THE UNIVERSITY OF OKLAHOMA

GRADUATE COLLEGE

HEAT TRANSFER WITH A FLOWING FLUID THROUGH POROUS MEDIA

A DISSERTATION

SUBMITTED TO THE GRADUATE FACULTY

in partial fulfillment of the requirements for the degree of

DOCTOR OF PHILOSOPHY

BY

DON WESLEY GREEN

Norman, Oklahoma

1962

HEAT TRANSFER WITH A FLOWING FLUID

THROUGH POROUS MEDIA

APPROVED BY

DISSERTATION COMMITTEE

ACKNOWLEDGMENT

Special appreciation is expressed to Dr. R. H. Perry who acted as research director during this work. His guidance and suggestions were truly helpful. The author is further appreciative of the personal friendship extended by Dr. Perry; a friendship which has helped to create within the author a fuller realization of the unlimited potentialities of the chosen vocation.

Several members of the Chemical Engineering Staff contributed to this work, especially Dr. R. L. Huntington and Dr. E. Weger. The advice and criticisms of fellow graduate students provided a good deal of assistance.

Many of the calculations were performed by Mr. R. Babcock, Mr. W. Pinto and Pat Green. Mr. Pinto also helped in the collection of most of the experimental data. The figures were prepared by Mr. J. Samaska. Typing and proofreading by Pat Green and typing by Mrs. Butler are appreciated.

The author is indebted to the National Science Foundation for financial support throughout this investigation and during the period of graduate study.

Don Wesley Green

TABLE OF CONTENTS

LIST OF TABLES

LIST OF ILLUSTRATIONS

HEAT TRANSFER WITH A FLOWING FLUID THROUGH POROUS MEDIA

CHAPTER I

INTRODUCTION

The rate of heat transfer in porous media with a flowing fluid present is determined by a combination of mechanisms. Broadly, these may be grouped as (1) bulk movement of the fluid, (2) conduction in the solid and fluid phases, (3) convective transfer of heat between the phases, (4) convective eddy mixing or dispersion of the fluid phase in the porous-media interstices, and (5) radiation.

A well known example of the effect of these mechanisms in porous-media heat transfer is illustrated in Figure 1. A fluid, at temperature T_o, is flowing in one-dimensional, steady, piston flow through a homogeneous, stationary porous prism, also at temperature T_o. At the point $x = 0$, the temperature of the input fluid is suddenly changed to a new value, T_i, and held constant. A thermocouple, placed at $x = L$, will yield an "S" shaped response curve as the heat front arrives, not a step function as was introduced into the prism. Thermal energy will have dispersed in the direction of fluid flow and away

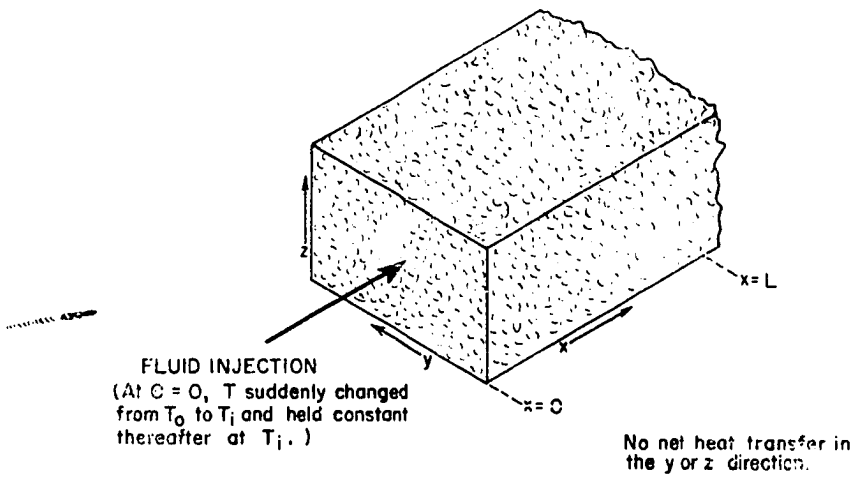

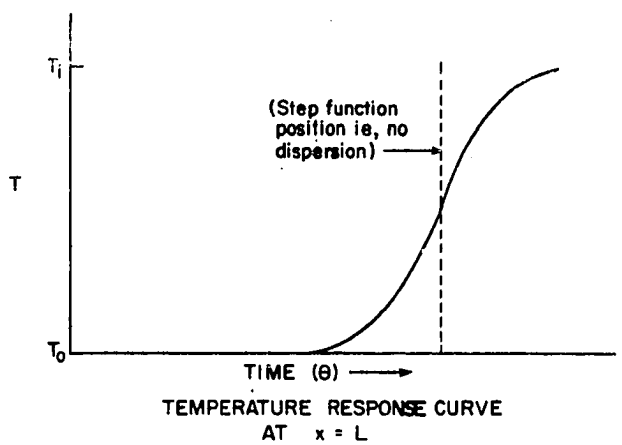

Figure 1- Longitudinal Heat Transfer in Porous Media

from the step-function position, the amount of dispersion being determined by the heat-transfer mechanisms which are important at the particular conditions of the experiment.

In the late 1920's, Anzelius (1), Schumann (159), and others (80, 132) presented papers dealing with the mathematical description of heat flow by bulk fluid movement with convective transfer between solid and fluid phases. These works showed that, as a consequence of the finite time required for heat transfer between the phases, there was a dispersion of the energy giving rise to a characteristic "S" shaped temperature response curve with a step-function input. The articles form a basis for much of the later research. Early experimental studies at low fluid rates utilized a convective transfer coefficient to characterize the data (75, 139).

More recently, investigators have shown that the presence of other heat-transfer mechanisms also results in temperature profiles of the same general form. Molecular conduction in one or both phases, superimposed on the bulk fluid flow, is one dispersion means. Jenkins and Aronofsky (92), examining this idea at the special condition of low fluid velocities, stated that earlier experimental work could be represented just as well by molecular-conduction parameters as by the convective transfer coefficient. In fact, they concluded that based on the then available data, the conduction mechanism was a more realistic explanation at very low fluid flow rates. Others have reached this same conclusion (7, 76, 77, 138).

Dispersion of heat by a convective mixing process occurs in packed beds due to the irregularities of fluid flow since fluid elements undergo a series of events such as acceleration, deceleration, or temporary trapping in eddies or stagnation points. Velocity profiles which develop in the interstices also tend to cause a spread of the thermal energy. These effects have been investigated by several workers in the area of mass transfer (25, 29, 38, 46, 114, 120) and have been found to be important both at low and high fluid velocities. In nearly all cases the diffusion equation has been used to fit the experimental data, with molecular diffusivity being replaced by an "eddy-dispersion" coefficient.

Examination of the general problem in which the different modes of heat transfer (e.g. conduction and convective transfer between phases) act simultaneously has also shown that the "S" shaped response curve results (73, 110, 148). Unfortunately then, the relative contributions of each to the overall rate are not easily determined from experimental data since measured temperature profiles have the same form for the individual mechanisms and for a combination of these. Only a very limited amount of data have been taken and analyzed for this latter case. The importance of interactions of the mechanisms has been little examined. Here, an analysis will necessarily need to rely on data taken at conditions where the different effects could be isolated.

Scope and Application of Rate Studies

A knowledge of rate processes in porous media is of considerable importance in the design of many commerical operations. Since about 1940, experimental and theoretical research has been accelerated in this broad field which includes heat transfer and the closely allied areas of mass and momentum transport. A fairly wide range of conditions has been investigated.

Packed-bed operations of the chemical and petroleum industries have increased in number and significance. Of prime concern in such equipment are the transfer rates between phases. Studies of mass and heat transport in the same direction as flow (axial) and in a direction normal to flow (radial) have found application. Regenerator heat exchangers, chromatography, and nuclear-reactor coolant systems are examples of other areas where this type of information is utilized.

In the last few years, rate processes at relatively low mass flow rates have become of concern. Low-velocity analyses are useful to the petroleum reservoir engineer. One heat-transfer application is in the design of thermal methods of oil recovery such as the in-situ combustion process. In this scheme a small part of the crude oil is burned "in-place" creating a moving heat front in the reservoir. The generated thermal energy raises the oil temperature, thereby decreasing its viscosity and increasing its mobility through the porous rock. Steam injection and hot-water injection have been proposed as

alternate means of getting heat to the oil.

More generally, the transport investigations at low velocities serve to complement the high-flow results and therefore to increase our understanding of the rate mechanisms.

Research Objectives

This research is the beginning of a longer range program to study dispersion of thermal energy in the same direction as fluid flow in porous media. The goal is a better understanding of the different heat-transfer mechansims, their interactions, and the conditions under which each is significant in establishing the overall rate.

The specific objective of the present work is a theoretical and experimental examination of unsteady-state heat transfer at relatively low fluid velocities and low temperatures where radiation is unimportant. One-dimensional, piston, liquid flow will be primarily investigated.

CHAPTER II

REVIEW OF PREVIOUS WORK

Previous theoretical and experimental work will be discussed according to the heat-transfer mechanisms considered. Unless otherwise specified, the physical model may be pictured by reference to Figure 1, Chapter I. A fluid is considered as being in one-dimensional, steady flow through a homogeneous porous medium. There is no net heat flow in the y or z directions, i.e., there are no heat "losses" from the system.

Square Front

Probably the simplest case of heat transfer in the direction of fluid flow is exhibited by the "square" heat front as discussed by several authors including Preston (138) and Churchill et al. (34). In this highly idealized case, two important assumptions are made.

(1) There is instantaneous thermal equilibrium between the solid and fluid phase.

(2) Dispersion of thermal energy by molecular conduction or any type of fluid convective eddy mixing does not occur. The first assumption is equivalent to an infinite heat-transfer coefficient and the second to zero molecular and eddy thermal

diffusivity. For this case, an energy balance on an increment of porous medium yields

$$\left[\rho_w C_w \phi + \rho_s C_s (1-\phi)\right] \frac{\partial T}{\partial \theta} = - v \rho_w C_w \phi \frac{\partial T}{\partial x} \qquad \text{(II-1)}$$

where $T = T_w = T_s$ at every bed location. Nomenclature is defined in Appendix A. For the boundary conditions,

$$\begin{aligned} T &= f_1(x), \quad \theta \leqq \frac{x}{v} \\ T &= f_2(\theta), \quad x = 0 \end{aligned} \qquad \text{(II-2)}$$

Churchill et al. (34) present the solution

$$\begin{aligned} T &= f_1(x - V_F\theta), \quad x > V_F\theta \\ T &= f_2(\theta - x/V_F), \quad x < V_F\theta \end{aligned} \qquad \text{(II-3)}$$

where $V_F = \dfrac{\rho_w C_w \phi\, v}{\rho_w C_w \phi + \rho_s C_s (1-\phi)}$.

For the special case of a step-function temperature input into a system initially at a constant temperature ($f_1(x) = T_o$, $f_2(\theta) = T_i$), the solution is

$$\begin{aligned} T &= T_o, \quad x > V_F\theta \\ T &= T_i, \quad x < V_F\theta \end{aligned} \qquad \text{(II-4)}$$

The temperature response curve or profile then shows a sharp break when the heat front arrives, going instantaneously from the initial temperature, T_o, to the input temperature, T_i. The time of arrival of the square front is given by

$$\theta = \frac{x}{V_F} \qquad \text{(II-5)}$$

so that V_F may be called the "square" heat-front velocity.

While this model is physically unrealistic, it does serve as an idealized reference case. Churchill points out that in some instances it is closely approached and serves as a good approximation. Hadidi (76) discusses this same type model for a system in which two fluid phases and a solid phase are present.

Finite Convective Transfer Coefficient

Theory

When the time taken for heat to be transfered between the solid and fluid phases is finite, the describing differential equations may be written:

For the fluid phase,

$$\rho_w C_w \phi \frac{\partial T_w}{\partial \theta} = - v \rho_w C_w \phi \frac{\partial T_w}{\partial x} - ha (T_w - T_s) \qquad \text{(II-6)}$$

For the solid phase,

$$\rho_s C_s (1-\phi) \frac{\partial T_s}{\partial \theta} = ha (T_w - T_s) \qquad \text{(II-7)}$$

The basic assumptions in the derivation of these equations are as follows:

a. Thermal diffusivities parallel to flow are zero.

b. No temperature gradients exist in the individual solid particles, i.e., the resistance to heat transfer between the phases lies entirely within a fluid "film" around the solid.

c. The rate of heat transfer between phases is proportional to their average temperature difference.

d. Solid and fluid physical properties are constant.

e. The fluid velocity is constant and "piston" flow exists.

These equations are commonly written as

$$-\frac{\partial T_w}{\partial Y} = T_w - T_s = \frac{\partial T_s}{\partial Z} \qquad \text{(II-8)}$$

where the dimensionless variables

$$Y = \frac{ha\ x}{\rho_w C_w \phi v} \quad \text{and} \quad Z = \frac{ha}{\rho_s C_s (1-\phi)} \quad (\theta - x/v)$$

have been introduced.

Anzelius (1), Schumann (159), and others (58, 80 139, 152) applied Equation (II-8) to the unsteady-state heating of porous solids or packed beds. Jakob (90) has discussed its application to regenerator-heat-exchanger problems and Klinkenberg (97) its application to cross-flow heat exchangers. This equation has also been used in adsorption and ion-exchange problems (63, 88, 180).

For the boundary conditions,

$$\begin{aligned} T_s &= T_o, \quad Z \leq 0 \\ T_w &= T_i, \quad Y = 0 \end{aligned} \qquad \text{(II-9)}$$

the solution is (97)

$$\frac{T_w - T_o}{T_i - T_o} = e^{-Y} \int_0^Z e^{-u}\, I_o(2\sqrt{Yu})\, du + e^{-Y-Z} I_o(2\sqrt{YZ}) \qquad \text{(II-10)}$$

$$\frac{T_s - T_o}{T_i - T_o} = e^{-Y} \int_0^Z e^{-u}\, I_o(2\sqrt{Yu})\, du \qquad \text{(II-11)}$$

where

$$I_o\ (2\sqrt{YZ}) = \sum_{n=o}^{\infty} \frac{(YZ)^n}{(n!)^2} \qquad \text{(II-12)}$$

By combining Equations (II-10) and (II-11), an expression is derived for the solid-fluid temperature difference (97).

$$\frac{T_w - T_s}{T_i - T_o} = e^{-Y-Z}\ I_o\ (2\sqrt{YZ}) \qquad \text{(II-13)}$$

Several alternate forms of the solution to Equation (II-8) have been derived and are discussed in detail by Klinkenberg (97), Reilly (144), and Hadidi (76). A typical form of the solution is shown in Figure 2a along with the square-front solution previously discussed.

Walter (180) has shown that Equations (II-10) and (II-11) approach from either side to

$$\frac{T - T_o}{T_i - T_o} = \frac{1}{2}\left[1 + \text{erf}\ (\sqrt{Z} - \sqrt{Y})\right] \qquad \text{(II-14)}$$

as Y and Z increase. The error function, erf, is defined to mean

$$\text{erf}(\xi) = \frac{2}{\sqrt{\pi}} \int_o^{\xi} e^{-u^2}\, du \qquad \text{(II-15)}$$

Klinkenberg (97, 98) developed approximations to the general solution which are applicable for smaller Y and Z values.

$$\frac{T_w - T_o}{T_i - T_o} = \frac{1}{2}\left[1 + \text{erf}\ (\sqrt{Z} - \sqrt{Y} + \frac{1}{8\sqrt{Z}} + \frac{1}{8\sqrt{Y}})\right] \qquad \text{(II-16)}$$

Figure 2a

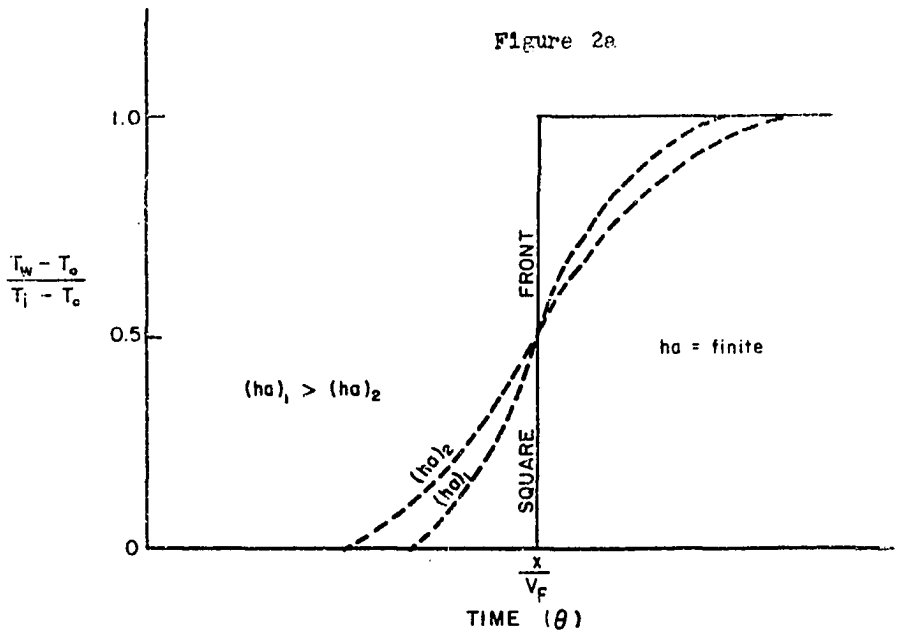

Figure 2b

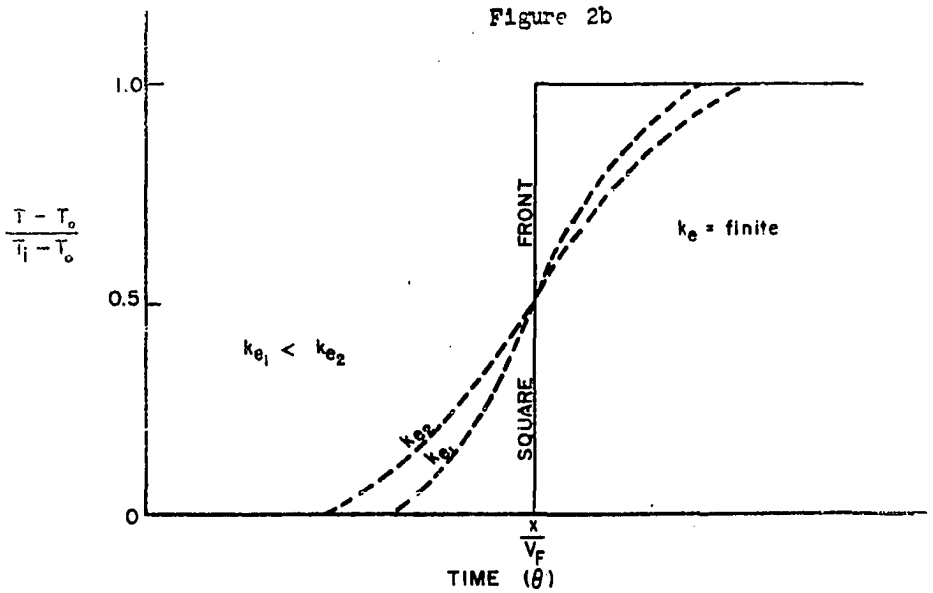

Figure 2- Simplified Analytical Solutions, Heat Transfer in Porous Media; 2a) ha=finite, k_w=k_s=0 2b) ha= ∞, k_w and k_s finite

$$\frac{T_s - T_o}{T_i - T_o} = \frac{1}{2}\left[1 + \text{erf} \left(\sqrt{Z} - \sqrt{Y} - \frac{1}{8\sqrt{Z}} - \frac{1}{8\sqrt{Y}} \right) \right] \qquad \text{(II-17)}$$

These are stated to be accurate to 0.006 for Y = 2 and 0.002 for Y = 4. They should not be used for Y less than 2. Other approximations are discussed also by Klinkenberg (97) and Hiester and Vermeulen (83).

The more general boundary conditions of an arbitrary initial temperature distribution and an arbitrary inlet temperature history has been treated by Churchill et al. (34). Their solutions are also generalized to a two-or three-dimensional flow field, where a knowledge of the point velocity as a function of distance along streamlines is required.

Klinkenberg and Sjenitzer (100) have shown that, for the case of a pulse input into a bed, the solution to Equation (II-8) approachs a Gaussian distribution with a mean of Y and a variance of 2Y. This is discussed in greater detail in Chapter III.

Experimental Work

Unsteady-State. Only a few investigators have conducted unsteady-state experiments to determine heat-transfer coefficients. Furnas (58), Saunders and Ford (152), and Lof and Hawley (116) injected air into beds of solid particles. A study by Coppage (37) utilized wire screening to simulate a packed bed. Values of the heat-transfer coefficient, ha, were determined by comparing the solution of Equation (II-8) with measured packed-bed effluent temperature response curves to a

step-function input. These investigations were generally in the turbulent region and h was found to vary with G^n, n varying between 0.7 and 1.0.

Greenstein and Preston (75), and Preston and Hazen (139) obtained data with liquids at relatively low liquid velocities, approximately 3 to 24 ft/hr. They flowed hot water through porous-media packs of sand grains, being primarily concerned with secondary oil-recovery processes. Application of Equation (II-8) yielded heat-transfer coefficients which correlated with fluid velocity as

$$ha = 0.196\ G^{1.82} \qquad \text{(II-18)}$$

Preston (138) and Hadidi (76), from later work at about the same experimental conditions, concluded that the thermal conduction mechanism (to be discussed) was more applicable at the low flow rates studied than the finite-transfer-coefficient model. The conclusion was based to a large degree on the size of the exponent in Equation (II-18).

Steady-State. A large number of investigators have measured heat-transfer coefficients with steady-state experiments. In some of these works, heat has been generated in metallic particles by the use of electrical energy. Green et al. (74), Baumeister and Bennett (10), Glaser and Thodos (66), and Denton (41) used this method with gas as a flowing fluid. In the latter two cases, both solid and fluid temperatures were measured at selected points in the bed, and ha

values were calculated from the measured differences and known heat-transfer rates. In the other papers, gas temperatures were measured at the bed inlet and outlet and mean temperature driving forces were used. The general correlation procedure has been to plot the "j_h" factor, introduced by Colburn (35), as a function of Reynolds number; where

$$j_h = \frac{h}{C_w G} \left(\frac{C_w \mu}{k_{wc}}\right)^{2/3} \qquad \text{(II-19)}$$

Gamson et al. (61) measured simultaneous heat-and mass-transfer rates from particle to fluid by drying beds of porous water-filled particles, and Satterfield and Resnick (151) obtained simultaneous rates in a system in which a "film-diffusion" controlled chemical reaction was taking place. Gamson et al. reported the ratio j_h/j_m to be 1.076 while Satterfield and Resnick gave the ratio as 1.37. The mass-transfer "j_m" factor is defined analogously to "j_h" as

$$j_m = \left(\frac{HMP}{G}\right) \left(\frac{\mu}{\rho_w D_m}\right)^{2/3} \qquad \text{(II-20)}$$

where H is the mass-transfer coefficient. Stewart (167) has indicated that the value 1.076, obtained by Gamson et al., resulted from use of humidity charts which were in error, and that actually the correction should be in the opposite direction. The percentage difference would not exceed 7%.

Several investigations of mass transfer in packed beds have been made (43, 52, 59, 60, 61, 84, 118, 190). Many of these works have been with liquid-solid systems (43, 52, 118)

and a few have been in the laminar flow region (43, 52, 59, 118, 190). Here again, the usual correlating procedure has been to plot j_m versus the Reynolds number. In general, the analogy between heat and mass transfer holds, making it possible to use mass-transfer results to predict heat-transfer rates. This has been discussed by Gamson (60), Denton (41), and Colburn (35), among others.

The agreement of results of different researchers has been fair to poor. Differences in type and mode of bed packing and bed geometries have been suggested as reasons for the disagreements.

Finite Convective Transfer Coefficient Plus Solid-Phase Resistance

In some cases, the assumption that solid temperature gradients within individual particles do not exist, i.e., that the solid offers no resistance to particle-fluid heat transfer, may be in error. The effect of this additional resistance is to spread the temperature response to a step-function input into a packed bed in the same manner as the fluid "film" resistance.

Saunders and Ford (152), using a dimensional-analysis approach, concluded that heat transfer in a packed bed should be governed by three groups: $\frac{\rho_w C_w \phi v \theta}{d_p \rho_s C_s}$, $\frac{\rho_w C_w \phi v\, d_p}{k_{sc}}$, and $\frac{L}{d_p}$. In their experimental work, the maximum value of the group,

$\frac{\rho_w C_w \phi v d_p}{k_{sc}}$, was approximately 4.0. At this magnitude it had no influence on the correlation, indicating that solid resistance was negligible compared to the gas "film." Their calculations further indicated that solid-phase resistance should be considered at $\frac{\rho_w C_w \phi v d_p}{k_{sc}}$ values of 8 to 12 and higher.

Rosen (147, 148) attacked this problem by solving differential equations which include both a finite "film" transfer coefficient and intra-particle conduction. His approach was to assume that each spherical pellet is surrounded by fluid at a constant temperature, i.e., the downstream fluid temperature gradient across one particle is so small that assuming it constant causes negligible error. The resulting partial differential equations, which describe transfer in the solid sphere and in the bulk fluid stream, were solved for a step-function input into the bed. As the complete solution involves complicated integrals, a simplified approximate solution was also presented. Babcock (6) discusses the application of these results to heat transfer at relatively low liquid flow rates.

Rosen and Winsche (149) have used a frequency response analysis, and by analogy with electric-circuit theory have derived expressions for the complex admittances for both the "film" resistance and intra-partical diffusional resistance mechanisms. Their work showed the total impedance for linear systems to be equal to the sum of the solid-phase impedance

plus a "film" resistance term. Kasten et al. (94) and Edeskuty and Amundson (48) have also mathematically treated the case of "film" diffusion combined with intra-particle diffusion in adsorption systems.

Effective-Thermal-Conductivity Model

Theory

An alternate assumption to the finite-heat-transfer-coefficient model is to take the bed thermal conductivity as finite and ha as infinite. Jenkins and Aronofsky (92) proposed this model to be applicable at relatively low flow rates in porous media. An energy balance on a porous-medium increment gives

$$\left[\rho_w C_w \phi + \rho_s C_s (1-\phi)\right] \frac{\partial T}{\partial \theta} = - v \rho_w C_w \phi \frac{\partial T}{\partial x} + k_e \frac{\partial^2 T}{\partial x^2} \qquad \text{(II-21)}$$

where, as in the square-front model, $T = T_w = T_s$ at each bed position. Equation (II-21) is the one-dimensional form of the more general Fourier-Poisson equation. The parameter k_e is the effective thermal conductivity of the porous medium. As proposed by Jenkins and Aronofsky, it is the "static" conductivity of the bed, i.e., the thermal conductivity of the porous medium in the absence of fluid flow.

Additional assumptions implied include the following:

a. The fluid is in steady, piston flow in the x direction only.

b. There are no temperature gradients normal to the fluid flow direction.

c. The physical properties of the system are constant.

For the boundary conditions,

$$\begin{aligned} T &= T_o, & \theta &= 0, & &\text{all } x \\ T &= T_i, & \theta &> 0, & x &= 0 \end{aligned} \qquad \text{(II-22)}$$

the solution is (92, 138)

$$\frac{T - T_o}{T_i - T_o} = \frac{1}{2} \operatorname{erfc}\left[\frac{1}{2\sqrt{K}}\left(\frac{x}{\sqrt{\theta}} - V_F\sqrt{\theta}\right)\right] + \frac{1}{2} e^{x \rho_w C_w \phi \, v/k_e} \operatorname{erfc}\left[\frac{1}{2\sqrt{K}}\left(\frac{x}{\sqrt{\theta}} + V_F\sqrt{\theta}\right)\right] \qquad \text{(II-23)}$$

where erfc, the co-error function, is equal to (1 - erf). The thermal diffusivity, K, is defined as $K = \frac{k_e}{\rho_w C_w \phi + \rho_s C_s (1-\phi)}$. As Illustrated in Figure 2b, the shape of the temperature profile curve is the typical "S" shaped response curve with the curve "spread" becoming larger as k_e increases.

Preston (138) and Hadidi (76, 77) have discussed the application of Equation (II-21). Preston discussed the possibility of the effective conductivity, k_e, varying with fluid velocity, being made up of a static component, k_e^o, and a component which is a function of velocity, $k_e(v)$.

The thermal-conductivity approach has generally been taken in petroleum reservoir studies of secondary methods of oil recovery since fluid velocities are very low. Bailey and

Larkin (8) and Ramey (141) obtained solutions for the case of a moving heat source where conduction is the only mechanism of heat transport (no heat flow by bulk fluid movement). Solutions were presented for both linear and radial heat flow. Vogel and Krueger (176) examined this same problem using an analog computer. Bailey and Larkin (7) have also solved the one-dimensional, moving-heat-source problem including both conduction and transport by bulk fluid flow.

Experimental Work

Unsteady-State. The early experimental investigations at low fluid velocities assumed a finite heat-transfer coefficient and zero thermal diffusivity (75, 139). Jenkins and Aronofsky (92) compared these very limited data to the effective-thermal-conductivity model and concluded that k_e was a more applicable characterizing parameter. Their conclusions were based primarily on the following:

1. Values of ha varied with fluid velocity to about the 1.8 power see Equation (II-18) , while at high velocities, previous investigators found ha to be a function of velocity to the 0.70 to 1.0 power (58, 116). Calculated k_e values did not vary with velocity, in agreement with the application of the "static" thermal conductivity.

2. Particle size did not influence ha. Again, at high velocities, workers have found particle diameter to affect ha (58, 116). The magnitude of k_e did not change with particle

size as predicted by static-conductivity correlations (51) [see Equation (II-26)].

3. Numerical values of calculated k_e's were more in agreement with previous works and were more reasonable than the ha values.

Hadidi (76), in a very few experimental runs at low velocities, reached the same conclusion.

A more extensive study was made by Preston (138). Preston concluded, in disagreement with his earlier work (75, 139), that the effective-conductivity concept was more reasonable at relatively low liquid velocities than the finite-ha model. He did find, however, that k_e varied with liquid velocity. The final correlation was

$$\frac{k_e/k_{wc}}{(k_{sc}/k_{wc})^{.12}} = 8.40 \left(\frac{d_p G}{\mu \phi}\right)^{.17} \qquad \text{(II-24)}$$

to be used at Reynolds numbers between 0.01 and 10. Data scatter was large. Preston's results are discussed further in Chapter V and in Appendix L.

Steady-State. Effective thermal conductivities in the same direction as fluid flow have been measured in steady-state systems by Kunii and Smith (106) and Yagi et al. (189). In these low-velocity studies, heat was injected into one end of a packed bed and fluid into the other. The resulting steady-state temperature profile across the bed was measured. Data were analyzed by comparing this temperature profile to the solution of the steady-state form of Equation (II-21).

$$- v \rho_w C_w \phi \frac{\partial T}{\partial x} + k_e \frac{\partial^2 T}{\partial x^2} = 0 \qquad \text{(II-25)}$$

These investigators found k_e to be a function of fluid velocity.

Static Thermal Conductivity

Theory. The use of the effective-thermal-conductivity model, Equation (II-21), requires a knowledge of the thermal conductivity of porous media when a fluid phase is present but not flowing. This is so even when k_e is a function of fluid velocity since it can then be thought of as being composed of a static contribution, k_e^o, and a velocity-dependent contribution, $k_e(v)$. Several predictive correlations have been presented for the static conductivity.

Euchen (51) modified an equation developed by Maxwell for the electrical conductivity through a two-phase system where one phase was continuous and the other consisted of spherical pellets of different conductivity. The Euchen equation is

$$k_e^o = \frac{k_{wc}\left[k_{sc} + 2k_{wc} - 2(1-\phi)(k_{wc} - k_{sc})\right]}{k_{sc} + 2k_{wc} + (1-\phi)(k_{wc} - k_{sc})} \qquad \text{(II-26)}$$

Hamilton (78) modified this expression to include non-spherical particles.

Kunii and Smith (105) developed a k_e^o expression for packed beds considering heat transfer by (1) conduction in the gas phase, (2) conduction in the solid phase, (3) a solid-fluid-solid conduction mechanism, and (4) radiation.

Preston (138), based on experimental data in several systems, modified a result due to Schumann and Voss (160). Preston's relationship should be applicable in systems of the particular type studied.

$$k_e^{\circ} = 1.536\ k_{sv}^{.959} \qquad \text{(II-27)}$$

The term, k_{sv}, is the Schumann and Voss conductivity given by the following equations.

$$k' = \frac{k_{wc}\ k_{sc}}{k_{wc}+p(k_{wc}-k_{sc})} \left[1 + \frac{p(1+p)(k_{wc}-k_{sc})}{k_{wc}+p(k_{wc}-k_{sc})} \ln \frac{k_{wc}(1+p)}{k_{sc}p} \right] \qquad \text{(II-28)}$$

$$k_{sv} = k_{wc}\ \phi^3 + k'\ (1-\phi^3) \qquad \text{(II-29)}$$

$$\phi = (p^2 + p)\ \ln\left(\frac{p+1}{p}\right) - p \qquad \text{(II-30)}$$

Tabulated values of k_{sv} as a function of $\frac{k_{sc}}{k_{wc}}$ and ϕ are given by Preston.

Experimental Work. Several experimental studies of the static thermal conductivities of two-phase porous-media systems appear in the literature (44, 55, 65, 105, 138, 166, 169). Preston (138) measured k_e° values for the same experimental systems as used in his dynamic heat-transfer experiments, making the work very useful for packed-bed, liquid-solid calculations. The data were correlated by modifying an earlier equation due to Schumann and Voss (160).

Radial Effective Thermal Conductivity

The effective-thermal-conductivity model has been

applied to the radial transfer of heat (perpendicular to fluid flow) by many investigators (3, 9, 21, 27, 127, 136, 163, 187). In these steady-state studies, longitudinal conduction is generally assumed negligible. Values of radial conductivities are taken to be composed of a static contribution and a component which is velocity dependent (127, 163, 187). Wall effects are also sometimes accounted for (27, 136). In many of the works, radiation is included as a heat-transfer means (3, 187).

Longitudinal Eddy Dispersion

Theory

Longitudinal "eddy dispersion" of thermal energy and mass is known to be a result of a convective mixing process which occurs in packed beds. This effect has been studied primarily in mass-transfer investigations.

Diffusion Model. The theoretical model usually applied is the ordinary "random-walk" concept. When a macroscopic element of fluid undergoes a statistical number of events, such as acceleration, deceleration, trapping, etc., it may be described by a law similar to Fick's law of molecular diffusion. The spreading therefore follows a Gaussian distribution, and for packed beds this may be assumed to hold in a bed of sufficient length (4, 22, 38). The differential equation describing this process is the diffusion equation. For mass transfer,

$$\frac{\partial C}{\partial \theta} = - v \frac{\partial C}{\partial x} + E_m \frac{\partial^2 C}{\partial x^2} \qquad \text{(II-31)}$$

where E_m, the dispersion coefficient, has replaced the

molecular-diffusion coefficient. Keulemans (95) and others (4,100) have reasoned that E is proportional to fluid velocity and particle diameter.

$$E = \eta v d_p \qquad \text{(II-32)}$$

The coefficient " η " is a constant characterizing the porous media.

The solution to Equation (II-31) is well known and has been discussed with reference to packed-bed dispersion in several articles (38, 46, 113). Danckwerts (38) has presented solutions for the boundary conditions of either a pulse-function or step-function input. Carberry and Bretton (29), Klinkenberg and Sjenitzer (100), and Levenspiel et al. (113) have treated the case of a pulse input. A frequency-response analysis has been used by Kramers and Alberda (104), Ebach and White (46) and McHenry and Wilhelm (120).

Cell-Mixing Model. A cell-mixing model has been proposed by Kramers and Alberda (104) and others (4, 29). A packed bed is assumed to consist of "n" perfect mixers in series, i.e., the fluid leaving a mixing cell has the same concentration of tracer material as the solution in the cell. Equations have been derived expressing the effluent from the nth cell as a function of time for a given input into the first cell. Carberry (28) extended the model by the introduction of a cell-mixing efficiency.

Aris and Amundson (4) compared the cell-mixing and diffusion models and, at distances equivalent to several mixing

lengths down the bed, the two models gave approximately the same distribution expressions for injected tracer material. By equating these distributions, an expression for the Peclet number resulted.

$$Pe = \frac{v\, d_p}{E} = \frac{2}{\gamma} \qquad \text{(II-33)}$$

where γ characterizes the distance between successive mixing layers and is approximately equal to 1.0 for random-packed spheres. This limiting value of 2.0 for the Peclet number was stated to be applicable at high fluid velocities where perfect mixing occurs in the mixing cells.

Alternate Statistical Model. Cairns and Prausnitz (23, 25) proposed a statistical model alternate to the random-walk model. Their work is based on the mathematics of Einstein (49). Fluid corpuscles are assumed to move through porous media in a series of "motion phases" and "rest phases;" that is, the corpuscle may be moving rapidly in one instant and in the next instant caught in an eddy or at a stagnation point. By consideration of a Galton plane, probability expressions were derived for the downstream concentration distribution of injected tracer material. Parameters for this model were obtained by equating the derived distribution to the Gaussian distribution of the diffusion model, at large values of time and distance down the bed. In this theory, upstream mixing of tracer material is not allowed.

Miscellaneous Models. The application to packed beds

of the theory of Taylor (171) for longitudinal dispersion of material in flow through a capillary tube has been discussed (17, 56). Here, the porous-media void spaces are viewed as small tubes in which velocity profiles develop causing a net concentration spread of tracer material. According to Taylor's theory, the dispersion in this case is inversely proportional to the molecular diffusivity of the tracer. This result was also reached by Frankel (56) who considered the effect on the mixing process of stagnant spheres of fluid or stagnant "pockets" of fluid. In these models,

$$E \sim \frac{v^2}{D} \qquad \text{(II-34)}$$

Frankel suggests combining this effect with the model of Keuleman's, Equation (II-32), and with molecular diffusion to yield a general expression for the total dispersion.

Experimental Work

Experimental investigations for the purpose of determining longitudinal dispersion coefficients have been limited to mass-transfer studies. In nearly all cases, the diffusion equation has been used to analyze experimental data. Primarily, the reason is the simplicity of analysis with this approach since the measured concentration response curves are characterized by a single parameter, E_m. Other theoretical models require knowledge of bed parameters which are difficult to obtain (e.g., in the mixing-cell theory the cell volume, mixing efficiency, and number of cells must be known). Values of E_m

reported by the different researchers are actually the sum of the molecular diffusion contribution, D_m, plus the convective mixing contribution. However, in many cases D_m is negligible.

Methods of injection of tracer material into the beds have varied, including approximations to pulse-function injection (29, 46), step-function input (17, 25, 38), and sinusoidal injection (40, 46, 104). Relatively low Reynolds numbers have generally been investigated, with flow ranging from purely laminar up through the flow-transition region.

Experimental data taken by different investigators in the laminar flow region with liquid-solid systems have yielded Peclet numbers on the order of $0.5 \pm 60\%$ (25, 29, 46, 114, 168). McHenry and Wilhelm (120), with gas-solid porous-media systems at about the same range of Reynolds number, gave an average Pe value of 1.88, in close agreement with the theoretical maximum of 2.0. The possibility of this nearly four-fold disagreement between liquid and gas systems being due to fluid "by-passing" in the liquid case has been discussed (17, 56, 71). The argument is that fluid next to solid particles and in the crevices formed by solid-solid contacts will tend to be by-passed by the main stream, causing a spread in the concentration profile. This by-passed fluid will approach the main stream concentration by molecular diffusion. The overall result of such a process is to increase the size of the measured dispersion coefficient, E, inversely proportional to the size of the molecular diffusion coefficient as predicted in the model of

Taylor (171) previously discussed. The high molecular diffusivity of gases, compared to liquids, markedly reduces the magnitude of this effect for gas-solid systems. Handy (79) examined the effect of molecular diffusivity on the dispersion coefficient by making experiments with liquids in which D_m had different values ($D_{m1}/D_{m2} \approx 4$). No positive conclusions could be made, but a qualitative trend of increased E_m with lower D_m values was noted.

The fluid flow mechanisms resulting in eddy dispersion in porous media are illustrated pictorily in movies taken by Chatenever (32). Events such as acceleration, deceleration, temporary trapping, and differences in velocity across a single pore opening are clearly shown.

Radial Dispersion. Radial convective dispersion occurs in porous-media systems but at a slower rate than longitudinal dispersion. Bernard and Wilhelm (12) experimentally determined radial Peclet numbers of approximately 10-12 with turbulent flow. Other investigators (91, 142) are in general agreement with the lower dispersion coefficients for radial transport of heat or mass. For heat transfer, the radial convective dispersion coefficients are combined with the static thermal conductivity of the packed bed to give the radial effective thermal conductivity previously discussed.

Combination of Transfer Mechanisms

Theory

Combination of the concepts of longitudinal dispersion

of heat or mass by molecular transport and convective mixing, and of finite times for transfer between the solid and fluid phases of a system has been theoretically considered. For a few specialized cases, differential equations have been solved.

Lapidus and Amundson (110) considered longitudinal mass transfer of an adsorbate in a column packed with porous adsorbent particles. The differential equations, assuming piston fluid flow, are

$$\frac{\partial C}{\partial \theta} = - v \frac{\partial C}{\partial x} + E_m \frac{\partial^2 C}{\partial x^2} - \frac{1}{\phi} \frac{\partial n}{\partial \theta} \qquad \text{(II-35)}$$

where here, E_m includes both molecular diffusion and eddy dispersion, and where n is the amount of adsorbate on the adsorbent in moles per unit volume of bed. For the adsorbed phase,

$$\frac{\partial n}{\partial \theta} = k_1 C - k_2 n \qquad \text{(II-36)}$$

where k_1 and k_2 are constants.

With the boundary conditions,

$$\begin{aligned} C = n = 0, \quad & \theta = 0, \quad \text{all } x \\ C = C_i, \quad & \text{all } \theta, \quad x = 0 \end{aligned} \qquad \text{(II-37)}$$

the solution is

$$\frac{C}{C_i} = e^{vx/2E_m} \left[F(\theta) + k_2 \int_0^\theta F(\theta)\, d\theta \right] \qquad \text{(II-38)}$$

$F(\theta)$ is defined as

$$F(\theta) = e^{-k_2\theta} \int_0^\theta I_0 \left[2 \sqrt{\frac{k_1 k_2 z}{\phi} (\theta - z)} \right] \frac{x}{2\sqrt{\pi E_m z^3}} \exp\left[\frac{-x^2}{4E_m z} - zg \right] dz \qquad \text{(II-39)}$$

with $g = \frac{v^2}{4E_m} + \frac{k_1}{\phi} - k_2$.

Van Deemter et al. (175) discussed an approximation to this solution, for the boundary conditions of a pulse input, which holds under certain assumptions concerning the size of the system parameters. This simplification, due mainly to Van der Waerden (unpublished report referred to by Van Deemter et al.), reduces the solution to a Gaussian distribution in which variances for the two mechanisms of longitudinal dispersion and a finite transfer rate between phases are simply additive. Klinkenberg and Sjenitzer (100) also proposed the idea of added variances for the different mechanisms. This is discussed in detail in Chapter III.

In the investigation of Rosen and Winsche (149) discussed earlier, heat transfer between phases was taken to be governed by both a "film" resistance around the solid and intra-particle conduction. Their work, using the analogy to electric-circuit theory, showed the complex impedances for the "film" resistance and intra-particle conduction to be additive. Deisler (39,40) extended this work by experimentally and theoretically investigating simultaneous diffusion into the pores of a catalyst, longitudinal diffusion, and convective eddy dispersion. Deisler's work is discussed further in Chapter III and Appendix K.

Bland (16) developed relations governing both the flow of gas in porous media and the heat-transfer rate. He combined

the energy balance, equation of continuity, an equation of state for the gas, and Darcy's law for fluid flow in porous media to derive the generalized equations. Analytical solutions were obtained for a few particular cases.

Amundson (2) has obtained solutions for several cases of heat transfer in which the different mechanisms are combined. In treatment of a bed packed with small particles, the mechanisms of radial and longitudinal conduction in the fluid phase, and solid-fluid convective transfer were included. The solid was assumed to contain a heat source. For a bed of large particles, the equations were extended to include intra-particle conduction in the solid phase, with the assumption that the temperature around each sphere was constant. Downstream solid conduction was not allowed.

Combination of the different heat-transfer mechanisms has been treated by Bailey and Larkin (7), and the case of a moving heat source with longitudinal conduction and particle-fluid transfer has been solved for quasi-steady-state conditions. The steady-state situation, not including a heat-source term, has been discussed by Kunii and Smith (106) and Yagi et al. (189).

Hadidi (76) attacked the problem of two fluid phases flowing simultaneously through porous media. Finite-difference equations describing heat transfer were set up but not solved.

Experimental Work

Deisler (39) measured total longitudinal dispersion

of mass in a gas-solid packed-bed system in which intra-particle diffusion, gas-phase molecular diffusion, and eddy dispersion were present. A frequency-response analysis was made. From response concentration curves, values were calculated for the apparent diffusion coefficient of the gas within the porous solid and for the gas-phase longitudinal diffusion coefficient, $(E_m + D_m)$. Longitudinal Pe numbers were slightly higher than 4.0, considerably above the results of McHenry and Wilhelm (120).

Van Deemter et al. (175) studied limited experimental data obtained in two chromatographic columns. The important mass-transfer mechanisms were considered to be molecular diffusion, eddy dispersion and a finite fluid-solid mass-transfer rate. Constants, characterizing the mechanisms, obtained from the data were the right order of magnitude for all mechanisms.

Velocity-Profile Considerations

Deviations from piston fluid flow in packed beds are known to occur. An effect of the tube wall on the particle packing arrangement, with a corresponding effect on fluid velocity near the wall, has been observed (26, 128, 161). The presence of the wall increases the void volume of the pack in the region of the wall. The result is a higher fluid velocity in this zone and, when the particle size is large compared to the tube diameter, significant deviation from piston flow can occur. Ratios of particle diameter to tube diameter, above

which the wall effect is important, have been reported from 0.04 (161) to 0.067 (26).

Flow channeling frequently appears in porous media as the result of an unfavorable viscosity ratio, i.e., when the fluid being displaced from a porous medium has a higher viscosity than the displacing fluid (17, 32, 154). Brigham et al. (17) discuss this phenomenon with reference to longitudinal dispersion of mass in a two-liquid system.

Natural convection can induce flow channeling. This has been observed in experimental studies of solid-fluid mass transfer at low Reynolds numbers (43, 59, 185). The effect is characterized by the Grashof number.

Cairns and Prausnitz (26) discuss the influence of deviations from plug flow on experimental longitudinal dispersion coefficients. When experimental concentration response curves are determined by measuring radially averaged packed-bed effluents, calculated parameters, (such as E), may be influenced by these deviations. A calculated longitudinal dispersion coefficient will be high unless radial transport is of sufficient magnitude to eliminate the radial concentration gradients induced by the non-plug flow.

CHAPTER III

THEORETICAL INVESTIGATION

The mechanisms of heat transfer considered which contribute to the dispersion of thermal energy are (1) longitudinal conduction in the fluid and solid phases, (2) convective eddy mixing or dispersion in the fluid phase, and (3) a finite rate of heat transfer between solid and fluid. These processes, combined with bulk fluid movement, are assumed to account for the total heat-transfer rate in the direction of fluid flow.

General differential equations resulting from an energy balance on the porous media were formulated. Since an analytical solution was not obtainable, numerical calculations were made, using a digital computer, for several specific values of the system parameters. Numerical calculations were time consuming and rather impractical for use in the evaluation of experimental data. Therefore, based on literature sources, an approximate solution was derived which in many instances allows the heat transfer to be well represented using the diffusion equation and an effective thermal conductivity accounting for the several individual dispersion mechanisms.

Physical Model

The system is a semi-infinite porous body through which a liquid is flowing in one-dimensional, steady, piston flow (see Figure 1). Solid and fluid temperatures are initially equal and constant throughout. At time zero, the injected fluid temperature is suddenly changed to a different value. No net heat transfer in a direction normal to the liquid flow occurs, i.e., there are no heat "losses" from the system. Radiation is assumed negligible. For any given set of conditions, fluid and solid physical properties are taken as independent of temperature.

Fluid and Solid Phase Energy Balances

An energy balance over a porous-medium increment yields the following differential equations.

For the fluid phase,

$$\rho_w C_w \phi \frac{\partial T_w}{\partial \theta} = - v \rho_w C_w \phi \frac{\partial T_w}{\partial x} + k_w \phi \frac{\partial^2 T_w}{\partial x^2} - ha(T_w - T_s) \qquad \text{(III-1)}$$

For the solid phase,

$$\rho_s C_s (1-\phi) \frac{\partial T_s}{\partial \theta} = k_s (1-\phi) \frac{\partial^2 T_s}{\partial x^2} + ha (T_w - T_s) \qquad \text{(III-2)}$$

Here, k_s is a pseudo thermal conductivity which characterizes the rate of apparent solid-phase conduction in the longitudinal direction. The fluid-phase coefficient, k_w, includes both a conduction contribution and the effect of eddy dispersion,

$$k_w = k_{wc} + k_{wm} \qquad \text{(III-3)}$$

where

k_{wc} = thermal conductivity of the fluid phase

k_{wm} = eddy-dispersion coefficient

Of these coefficients, k_{wm} is a function of fluid flow rate while k_{wc} and k_s are assumed to be independent of fluid velocity. The rate of heat transfer between the phases at any point is assumed proportional to their average temperature difference, ha being the constant of proportionality. An implicit assumption in the derivation of Equations (III-1) and (III-2) is that the solid phase is an evenly distributed source or sink, also having the property of allowing conduction only in the direction of the flowing liquid. However, temperature gradients in the solid normal to the fluid flow are assumed non-existent, that is, the resistance to heat transfer between fluid and solid lies entirely within a fluid "film" around the solid.

Applicable boundary conditions for the model are

$$\begin{aligned} T_w = T_s = T_o, &\qquad \text{all } x, &&\qquad \theta = 0 \\ T_w = T_s = T_i, &\qquad x = 0, &&\qquad \text{all } \theta > 0 \\ T_w = T_s = T_o, &\qquad x \to \infty, &&\qquad \text{all } \theta \end{aligned} \tag{III-4}$$

The second condition, of an instantaneously reached solid temperature, T_i, at the boundary $x = 0$, is an approximation which should be sufficiently accurate for times slightly larger than zero. An analytical solution to Equations (III-1) and (III-2) was not obtained and numerical methods were therefore used.

Numerical Solution

Equations (III-1) and (III-2) can be written in a dimensionless form as

$$\frac{\partial t_w}{\partial \tau} = - \frac{\partial t_w}{\partial y} + \lambda \frac{\partial^2 t_w}{\partial y^2} - \lambda (t_w - t_s) \qquad \text{(III-5)}$$

$$\frac{\partial t_s}{\partial \tau} = \lambda \frac{a_s}{a_w} \frac{\partial^2 t_s}{\partial y^2} + \lambda \frac{a_s}{a_w} \frac{k_w'}{k_s'} (t_w - t_s) \qquad \text{(III-6)}$$

where

$$\lambda = \left(\frac{ha}{k_w'}\right)^{\frac{1}{2}} \frac{a_w}{v}, \quad \tau = \left(\frac{ha}{k_w'}\right)^{\frac{1}{2}} v\,\theta, \text{ and } y = \left(\frac{ha}{k_w'}\right)^{\frac{1}{2}} x \,.$$

The dependent variables t_w and t_s are "accomplished temperature fractions" and may have values between zero and one. All nomenclature is defined in Appendix A.

These equations were reduced to finite-difference equations and solved for several values of the parameters on an IBM 650 digital computer. Equations of the forward-difference type were used in the solution. Convergence of the numerical solutions was checked by reducing increment size until convergence was obtained and by checking computer results against the analytical solution for the case, $k_w = k_s = 0$ and ha = finite. The difference equations and convergence criteria of the type presented by Dusinberre (45) are presented in Appendix B. To obtain solutions, it was necessary to use very small time and distance increments necessitating long runs on the computer.

The parameter range studied corresponded primarily to

water-silica and water-glass porous-media systems. In Figures 3 and 4 are shown some typical time-fluid temperature profiles. A decrease in λ which is equivalent to decreasing ha or increasing fluid velocity, all other properties held constant, causes an earlier appearance of the heated zone at a given position and a greater "spread" of the profile curve (Figure 3). Similarly, an increase in solid thermal conductivity results in the heated zone appearing earlier with a greater spread of the curve (Figure 4). Also shown in these plots is the position of the square heat front for the simplest case discussed in Chapter II, i.e., $t_w = t_s$, $k_s = k_w = 0$.

The influence of the parameter λ on the solid-fluid temperature difference is seen in Figure 5, where $(t_w - t_s)$ decreases significantly as λ increases. The curves are plotted at different dimensionless y and τ values to allow them to be clearly presented on one graph, and such small changes in time or distance will not markedly affect the magnitude of $(t_w - t_s)$.

The effect of a finite heat-transfer coefficient resulting in these solid-liquid temperature differences is shown by a comparison of the analytical solutions for the simplified cases (discussed in Chapter II) with the more general numerical-solution results. This is done for different parametric values in Figure 6. The simplified cases used for comparison are (1) $k_w = k_s = 0$ [Equation (II-8)], and (2) $t_w = t_s$ [Equation (II-21)]. The value of k_e used in the analytical solution for the

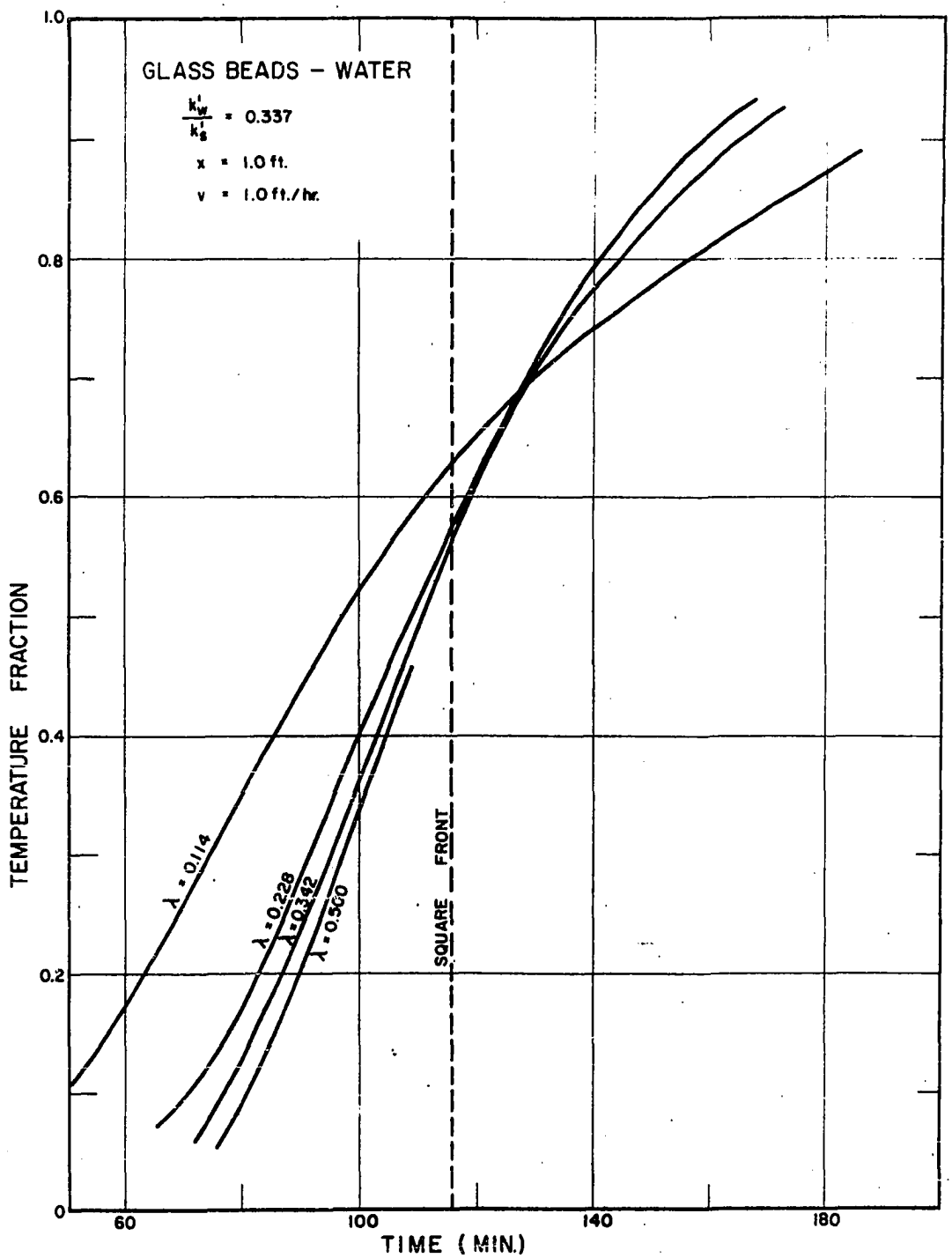

Figure 3- Fluid Temperature Profiles; Effect of Dimensionless Parameter λ

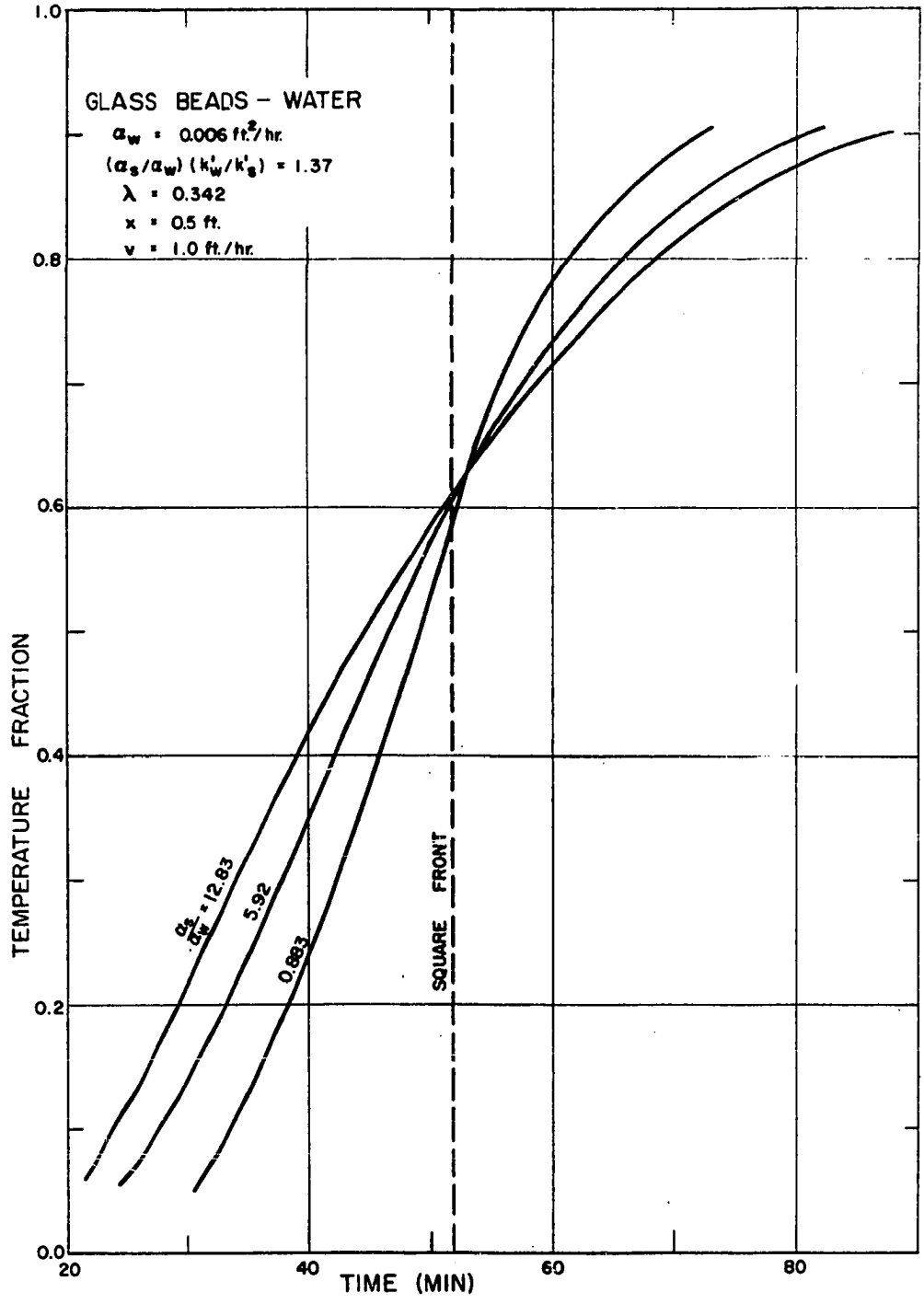

Figure 4- Fluid Temperature Profiles; Effect of Solid-Phase Thermal Conductivity

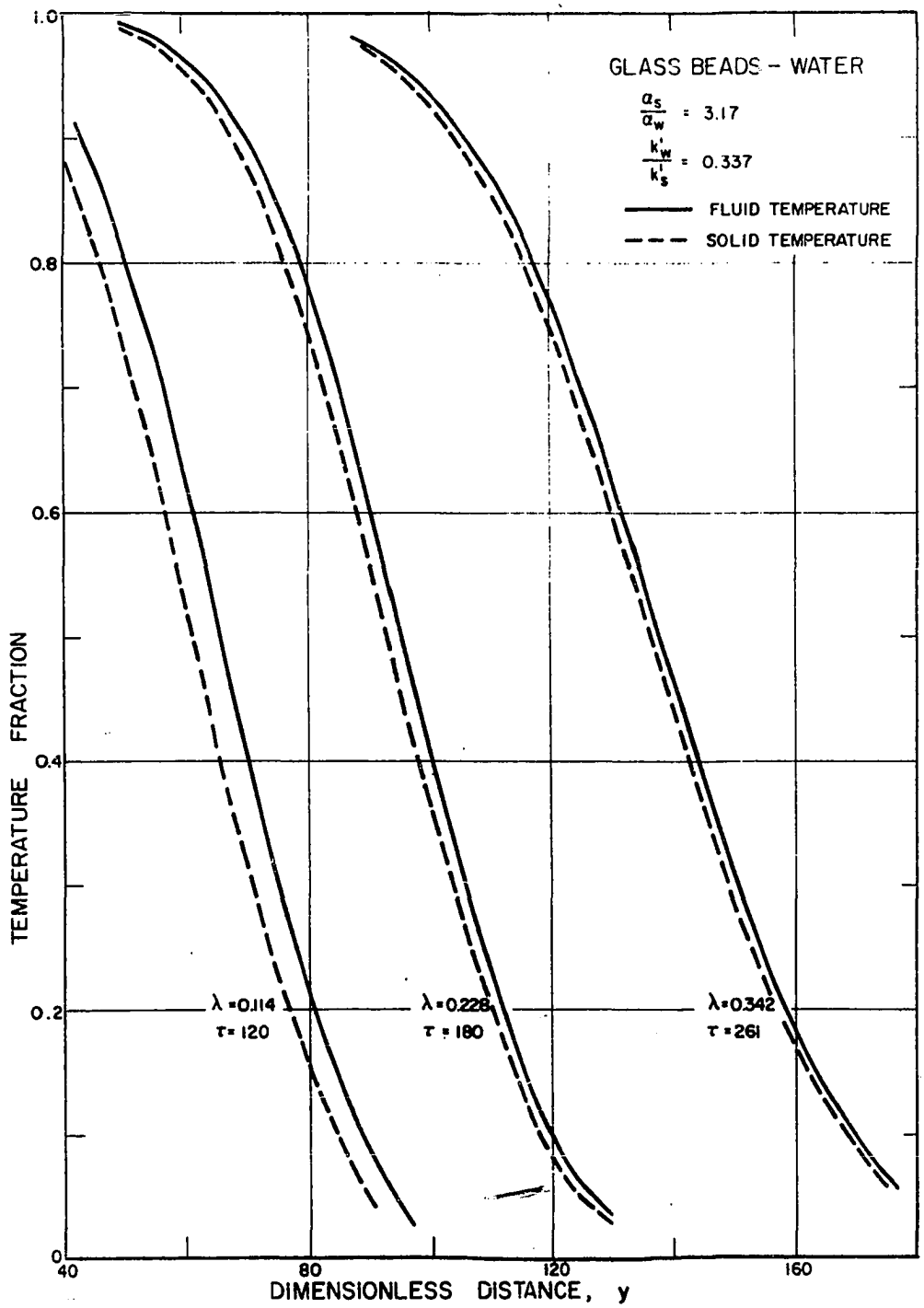

Figure 5- Fluid-Solid Temperature Differences; Effect of Dimensionless Parameter λ

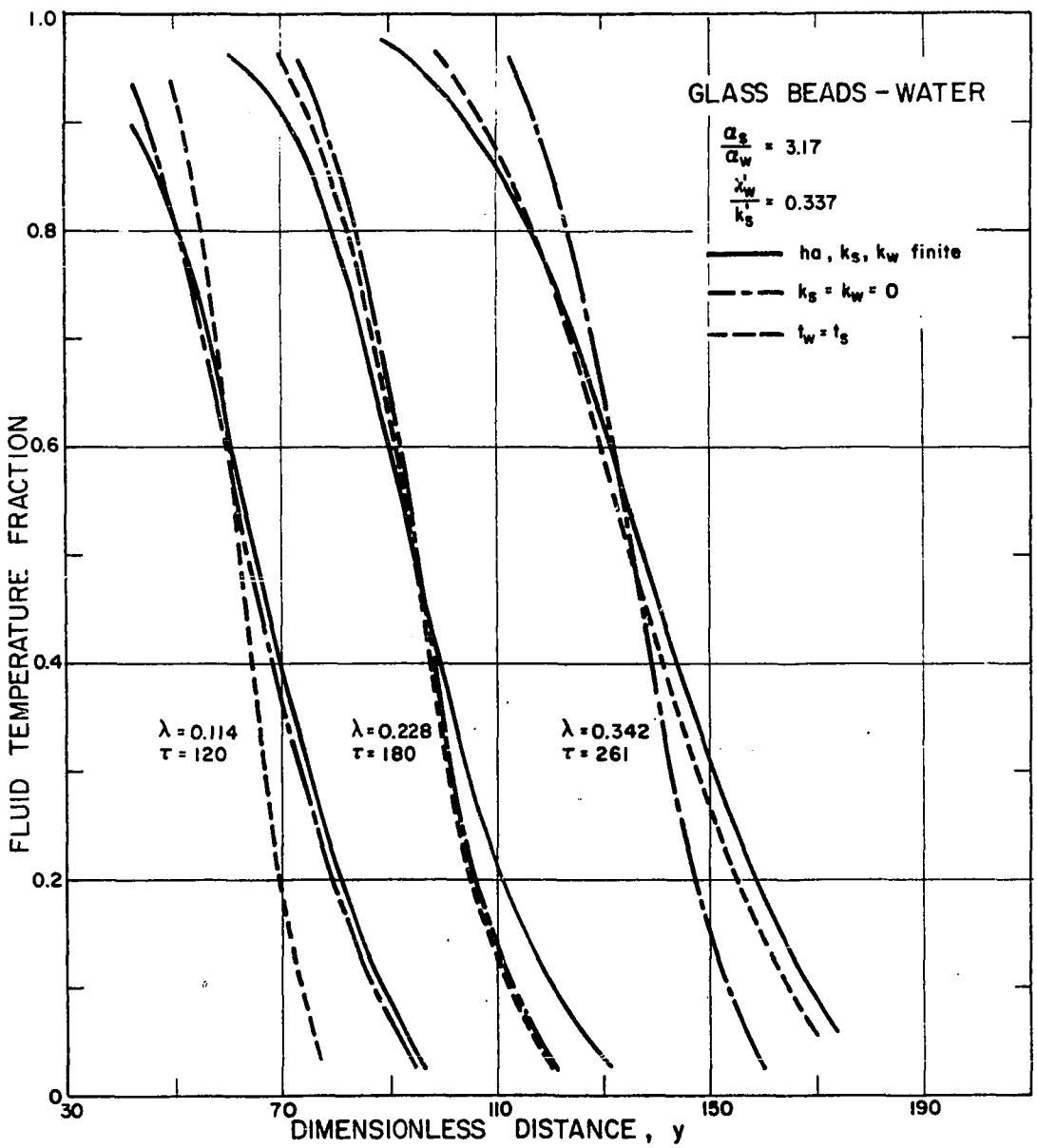

Figure 6- Approach of Generalized Numerical Solutions to Simplified Analytical Solutions; Dependence on Parameter λ

conduction case, where $t_w = t_s$, is $k_e = k_w\phi + k_s(1-\phi)$. At λ values of 0.114 or less for these liquid-solid systems, the numerical solution approaches the curve assuming $k_w = k_s = 0$ which indicates that the fluid-to-solid heat transfer is essentially controlling the profile shape. When λ is increased to 0.342 and above, the numerical solution approaches the analytical solution based on an assumption of $t_w = t_s$, i.e., the solid-fluid boundary resistance is neglibible. It is also shown in Figure 6 that in the intermediate λ range, both the heat-transfer coefficient and the thermal conductivity should be considered to accurately describe the temperature profiles.

Approximate Solution

The derivation of an approximate solution to Equations (III-1) and (III-2) follows the work of Klinkenberg and Sjenitzer (100), and Van Deemter et al. (175). Klinkenberg and Sjenitzer have shown that for a pulse input into a packed bed the heat-or mass-transfer mechanisms of molecular conduction, eddy dispersion, and convective transfer between phases all individually give rise to Gaussian distributions in the bed holding-time variable. This is true under certain conditions of bed parameters. They postulate that when these transport mechanisms act simultaneously in a system, the distribution of holding times is still normal and the individual variances may be simply additive. Van Deemter et al. arrived at the same conclusion by starting with the solution to the

differential equations which include both a diffusivity term in the fluid phase and a finite rate of heat transfer between phases. The solution, with the boundary condition of a pulse input, was reduced to a simplified form which is Gaussian and in which the variances for the two mechanisms of conduction and convective transfer between phases are additive.

It will first be shown that the different heat-transfer mechanisms, treated separately, give rise to normal distributions. The individual variances are then added to yield an approximate solution for the case of multi-mechanistic heat transfer. The work of Van Deemter et al. justifying this addition for a special case is outlined. Finally, the numerical solution to Equations (III-1) and (III-2) is used to further support the application of this assumption to the model considered here.

Convergence to Normal Distribution

Conduction. If it is assumed that at every point in the porous media, $t_w = t_s$, i.e., ha = ∞, and that eddy dispersion is negligible, then Equations (III-1) and (III-2) may be combined to yield

$$\left[\rho_w C_w \phi + \rho_s C_s (1-\phi)\right] \frac{\partial T}{\partial \theta} = -v\, \rho_w C_w \phi \frac{\partial T}{\partial x} + k_e^{o} \frac{\partial^2 T}{\partial x^2} \qquad \text{(III-7)}$$

where k_e^{o} is the static thermal conductivity of the bed,

$$k_e^{o} = k_s(1-\phi) + k_{wc}\phi \qquad \text{(III-8)}$$

As previously discussed, Equation (II-23), Jenkins and

Aronofsky (92) give as the solution to Equation (III-7) with a step-function temperature input and constant initial temperature throughout,

$$t = \frac{1}{2}\,\mathrm{erfc}\left[\frac{1}{2\sqrt{K^o}}\left(\frac{x}{\sqrt{\theta}} - V_F\sqrt{\theta}\right)\right] + \frac{1}{2}\,e^{x\rho_w C_w \phi v/k_e{}^o}\,\mathrm{erfc}\left[\frac{1}{2\sqrt{K^o}}\left(\frac{x}{\sqrt{\theta}} + V_F\sqrt{\theta}\right)\right] \qquad \text{(III-9)}$$

where $K^o = \dfrac{k_e{}^o}{\rho_w C_w \phi + \rho_s C_s (1-\phi)}$.

Now, rather than a step temperature or energy input, consider an energy input over only a very small increment of time θ_o. That is, with the porous medium initially at T_o and the injected fluid temperature at T_o, introduce a pulse of fluid at temperature T_i over the time interval θ_o, at $\theta = 0$. The resulting temperature distribution in the porous media, $T(x,\theta)$, as a result of this input may be derived by differentiating Equation (III-9) to give

$$\frac{t}{\theta_o} = \left[\frac{V_F}{4\sqrt{\pi K^o\theta}} + \frac{x}{4\sqrt{\pi K^o\theta^3}}\right]\exp\left[-\left(\frac{x-V_F\theta}{2\sqrt{K^o\theta}}\right)^2\right] - \left[\frac{V_F}{4\sqrt{\pi K^o\theta}} - \frac{x}{4\sqrt{\pi K^o\theta^3}}\right]\exp\left[-\left(\frac{x+V_F\theta}{2\sqrt{K^o\theta}}\right)^2 + \frac{xv\rho_w C_w\phi}{k_e{}^o}\right] \qquad \text{(III-10)}$$

Equation (III-10) may be simplified. If it is assumed that all energy-retention times in the bed are close to the mean time of $\frac{x}{V_F}$, then θ may be replaced by $\frac{x}{V_F}$ in all terms <u>except</u> the numerators of the exponent arguments. With this assumption, the second term of Equation (III-10) is eliminated

and the resulting simplified expression is a normal distribution.

$$\frac{t}{\theta_o} = \frac{1}{\sqrt{2\pi}\,\sigma_1} \exp\left[\frac{-(\frac{x}{V_F} - \theta)^2}{2\ \sigma_1^2}\right] \qquad \text{(III-11)}$$

where

$$\sigma^2_1 = \frac{2K^o x}{V_F^3} = \frac{2\ k_e{}^o x}{\rho_w C_w \phi v V_F^2} \qquad \text{(III-12)}$$

Plots of Equation (III-11), with a comparison to the complete expression, Equation (III-10), are shown in Figure 7. The necessary assumption for the substitution, $x/V_F = \theta$, as made, is

$$\frac{2\ K^o\ x}{V_F^3} \ll \left|\frac{x}{V_F}\right|^2 \qquad \text{(III-13)}$$

or

$$\frac{2\ k_e{}^o}{\rho_w C_w \phi v x} \ll 1 \qquad \text{(III-14)}$$

i.e., the "spread" in time of the temperature profile due to conduction is much less than the total time of travel of the heated zone.

Eddy Dispersion. Since the diffusion equation applies to eddy dispersion in porous media, the results of the simplification, Equation (III-11), are also applicable to this heat-transfer mechanism with $k_e{}^o$ replaced by $k_{wm}\phi$, the dispersion coefficient. However, as discussed by Aris and Amundson (4), the boundary condition

$$T = \text{constant}, \qquad x = 0, \qquad \theta > 0 \qquad \text{(III-15)}$$

used by Jenkins and Aronofsky in the derivation of Equation

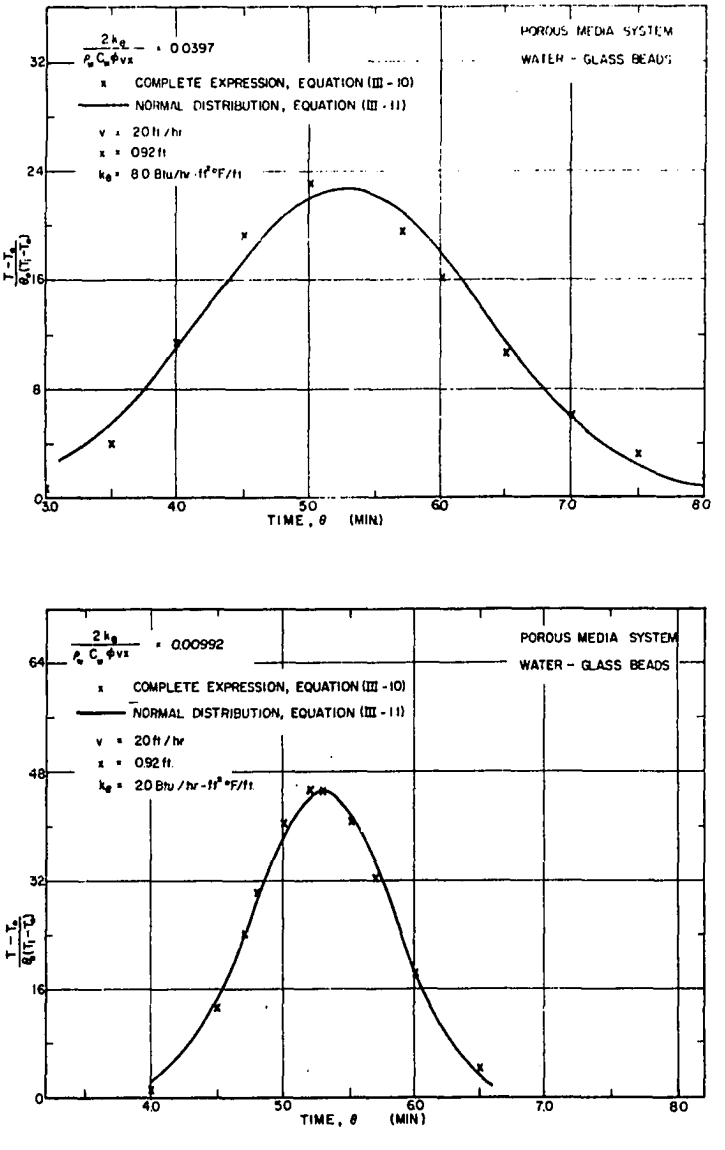

Figure 7 - Convergence of Conduction-Equation Solution to Normal Distribution

(III-9) is not strictly applicable to the eddy-dispersion case. With boundary condition (III-15), back diffusion of energy out of the bed is allowed, a condition which does not seem reasonable for eddy dispersion. The error introduced by use of this condition will be small for relatively small values of the thermal diffusivity, and this boundary condition will be assumed sufficiently accurate.

The condition for convergence to a normal distribution follows from Equation (III-14),

$$\frac{2\, k_{wm}\phi}{\rho_w C_w \phi v x} \ll 1 \qquad \text{(III-16)}$$

Finite Heat-Transfer Coefficient. When the heat transfer in a packed bed is controlled by the rate of transfer between solid and fluid, and conduction and eddy dispersion are negligible (ha = finite, $k_w = k_s = 0$), an energy balance gives

$$\rho_w C_w \phi \frac{\partial T_w}{\partial \theta} = - v \rho_w C_w \phi \frac{\partial T_w}{\partial x} - ha\,(T_w - T_s) \qquad \text{(III-17)}$$

$$\rho_s C_s (1-\phi) \frac{\partial T_s}{\partial \theta} = ha\,(T_w - T_s) \qquad \text{(III-18)}$$

The solution for the fluid phase with a step-function temperature input into a bed initially at constant temperature is (97)

$$t_w = \int_{\frac{x}{v}}^{\theta} \frac{ha}{\rho_s C_s (1-\phi)} \exp\left[\frac{-hax}{\rho_w C_w \phi v} - \frac{ha}{\rho_s C_s (1-\phi)}(\theta - x/v)\right] I_o\left[2\sqrt{\frac{(ha)^2 x\,(\theta - x/v)}{\rho_w C_w \phi v\ \rho_s C_s (1-\phi)}}\right] d\theta + \exp\left[\frac{-hax}{\rho_w C_w \phi v} - \frac{ha}{\rho_s C_s (1-\phi)}(\theta - x/v)\right] I_o\left[2\sqrt{\frac{(ha)^2 x\,(\theta - x/v)}{\rho_w C_w \phi v\ \rho_s C_s (1-\phi)}}\right] \qquad \text{(III-19)}$$

The corresponding solution for the injection of an energy pulse over a small time interval θ_o may be derived from Equation (III-19).

$$\frac{t_w}{\theta_o} = \frac{\exp\left[\frac{-hax}{\rho_w C_w \phi v} - \frac{ha}{\rho_s C_s (1-\phi)}(\theta - x/v)\right]}{\left[\rho_s C_s (1-\phi)\ 4\pi\ ha \sqrt{\frac{x(\theta-x/v)}{\rho_w C_w \phi v\ \ \rho_s C_s (1-\phi)}}\right]^{\frac{1}{2}}} \cdot \frac{\exp\left[2ha\sqrt{\frac{x(\theta-x/v)}{\rho_w C_w \phi v\ \ \rho_s C_s (1-\phi)}}\right]}{\left[x(\theta-x/v)\ \ \rho_w C_w \phi v\right]^{\frac{1}{2}}} \qquad \text{(III-20)}$$

The asymptotic expansion for the Bessel function has been used, implying

$$2\left[\frac{(ha)^2\, x\,(\theta - x/v)}{\rho_w C_w \phi v\ \ \rho_s C_s (1-\phi)}\right]^{\frac{1}{2}} \approx \frac{2\ ha\ x}{\rho_w C_w \phi v} \gg 1 \qquad \text{(III-21)}$$

Equation (III-20) may be simplified as previously done in the conduction case by the substitution of $\theta = \frac{x}{V_F}$ in all terms but the numerator of the exponent. Details are given in Appendix C. The result is the Gaussian distribution

$$\frac{t_w}{\theta_o} = \frac{1}{\sqrt{2\pi}\ \ \sigma_2} \exp\left[\frac{-(x/V_F - \theta)^2}{2\ \sigma_2^{\,2}}\right] \qquad \text{(III-22)}$$

where

$$\sigma_2^{\,2} = \frac{2\ x\ \left[\rho_s C_s (1-\phi)\right]^2}{\rho_w C_w \phi\ v\ ha} \qquad \text{(III-23)}$$

The assumption leading to the substitution $\theta = x/V_F$ is

$$\frac{2x\ \left[\rho_s C_s (1-\phi)\right]^2}{ha\ \ \rho_w C_w \phi\ v} \ll \left(\frac{x}{V_F}\right)^2 \qquad \text{(III-24)}$$

or
$$\frac{2V_F^2 \left[\rho_s C_s(1-\phi)\right]^2}{ha \ \rho_w C_w \phi \ v \ x} \ll 1 \qquad \text{(III-25)}$$

The spread of the injected thermal-energy pulse is much less than the total time of travel in the bed. It is noted that Equation (III-25) is always satisfied if condition (III-21) holds since the former may be rearranged to give

$$\frac{4 \left[\frac{\rho_s C_s(1-\phi)}{\rho_w C_w \phi + \rho_s C_s(1-\phi)}\right]^2}{2 \frac{ha \ x}{\rho_w C_w \bar{v}}} \ll 1 \qquad \text{(III-26)}$$

Addition of Variances

Klinkenberg and Sjenitzer (100) have proposed that when the different heat-transfer mechanisms act simultaneously, and conditions are such that each would approach a Gaussian curve, individual variances are simply additive. This assumption results in the following approximate solution with a pulse thermal-energy input into a packed bed.

$$\frac{t_w}{\theta_o} = \frac{1}{\sqrt{2 \ \Pi \ \sigma^2}} \exp\left[\frac{-\left|\frac{x}{V_F} - \theta\right|^2}{2 \ \sigma^2}\right] \qquad \text{(III-27)}$$

with

$$\sigma^2 = \sigma_1^2 + \sigma_2^2 + \sigma_3^2 + \ldots\ldots \qquad \text{(III-28)}$$

For the specific mechanisms considered here,

$$\sigma^2 = \frac{2 \ k_e^o \ x}{\rho_w C_w \phi v \ V_F^2} + \frac{2 \ k_{wm} \phi \ x}{\rho_w C_w \phi v \ V_F^2} + \frac{2 \left[\rho_s C_s(1-\phi)\right]^2 x}{\rho_w C_w \phi \ v \ ha} \qquad \text{(III-29)}$$

where k_e^o is the bed "static" thermal conductivity

$\left[k_e^{\circ} = k_{wc}\phi + k_s(1-\phi)\right]$, and $k_{wm}\phi$ is the eddy-dispersion coefficient. From Equation (III-29), it is seen that an "apparent" longitudinal effective conductivity for the heat-transfer-coefficient contribution to the dispersion may be defined as

$$k_{ha} = \frac{V_F^2 \left[\rho_s C_s(1-\phi)\right]^2}{ha} \qquad \text{(III-30)}$$

reducing Equation (III-29) to

$$\sigma^2 = \frac{2x\ (k_e^{\circ} + k_{wm}\phi + k_{ha})}{\rho_w C_w \phi\ v\ V_F^2} \qquad \text{(III-31)}$$

Thus, an overall effective thermal conductivity, k_e, is defined

$$k_e = k_e^{\circ} + k_{wm}\phi + k_{ha} \qquad \text{(III-32)}$$

Equations (III-27) and (III-28) are based on the general principle of probability theory that the variance of the sum of two or more statistically independent random variables is the sum of the individual variances (5). Use of these equations therefore assumes that the different heat-transfer mechanisms act independently, and that the spread of thermal-energy, bed-holding times away from the mean time, x/V_F, is the sum of the spreads due to each mechanism taken separately.

The corresponding form of the solution for a step-function temperature input is

$$t_w = \frac{1}{2}\left[1 - \operatorname{erf}\left(\frac{\frac{x}{V_F} - \theta}{\sqrt{2\ \sigma^2}}\right)\right] \qquad \text{(III-33)}$$

Rearrangement of the error-function argument leads to

$$t_w = \frac{1}{2}\left[1 - \text{erf}\left(\frac{x - V_F\theta}{\sigma^*\sqrt{2\theta}}\right)\right] \qquad \text{(III-34)}$$

where

$$\sigma^* = \sqrt{2K} \qquad \text{(III-35)}$$

$$K = \frac{k_e^{\,o} + k_{wm}\phi + k_{ha}}{\rho_w C_w \phi + \rho_s C_s(1-\phi)} = \frac{k_e}{\rho_w C_w \phi + \rho_s C_s(1-\phi)} \qquad \text{(III-36)}$$

and where θ has been re-substituted for x/V_F in the denominator of the error function. Equation (III-34) is the first term of the conduction-equation solution, Equation (III-9), with $k_e^{\,o}$ replaced by k_e.

Van Deemter et al., Summation of Variances

The work of Van Deemter et al. (175) adds strong justification to the assumption of added variances. These results are outlined in brief here and in detail in Appendix D.

The heat-transfer mechanisms affecting the longitudinal dispersion are (1) conduction and eddy dispersion in the fluid phase, and(2) a finite rate of heat transfer between the solid and fluid phases. From an energy balance, the describing differential equations are

$$\rho_w C_w \phi \frac{\partial T_w}{\partial \theta} = - v\, \rho_w C_w \phi \frac{\partial T_w}{\partial x} + k_w \phi \frac{\partial^2 T_w}{\partial x^2} - ha\,(T_w - T_s) \qquad \text{(III-37)}$$

$$\rho_s C_s (1-\phi) \frac{\partial T_s}{\partial \theta} = ha\,(T_w - T_s) \qquad \text{(III-38)}$$

The solution corresponding to the injection of an energy pulse $\left[\rho_w C_w \phi\, v\,(T_i - T_o)\,\theta_o\right]$, over the small time increment θ_o, into

a bed initially at temperature T_o, is given by Van Deemter et al. and was derived from a solution of Lapidus and Amundson (110).

$$\frac{t_w}{\theta_o} = \frac{x}{2\theta\sqrt{\Pi\, a_w \theta}} \exp\left[\frac{-(x-v\theta)^2}{4\, a_w \theta} - \frac{ha\,\theta}{\rho_w C_w \phi}\right] + \int_o^\theta \frac{x}{2z\sqrt{\Pi\, a_w z}} \exp\left[\frac{-(x-vz)^2}{4 a_w z}\right] F(z)\, dz \qquad \text{(III-39)}$$

where

$$F(z) = \left[\frac{(ha)^2 z}{\rho_w C_w \phi\, \rho_s C_s (1-\phi)(\theta-z)}\right]^{\frac{1}{2}} \exp\left[\frac{-ha\,(\theta-z)}{\rho_s C_s (1-\phi)} - \frac{ha\, z}{\rho_w C_w \phi}\right] I_1\left[2\sqrt{\frac{(ha)^2 z\,(\theta-z)}{\rho_w C_w \phi\, \rho_s C_s (1-\phi)}}\right] \qquad \text{(III-40)}$$

Simplification of these equations by use of the asymptotic expansion for the Bessel function and substitution for θ, $\theta = x/V_F$, in all terms but the numerators of exponents yields

$$\frac{t_w}{\theta_o} = \beta \int_o^\theta \frac{1}{\sigma_1\sqrt{2\,\Pi}} \exp\left[\frac{-\left(\frac{x}{V_F} - \frac{z}{\beta}\right)^2}{2\,\sigma_1^2}\right] \frac{1}{\sigma_2\sqrt{2\Pi}} \exp\left[\frac{-\left(\theta - \frac{z}{\beta}\right)^2}{2\,\sigma_2^2}\right] dz \qquad \text{(III-41)}$$

where: $\beta = \dfrac{\rho_w C_w \phi}{\rho_w C_w \phi + \rho_s C_s (1-\phi)}$, σ_1^2 was previously defined in Equation (III-12) with $k_w\phi$ replacing k_e^o, and σ_2^2 was defined in Equation (III-23). This integral may be approximated to give as a final expression

$$\frac{t_w}{\theta_o} = \frac{1}{\sqrt{2\pi(\sigma_1^2 + \sigma_2^2)}} \exp\left[\frac{-(\frac{x}{V_F} - \theta)^2}{2(\sigma_1^2+\sigma_2^2)}\right] \quad \text{(III-42)}$$

The solution has therefore been simplified to a form which is Gaussian and in which the variances for the heat-transfer mechanisms considered are summed.

Numerical Solution to the General Equations, Summation of Variances

It is proposed that the general equations, Equations (III-1) and (III-2), may be approximated by the conduction equation, Equation (III-7), in which, k_e^o is replaced by k_e, given by

$$k_e = k_e^o + k_{wm}\phi + k_{ha} \quad \text{(III-32)}$$

where k_{ha} was defined in Equation (III-30). The previously discussed numerical solutions to these general equations show that the addition of conductivities (equivalent to addition of variances) is justifiable under the conditions (III-14), (III-16) and (III-25). This is demonstrated in the following by first determining an effective conductivity, k_e, representative of the numerical solution. This k_e calculated from the numerical data (termed $k_{e(num)}$) is then shown to agree with the summed effective conductivity, i.e., Equation (III-32).

Numerical Solution, Effective Thermal Conductivity. For specific system parameter values, the numerical solution yields the fluid temperature, t_w, as a function of x and θ, and this

temperature profile may be approximated by the use of the conduction-equation solution, Equation (III-9), with the proper value of $k_{e(num)}$. Several methods of calculating $k_{e(num)}$ from temperature profiles are available and these are discussed by Preston (138). The procedure used here is to determine $k_{e(num)}$ from the "spread" or variance of the temperature profile.

Preston (138) developed an approximation to the second term of Equation (III-9) by using an expansion for the error function. Define the second term of the solution as R.

$$R = \frac{1}{2} e^{\rho_w C_w \phi v x / k_e} \left[1 - \operatorname{erf} \frac{1}{2\sqrt{K}} \left(\frac{x}{\sqrt{\theta}} + V_F \sqrt{\theta} \right) \right] \quad \text{(III-43)}$$

Then by Preston's simplification, for values of the error-function argument greater than 3.0,

$$R = \frac{e^{(z-w^2)}}{2w\sqrt{\pi}} \quad \text{(III-44)}$$

where $z = \dfrac{xv\,\rho_w C_w \phi}{k_e}$, and $w = \dfrac{1}{2\sqrt{K}} \left(\dfrac{x}{\sqrt{\theta}} + V_F \sqrt{\theta} \right) = \dfrac{A}{2\sqrt{K}}$.

The error in this approximation is about 5% of R at $A/2\sqrt{K}$ values of 3.0 and the error decreases as $A/2\sqrt{K}$ increases. The maximum value of R was determined by Preston to be

$$R_{max} = \frac{1}{2} \sqrt{\frac{k_e}{\pi\, \rho_w C_w \phi\, v\, x}} \quad \text{(III-45)}$$

Comparison of R_{max} to conditions (III-14), (III-16), and (III-25) shows that when these conditions are satisfied R_{max} is necessarily small. In the calculations performed here, the

contribution of R to the total was generally less than 0.03, and as shown in Appendix E, R values of this magnitude can be neglected with only a small error introduced into the calculated $k_{e(num)}$ value. Equation (III-9) therefore reduces to the simplified form

$$t_w = \frac{1}{2}\left[1 - \text{erf}\left(\frac{x/V_F - \theta}{\sigma^* \sqrt{2\theta}}\right)\right] \qquad \text{(III-34)}$$

or defining

$$F = \frac{x}{\sqrt{\theta}} - V_F \sqrt{\theta} \qquad \text{(III-46)}$$

$$t_w = \frac{1}{2}\left[1 - \text{erf}\frac{F}{2\sqrt{K}}\right] \qquad \text{(III-47)}$$

where $\sigma^* = \sqrt{2K}$ and $K = \dfrac{k_{e(num)}}{\rho_w C_w \phi + \rho_s C_s (1-\phi)}$.

An effective thermal conductivity, $k_{e(num)}$, is now calculated for a numerical solution as follows. A plot of t_w vs. F is made on probability paper, at constant θ or constant x, with t_w being plotted on the probability scale. This graph paper gives a linear representation of the function

$$y = \frac{1}{2}\left[1 - \text{erf } bx\right] \qquad \text{(III-48)}$$

where y and x are dependent and independent variables and b is a constant. The best straight line is therefore drawn through the plotted points. At $t_w = .16$, Equation (III-34) reads

$$-.68 = -\text{erf}\frac{F_{t=.16}}{2\sqrt{K}} \qquad \text{(III-49)}$$

and from error-function tables,

$$\frac{F_{t=.16}}{2\sqrt{K}} = + .7032 \qquad \text{(III-50)}$$

At $t_w = .84$

$$.68 = - \operatorname{erf} \frac{F_{t=.84}}{2\sqrt{K}} \qquad \text{(III-51)}$$

and

$$\frac{F_{t=.84}}{2\sqrt{K}} = - .7032 \qquad \text{(III-52)}$$

If the error-function arguments are subtracted,

$$1.406 = \frac{1}{2\sqrt{K}} \left[F_{t=.16} - F_{t=.84} \right] \qquad \text{(III-53)}$$

or

$$F_{t=.16} - F_{t=.84} = 2 \sigma^* \qquad \text{(III-54)}$$

Thus,

$$K = \frac{1}{7.897} \left[F_{t=.16} - F_{t=.84} \right]^2 \qquad \text{(III-55)}$$

A plot of t_w vs. F on probability paper for one of the numerical calculations is shown in Figure 8. This method determines a $k_{e(num)}$ which will give excellent agreement in temperature-profile shape between the numerical solution and Equation (III-34). However, the two solutions will not coincide completely. That is, if the numerical temperature profile and Equation (III-34) with the calculated $k_{e(num)}$ are plotted on linear graph paper (Figure 9), there will be a small displacement between the curves along the x or θ axis. This is because the numerical solution, at these values of x and θ, and the conduction-equation solution have not completely converged. Continuation of numerical calculations to large x and θ values was impractical because of the time necessary for the calculation. It was indicated in the numerical results that, as long

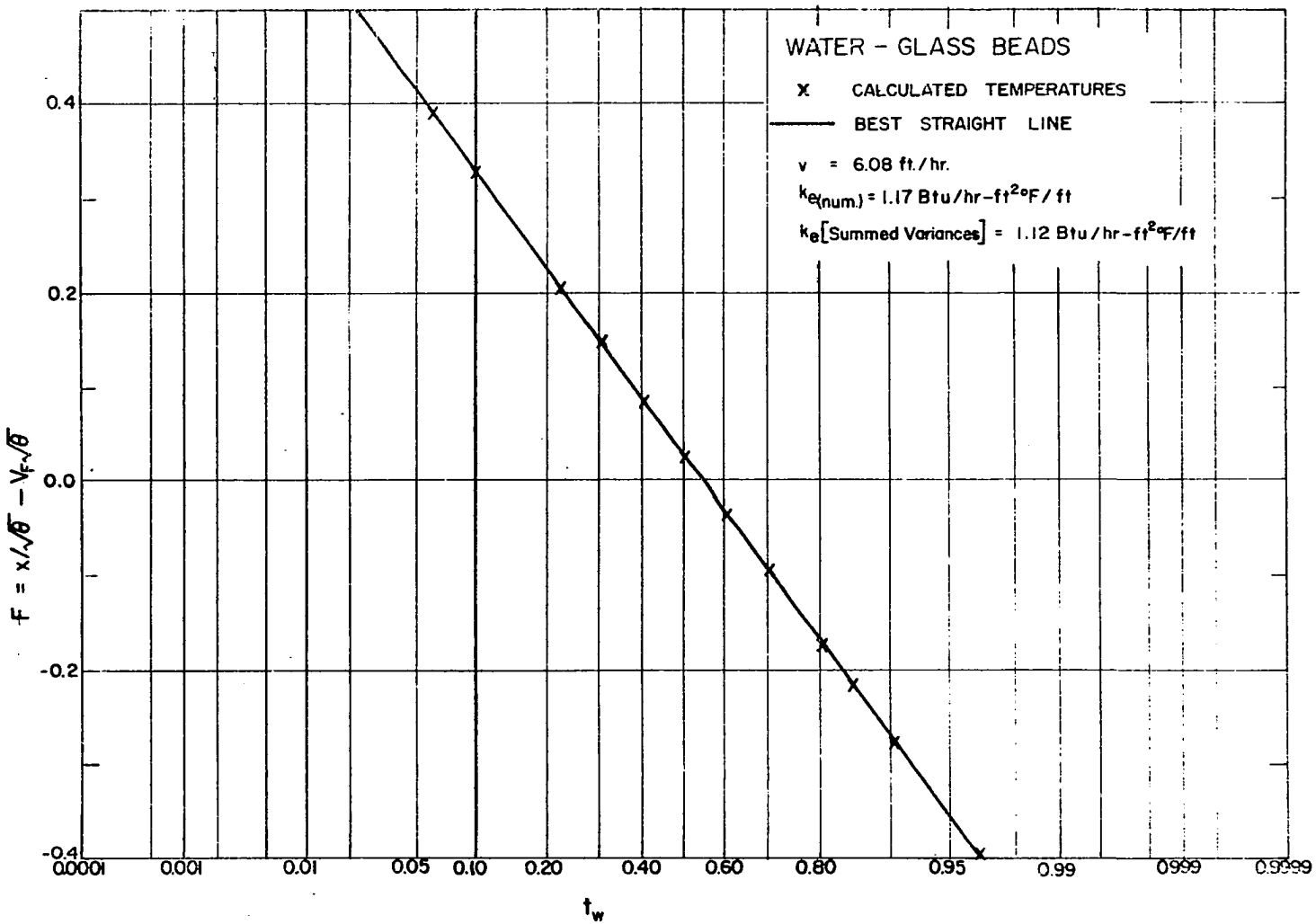

Figure 8- Numerical Solution; Calculation of $k_{e(num)}$

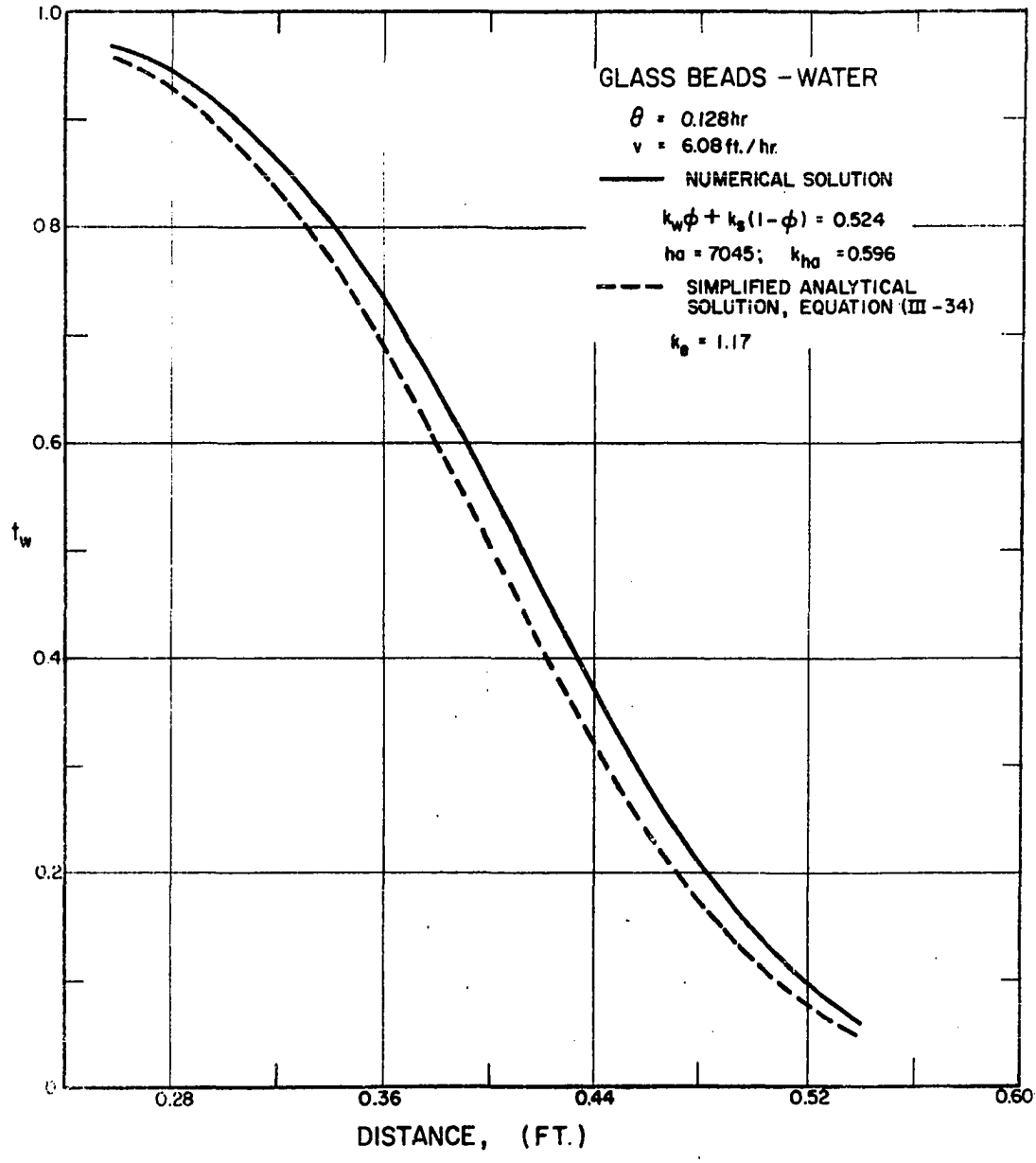

Figure 9- Comparison of Numerical Solution and Conduction-Equation Solution

as conditions (III-14), (III-16), and (III-25) were satisfied, the above procedure was satisfactory for the estimation of $k_{e(num)}$ values from the numerically calculated temperature profiles. A sample calculation of $k_{e(num)}$ is shown in Appendix F.

Summation of Conductivities. The effective conductivities for the numerical solutions are now estimated assuming the variances for the individual mechanisms are additive,

$$k_e = k_e^{\circ} + k_{wm}\phi + k_{ha} \qquad \text{(III-32)}$$

where, for a given numerical solution, the individual k's are determined from the parameter values of the numerical calculation. That is,

$$k_e = k_s(1-\phi) + k_w\phi + \frac{V_F^2 \left[\rho_s C_s(1-\phi)\right]^2}{ha} \qquad \text{(III-56)}$$

where the terms on the right hand side of the equation are the quantities used in the numerical solution. The validity of Equation (III-56) may be checked by comparing this k_e to the $k_{e(num)}$ determined from the corresponding temperature profile. The results of these calculations for several numerical solutions are shown in Table 1 where the difference is generally less than about 8.0%. System parameter sizes, as well as the approach to conditions (III-14), (III-16), and (III-25) are also included in the table.

These results indicate, for the conditions specified, that the solution to Equations (III-1) and (III-2) may be

TABLE 1

NUMERICAL SOLUTIONS - EFFECTIVE THERMAL CONDUCTIVITIES

λ	$\frac{\alpha_w}{\alpha_s}$	$\frac{k_w \phi}{k_s(1-\phi)}$	$k_w\phi+k_s(1-\phi)$	k_{ha}	k_e Summed Variances	$k_{e(num)}$	% Difference	At t=.5;* $\frac{2\left[k_w\phi+k_s(1-\phi)\right]}{\rho_w C_w \phi\ v\ x}$	At t=.5;‡ $\frac{2V_F^2\left[\rho_s C_s(1-\phi)\right]^2}{ha\ \rho_w C_w \phi\ v}$
.114	.316	.337	.524	2.38	2.90	3.04	4.7	.0095	.042
.228	.316	.337	.524	.596	1.12	1.17	4.4	.024	.022
.500	.316	.337	.524	.124	.648	.686	5.7	.053	.0125
.342	.169	.231	.809	.657	1.04	1.07	2.8	.043	.0179
.228	1.48	1.20	.242	.775	1.02	1.09	6.6	.024	.060
.342	.0779	.106	1.58	.23	1.81	1.73	4.5	.136	.027
.167	.123	.167	1.67	1.53	3.20	2.95	8.1	.045	.097
.520	2.44	1.57	.524	.438	.962	1.04	8.0	.085	.071
.398	1.43	.922	.392	.439	.831	.900	8.0	.055	.063

*Condition (III-14) and (III-16) combined.

‡Condition III-25

approximated by the conduction equation in which the variances for the different heat-transfer mechanisms are simply additive. Since this conclusion was made from specific numerical calculations, its generality has not been shown.

Improved Approximate Solution

An improved approximate solution to Equations (III-1) and (III-2) was found in which the displacement between the approximation and the numerical solution (previously discussed, see Figure 9) was essentially eliminated. This equation is presented in Appendix G. The solution was checked against the numerical calculations for several systems and agreement was good, although its generality has not been ascertained.

Summary

Numerical solutions to Equations (III-1) and (III-2) were obtained. Because it was necessary to use small increment sizes in these calculations, the computing time necessary to run the solutions out to x and θ values of interest was prohibitive. An approximate solution to Equations (III-1) and (III-2) was developed utilizing the previous work of Klinkenberg and Sjenitzer (100) and Van Deemter et al. (175). This approximation is based on the supposition that the different heat-transfer mechanisms are independent, at least for statistical purposes, and therefore, the individual variances are additive. With this assumption, Equations (III-1) and (III-2) may be adequately represented by the conduction equation

(III-7) where k_e is the sum of the different contributing conductivities. Equation (III-34) is the applicable form of the solution for a step-function temperature input. The approximate solution was checked through use of the numerical solutions and was found to be satisfactory. Necessary conditions for the use of Equation (III-34) were given as Equations (III-14), (III-16), and (III-25).

In the following chapters, the approximate solution is checked experimentally. Effective conductivities are calculated from experimental data using Equation (III-34). These k_e values are assumed to be the sum of the molecular-conduction, eddy-dispersion, and heat-transfer coefficient contributions, and conductivities are determined for each mechanism. The conductivities obtained from the data are shown to be consistent with available literature data.

CHAPTER IV

EXPERIMENTAL INVESTIGATION

The experimental model was designed to simulate the basic requirements of the real physical system. The main requirements were:

(a) Piston flow of a liquid in one direction (axial) through a homogeneous packed bed.

(b) The establishment of a known initial constant temperature throughout the bed.

(c) The introduction of a step function in temperature into one end of the bed.

(d) The measurement of the response temperature profile at a known position down the bed.

(e) Negligible heat losses in the direction perpendicular (radial) to the fluid flow.

Early considerations indicated that a design similar to that used by Preston (138) and Hadidi (76) would be satisfactory. The heat-transfer section in these investigations consisted of a homogeneous packed bed of particles contained in a thin-walled, insulated, cylindrical tube. An open-volume section immediately above the bed face served to distribute

the flow evenly across the pack. A step-function temperature input was approximated by first bringing the bed to a desired temperature, T_o, using the test liquid as heating media. Then, the entrance-face temperature was quickly changed by "flushing out" the open volume above the bed with liquid at the different input temperature, T_i. These design concepts were followed in this work.

Experimental Apparatus

Flow System

A schematic diagram of the flow system is shown in Figure 10. Fluid storage was in an 8 gallon closed tank. Flow rates through the system were controlled by regulated air pressure on the liquid in the storage tank. Liquid leaving the storage passed through a rotameter (C). To maintain constant volumetric flow rates during an experimental run, a setting on this meter was held by manually adjusting the storage pressure.

To preheat the liquid, it was passed through the heat-transfer coils in two heating baths in series. Water was used as the heating media. In the first bath, a crude temperature control was maintained with the test liquid being heated to within a few degrees of the final temperature. The heat source was a 1000 watt immersion heater (D) which contained its own thermostat. The second bath maintained a fine temperature control ($\pm 0.1^{\circ}F$) and brought the liquid entering the packed

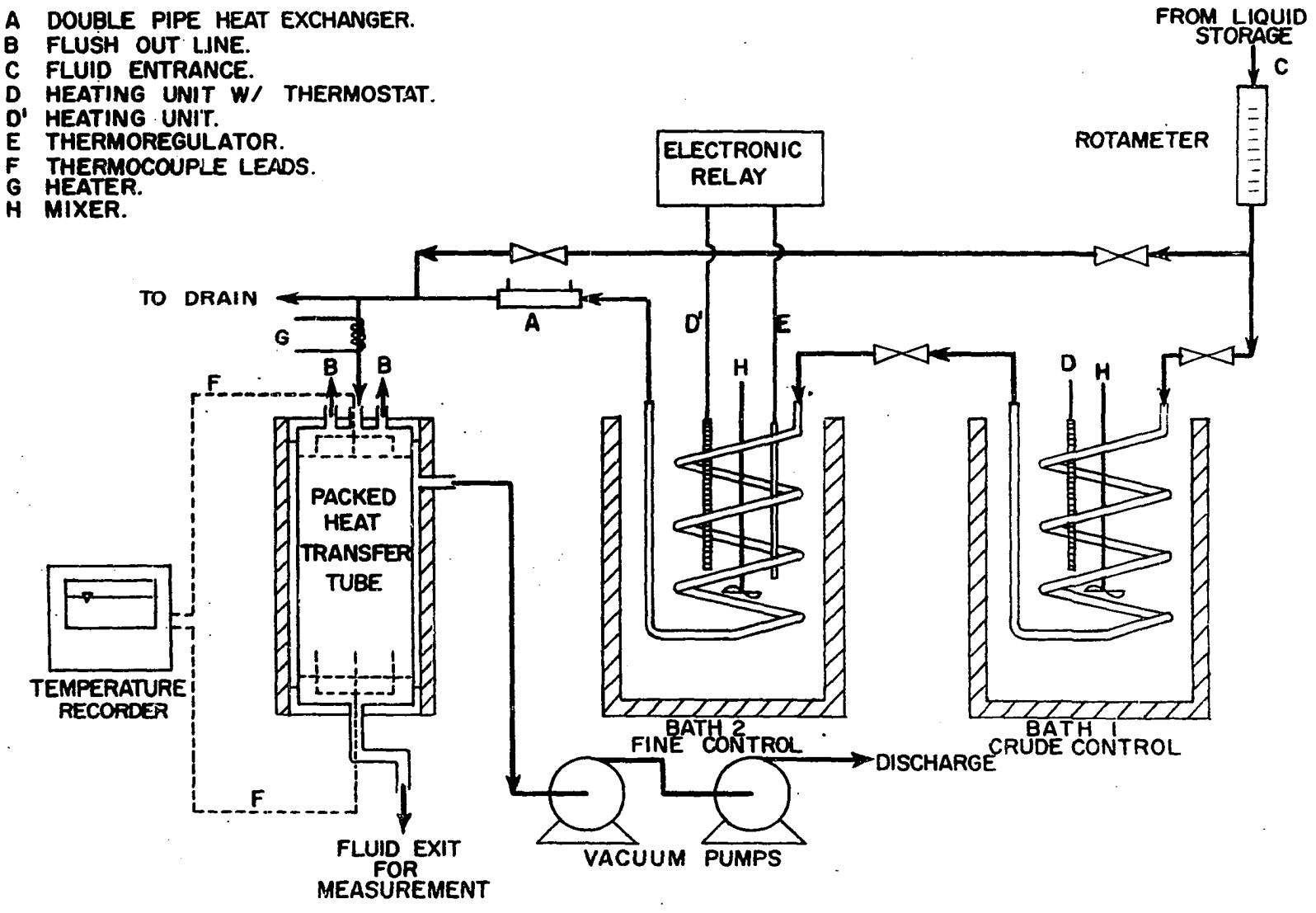

Figure 10- Flow System

tube to a set temperature level. The control in this second bath consisted of a mercury temperature regulator (E) and an electronic relay in conjunction with electric immersion heaters (D).

The test liquid went directly from the heating baths to the packed-bed test section. To reduce heat losses between the temperature baths and the test cell, a double-pipe heat exchanger insulated the flow line (A). Hot water from the second constant-temperature bath was circulated through the annulus of this exchanger.

When the test liquid was not preheated, it went immediately from the flow meter (C) to the test cell, by-passing the heating baths. With a constant flow rate, the temperature at the entrance to the cell was found to hold steady ($\pm 0.1^{\circ}F$) over the time of an experimental run.

A small resistance heater (G), manually controlled by means of a rheostat, was wound around the liquid flow line just above the cell entrance. The need for this heater is discussed later. When desired, the packed bed could be by-passed by closing the exit flow line and opening the flush-out line (B) from the entrance cap. Provision was made to catch timed samples of the packed-bed effluent in order to determine volumetric flow rates.

Temperatures were measured using iron-constantan thermocouples and a Minneapolis-Honeywell multipoint temperature recorder (Y 153 x 87-C-11-111-106-8-B-V). Up to 24 separate

points could be recorded during a given run, however, a maximum of six were used in this work. Print speed was two seconds per point, with a recording chart speed of one inch per minute. The temperature range was 60 to 220°F. The chart was graduated at 1.0°F and temperature recordings could easily be read to 0.2°F. Both 30 and 24 gauge, spun-glass insulated thermocouples were used. In order to obtain small thermocouple beads, an electric arc was made to form the wire junctions.

Test Cell

More detailed sketches of the test cell are shown in Figures (11), (12), (13), and (14), and a photograph in Figure (15). The packed bed, consisting of solid spheres, was held in a cylindrical metal container which was 3.66±.01 inches ID and 13.67 inches in length (including threaded end pieces). The spheres were held in place between two end retaining screens, each of which was composed of a 200 mesh over an 18 mesh screen. The outlet retaining screen was soldered permanently in place while the entrance screen was fixed using Armstrong A-1 adhesive (Armstrong Company, Warsaw, Indiana).

The wall of the packed bed was made of 0.010 inch stainless steel sheet formed into a cylindrical shape and soldered at the seam. Threaded end pieces were soldered to the tube. The thinness of the tube resulted both in a low wall heat capacity and small heat conduction down the tube in the direction of fluid flow. The heat capacity of the tube

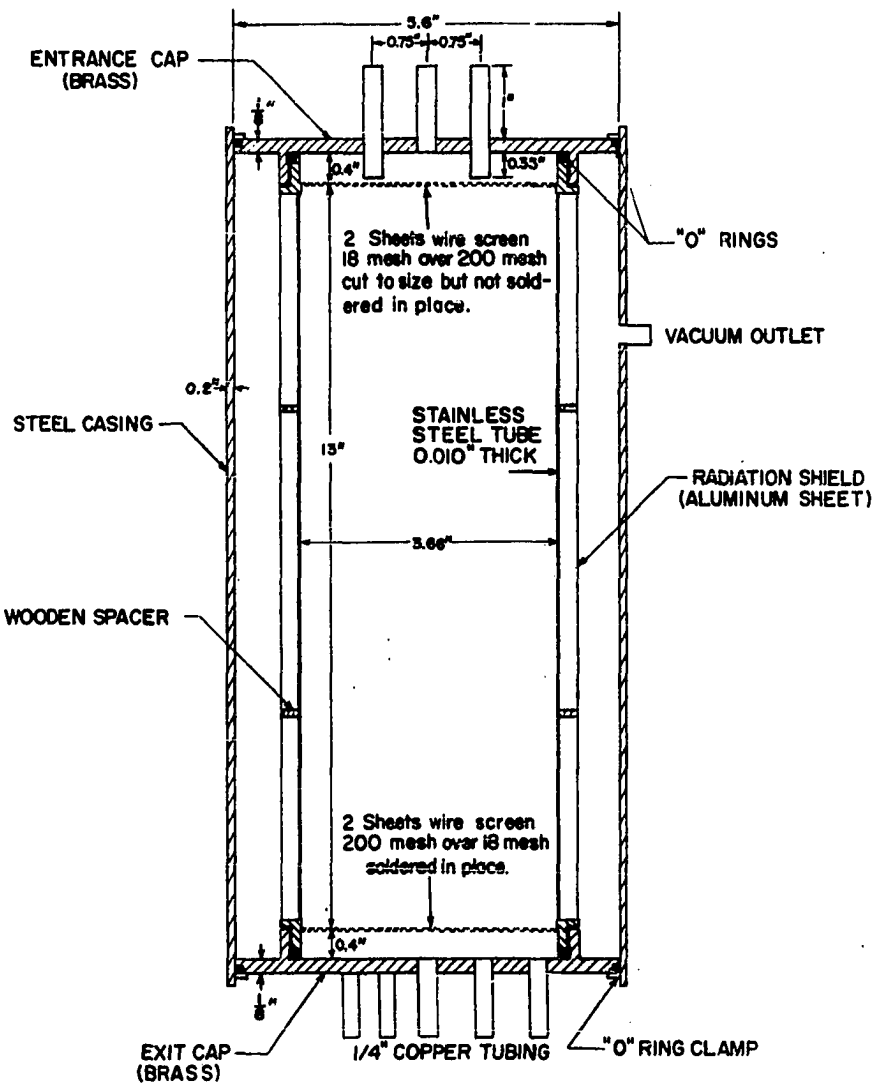

Figure 11- Test Cell

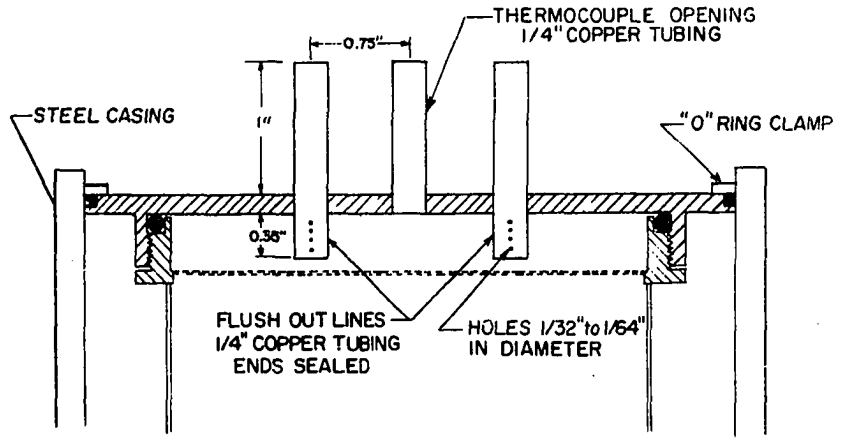

ENTRANCE CAP
FLUSH OUT LINES AND THERMOCOUPLE OPENING

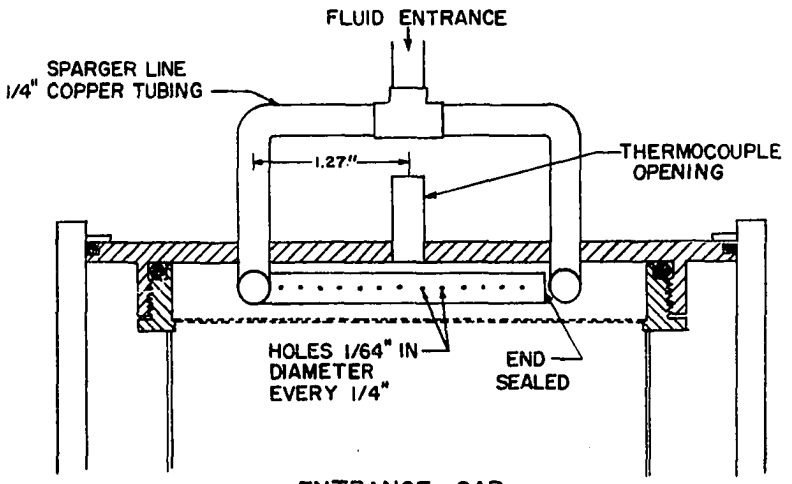

ENTRANCE CAP
SPARGER LINE

Figure 12- Test-Cell Entrance Cap; Flow Sparger and Flush-Out Lines

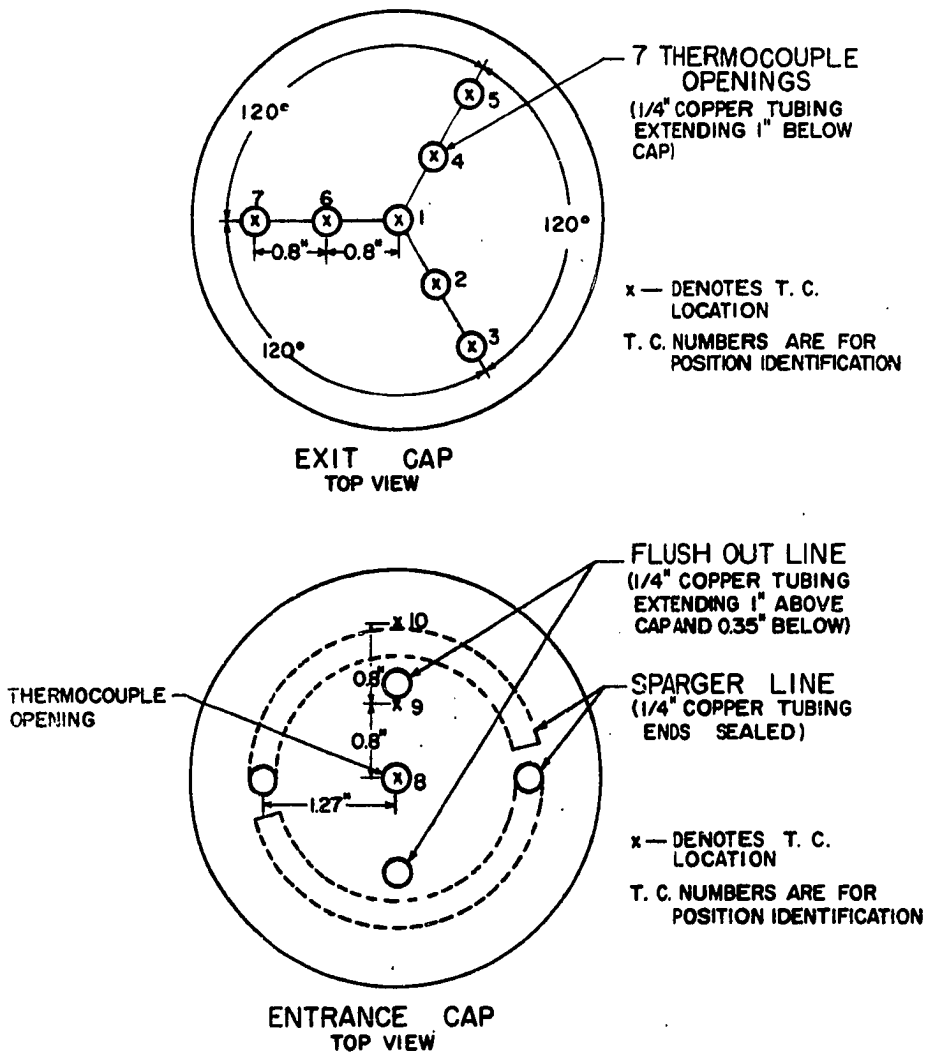

Figure 13- Test-Cell Entrance and Exit Caps; Thermocouple Openings

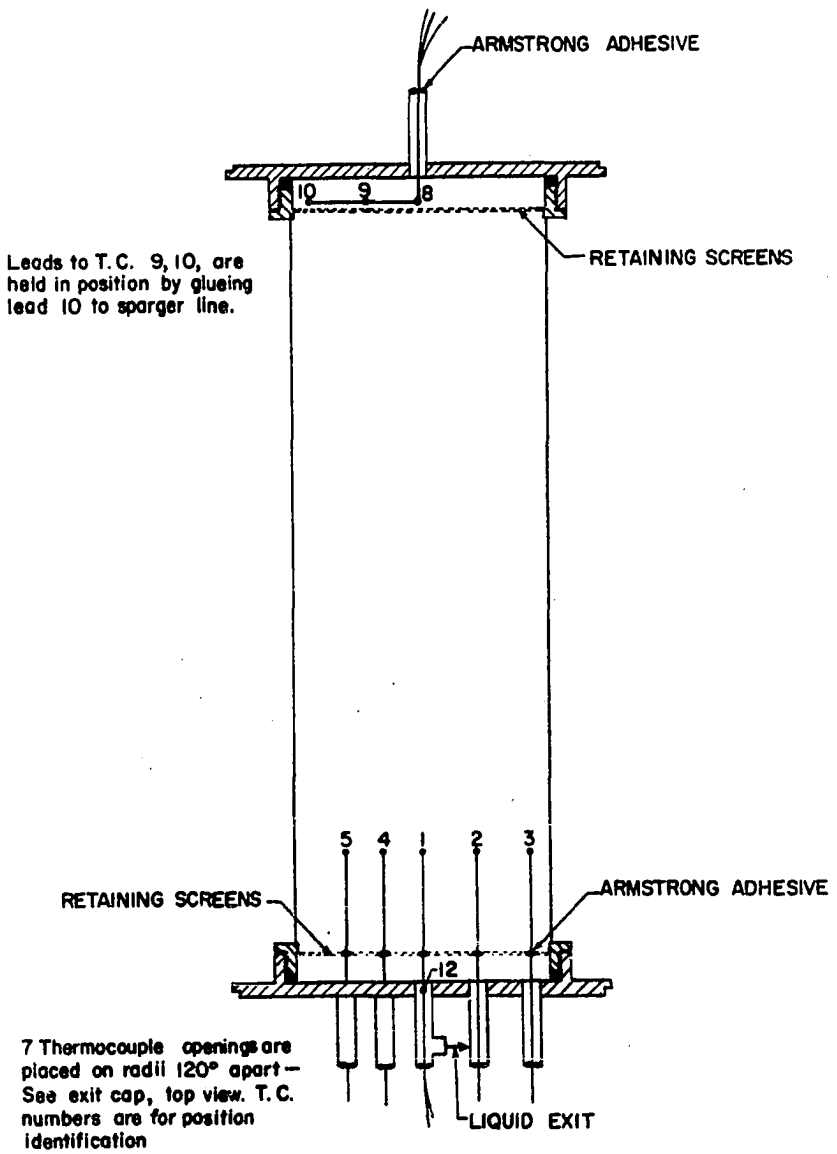

Figure 14- Test Cell; Thermocouple Positions

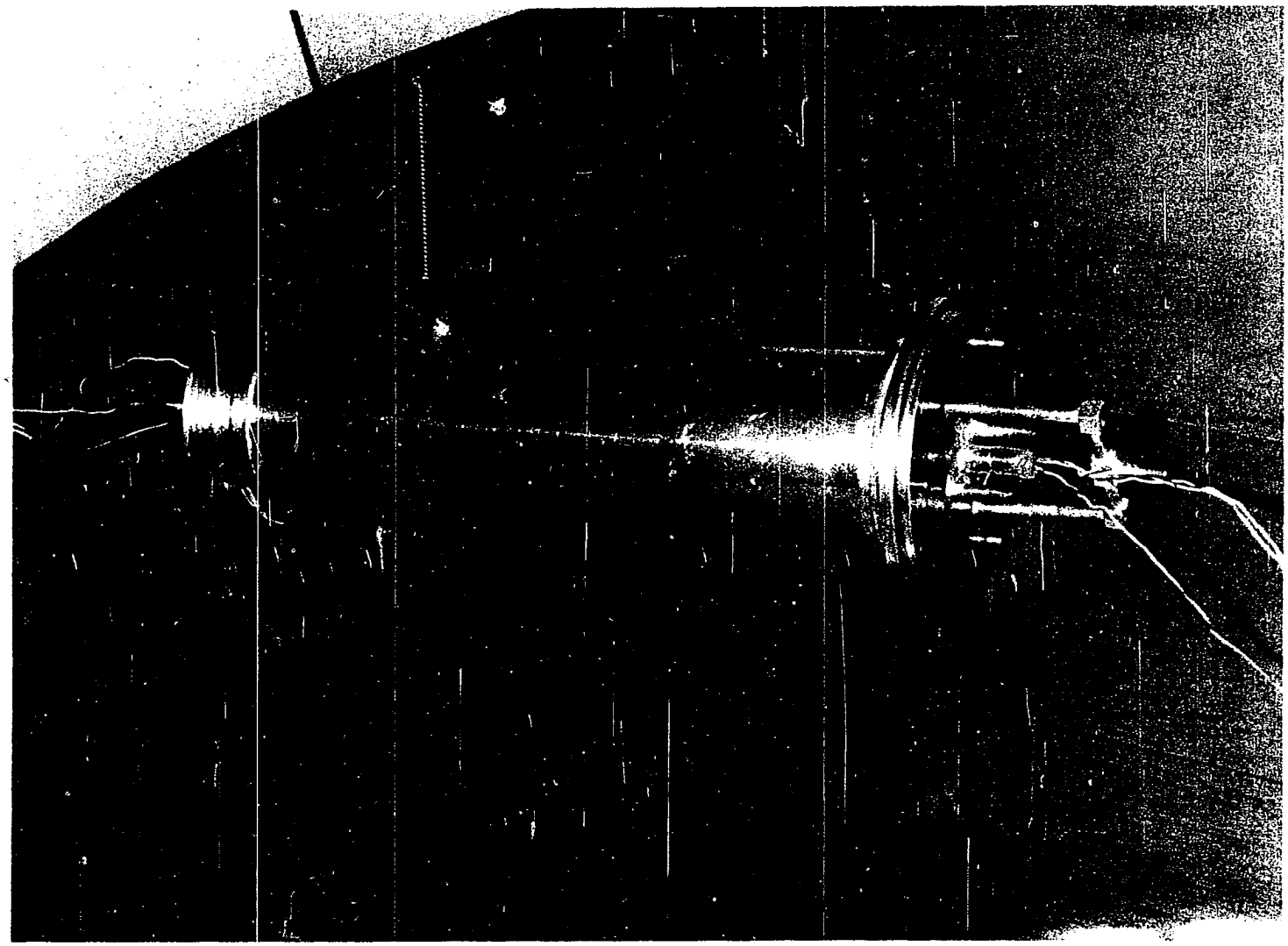

Figure 15- Photograph of Test Cell

wall was approximately 1.4% of the total packed-bed heat capacity, with water as the test liquid.

Fluid entrance and exit caps were threaded to match the tube end pieces. The use of "O" rings at this point prevented fluid leak (Figure 12). The thin-walled retaining tube, plus end caps, were inserted into a heavy-walled, steel casing. "O" rings were also used here to hold the inner tube in place and to seal off the annular space. This arrangement allowed a vacuum to be pulled around the packed bed, providing insulation. Vacuums on the order of 0.5 mm total pressure were used. An alumina-foil radiation shield around the inner tube, at a distance of about 0.25 inches from the tube, provided further against heat losses from the packed bed.

The entrance cap contained a flow sparger which served to distribute the incoming fluid over the face of the packed bed (Figure 12). There was a void space of 0.4 inches above the bed in which mixing of the feed liquid occurred. Two flush-out exit lines were fitted into the entrance cap allowing the bed to be by-passed. The use of this flush-out will be discussed in the Procedure Section. Thermocouples were fixed at different radial positions just above the entrance retaining screen (Figures 13 and 14). The thermocouples were sealed by taking the leads in through 1/4 inch copper tubing and applying Armstrong adhesive at the outlets.

The exit cap contained seven openings for thermocouple leads (Figures 13 and 14). Thermocouples (30 gauge) located

in the packed bed itself were run into the cap openings, through small holes in the bottom retaining screen, and up into the bed. These were fixed in place with Armstrong adhesive prior to packing the bed. Lead wires were sufficiently rigid to hold the thermocouples in upright positions. Thermocouples could thus be placed at any selected depth in the bed, or at the packed-section exit, just below the retaining screen. The thermocouple openings were designed to serve as fluid flow outlets, however, it was found satisfactory to use only the center exit line. A thermocouple placed in this center exit line could be used to give the average temperature of the leaving liquid.

Experimental Materials

Four different liquids were used in the experimental program. These were distilled water, 30% by wt. glycerol (aqueous), 60% by wt. glycerol (aqueous), and ethyl alcohol. Sources and specifications of the liquids are given in Table 9 of Appendix H.

Solid glass spheres made up the packed beds. The four sizes used were 0.0038, 0.0181, 0.0425, and 0.118 inches in diameter. Sources and descriptions of the beads are listed in Table 10 of Appendix H. The spheres were screened until a minimum of 95% were within two closest standard sizes in the U.S. Sieve series. The diameter was then taken as the mean of the two screen openings.

Physical properties of the liquids and solids are presented in Appendix H for temperatures over the range of interest in this research. The densities of the glass spheres were determined to within 1% by measuring the liquid volume displaced by a bead sample of known weight.

Experimental Procedure

Preliminary Procedures

The Minneapolis-Honeywell Temperature Recorder was calibrated using a Leeds and Northrup Potentiometer #8662, as prescribed in the Leeds and Northrup manual.

Thermocouples were checked against the best available thermometers over the experimental temperature range. The precision of all thermocouples used was judged to be better than $\pm 0.2^{\circ}F$ between $70^{\circ}F$ and $175^{\circ}F$. Accuracy was within $0.5^{\circ}F$.

Prior to packing the spheres, thermocouples which were to be located within the bed were fixed in position and their locations measured. Position measurements with respect to the top of the tube were within ± 0.04 inches. The thermocouples generally were placed approximately 2.0 inches from the outlet end of the bead pack and approximately 11.0 inches from the entrance face. Also, prior to packing, the empty volume of the tube between the retaining screens was measured to allow a calculation of bed porosity.

The beads were wet packed using a mechanical shaker, with two to four inches of water maintained above the beads

during packing. When the final bed height was reached, the top was smoothed, and the retaining screen fixed in position using Armstrong adhesive. Once the top screen was fixed and the entrance cap threaded on, the complete tube could be inverted with no shifting of the bed. Fluid flow could be in either an upward or downward direction.

Bed porosity was calculated, knowing the empty tube volume, bead density, and total weight of beads in the bed. Packing as described gave porosities reproducible to within one per cent.

The packed heat-transfer tube, with the radiation shield in place, was next inserted into the heavy-walled outside cylinder which was fixed in a tri-pod metal stand. The "O" rings were clamped into place. The assembled tube was placed in its operating location, leveled, and a vacuum was pulled on the annular space. The tube was now ready for operation.

Experimental Run Procedure

The experimental procedure consisted of bringing the bed to a constant temperature, injecting a step function in temperature at one end, and measuring the response curve at fixed positions.

In cooling runs, the packed section was heated to a constant specified temperature throughout by preheating the test liquid in the constant-temperature baths and flowing it

through the section until thermocouple readings at the inlet and outlet agreed. Initial bed temperatures between 115°F and 180°F were used, with about 130-150°F being the usual value. The hot flow through the bed was stopped. The entrance cap (space above packing) was flushed out at a high flow rate with cool (room temperature) test fluid. This was done by closing in the tube exit line and opening the entrance-cap, flush-out line. Flush-out was continued until the entrance thermocouples indicated a constant temperature. The approximate flow rate for the run was set using the flow meter. After allowing a few seconds for further temperature adjustment at the entrance, flow was started through the test section by simultaneously opening the tube exit line and closing the flush-out line. The temperature recorder was started at this same instant. Total time of flush-out was held to one minute or less and, as discussed in the next section, this procedure resulted in a satisfactory approximation to a temperature step function.

Even with flush-out, the entrance temperature tended to drift downward 1-3°F during a run. This was apparently due to a combination of initial incomplete cooling of the entrance cap and back diffusion of heat out of the bed. To offset this drift, a small resistance heater was wound around the feed line, just above the entrance cap. By manually controlling the input from this heater, a constant temperature of ± 0.5°F was maintained at the packed-section face except during

approximately the first 20 seconds of a run. A drift of 1-2°F sometimes occurred in this short initial period. These tolerances were exceeded very slightly in a few of the runs, with no noticeable effect on the measured temperature profile. At interstitial velocities of 2-4 ft/hr or less, back diffusion of heat out of the bed prevented complete control of the input temperature.

During a run the flow rate was held constant to ± 1% by using the rotameter as an indicator and manually controlling the reservoir air pressure. Flow was measured by catching timed samples of the effluent. Rates had to be adjusted during a run because of changing pressure drop across the packed bed as the heat front progressed down the bed.

The temperatures at six pre-selected points in the system were recorded during the run. The two center positions, at the bed face and within the packed section (positions 1 and 8, see Figure 14) were always recorded. These points were all that were really necessary to the data calculations. The other thermocouples provided auxilliary information on radial temperature gradients and length effects. An experimental run concluded when all thermocouples in the bed reached the temperature of the input fluid. A typical cooling-run data sheet and temperature recorder chart are shown in Figures 16 and 17.

Heating runs involved the same procedure, the difference being that the test section was first cooled with

Run # - 71C Date - June 20, 1961

Barometric Pressure - 732.6 Room Temperature -

Solid - glass beads + 170 U.S. Sieve (see 25C)

Fluid - distilled H_2O Insulation Shell Pressure - < 1 mm

Heat Transfer Tube - B-1

Porosity, ϕ - 0.355 Initial Temperature - 147.5

Inlet Temperature - 83.8

Flow Reading (Rotameter) - 8.0

Measured Flow Rates

Q_3 cm	t min	q_3 cm/min	v ft/hr
102.5	0-36.0	170.8	
93.7	0-32.7	171.9	V = 17.075
94.2	0-32.8	172.3	

Avg q(cm^3/min) - 171.7; 0.5% drift

Entrance Preheat - 0.55"

Effective Thermal Conductivity, k_e = .7883

Remarks -

Figure 16- Sample Data Sheet; Run 71C

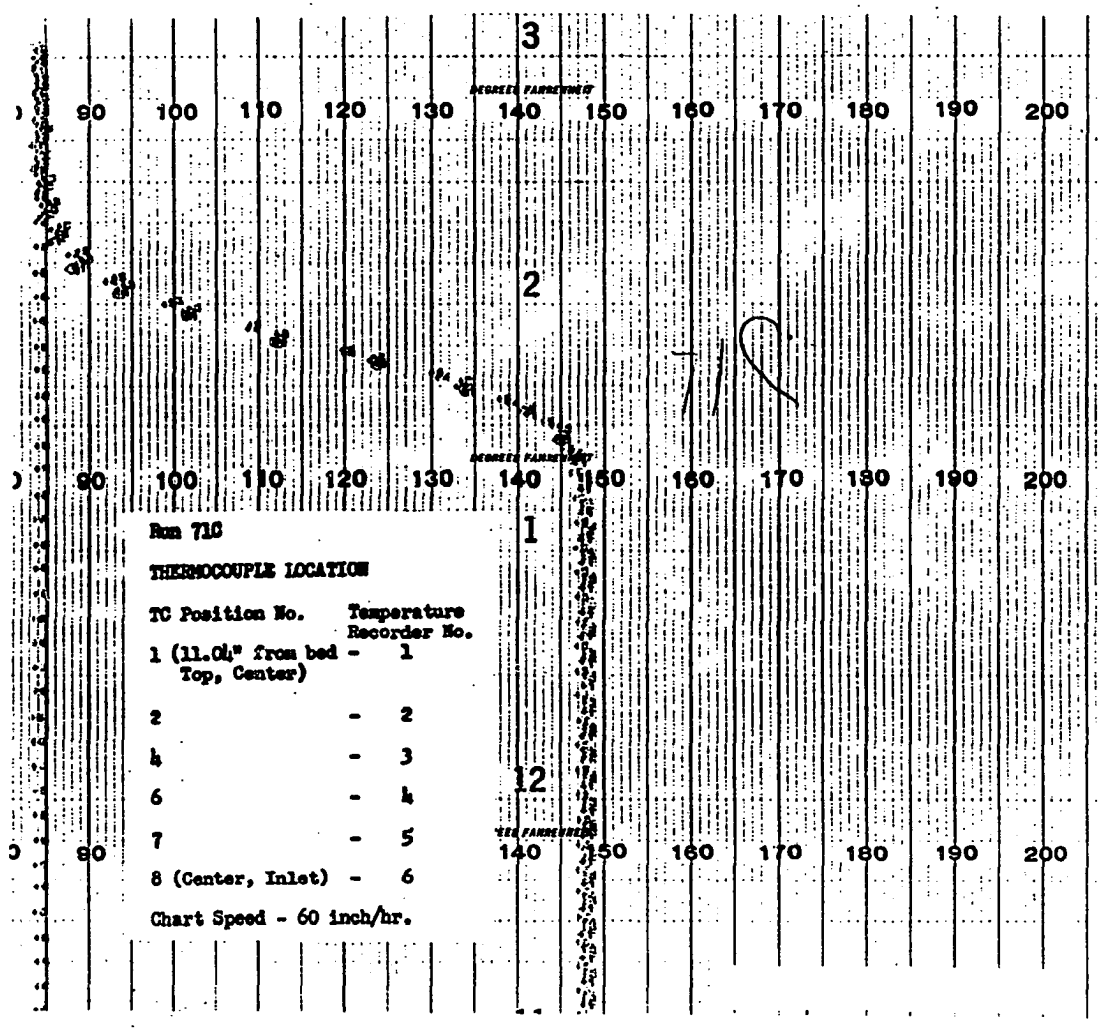

Figure 17- Sample Cooling-Run Temperature Recorder Chart; Run 71C

room-temperature test liquid followed by step-function injection of hot test liquid.

In changing from one fluid system to another, the old liquid was simply flushed out of the bed with the new liquid. This procedure was satisfactory since all liquids used were miscible. The completion of a flushing operation was checked using a refractometer to compare the input liquid to the effluent.

Air saturation of liquids which were reused was prevented by periodically heating the liquids to temperatures considerably above the experimental temperature range to drive off absorbed air.

Both vertically upward and downward flows were used in the experimental work and some complications are discussed in the next section under natural-convection considerations.

Operating Characteristics of the Apparatus - Exploratory Data

Preliminary data were taken to analyze the operating characteristics of the selected experimental system. Part of this exploratory work was carried out in a cell of a design similar to that previously discussed. The packed section was held between two retaining screens in a thin-walled stainless steel tube of approximately 3.5 inches in diameter and 7 inches in length. The cell was insulated by inserting it into a box packed with spun glass.

Step Function Injection

One of the weaker points of the apparatus appeared to be the method of injecting a temperature step function into the bed. A preliminary calculation was made to estimate the amount of heat conduction into or out of the bed during a two-minute flush-out. This indicated that the very maximum heat conduction would be about 2% of the total heat input. An experimental check was made by conducting entrance-cap, flush-out tests with thermocouples at known positions just under the packed-bed face. These tests showed the calculated maximum conduction rate to be high, and that a negligible amount of mixing between the bed liquid and entrance-cap liquid occurred. A one-minute flush-out period would therefore not cause adverse effects, and actually flush-out times up to two minutes resulted in no appreciable effects on the temperature response curves of the bed.

The temperature of the injected fluid was constant across the inlet face of the packed section to $\pm$ 0.5°F in nearly all runs. In some of the lower velocity, 60% glycerol runs there was as much as a 3°F temperature difference between the center and outside radius.

It is expected that the results will not be affected due to the use of a static injection, i.e., fluid flow through the bed stopped during flush-out. This has been checked in a study on the longitudinal dispersion of mass in porous media (29).

Wall Conduction and Bed Heat Losses

Calculations indicated that conduction down the wall of the heat-transfer tube would be negligible. This was experimentally verified by conducting preliminary runs in which the wall temperature was measured along with the bed temperature. The wall temperature did not lead that of the bed. Also, the appearance of radial temperature gradients within the bed, in which the outside recording points read different from the inner points would have indicated a possibility of significant wall conduction. No such results were observed.

Calculated heat losses from the bead pack were on the order of 1.5-3% of the heat input at a water flow velocity of 4.5 ft/hr, decreasing with increasing flow rate. The use of a vacuum did not significantly reduce the air thermal conductivity (89), but convective transfer was essentially eliminated. An estimation of radiation indicated that the radiation shield reduced these losses to a negligible value.

Temperature Measurement

Thermocouples were made of 30 gauge wire allowing small junction beads to be formed (on the order of .02 inches). However, a slight time lag would occur in the heating of the thermocouple bead. Recorded temperatures therefore represent some intermediate value between the true liquid temperature and the solid-sphere temperature. Estimations of this time lag, based on literature heat-transfer coefficient correlations

(see Chapter II) indicated that it had negligible effect on the data, with the dimensionless temperature difference between fluid and thermocouple being less than .01.

Velocity Profiles

Tube-Wall Effects. It is known that velocity profiles do occur across a packed tube (26, 128, 161). The flow deviates more from piston flow in a given tube as the particle size is increased. Experimental studies (26, 128, 161) have shown that as long as the ratio d_p/d_t (particle diameter/tube diameter) is less than about 0.04, the assumption of piston or plug flow is good. The ratio did not exceed 0.032 in this work.

The presence of significant deviations from piston flow due to tube-wall effects was checked for by placing thermocouples at the same height but at different radial locations in the bed. The occurance of symmetrical velocity profiles would have resulted in symmetrical radial temperature gradients. Radial heat flow would not be of sufficient magnitude to erase any large temperature gradients. No such symmetrical radial temperature gradients occurred in the test program. Since temperature response curves were measured at "points" in the bed and an average or mixing-cup value was not used, any small deviations from piston flow should not significantly affect the results (22, 25).

Channeling. A distortion of the fluid flow pattern

termed "channeling" or fingering" often occurs in porous media. Petroleum engineers are familiar with this phenomenon is systems where the viscosity ratio is unfavorable (17, 32, 154). That is, when the fluid being displaced from a porous medium has a higher viscosity than the displacing fluid, channeling nearly always results. In the present work, the possibility of channeling due to an unfavorable viscosity ratio did exist in heating-run experiments.

It is also known that natural convection can cause fingering in packed beds (43, 185). When one fluid flows downward, displacing a less-dense fluid, flow "fingers" may develop. This is also possible if the direction of flow is upward and a more-dense fluid is being displaced by a less-dense fluid.

In the preliminary data, it was found very early that under certain conditions large radial temperature gradients appeared. These gradients were not symmetrical across the bed. Under different conditions they ranged from about a $3^{\circ}F$ temperature difference between the center and outside radial thermocouples to a difference several times this. The occurence of such radial temperature gradients was taken as direct evidence of flow channeling or fingering. Table 2 gives a summary of data in which channeling occurred. For this study, data had to be obtained at conditions where channeling was insignificant and thus, cooling runs were of primary interest.

TABLE 2

SUMMARY OF CHANNELING APPEARANCES

Run Type	Flow Direction	d_p(in)	Channeling*	Cause of Channeling	Comments
Cooling	Up	0.0425	All systems-No		
		0.118	All systems-No		
Heating	Down	0.0038	All systems-Sev	Unfavorable Viscosity Ratio	
		0.0181	All systems-Sev	Unfavorable Viscosity Ratio	
		0.118	Water Alcohol -No 30% Glycerol-Slt-Sev 60% Glycerol-Sev	Unfavorable Viscosity Ratio	
Cooling	Down	0.0038	All systems-No		
		0.0181	All systems-No		
		0.0425	Water-Slt-Sev (Other systems not tested)	Natural Convection	Calculated k_e values agree with those for up-flow cooling runs; water, d_p = 0.0425", Data scatter-high
		0.118	Water Alcohol -Sev 30% Glycerol-Slt-Sev 60% Glycerol-No-Slt	Natural Convection	Calculated k_e values agree with those for up-flow cooling runs; 60% glycerol, d_p = 0.118"
Heating	Up	0.118	Water-Sev Alcohol-Sev	Natural Convection	

*Nomenclature in this column
No - No significant channeling, Radial Gradients 0 - 3° F
Slt - Slight channeling, Radial gradients 5° F
Sev - Severe channeling, Radial gradients > 5° F

In the up-flow cooling runs and down-flow heating runs, natural convection should not have been a cause of fingering. Yet in down-flow heating run experiments with 0.0038 and 0.0181 inch beads, severe channeling was present in all liquid systems. The magnitude of the effect was a function of particle size as well as liquid viscosity, indicating its dependence on viscous forces within the bed. Channeling decreased with increasing particle size and with decreasing liquid viscosity, and, in fact, was insignificant in water and alcohol down-flow heating runs with 0.118 inch beads. Temperature level was also important, in that, the larger the initial temperature difference between displaced and displacing liquid, the larger the radial temperature gradients. The radial temperature profiles were very flat in all up-flow cooling experiments, being generally on the order of 1-3°F between the center and outside thermocouples.

The cause of fingering in the heating data was apparently an unfavorable viscosity ratio. Since the displacing fluid had a lower viscosity than the original bed fluid, it seems reasonable that flow fingers would develop just as in the case of a two-liquid system in which the different liquids have different viscosities. Experiments with two-liquid systems have shown that with only slightly unfavorable viscosity ratios, severe channeling can result (17). A typical heating-run temperature data chart with channeling is shown in Figure 18. A cooling run with no significant channeling is seen

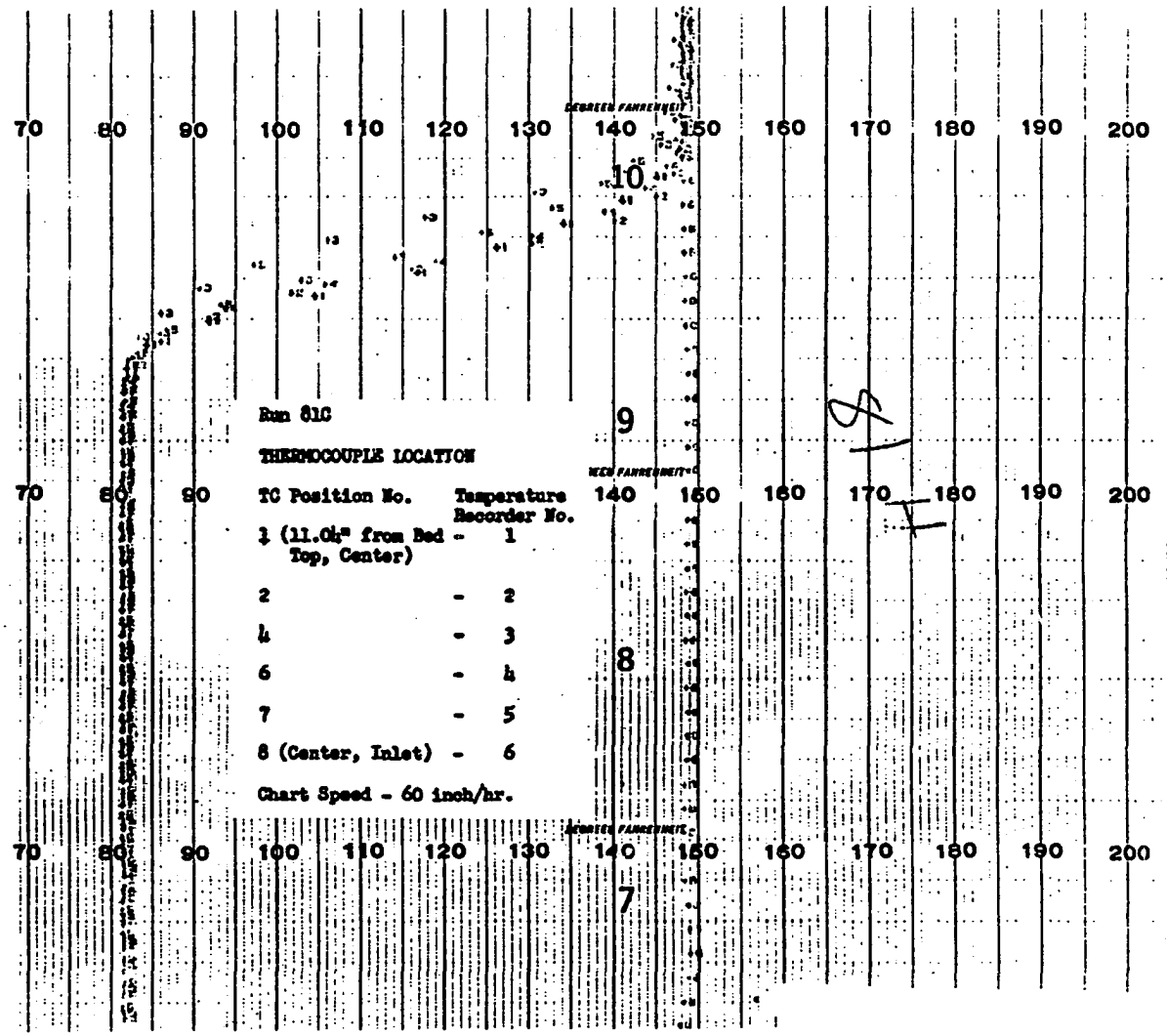

Figure 18- Heating Run with Channeling Caused by an Unfavorable Viscosity Ratio; Run 81H

in Figure 17.

As shown in Table 2, piston flow occurred in both heating and cooling runs in the 0.118 inch bead system with water and alcohol as the liquid phases. These were the only heating runs in which fingering was not present. A comparison of the heating-and cooling-run data is made in Appendix L.

In down-flow cooling runs and up-flow heating runs the possibility of fingering due to natural convection would exist, and such fingering did occur with the larger size beads. This was most apparent in the 0.118 inch sphere pack. Water and alcohol down-flow cooling runs gave extreme radial temperature profiles. One such run is shown in Figure 19. When the flow direction was reversed, the radial gradients were flat for cooling runs, but heating data yielded severe gradients. These heating-run gradients could not be explained by an unfavorable viscosity ratio since, as shown in Table 2, viscosity ratio channeling did not appear in the water and alcohol down-flow heating runs. The gradients were also larger and more irregular than those caused by an unfavorable viscosity ratio.

Natural convection effects are correlated by the Grashof number.

$$Gr = \frac{g_c L^3 \rho^2 \beta |(T_i - T_o)|}{\mu^2} \qquad \text{(IV-1)}$$

where, L = characteristic length

β = coefficient of thermal cubical expansion

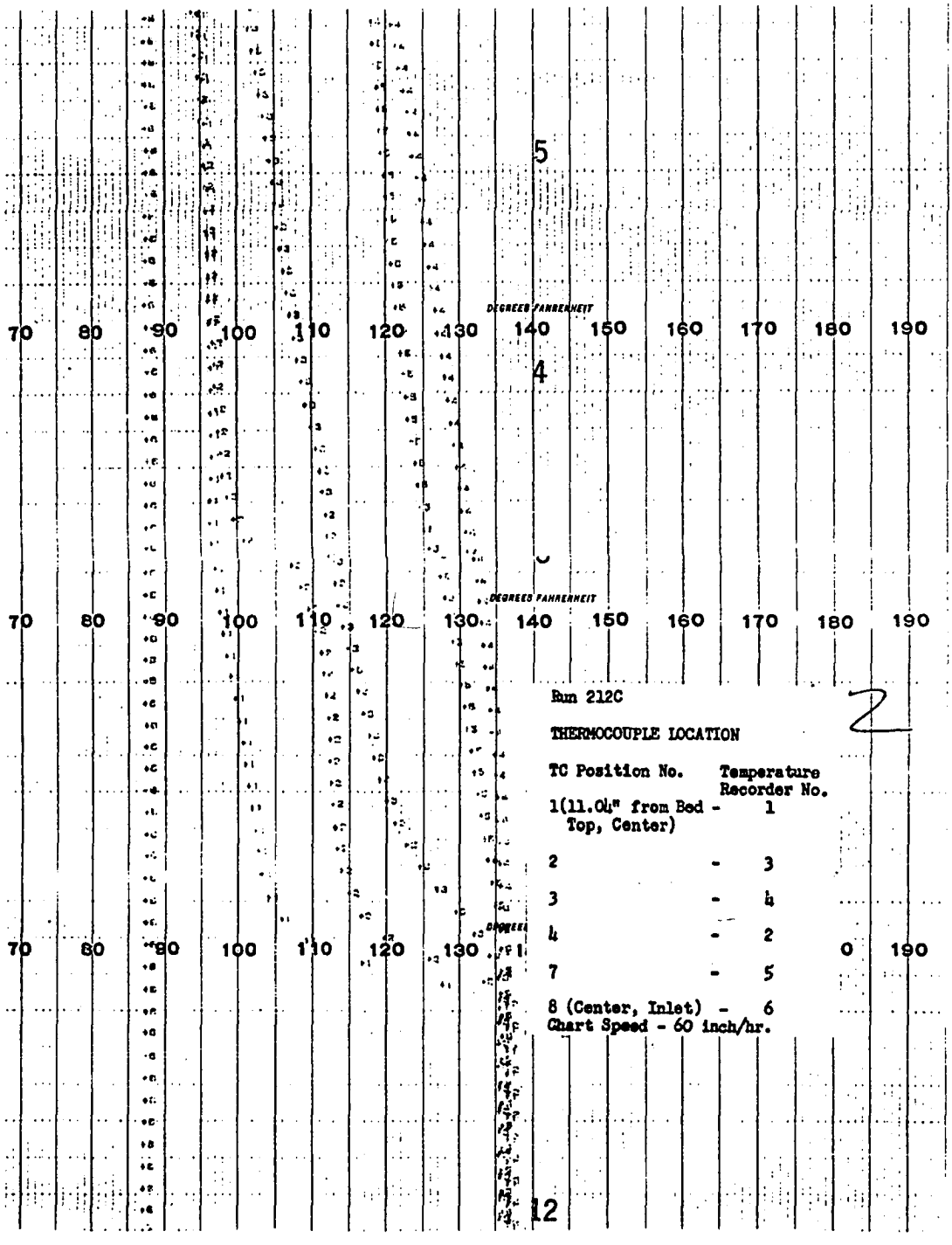

Figure 19- Cooling Run with Channeling Caused by Natural Convection; Run 212C

The Grashof number as used here is based on the difference between the initial bed temperature and the injected liquid temperature. The characteristic length used was the particle diameter. Some typical values are shown in Table 3. The severity of channeling increased with increasing Grashof number as is especially noticed by examination of the down-flow cooling data. In the water-0.118 inch sphere system there was extreme channeling at a Grashof number of about 7100, while only slight channeling appeared in the 0.0425 inch bead pack at a value of 331. The fingering almost disappeared with the 60% glycerol-0.118 inch bead system at Gr equal to 162.

Even though natural convection did not cause measurable channeling in systems with the lower Grashof numbers it might be reasoned that in down-flow cooling runs there could still be an effect on temperature profiles resulting in an increase of calculated effective thermal conductivities (See Chapter V, Data Reduction Section, for discussion on effective thermal conductivity calculation procedure). This was checked in two systems. In the water-0.0425 inch sphere system, at a Grashof number of 331, slight channeling occurred in most of the down-flow cooling runs. Calculated effective thermal conductivities for this down-flow data were in general agreement with the up-flow results, but the data scatter was approximately 15% greater when the down-flow values were included. With 60% glycerol-0.118 inch beads, at Gr equal to

TABLE 3

TYPICAL SYSTEM GRASHOF NUMBERS

Liquid	d_p(in)	$\lvert T_i - T_o \rvert$ (^oF)	T_{avg}(^oF)	Gr
Water	0.0181	40	115	25.6
Ethyl Alcohol	0.0181	40	115	24.6
Water	0.0425	40	115	331
Water	0.118	40	115	7085
Ethyl Alcohol	0.118	40	115	6813
30% Glycerol (Aqueous)	0.118	40	115	1787
60% Glycerol (Aqueous)	0.118	40	115	162

162, natural-convection channeling almost disappeared and a better check was obtained. Here, calculated effective thermal conductivity values were in excellent agreement for both up- and down-flow cooling data (see Figure 54). Based on this, natural convection was assumed not to influence the data except as it caused fingering in the flow pattern. Where this fingering did occur to a measurable degree (0.0425 inch and 0.118 inch spheres), the cooling runs were conducted with an upward flow direction.

Summary, Velocity Profiles. The conclusions concerning velocity profile effects are summarized as follows.

(1) The tube wall had insignificant influence on the bed packing, and the effects of deviation from piston flow near the wall were negligible.

(2) Channeling occurred in nearly all heating experiments due to an unfavorable viscosity ratio between the liquid being displaced and the injected liquid. Cooling runs were therefore of primary interest in the experimental program.

(3) Natural convection channeling appeared in down-flow cooling data at high Gr values. This fingering was eliminated by using up-flow experiments. Where measurable natural convection channeling was not present, up-flow and down-flow cooling data were in agreement.

Bed Length Effect

Bed-length effects were determined by measuring

temperature response curves at bed depths of 6.77 and 11.04 inches. The results are discussed in Chapter V.

Data Reproducibility

Experimental results were reproducible. For two sphere sizes, 0.0038 and 0.0181 inch, experimental runs were made, the bed was repacked and repeat runs were made. In both cases the data agreement between the first pack and the repack was excellent and statistical analysis showed that at a 95 per cent confidence level there was no difference in the data from the different packs.

Experimental Data Sets

The experimental systems investigated are summarized in Table 4.

Primary Data. Primary data consist of cooling-run experiments in which the bulk fluid flow pattern was one of piston flow. The average interstitial fluid velocity range in all cases was between 2 ft/hr and 25 ft/hr. The temperature range did not exceed 70°F to 180°F. The data are tabulated in Appendix I, and the results are discussed in Chapter V.

Additional Data. Additional data consist, for the most part, of runs in which channeling was present due either to viscosity-ratio effects or natural convection. These data are discussed in Appendix L, however, a quantitative analysis

TABLE 4

EXPERIMENTAL SYSTEMS

US Sieve*	d_p(in)	Φ	Liquids
140-170	0.0038	0.355	Water 30% Glycerol (Aqueous) 60% Glycerol (Aqueous)
35-40	0.0181	0.356	Water 30% Glycerol (Aqueous) 60% Glycerol (Aqueous) Ethyl Alcohol
16-18	0.0425	0.360	Water 30% Glycerol (Aqueous) 60% Glycerol (Aqueous) Ethyl Alcohol
6-7	0.118	0.353	Water 30% Glycerol (Aqueous) 60% Glycerol (Aqueous) Ethyl Alcohol

*All solid-phase particles were glass spheres

of channeling was not attempted.

Some heating-run data were taken in which no channeling appeared (0.118 inch beads). These are tabulated and discussed in Appendix L.

CHAPTER V

PRESENTATION AND INTERPRETATION OF EXPERIMENTAL RESULTS

In Chapter III, differential equations describing longitudinal dispersion of thermal energy resulting from conduction, eddy dispersion, and a finite fluid-solid heat-transfer rate were presented. An approximation was developed which allows the general solution to be represented by the simpler thermal-conduction equation, with the dispersion characterized by a single parameter, k_e. This effective thermal conductivity was shown to be the sum of the contributions due to each individual mechanism. Data obtained using the equipment and procedure described in Chapter IV provide a means of testing the applicability of this model. The data and interpretation of results are presented in this chapter which is concerned with work of primary interest, the cooling-run experiments where no flow channeling occurred.

The results are presented in three major sections. In the first of these three sections, the method of determining effective conductivities from the data and the "fit" of the data to the conductivity equation are discussed. Secondly,

the results of the conductivity calculations are presented. In the third section, the data are correlated assuming the calculated effective thermal conductivities are the sum of the molecular-conduction, eddy-dispersion, and heat-transfer coefficient contributions. The results are compared to other data available in the literature.

A discussion of additional data taken (heating runs, flow channeling) is presented in Appendix L.

Reduction of Data

As proposed in Chapter III, the conduction equation (III-7) is used to describe the experimental results. The applicable form of the solution was given as Equation (III-34),

$$t_w = \frac{1}{2}\left[1 - \text{erf}\,\frac{F}{\sigma^*\sqrt{2}}\right] \qquad \text{(III-34)}$$

where $F = \frac{x}{\sqrt{\theta}} - V_F\sqrt{\theta}$, $\sigma^* = \sqrt{2K}$ and where R, the second term of the Jenkins-Aronofsky solution, has been neglected. The maximum values of R encountered in the data were generally less than 0.03. As shown in Appendix E, R could thus be neglected introducing only a small error into the k_e calculation. Simplified expressions for R and for R_{max} are also given in Appendix E.

The procedure used for the determination of k_e values from experimental data was discussed in Chapter III in connection with k_e calculations for the numerical solutions.

Briefly the method is as follows:

1) Plot F vs. t_w on probability graph paper, t_w being plotted on the probability scale.

2) Draw the best straight line through the data points.

3) Read the F values at two points, e.g., at t_w=.1 and t_w=.9 (t_w=.16 and t_w=.84 could just as well be used).

4) Since subtraction of F values at these two points leads to,

$$1.8124 = \frac{1}{2\sqrt{K}} (F_{t=.1} - F_{t=.9}) \qquad \text{(V-1)}$$

then k_e may be calculated from,

$$K = \frac{1}{13.139} (F_{t=.1} - F_{t=.9})^2 \qquad \text{(V-2)}$$

Physical-property values were calculated at the average temperature of the system, $(T_i+T_o)/2$. This method of calculation determines k_e from the "spread in time" or dispersion of the measured temperature response curves. A typical data plot on probability paper is seen in Figure 20. In nearly all cases, the fit of the data to a straight line on the probability paper was excellent, except at small and large temperatures ($t_w < .05$ or $t_w > .95$) where deviations sometimes occurred. In a few runs, deviations from the straight line appeared at about t_w = .1 and t_w = .9. A comparison plot of an experimental temperature profile and the calculated profile using Equation (III-34) is shown in Figure 21. The dispersion and shape of the experimental profile is well represented, but there is slight displacement between the two curves along the

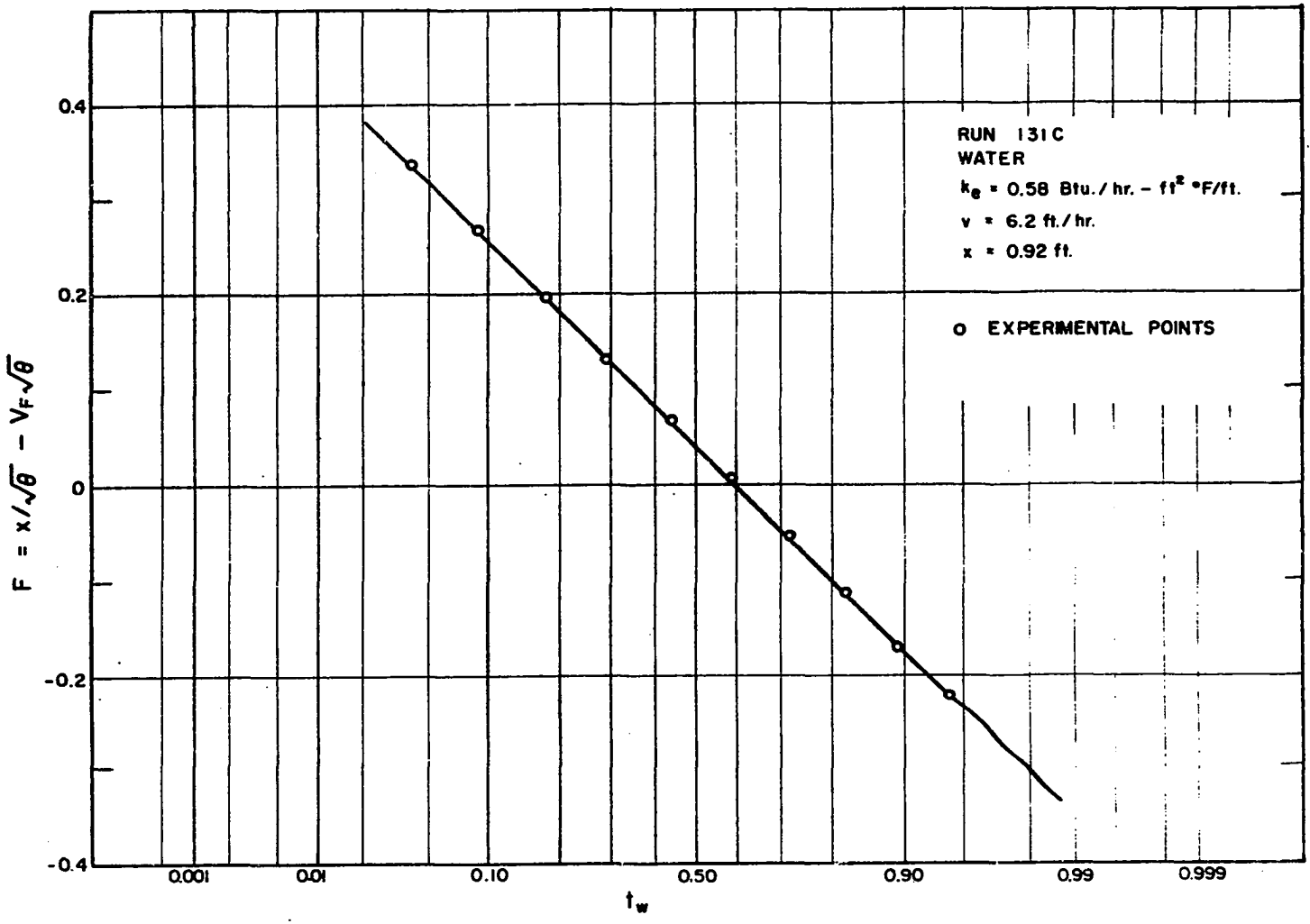

Figure 20- Calculation of k_e; t_w vs. F on Probability Paper; Run 131C

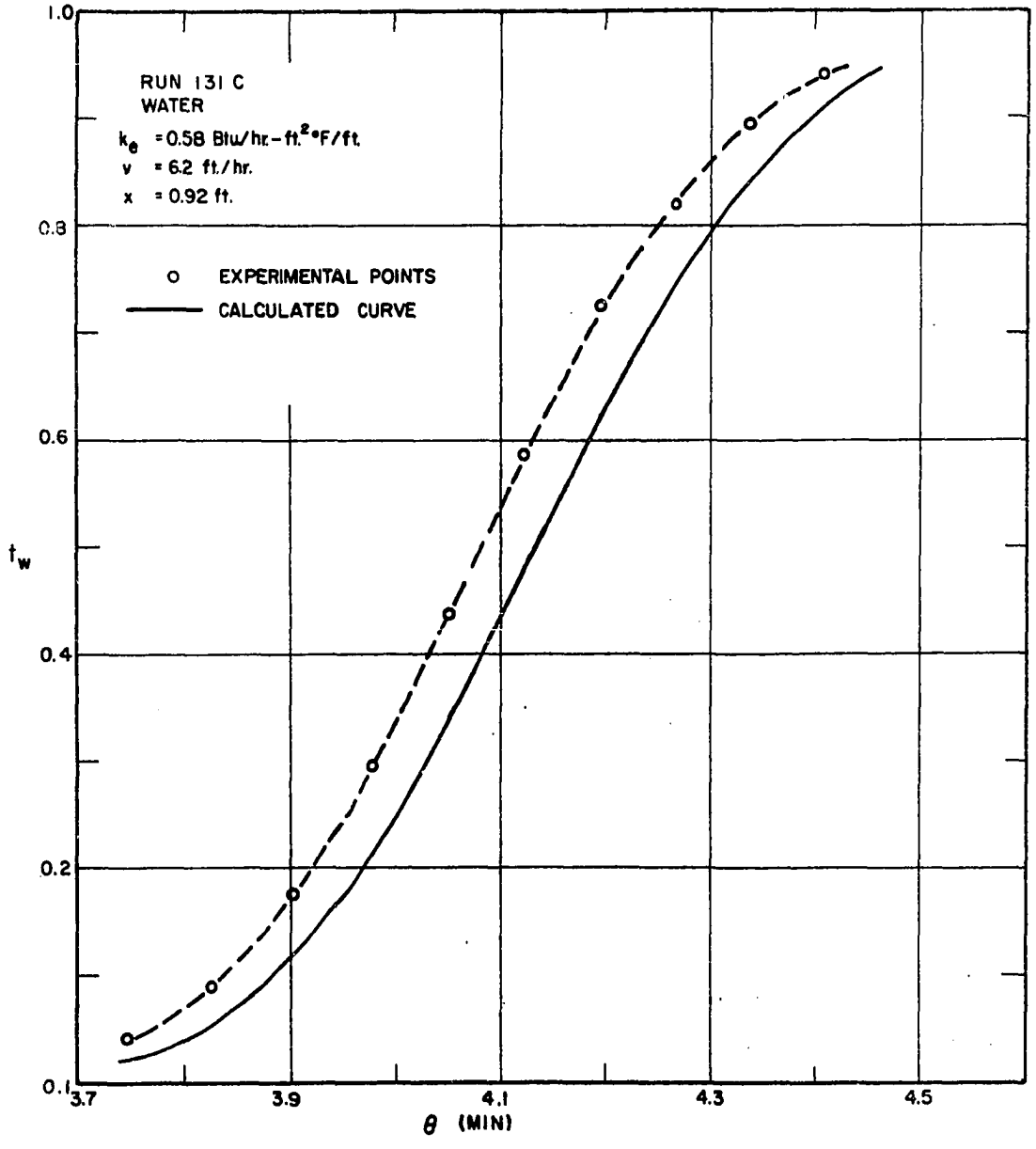

Figure 21- Experimental and Calculated Temperature Profiles; Run 131C

time axis. This displacement was also noted and previously discussed in Chapter IV with reference to the numerical solutions. The omission of the second term of the solution, R, accounts for a small fraction of the displacement. Small errors in system properties such as the solid-phase heat capacity or fluid-phase velocity also affect this "shift" along the axis.

Calculated effective conductivities for all cooling runs, in which no flow channeling appeared, are tabulated in Appendix I. A sample calculation and additional probability-paper plots are presented in Appendix F.

Alternate Methods of k_e Calculation

Alternate methods of determining k_e values from the data were also used, primarily for comparison with the procedure discussed above.

Normal Distribution in θ. As shown in Chapter III, as long as Equations (III-14), (III-16), and (III-25) were satisfied, the solution for a pulse input into a packed bed was approximately normal in the holding-time variable, θ. Correspondingly, for a step-function input as used in the experimental program, a plot of t_w vs. θ on probability paper should yield a straight line. Since the magnitude of $(2\ k_e/\rho_w C_w \phi\ v\ x)$ was generally on the order of .01 to .025, this postulate was checked. The curves obtained on probability paper were approximately linear as shown in Figure 22.

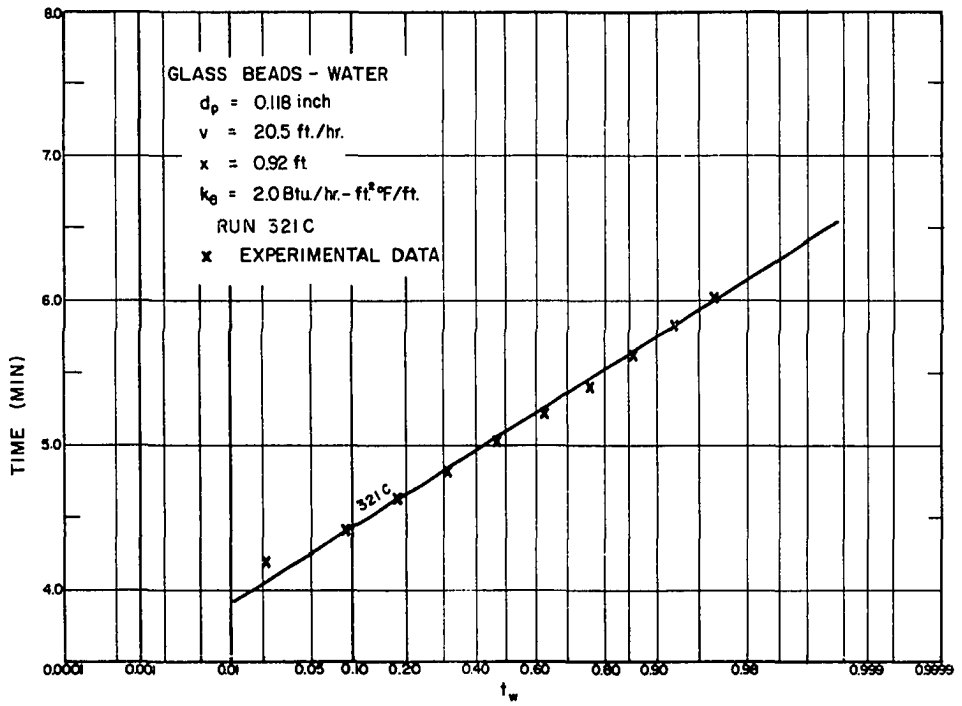

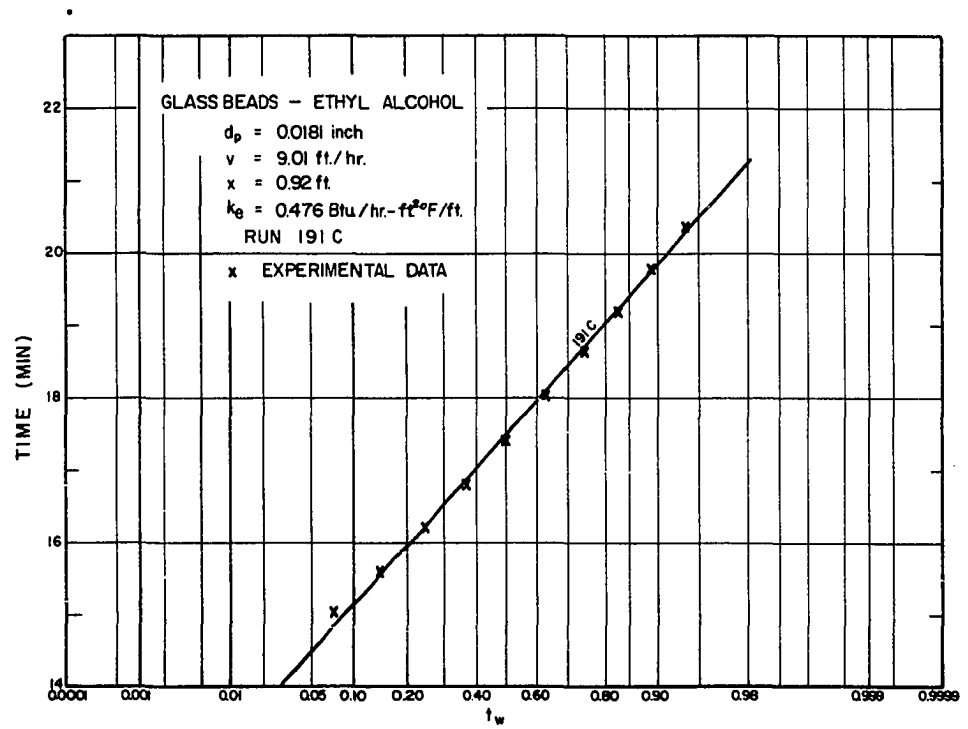

Figure 22- Calculation of k_e; t_w vs. θ on Probability Paper; Runs 191C, 321C

Effective thermal conductivities were calculated by utilizing the fact that the time difference between the 16th and 84th percentiles is equal to 2 σ, i.e.,

$$(\theta_{t=.84} - \theta_{t=.16}) = 2\sigma \qquad (V\text{-}3)$$

where σ^2 was previously defined in Equation (III-31) as

$$\sigma^2 = \frac{2 k_e x}{\rho_w C_w \phi v V_F^2} \qquad (III\text{-}31)$$

The k_e values calculated by this procedure were within 5% agreement with values determined from the plots of F vs. t_w. The error between the two methods was random.

Slope Method. Preston (138) developed an expression for the slope of the t vs. θ profile, evaluated at the time, $\theta = x/V_F$.

$$\frac{dt}{d\theta} = \frac{x}{2\theta\sqrt{\pi K \theta}} \qquad (V\text{-}4)$$

To use this equation, a plot of experimental values of t_w vs. θ is made and the slope estimated graphically at the point t=.5. The conductivity is then determined from Equation (V-4). The resulting agreement between this procedure and the probability-paper method was within approximately 5% for the runs checked.

Single-Point Method. In this method, a single value of t_w is selected from the data at a fixed x and θ. These values are substituted into Equation (III-9) and a value of K is calculated. Unless the data coincide exactly with Equation (III-9), a different K will be determined for each t_w selected,

and a suitable averaging process would then be necessary. This method of k_e calculation was not used because of this difficulty.

Length Effects

To check for length effects, i.e., for a changing k_e with length of travel in the porous media, thermocouples were located at positions of 6.77 inches and 11.04 inches from the bed entrance. Calculated conductivities at these two positions were compared statistically for the water-.0181 inch bead system. A statistical "t" test showed the data at the two locations to be in agreement at a 95% confidence level. A similar evaluation in the water-.118 inch bead system also indicated no change of the calculated k_e with length of travel. Literature data on longitudinal heat and mass transfer in packed beds indicate that length effects should not be significant (29, 46, 76, 161).

Effective Thermal Conductivities

Effective thermal conductivities were calculated for all cooling runs in which no flow channeling occurred. A plot of k_e versus vd_p for each liquid system was found to give a smooth continuous curve over all particle sizes investigated. In Figures 23, 24, and 25, these results are shown for the water and ethyl alcohol liquid systems. Data scatter is on the order of $\pm$ 5 to 8 per cent. Plotting k_e as a function of Reynolds number was not satisfactory, as the

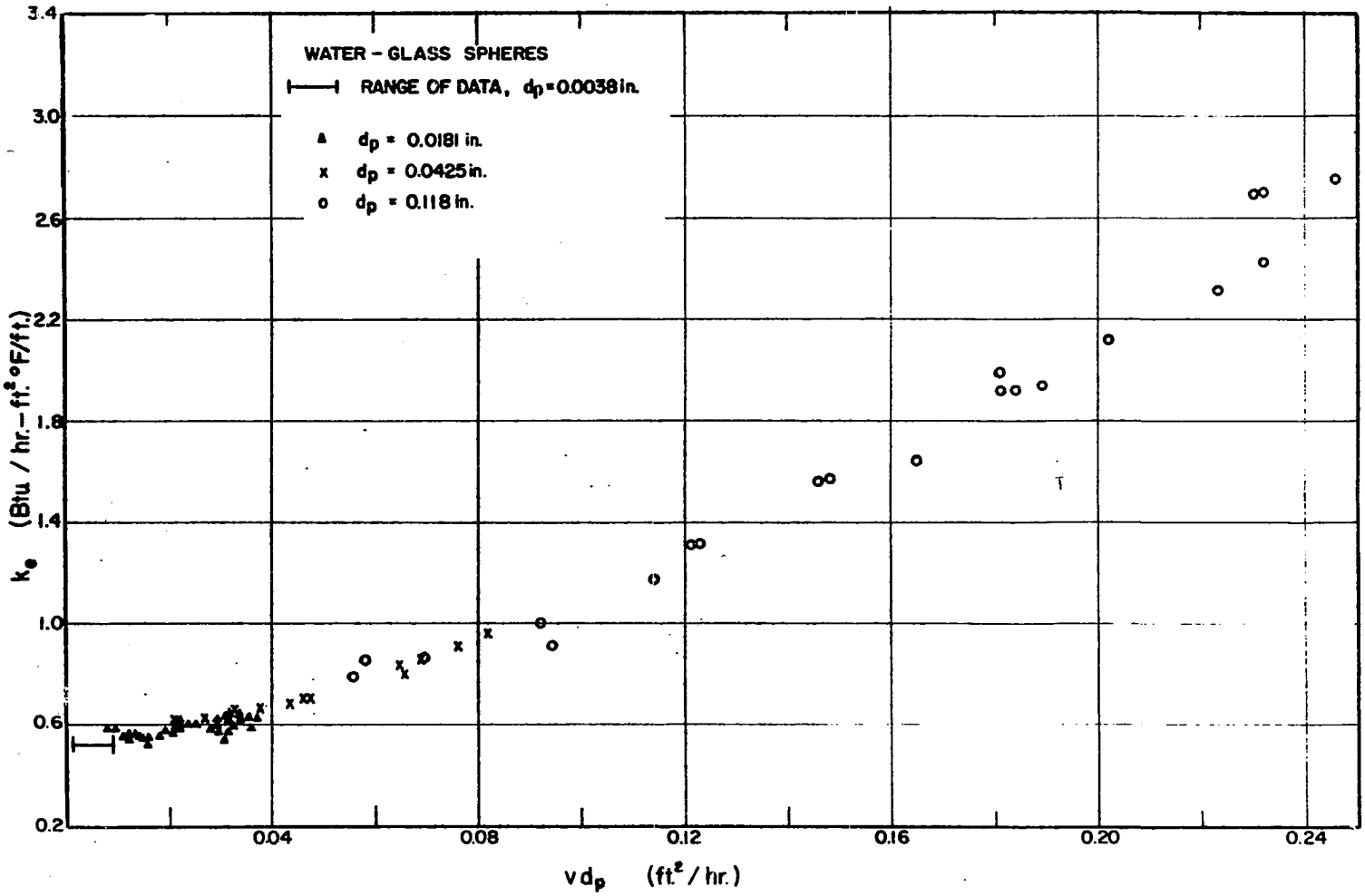

Figure 23- Effective Thermal Conductivity vs. vd_p; Water System

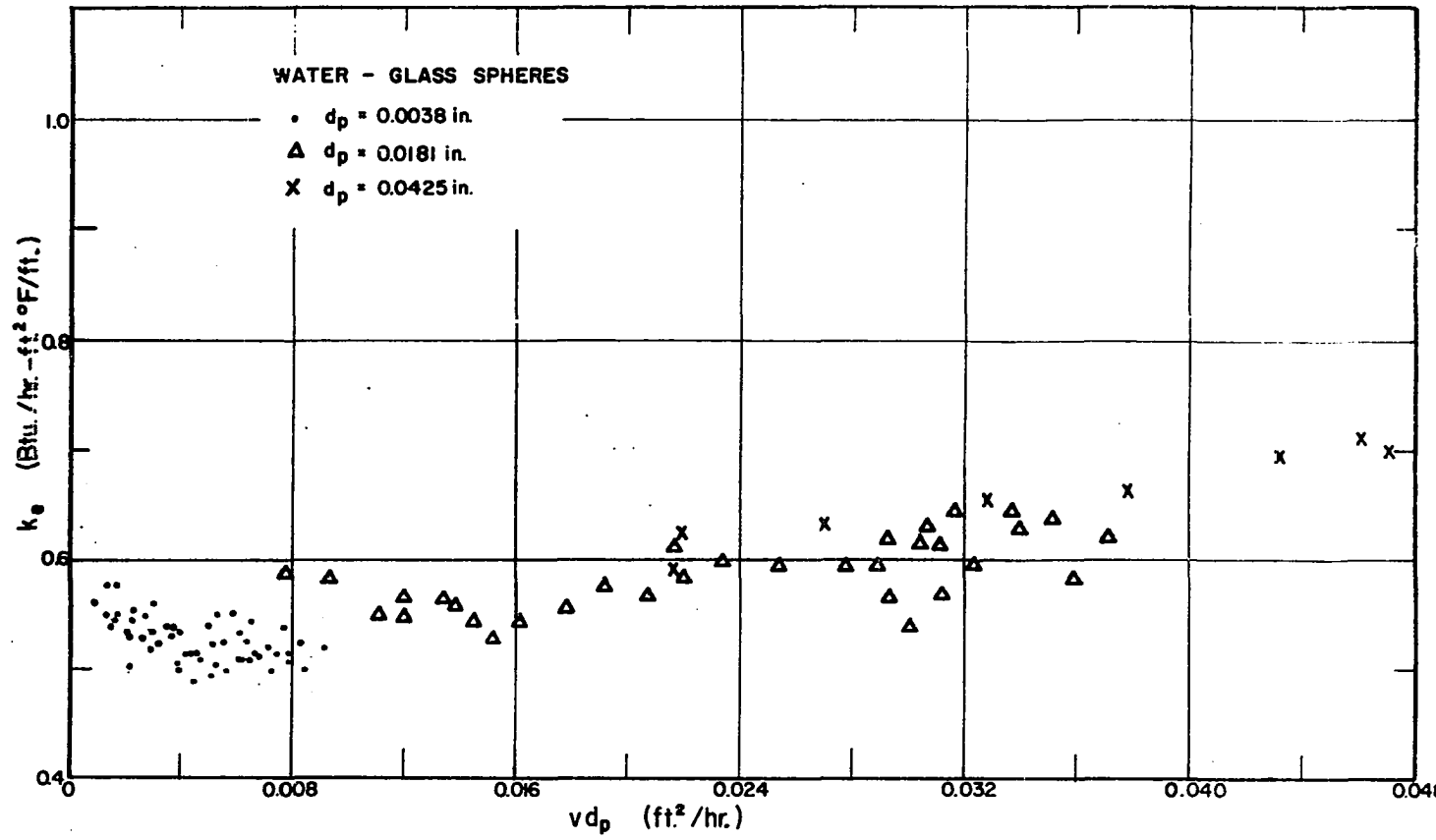

Figure 24- Effective Thermal Conductivity vs. vd_p; Small Spheres; Water System

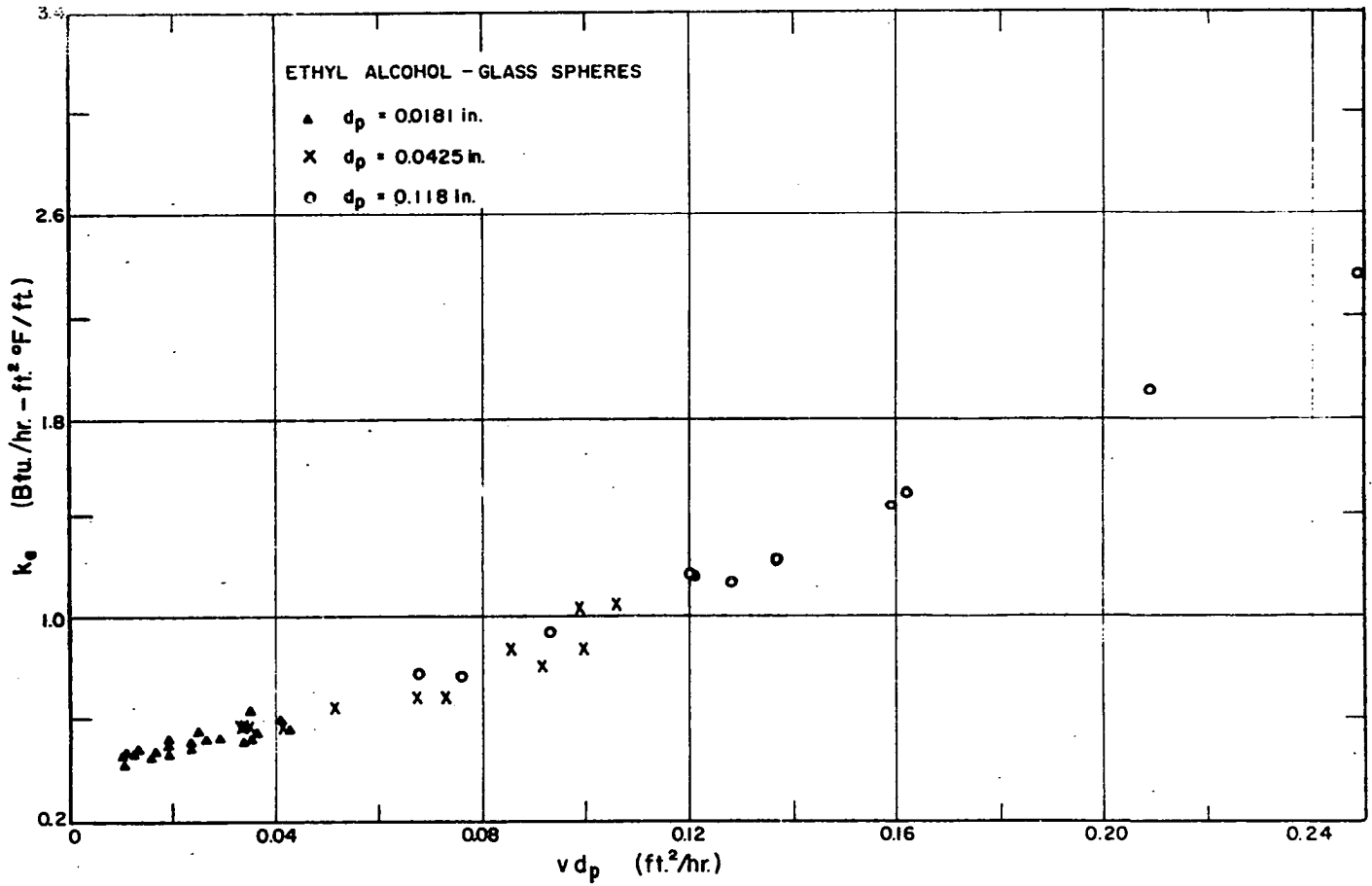

Figure 25- Effective Thermal Conductivity vs. vd_p; Ethyl Alcohol System

introduction of viscosity caused the data to scatter (Figure 26).

Static Thermal Conductivity

The static thermal conductivity, k_e^o, was not measured directly in the experimental program. These were obtained by extrapolation of k_e values back to zero velocity. Values of k_e^o thus determined were in good agreement with the predictive equation of Euchen (51) previously discussed, Equation (II-26), except for the ethyl alcohol system where the predicted value was low. Calculated and extrapolated values are presented in Table 5.

Preston (138) measured k_e^o in porous-media systems very similar to those of this investigation. Glass-water and glass-20% glycerol systems were included in the Preston investigation, and the reported k_e^o values are within 4% of the water and 30% glycerol extrapolated values of this work. Application of Preston's predictive equation, Equation (II-27), to ethyl alcohol yields a k_e^o of 0.41, substantiating the extrapolated number found in this work.

Velocity Component, $k_e(v)$

The velocity component of the overall effective conductivity is defined as

$$k_e(v) = k_e - k_e^o \qquad (V-5)$$

where k_e is the measured effective thermal conductivity. Calculated velocity components of k_e are tabulated in Appendix

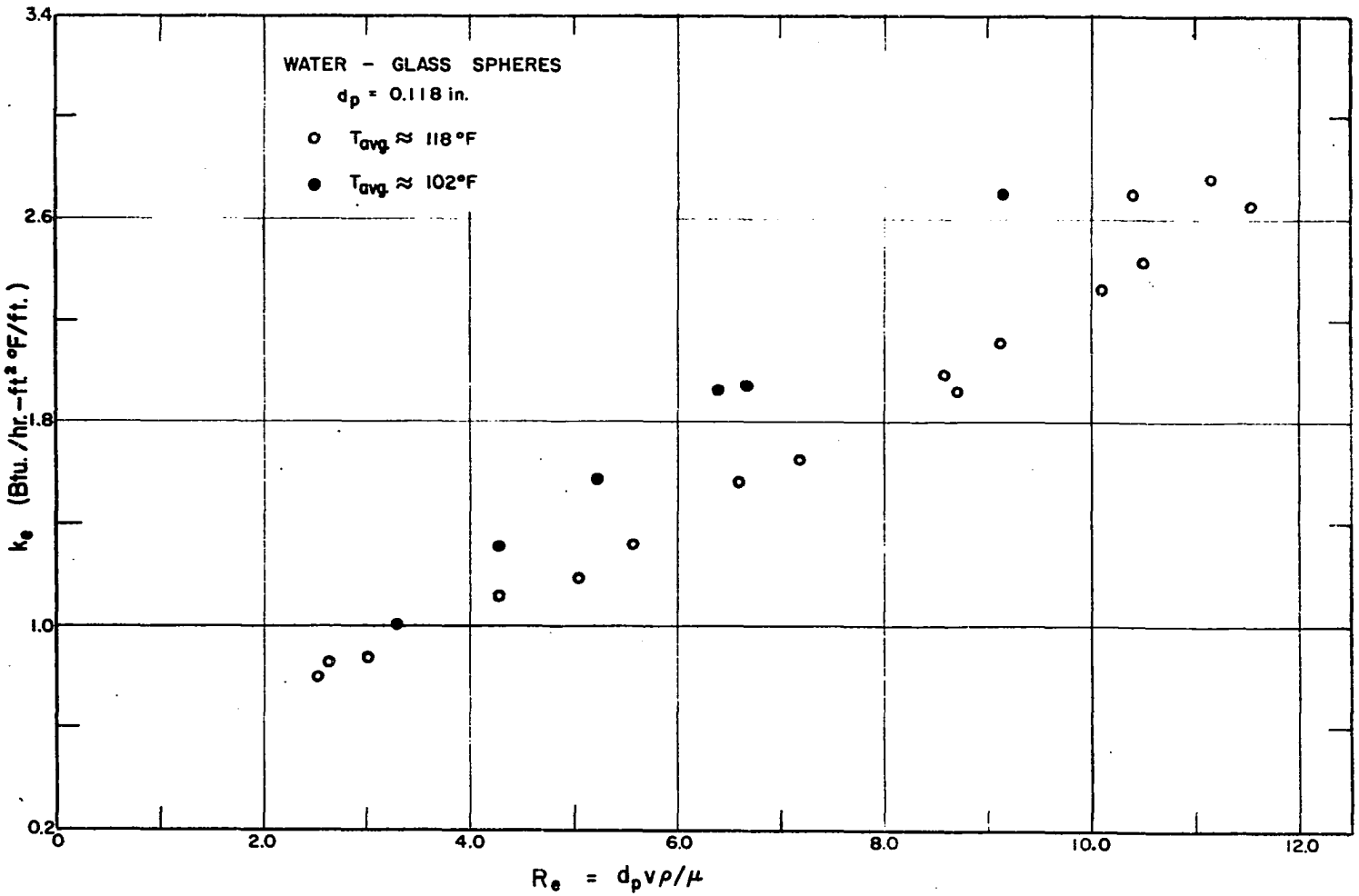

Figure 26- Effective Thermal Conductivity vs. Reynolds Number; Water System

TABLE 5

STATIC THERMAL CONDUCTIVITIES

Liquid System	Extrapolated k_e^o	Euchen Equa. (II-26) k_e^o	ϕ
Water	.51	.49	.355
30% Glycerol (Aqueous)	.50	.45	.355
60% Glycerol (Aqueous)	.45	.41	.355
Ethyl Alcohol	.40	.27	.355

I, and are plotted for all systems on log-log paper as a function of vd_p in Figure 27. The individual liquid systems are also presented in Figures (47) - (50) of Appendix M. Calculated $k_e(v)$ data for the smallest glass beads used, .0038 inch, are not shown on the graphs. Data scatter increases markedly as vd_p decreases since k_e^o becomes the major portion of k_e, and $k_e(v)$ is obtained as the difference between two numbers of the same order of magnitude.

A straight line fit to all the data points in the experimental series with the two largest bead sizes resulted in the equation,

$$k_e(v) = 16(vd_p)^{1.4} \qquad \text{(V-6)}$$

At the larger values of vd_p, the data fit Equation (V-6) within $\pm$ 14%. As seen from the discussion in the next section, the excellent fit of the data to this equation is fortuitous. A significant change in system properties such as fluid physical properties, bead size or bead physical properties, would result in deviations from this curve.

Data Correlation, Summation of Conductivities

The theoretical analysis of Chapter III indicated that as long as the condition,

$$\frac{2\,k_e}{\rho_w C_w \Phi\, v\, x} \ll 1 \qquad \text{(V-7)}$$

is met, then, k_e is approximately equal to the sum of the individual conductivities. In the experimental data, the

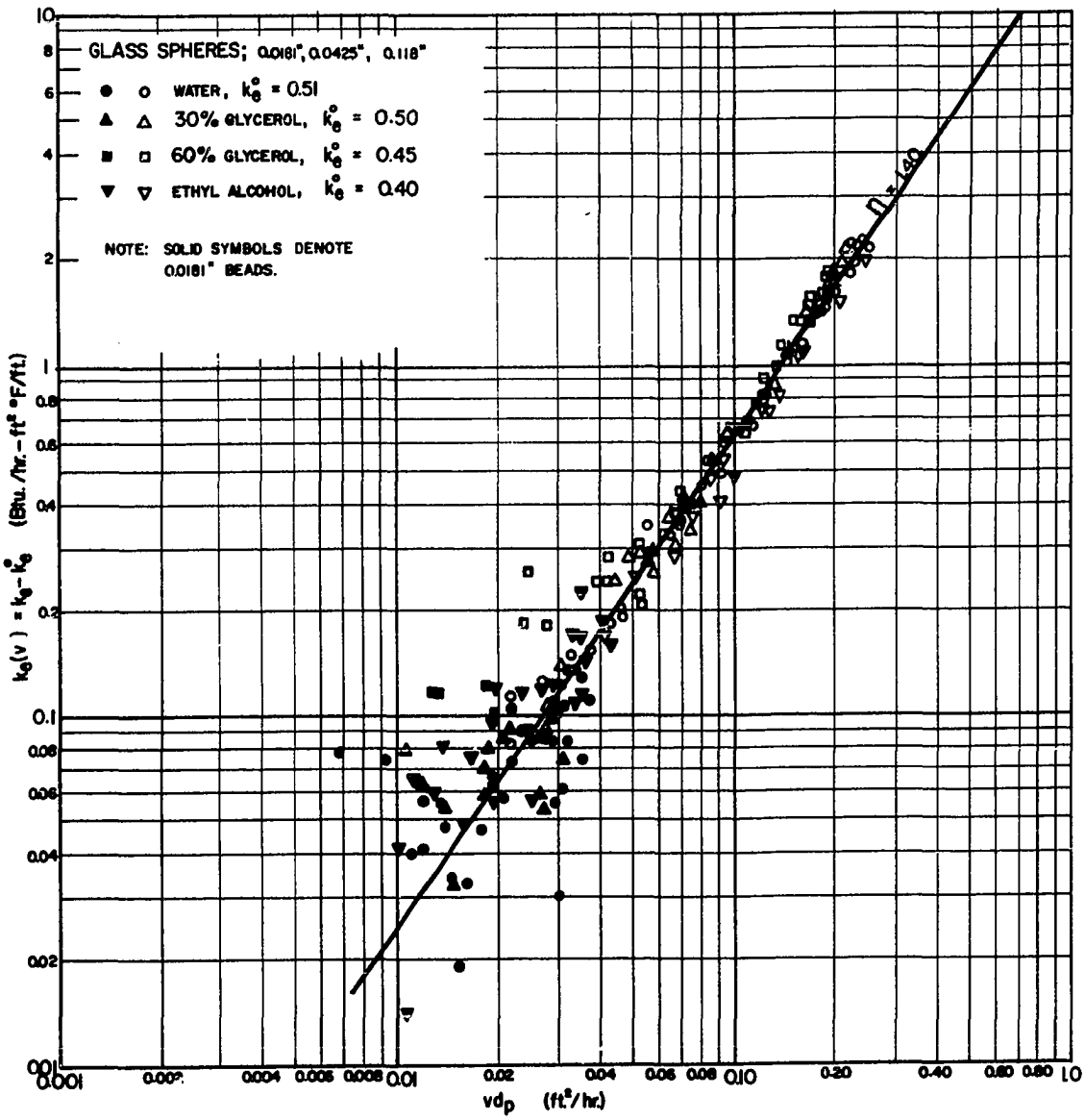

Figure 27- Velocity Component of the Effective Thermal Conductivity; All Liquid Systems

value of the group $(2k_e/\rho_w C_w \phi\ v\ x)$ was between about .010 and .025. Therefore, the concept of added variances, or equivalently added conductivities, was used as a correlating technique.

$$k_e = k_e^{\circ} + k_{wm}\phi + k_{ha} \qquad \text{(III-32)}$$

It is assumed in this section that the rate of fluid-solid heat transfer is controlled primarily by the "film" resistance around the solid spheres. The intra-particle conduction resistance was calculated and is sufficiently small to be negligible within the accuracy of these data. The magnitude of the "film" resistance, characterized by k_{ha}, is determined from existing heat-transfer data. An eddy-dispersion contribution is then calculated as the remainder of $k_e(v)$ after subtraction of k_{ha}, and a correlating curve is developed for $k_{wm}\phi$. Eddy-dispersion values thus obtained are shown to be consistent with longitudinal mass-transfer data in the literature. Data from the two smaller bead-size packs were not used in the development of a correlation because of the large scatter of $k_e(v)$ at the lower vd_p range. However, the final correlating curve is compared to all of the experimental systems.

Fluid-Solid Heat Transfer

A finite rate of heat transfer between the fluid and solid particles results in a dispersion of thermal energy which, under the restrictions given, may be characterized by

Equation (III-34) where

$$K = \frac{k_{ha}}{\rho_w C_w \phi + \rho_s C_s (1-\phi)} \qquad \text{(V-8)}$$

and

$$k_{ha} = \frac{V_F^2 \left[\rho_s C_s (1-\phi)\right]^2}{ha} \qquad \text{(III-30)}$$

The assumption (to be checked later) has been made that the solid intra-particle resistance is negligible. Knowing the system properties, k_{ha} may be determined from heat-transfer coefficient data. The literature data available were previously discussed in Chapter II and a summary plot of representative low-velocity data is shown in Figure 51, Appendix M. Data at low Reynolds numbers Re <10, are relatively scarce.

The correlating curve (j_m vs. Re) of Dryden, Strang, and Withrow (43) was used to calculate ha. This curve was selected primarily because Dryden et al. obtained data in liquid systems at low flow rates, and further, the data are in good agreement with other available results. Thus, values of ha determined should be reasonably close to the true bed value for this work. To check on the effects of using an alternate "j" factor correlation, calculations were also made using the correlation of Yoshida, Ramasuami, and Hougen (190).

The particle surface area per unit volume of bed, "a," was calculated from

$$a = \frac{6(1-\phi)}{d_p} \qquad \text{(V-9)}$$

In Figure 28, a typical plot of k_{ha} vs. vd_p, as determined from the data of Dryden et al., is presented for all the liquid systems. Calculated values for runs of the .0425 inch and .118 inch sphere systems are given in Appendix J. Also, in Figure 52, Appendix M, k_{ha} as determined from the Yoshida et al. correlation is presented.

Solid Intra-Particle Resistance. The solid-phase, intra-particle resistance to heat transfer results in an effective longitudinal conductivity shown in Appendix K to be

$$k_{s(ha)} = \frac{V_F^2 \left[\rho_s C_s (1-\phi)\right]^2 d_p^2}{60\, k_{sc}(1-\phi)} \qquad \text{(V-10)}$$

The total thermal-energy dispersion resulting from a finite fluid-solid heat-transfer rate is then characterized by $\left(k_{ha} + k_{s(ha)}\right)$. This expression (V-10) was derived from the work of Deisler (39). A basic assumption is that any given solid particle is surrounded by fluid at a constant temperature. While this assumption is not compatible with the idea of longitudinal molecular conduction through the solid phase, Equation (V-10) may be used as a first estimate of the intra-particle resistance.

Calculated values of $k_{s(ha)}$ are tabulated in Table 6 for the water and ethyl alcohol systems. The maximum values of $k_{s(ha)}$ are as high as .30 for water at a vd_p of .246, and .13 for ethyl alcohol at the same vd_p. This amounts to about 10% and 5% respectively of the total measured k_e for these systems at the given conditions. Intermediate percentages

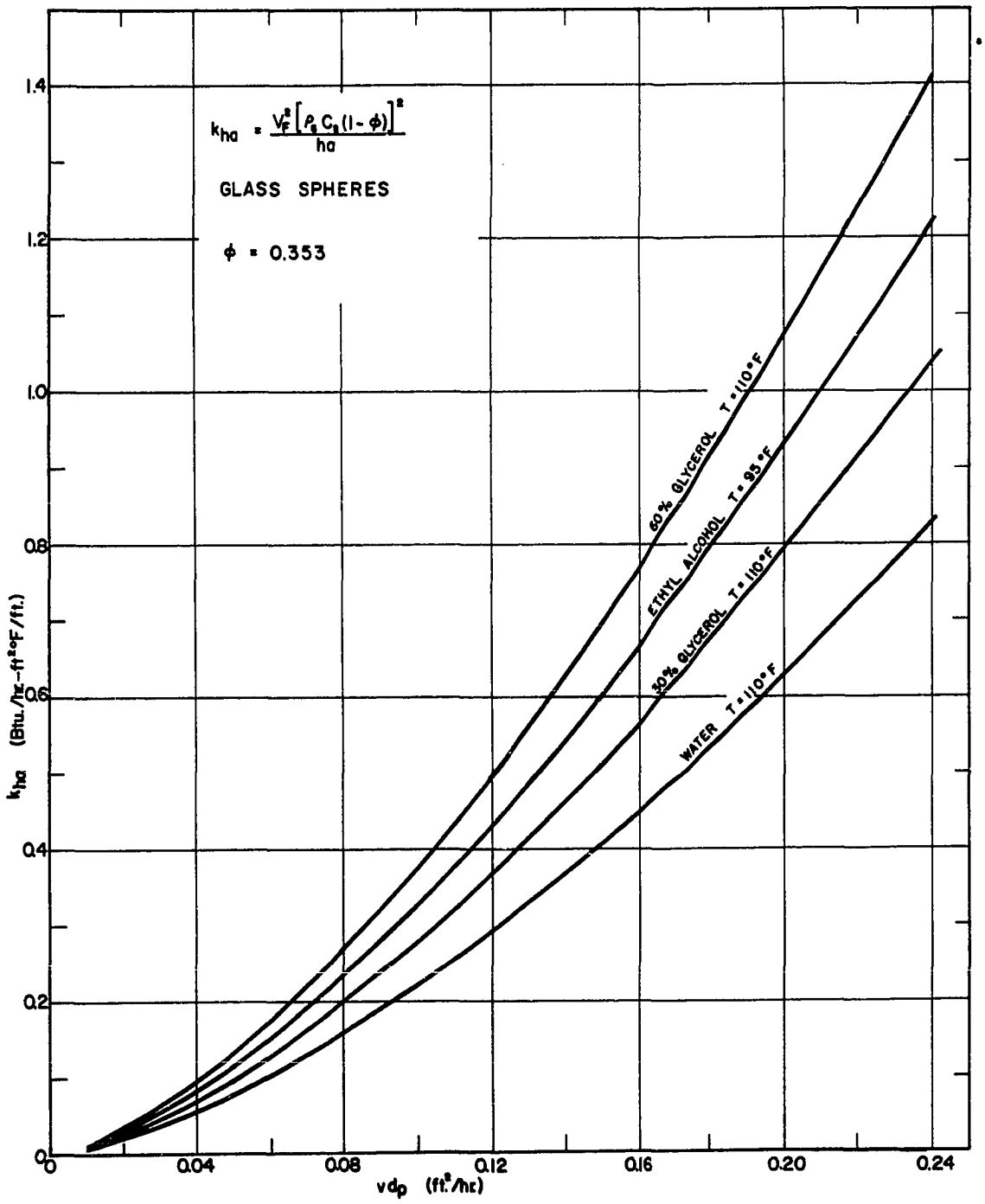

Figure 28- k_{ha} vs. vd_p; Heat-Transfer Coefficient Data from Dryden, Strang, Withrow

TABLE 6

SOLID-PHASE, INTRA-PARTICLE RESISTANCE

I. System: Water-Glass Spheres
T_{avg} = 120°F ϕ = .353

vd_p	$k_{s(ha)}$
.246	.30
.197	.19
.147	.11
.098	.049
.049	.012

II. System: Ethyl Alcohol - Glass Spheres
T_{avg} = 100°F ϕ = .353

vd_p	$k_{s(ha)}$
.246	.13
.197	.085
.147	.048
.098	.021
.049	.005

were obtained for the glycerols. While the magnitude of these numbers is noteworthy, the contribution of $k_{s(ha)}$ in the experimental range investigated is considerably smaller than the other mechanisms considered. At its maximum contribution, it is just at the limits of experimental error. Further, the uncertainty in the ha data used to obtain k_{ha} does not seem to warrant inclusion of $k_{s(ha)}$ in the present correlation calculations. It is stressed that under other experimental conditions (e.g., beads of lower molecular conductivity, larger vd_p) the effects of $k_{s(ha)}$ should be accounted for. Babcock (6) has treated this problem.

Data taken by Babcock (6) on overall longitudinal effective thermal conductivities in a water-lead bead (.118 inch) porous medium also substantiate the assumption that $k_{s(ha)}$ may be neglected here. Values of $k_e(v)$, at measurements taken over a vd_p range of .07 to .25, were essentially in agreement with glass-water data. However, a large absolute error in the water-lead $k_e(v)$ data, resulting because k_e^o was relatively large, prevented the dectection of small differences between the two data sets.

Eddy Dispersion

The eddy-dispersion component of $k_e(v)$ was calculated as the difference between $k_e(v)$ and k_{ha}.

$$k_{wm}\phi = (k_e - k_e^o) - k_{ha} \qquad \text{(V-11)}$$

These data (for the .0425 and .118 inch beads) are plotted in Figure 29 as a function of vd_p and are tabulated in Appendix

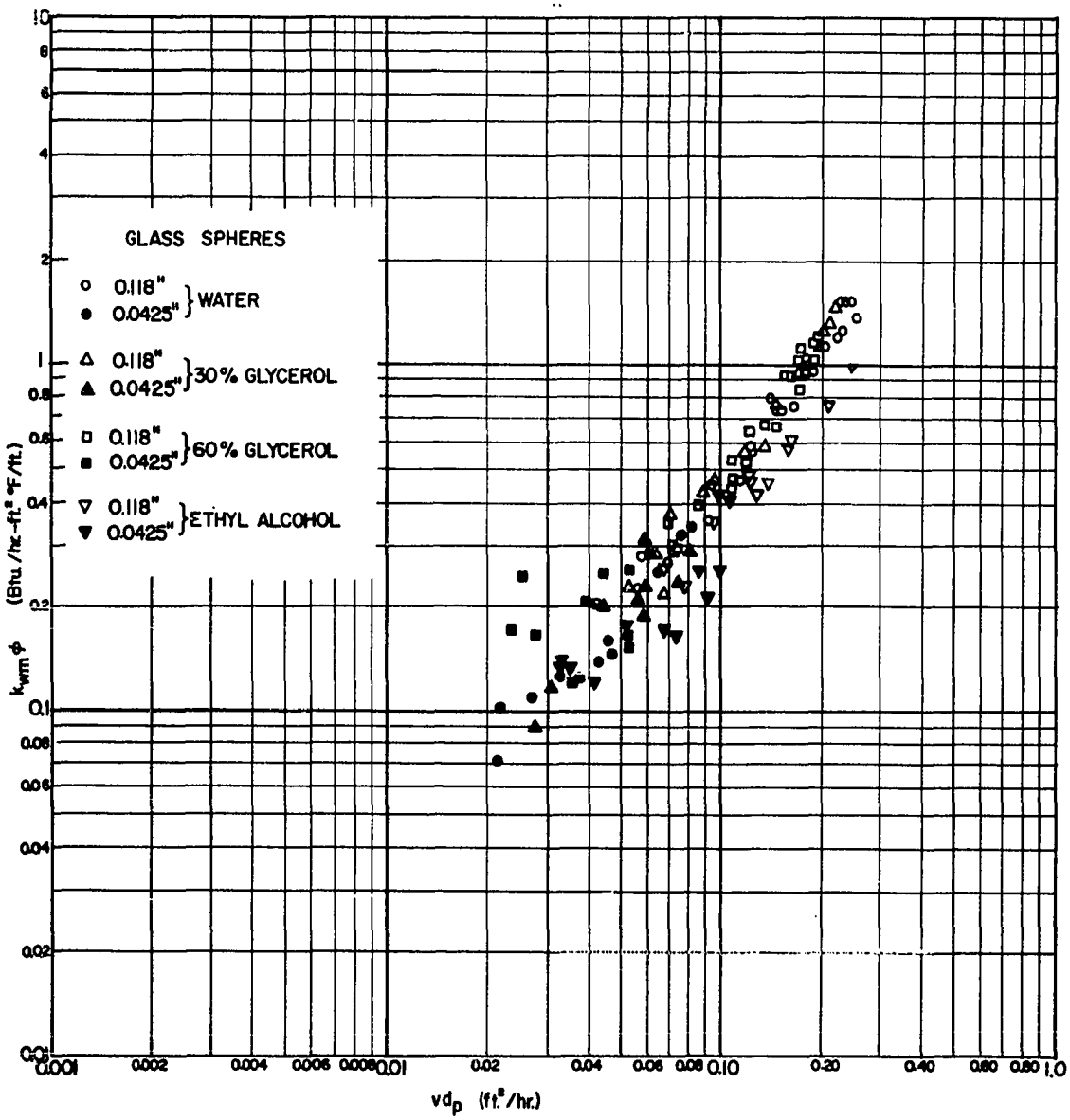

Figure 29- Eddy-Dispersion Component of the Effective Thermal Conductivity; k_{ha} from Dryden, Strang, Withrow Data; All Liquid Systems

J. A regression analysis of the water and ethyl alcohol data showed the best lines through the two data sets to be parallel but not coincident at a 95% confidence limit.

The eddy-dispersion conductivities are shown to be in agreement with available literature data and a correlating curve for $k_{wm}\phi$ is then developed.

Comparison of $k_{wm}\phi$ to Literature Data. While no thermal-energy longitudinal eddy-dispersion data are available at the experimental conditions of this investigation, several studies have been made for mass transfer. These were discussed in Chapter II, where the difference in results obtained in liquid systems and gas systems was described.

In Figure 30, data from this study for the water and alcohol systems, as well as the literature mass-transfer data, are shown as a plot of Pe versus Re, where

$$Pe = \frac{vd_p}{E + D} \qquad (V\text{-}12)$$

and for heat transfer

$$E_h + D_h = \frac{(k_{wm}\phi + k_{wc}\phi)}{\rho_w C_w \phi} \qquad (V\text{-}13)$$

This plot is only for comparison purposes. The heat-transfer results are in good agreement with the gas-phase mass-transfer work of McHenry and Wilhelm (120) and are somewhat below the Pe_m values of Deisler (39, 40). The heat-transfer Pe numbers are considerably above those for eddy dispersion of mass in liquid systems. For the systems shown, the molecular contributions are as follows; (1) D_m is negligible in the

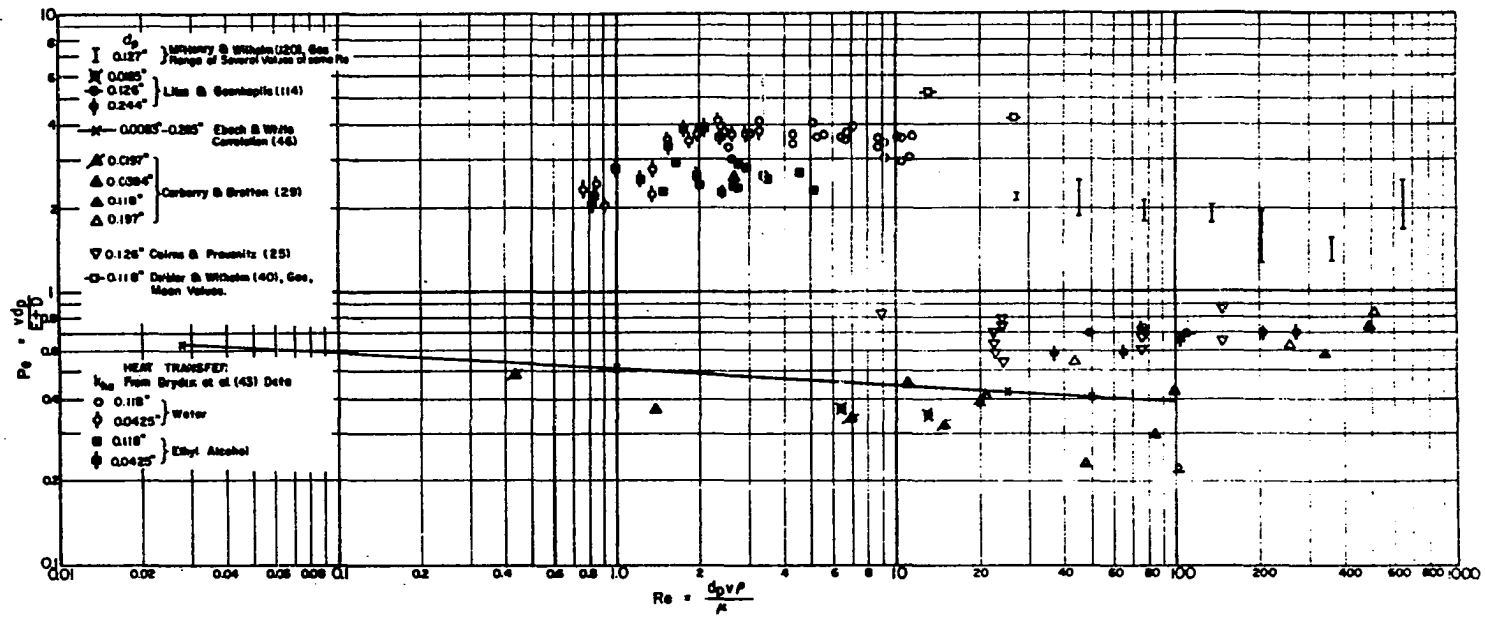

Figure 30- Peclet Number vs. Reynolds Number; Heat-and Mass-Transfer Data

liquid-phase mass-transfer data, (2) D_m is approximately 30% of $(E_m + D_m)$ in the gas-phase mass-transfer data at a Reynolds number of 27, and (3) D_h is about 8% of $(E_h + D_h)$ in the heat-transfer results at a Reynolds number of 11. The relative importance of D decreases with increasing Re.

In Figure 31, water and ethyl alcohol data of this investigation are compared to the mass-transfer results in a plot of E versus vd_p. It is shown in this graph also that the eddy diffusivities for heat transfer and gas-phase mass transfer fall below the liquid-phase mass-transfer results.

According to the model of Keulemans (95) for eddy dispersion,

$$E = \eta \ vd_p \qquad \text{(II-32)}$$

where η is a constant characteristic of the porous medium. At the same Reynolds number therefore, two geometrically similar packed-bed systems should have the same η value, resulting in the Pe numbers being equal for the two systems (provided molecular diffusivities are equal). However, mass-transfer results with liquids and gases are quite different, necessitating an explanation.

A proposed reason has been discussed by several authors (17, 56, 71), and is based on the results obtained by Taylor for dispersion in flow through a capillary tube. Because of velocity profiles which develop in the pores and due to fluid "trapping" etc., some of the fluid in the pores will be by-passed by the displacing fluid, at least temporarily.

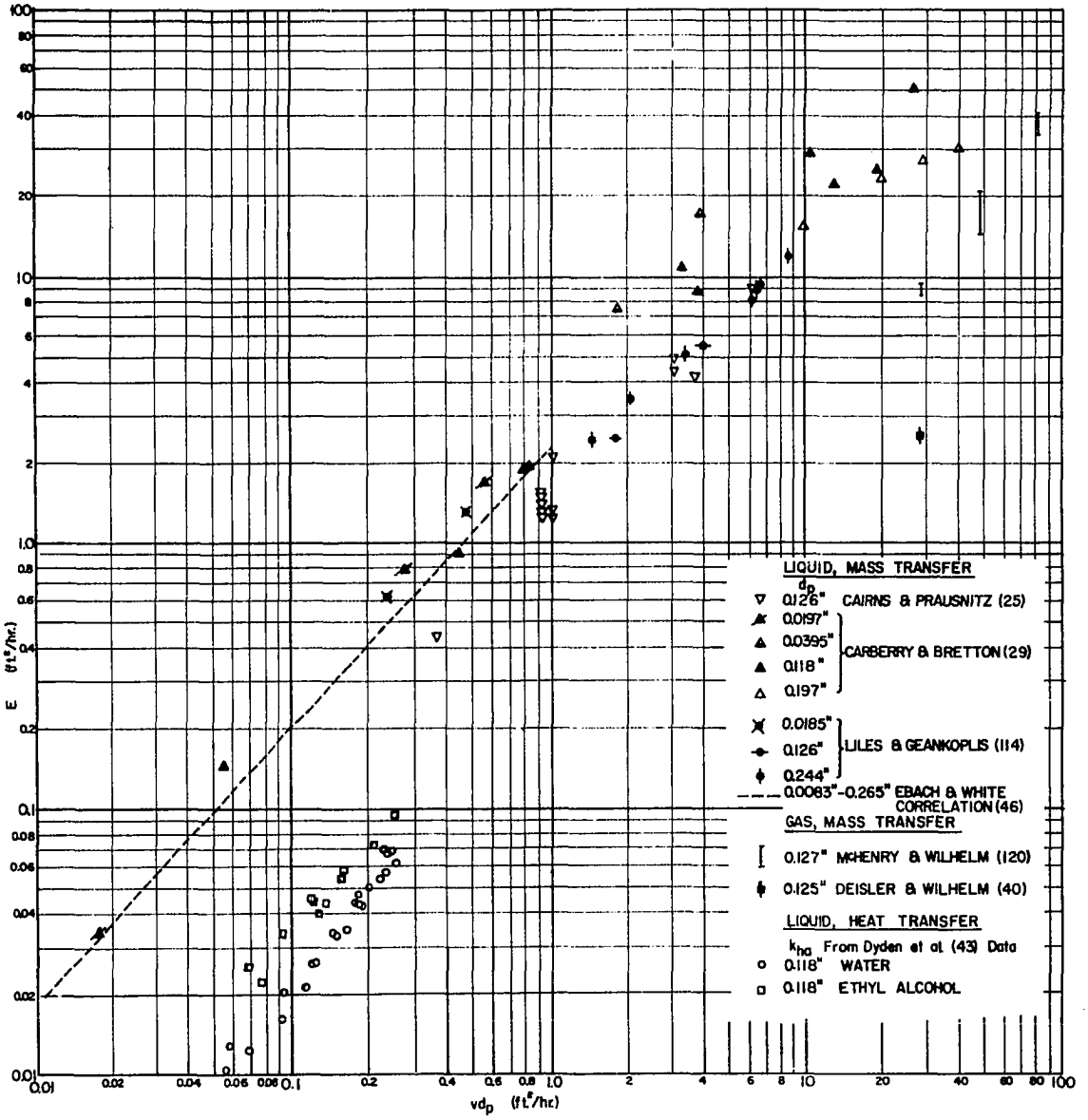

Figure 31- Eddy Diffusivity vs. vd_p; Heat-and Mass-Transfer Data

This by-passed fluid will approach the main stream concentration by a molecular conduction process. The result of this by-passing is a greater longitudinal dispersion of mass, the dispersion becoming greater as the molecular diffusivity is decreased. Conversely, if the fluid has a very high molecular diffusivity, concentration gradients normal to the flow direction which result because of by-passing will be quickly diminished and the resulting longitudinal eddy dispersion will be reduced. This effect is characterized by (56)

$$E \sim \frac{v^2}{D} \qquad \text{(II-34)}$$

Thus, on this basis, the difference between the gas-and liquid-phase mass-transfer data is at least qualitatively explained.

For the case of heat transfer, the molecular thermal diffusivity lies intermediate to the values for liquid and gas mass diffusion. In addition, molecular conduction through the solid particles, as well as conduction from the bulk fluid, will act to bring the "by-passed" fluid up to the main-stream temperature. Therefore, the effect of molecular conduction through the solid should be to decrease the longitudinal eddy dispersion. Qualitatively then, with liquids flowing, the eddy-dispersion coefficient for heat transfer would be expected to be smaller than for the corresponding mass-transfer case. This was the result obtained experimentally.

Correlation of Eddy Diffusivity. The two mechanisms, Equation (II-32) and (II-34), are not additive but, a correlating equation of the following form is suggested (15, 17),

$$\frac{E}{D} = \eta \left(\frac{vd_p}{D}\right)^m \qquad (V\text{-}14)$$

where η and m are constants obtained from experimental data and where m is greater than one. The $k_{wm}\phi$ data are plotted in Figure 32 with E/D as a function of vd_p/D. A least squares fit to all the data with a vd_p value greater than .03 yielded $\eta = .115$, and $m = 1.25$.

$$\frac{E}{D} = .115 \left(\frac{vd_p}{D}\right)^{1.25} \qquad (V\text{-}15)$$

This curve is also shown in Figure 32.

Equation (V-15) was tested against the mass-transfer data of several investigators. A plot of this equation and the gas-phase dispersion results of McHenry and Wilhelm (119, 120) and Deisler (39, 40) is given in Figure 33. In Figure 34, the equation is compared to the results of liquid-phase mass-transfer investigations (12, 29, 114). Sample calculations are shown in Appendix F. Over this wide range of fluid systems, Equation (V-15) does appear to satisfactorily correlate the effect of the fluid-phase molecular diffusivity. However, as previously discussed, for heat transfer conduction through the solid particles should act to decrease the measured eddy-dispersion coefficient. This effect has not been included in Equation (V-15). Further investigation with solid

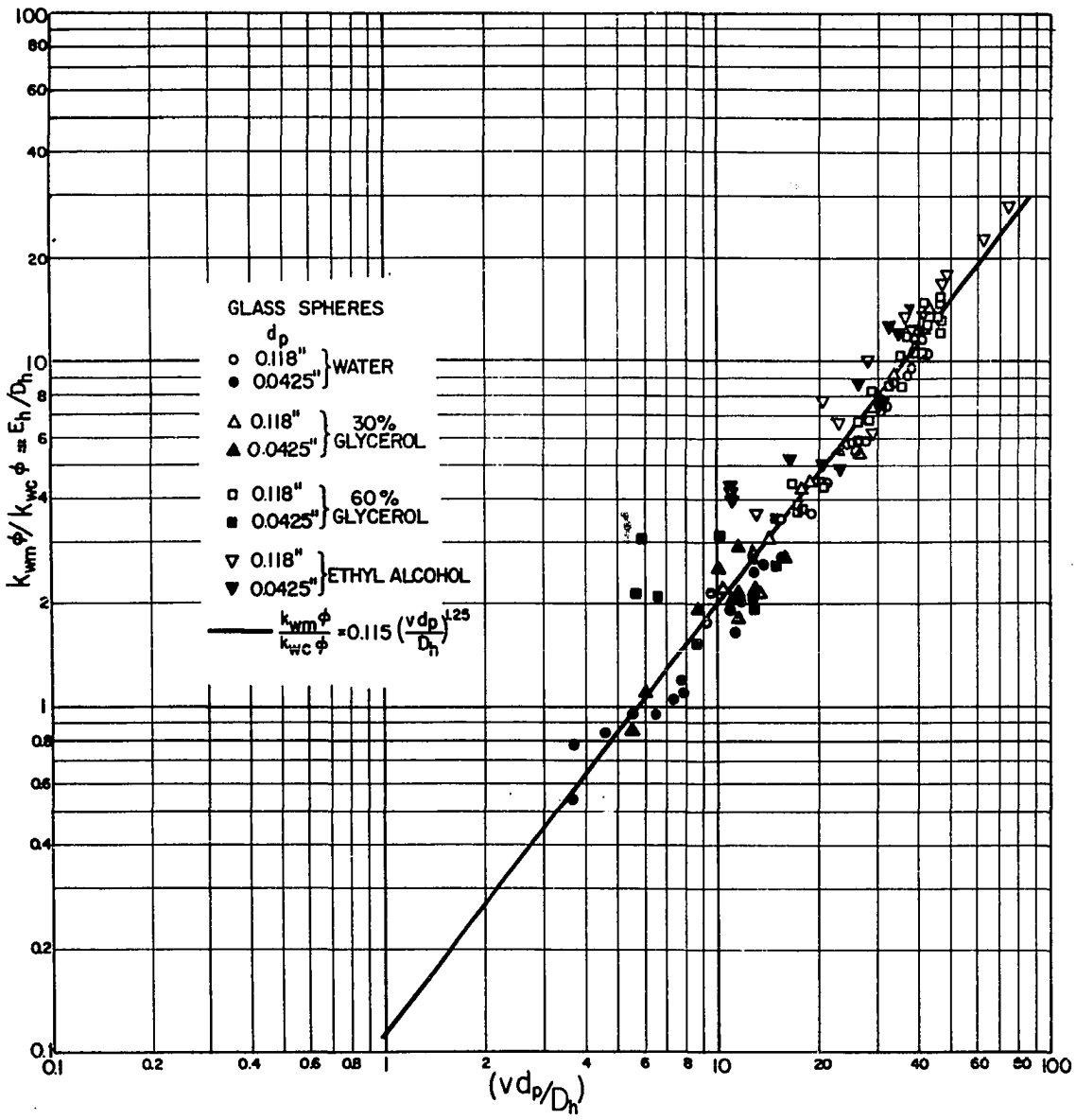

Figure 32- Correlation of Eddy-Dispersion Data; E/D vs. (vd_p/D); k_{ha} from Dryden, Strang, Withrow Data

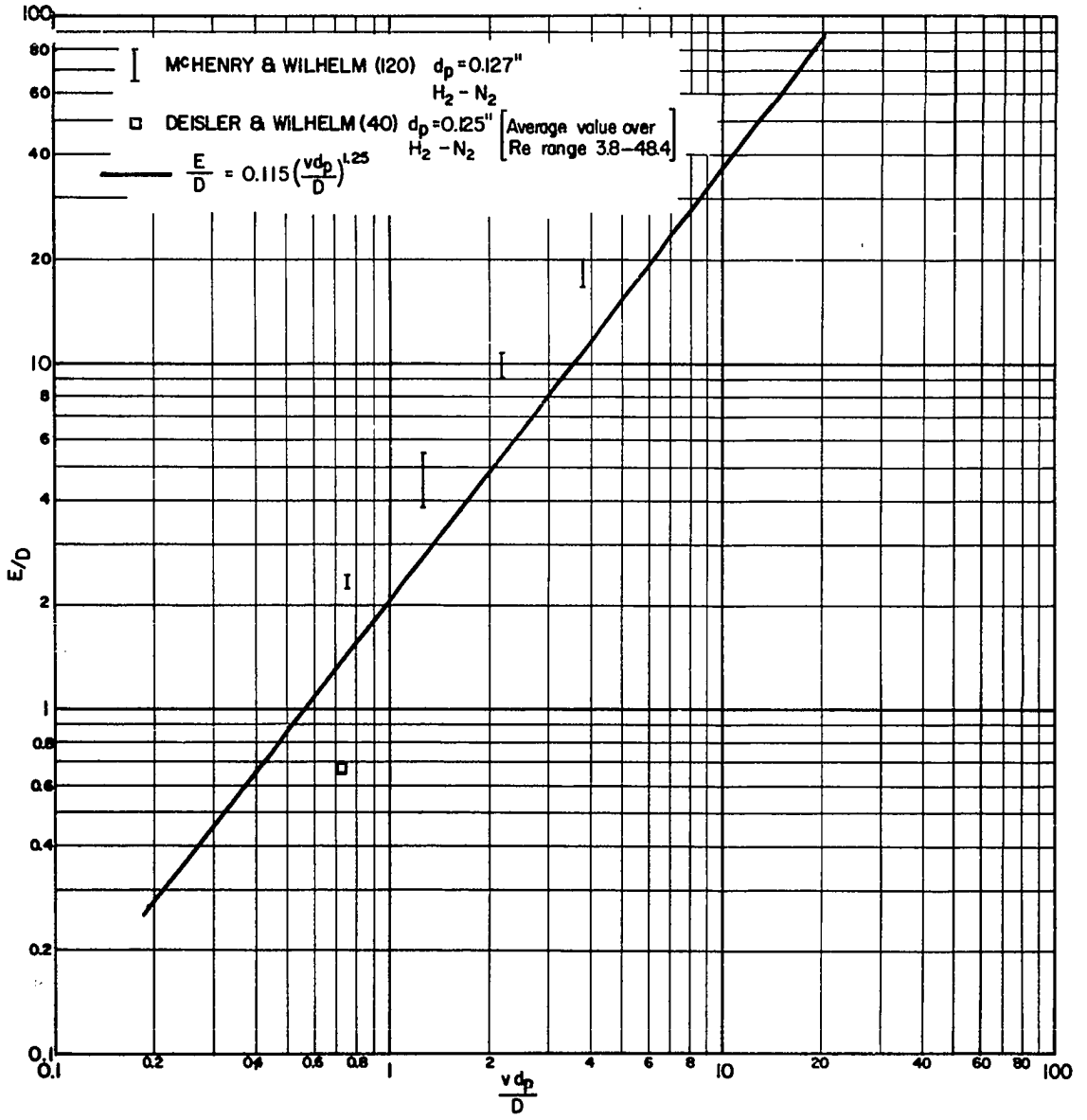

Figure 33- Comparison of Equation (V-15) with Gas-Phase, Mass-Transfer Data

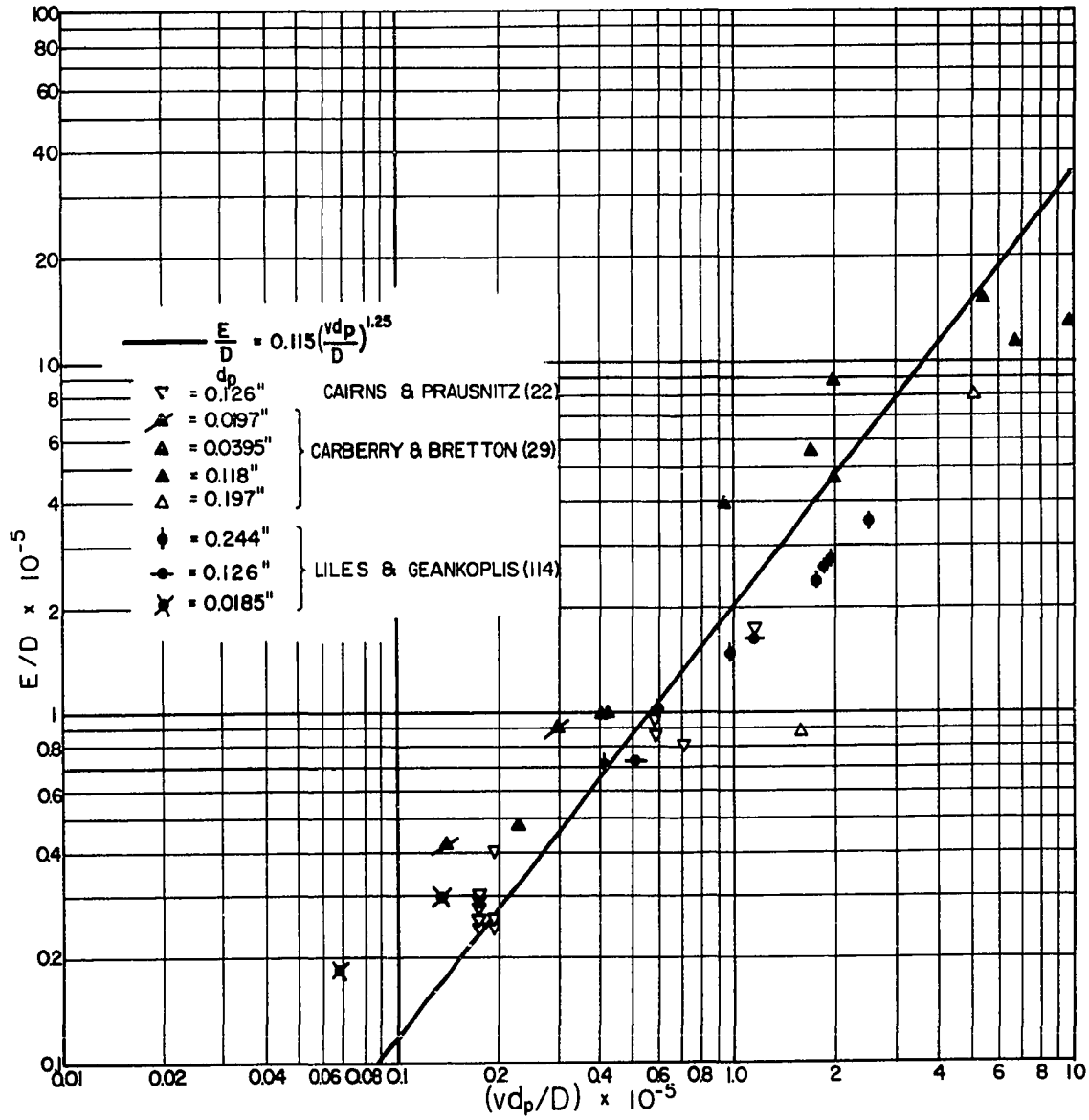

Figure 34- Comparison of Equation (V-15) with Liquid-Phase, Mass-Transfer Data

packing of different characteristics is required to establish the importance of this solid-conduction mechanism.

Babcock (6) measured the longitudinal effective thermal conductivities in a system of glass beads (.118 inch) and Soltrol "130" (Phillips Petroleum Company trade name for a hydrocarbon mixture; see Table 16 for physical properties). Eddy diffusivities were determined from the Babcock data in the same manner as for data of this investigation. These are plotted in Figure 35 along with Equation (V-15), where the agreement is poor. This discrepancy has not been explained, but two possible reasons may be:

(1) The calculated heat-transfer coefficients used in the determination of k_{ha} and subsequently $k_{wm}\phi$, are too high. A lower ha would increase k_{ha}, decreasing $k_{wm}\phi$, and bring the data into better agreement.

(2) As discussed, the conduction of heat through the solid beads serves to decrease the eddy-dispersion coefficient. This effect has not been included in Equation (V-15) as its importance is not known.

Correlation of Eddy Diffusivity; k_{ha} From Correlation of Yoshida, Ramasuami, Hougen. An analysis was made for all experimental data of this investigation, in which, k_{ha} values were calculated from the "j" factor correlation of Yoshida et al. (190) rather than the Dryden, et al. curve. The eddy-dispersion coefficient, $k_{wm}\phi$, was again taken as the remainder of $k_e(v)$ after subtraction of k_{ha}. The resulting plot of

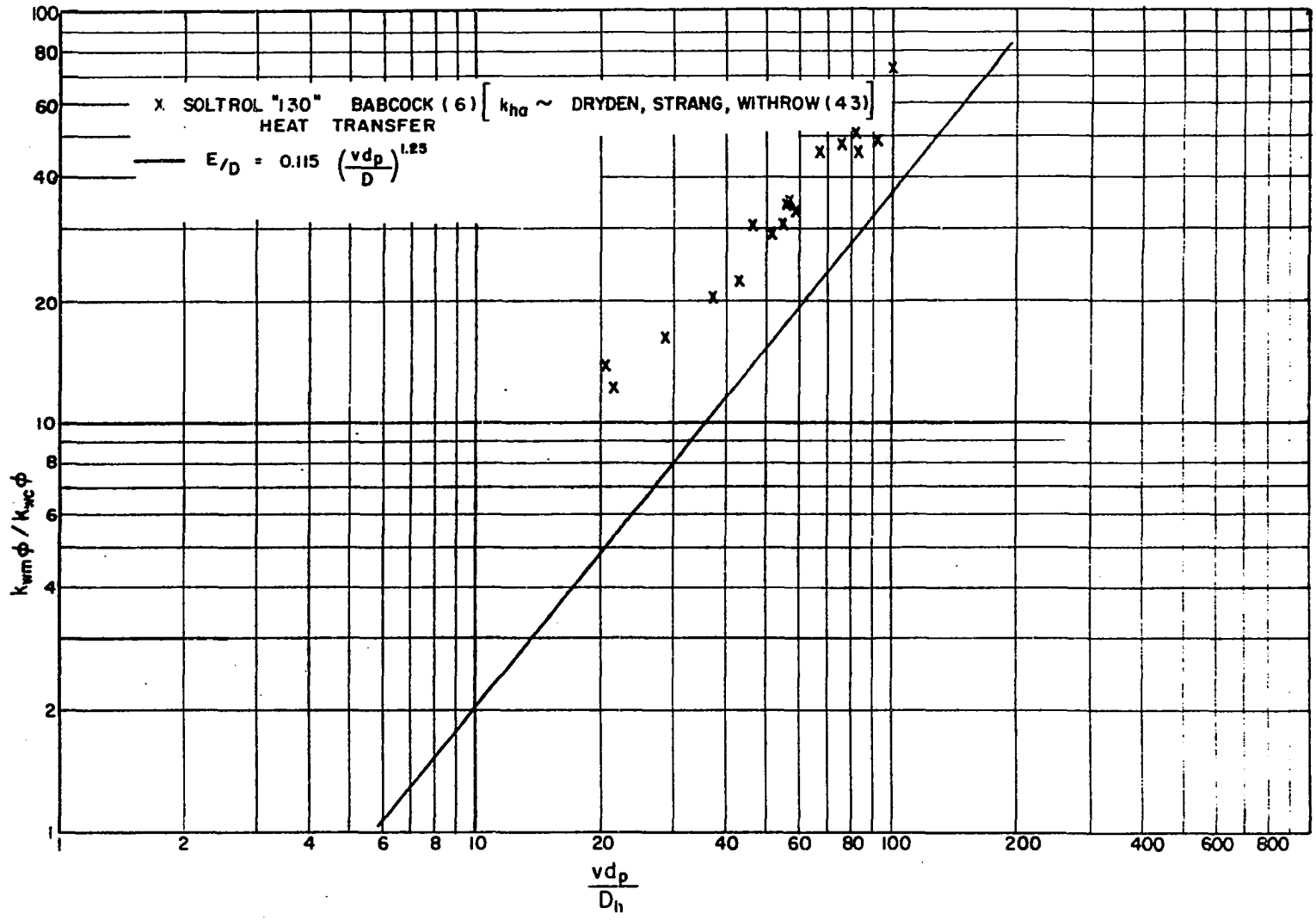

Figure 35- Comparison of Equation (V-15) with Heat-Transfer Data of Babcock

$(k_{wm}\phi/k_{wc}\phi)$ vs. (vd_p/D_h) is shown and the calculations discussed in Appendix M.

Summation of Conductivities

The total effective conductivity, k_e is assumed to be the sum

$$k_e = k_e^o + k_{wm}\phi + k_{ha} \qquad \text{(III-32)}$$

In summary, the individual conductivities on the right hand side of the equation have been determined as follows:

(1) The static conductivity, k_e^o, was obtained by extrapolation of the k_e data to zero fluid velocity. Values of k_e^o are given in Table 5.

(2) The effective dispersion coefficient, k_{ha}, was calculated from Equation (III-30), with the 'j' factor correlation of Dryden et al. (43) being used to obtain ha (Figure 28).

(3) A correlating curve, Equation (V-15), was developed for the eddy-dispersion coefficient, $k_{wm}\phi$. This curve resulted from an empirical "fit" to the $k_{wm}\phi$ values calculated from experimental data.

The resulting predictive curves of k_e are presented along with the data for the water and ethyl alcohol systems in Figures 36 and 37. Calculated conductivities are given in Table 7. The glycerol data of this investigation are shown as Figures 54 and 55 and Table 28 of Appendix M. The maximum deviation of the data from the predictive curves is $\pm$ 15%.

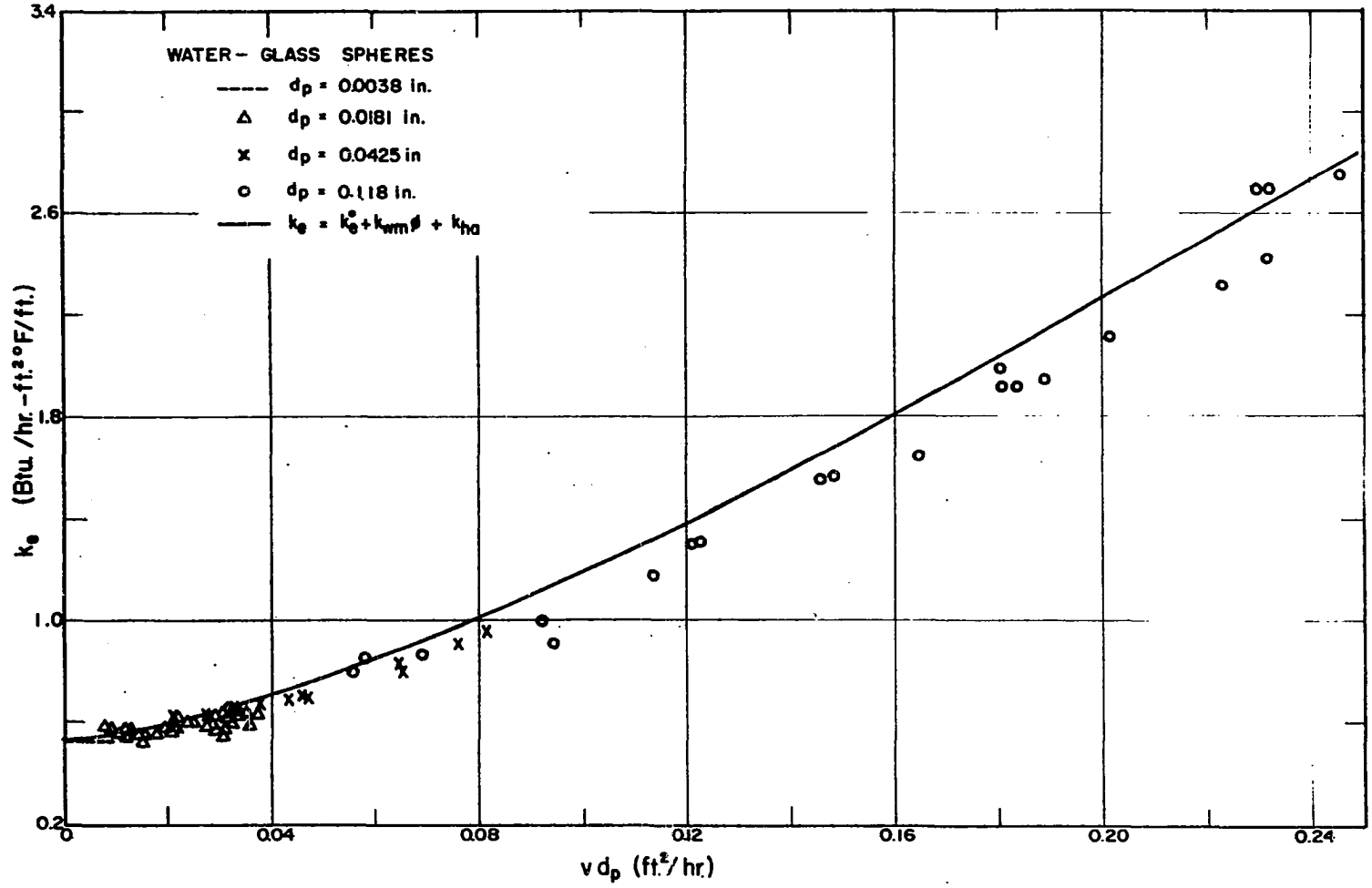

Figure 36- Summation of Conductivities; k_{ha} from Dryden, Strang, Withrow Data; Water System

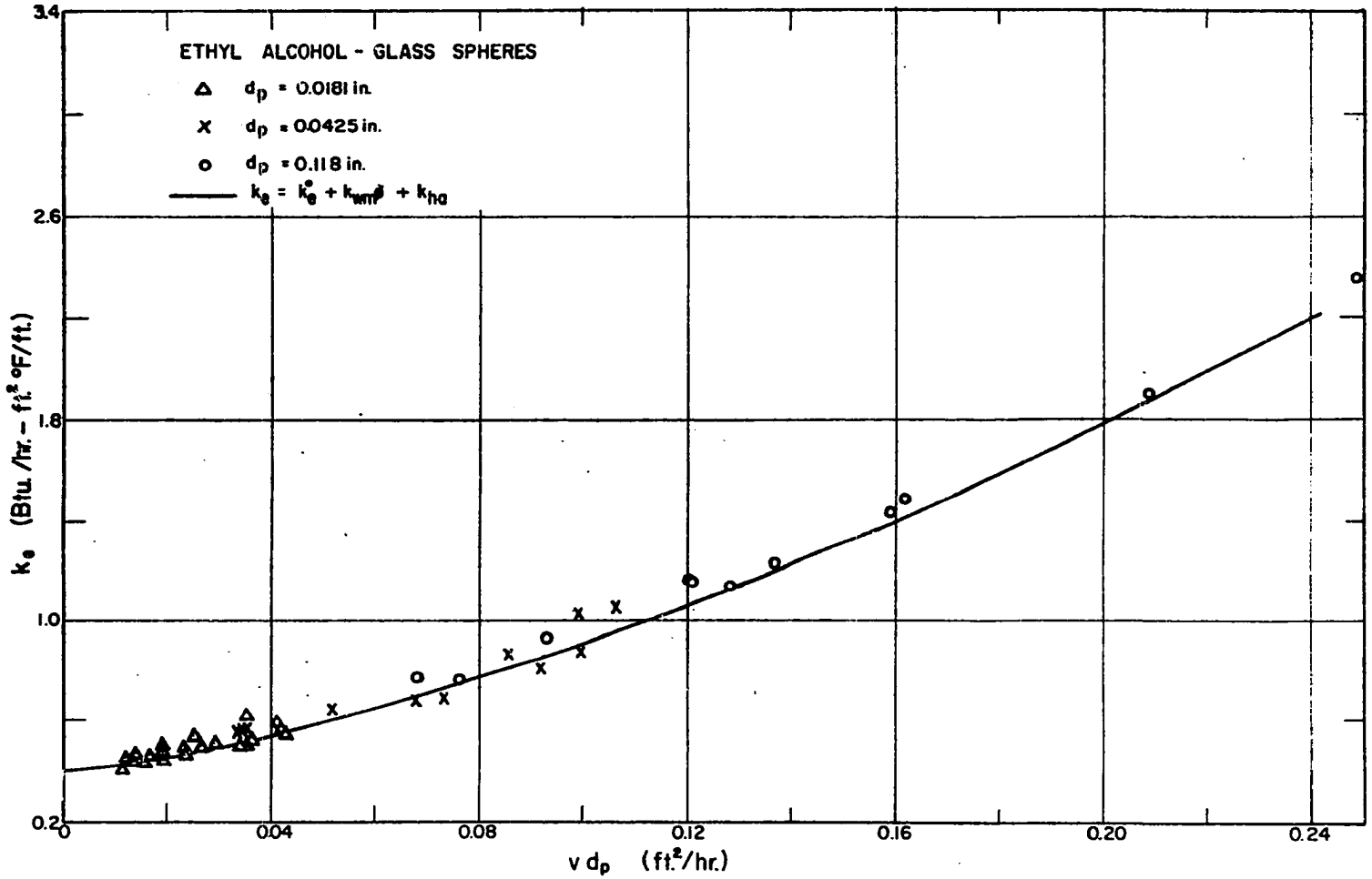

Figure 37- Summation of Conductivities; k_{ha}
from Dryden, Strang, Withrow Data; Ethyl Alcohol System

TABLE 7

SUMMATION OF CONDUCTIVITIES; k_{ha} FROM DRYDEN, STRANG, WITHROW DATA; WATER AND ETHYL ALCOHOL SYSTEMS

Water: T = 110°F ϕ = .356

vd_p	k_e^o	k_{ha}	$k_{wm}\phi$	k_e
.01	.51	.003	.029	.542
.02		.009	.069	.588
.05		.050	.218	.778
.10		.161	.520	1.191
.15		.319	.860	1.689
.20		.520	1.230	2.260
.24		.705	1.53	2.745

Ethyl Alcohol: T = 95°F ϕ = .356

vd_p	k_e^o	k_e(ha)	$k_{wm}\phi$	k_e
.01	.40	.004	.016	.420
.02		.027	.038	.465
.05		.065	.121	.586
.10		.213	.288	.901
.15		.422	.475	1.297
.20		.698	.680	1.778
.24		.933	.850	2.183

Literature Data. Babcock (6) measured overall effective thermal conductivities in a Soltrol "130" (Phillips Petroleum Co.) - glass bead system. These data and the predicted curve are shown in Figure 56, of Appendix M. The predicted curve is approximately 35% low.

Hadidi (76) conducted a limited number of cooling run experiments in a water-glass sphere (140-170 mesh) system of the same general type as used in this investigation. He found k_e to be a constant, equal to 0.6 Btu/hr-ft^2°F/ft, at liquid velocities up to 7.6 ft/hr. This is in agreement with the present work.

Preston (138) made a similar analysis to that of Hadidi. However, his experimental runs were all heating runs, i.e., the packed bed was first cooled and then hot liquid was injected into the bed. These results are discussed in Appendix L along with additional work of this investigation.

Steady-state longitudinal effective thermal conductivities were measured by Kunii and Smith (106) in both liquid and gas systems and by Yagi et al. (189) in gas systems. However, the results of the present investigation do not appear to be directly applicable to the steady-state case. This is so for two reasons:

(1) At steady state, the longitudinal heat-transfer rate is not characterized by an addition of the variances for the different contributing heat-transfer mechanisms.

(2) The correlation for eddy dispersion, Equation

(V-15), includes the effect of interaction between temporary fluid by-passing and trapping within the bed, and molecular conduction which serves to bring the fluid in these "trapped" areas up to the main-stream temperature. As discussed by Gottschlich (71), this effect should not be a significant contribution at steady state.

CHAPTER VI

SUMMARY AND CONCLUSIONS

A fluid is considered as being in one-dimensional, steady, piston flow through a homogeneous porous medium. At the entrance face, a step function in temperature is imposed on the injected fluid. The resulting heat front (or cold front), moves through the porous medium, with thermal energy being dispersed in the direction of fluid flow and away from the mean heat-front position by a combination of heat-transfer mechanisms. The particular dispersion mechanisms of molecular conduction, eddy dispersion, and a finite fluid-solid heat-transfer rate were considered.

General differential equations describing the rate of heat transfer were solved numerically using a digital computer. Since the computing time necessary to carry out the numerical calculations was prohibitive, an approximate solution was developed based on the previous work of Van Deemter et al. (175), and Klinkenberg and Sjenitzer (100). To arrive at the approximation, variances for the different heat-transfer mechanisms were shown to be additive under prescribed conditions of parameter sizes.

The mathematical model was checked experimentally with a system which consisted essentially of a homogeneous packed bed of spherical particles. Provision was made to approximate the injection of a temperature step function at the bed entrance, and to measure the response temperature profile at a position down the bed. Liquid systems flowing at relatively low velocities were investigated.

Effective longitudinal thermal conductivities were determined from experimental time-temperature data using the conduction-equation solution. These k_e values were correlated assuming them to be the sum of the contributions from the individual mechanisms, k_e^o, $k_{wm}\phi$, and k_{ha}, in accordance with the mathematical model. The static component, k_e^o, was obtained by extrapolation of k_e data to zero velocity. The "j" factor correlation of Dryden et al. (43) provided a means of calculating ha and correspondingly k_{ha}. Finally, the eddy-dispersion contribution was obtained as the remainder of k_e after subtraction of k_e^o and k_{ha}. These $k_{wm}\phi$ values were compared to literature mass-transfer data, and an empirical correlating curve was developed for eddy dispersion.

Conclusions

The following main conclusions may be drawn from the results of this investigation.

1. The solution to the general differential equations, which include several mechanisms for transient longitudinal

dispersion of thermal energy, may be approximated by a simple conduction-equation solution using an effective thermal conductivity which is equal to the sum of the contributing conductivities, where each is a measure of a separate mechanism. This is true within prescribed conditions of parameter sizes.

2. Experimental, longitudinal, thermal-energy dispersion data fit the conduction-equation solution as long as piston flow occurred. Values of the effective thermal conductivity, k_e, calculated from the data substantiate the additivity of the individual contributing conductivities: k_e^o, $k_{wm}\phi$, and k_{ha}.

3. Under prescribed conditions, transient longitudinal dispersion of thermal energy resulting from a finite heat-transfer coefficient between fluid and solid may be characterized by an effective conductivity, k_{ha}, and the equation for thermal conduction.

4. Values of k_e obtained from data for a given liquid increase as a smooth function of the product of interstitial velocity and particle size, i.e., vd_p. For the systems studied, at vd_p values less than about .01, k_e may be assumed a constant equal to the static conductivity, k_e^o, with only small error.

5. The correlation developed for eddy dispersion adequately describes the effect of the molecular diffusivity on the eddy-dispersion coefficient. The effect of solid-phase conduction on eddy dispersion should be investigated further.

BIBLIOGRAPHY

1. Anzelius, A., Zeit. fur angew. Math. und Mech, 6 (1926), p. 291.

2. Amundson, N. R. "Solid-Fluid Interactions in Fixed and Moving Beds," Ind. and Eng. Chem., 48 (January, 1956), p. 26.

3. Argo, W. B. and Smith, J. M. "Heat Transfer in Packed Beds," Chem. Eng. Prog., 49 (August, 1953), p. 443.

4. Aris, R. and Amundson, Neal R. "Some Remarks on Longitudinal Mixing or Diffusion in Fixed Beds," A.I.Ch.E. Journal, 3 (1957), p. 280.

5. Arley, N. and Buch, K. R. Introduction to the Theory of Probability and Statistics. New York: John Wiley and Sons, 1950.

6. Babcock, R. E. "Axial Effective Thermal Conductivity of Porous Media," University of Oklahoma Thesis (M.Ch.E.), 1962.

7. Bailey, H. R. and Larkin, B. K. "Conduction-Convection in Underground Combustion," Paper presented at San Francisco, California Meeting of A.I.Ch.E., December 6-9, 1959.

8. _____. "Heat Conduction in Underground Combustion," Paper #1134-G, 33rd Annual Meeting of the Society of Petroleum Engineers, (October, 1958).

9. Baron, T. "Generalized Graphical Method for the Design of Fixed Bed Catalytic Reactors," Chem. Eng. Prog., 48 (March, 1952), p. 118.

10. Baumeister, E. B. and Bennett, C. O. "Fluid-Particle Heat Transfer in Packed Beds," A.I.Ch.E. Journal, 4 (1958), p. 69.

11. Beran, M. J. Harvard University Dissertation (Ph.D.), May, 1955.

12. Bernard, R. A. and Wilhelm, R. H. "Turbulent Diffusion in Fixed Beds of Packed Solids," Chem. Eng. Prog., 46 (May, 1950), p. 233.

13. Berry, V. J., Jr. and Parrish, D. R. "A Theoretical Analysis of Heat Flow in Reverse Combustion," Paper presented at San Francisco, California Meeting of A.I.Ch.E., (December 6-9, 1959).

14. Bird, R. B., Stewart, W. E. and Lightfoot, E. N. Notes On Transport Phenomena. New York: John Wiley and Sons, 1959.

15. Blackwell, R. J., Terry, W. M. and Rayne, T. R. "Factors Influencing the Efficiency of Miscible Displacement," Trans. A.I.M.E., 217 (1959), p. 1.

16. Bland, D. R. "Mathematical Theory of the Flow of Gas in a Porous Media and Associated Temperature Distribution," Proceedings of the Royal Society, London, A 221, (1954), p. 1.

17. Brigham, W. E., Reed, P. W. and Dew, J. H. "Experiments on Mixing During Miscible Displacement In Porous Media," Presented at 52nd Annual Meeting, A.I.Ch.E., San Francisco, California, (December 6-9, 1959).

18. Brotz, W. "Transport Processes in Fixed and Fluidized Beds of Solids," Chem. Eng. Tech., 28 (1956), p. 165.

19. Brown, G. G. Unit Operations. New York: John Wiley and Sons, 1951.

20. Brownlee, K. A. Statistical Theory and Methodology in Science and Engineering. New York: John Wiley and Sons, Inc., 1960.

21. Brunnell, D. G., Irvin, H. B., Olson, R. W. and Smith J. M. "Effective Thermal Conductivities in Gas-Solid Systems," Ind. and Eng. Chem., 41 (September, 1949), p. 1977.

22. Cairns, E. J. "Mixing Properties and Chemical Kinetics in Chemical Flow Reactors," University of California Dissertation (Ph.D.), 1959.

23. Cairns, E. J. and Praunitz, J. M. "Longitudinal Mixing in Packed Beds," Part I, Paper, University of California, Berkeley, (1958).

24. _____. "Longitudinal Mixing in Packed Beds," Part II, Paper, University of California, Berkeley, (1958).

25. _____. "Longitudinal Mixing in Packed Beds," Chem. Eng. Sci., 12 (1960), p. 20.

26. _____. "Velocity Profiles in Packed and Fluidized Beds," Ind. and Eng. Chem., 51 (1959), p. 1441.

27. Campbell, J. M. and Huntington, R. L. "Heat Transfer and Pressure Drop in Fixed Beds of Spherical and Cylindrical Particles, II, Heat Transfer and Temperature Gradients," Pet. Refiner, 31 (1952), p. 123.

28. Carberry, J. J. "Axial Dispersion and Void Cell Mixing Efficiency in Fluid Flow in Fixed Beds," A.I.Ch.E. Journal, 4 (March, 1958) p. 13M.

29. Carberry, J. J. and Bretton, R. H. "Axial Dispersion of Mass in Flow Through Fixed Beds," A.I.Ch.E. Journal, 4 (1958), p. 367.

30. Carslaw, H. S. Introduction to the Mathematical Theory of the Conduction of Heat in Solids. New York: Dover Publications, 1945.

31. Carslaw, H. S. and Jaeger, J. C. Conduction of Heat in Solids. New York: Oxford at the Clarendon Press (Oxford University Press), 1959.

32. Chatanever, A. A.P.I. Research Project 49-B, Final Report, University of Oklahoma, Norman, Oklahoma, (1957).

33. Chu, P. C. and Storrow, J. A. "Heat Transfer to Air Flowing Through Packed Tubes," Chem. Eng. Sci., 1 (1952), p. 230.

34. Churchill, S. W., Abbrecht, P. H. and Chiao-Min, C. "Regenerative Heat Transfer in Two and Three Dimensional Flow Through Porous Media," Ind. and Eng. Chem., 49 (1957), p. 1007.

35. Colburn, A. P. "A Method of Correlating Forced Convection Heat Transfer Data and a Comparison with Fluid Friction," A.I.Ch.E. Transactions, 29 (1933), p. 174.

36. Collins, R. E. Flow of Fluids Through Porous Materials. New York: Reinhold Publishing Corporation, 1961.

37. Coppage, J. E. and London, A. L. "Heat Transfer and Flow Friction Characteristics of Porous Media," Chem. Eng. Prog., 52 (1956), p. 57.

38. Danckwerts, P. V. "Continuous Flow Systems," Chem. Eng. Sci., 2 (1953), p. 1.

39. Deisler, P. F. Jr., "Analogue of Alternating Current Theory Applied to Diffusion Processes in Beds of Porous Catalyst Carriers," Princeton University Dissertation (Ph.D.), 1952.

40. Deisler, Paul F. Jr. and Wilhelm, Richard H. "Diffusion in Beds of Porous Solids," Ind. and Eng. Chem., 45 (1953), p. 1219.

41. Denton, W. H. "The Heat Transfer and Flow Resistance for Fluid Flow Through Randomly Packed Spheres," Proceedings of the General Discussion on Heat Transfer, London, (September 11-13, 1951), pp. 370-373, 386-387.

42. Douglas, J. Jr. and Peaceman, D. W. "Numerical Solution of Two-dimensional Heat-flow Problems," A.I.Ch.E. Journal, 1 (December, 1955), p. 505.

43. Dryden, C. E., Strang, D. A. and Withrow, A. E. "Mass Transfer in Packed Beds at Low Re," Chem. Eng. Prog., 49 (1953), p. 191.

44. Dunn, J. E. and Fluker, B. J. "Experimental Determination of Heat-Transfer Coefficients of Porous Solid-Liquid Systems," Status Report to API, (May 6, 1959).

45. Dusinberre, G. M. Numerical Analysis of Heat Flow. McGraw-Hill Book Co., Inc., 1949.

46. Ebach, Earl A. and White, Robert R. "Mixing of Fluids Flowing Through Beds of Packed Solids," A.I.Ch.E. Journal, 4 (June, 1958), p. 161.

47. Eckert, E. R. G., Hartnett, J. P. and Irvine, T. F. Jr. "Heat Transfer," Ind. and Eng. Chem., 50 (March, 1958), p. 543.

48. Edeskuty, F. J. and Amundson, N. R. "Effect of Intraparticle Diffusion-Agitated Nonflow Adsorption Systems," Ind. and Eng. Chem., 44 (1952), p. 1699.

49. Einstein, H. A. Dissertation. Eidg. techn Hochschule, Zurich, (1937).

50. Elrod, H. G. "New Finite Difference Technique For Solution of the Heat Conduction Equation, Especially Near Surfaces With Convective Heat Transfer," Transactions of the A.S.M.E., 79 (1959), p. 1519.

51. Euchen, A. "Die Warmeleitfahigkeit keramischer feuerfester staffe," VDI Forschungsheft 353, Forschung auf clem Gebeite des Ingenieurwesens Ausgabe B, (March-April, 1932).

52. Evans, G. C. and Gerald, C. F. "Mass Transfer From Benzoic Acid Granules to H_2O in Fixed and Fluidized Beds at Low Re," Chem. Eng. Prog., 49 (1953), p. 135.

53. Fahien, R. W. and Smith, J. M. "Mass Transfer in Packed Beds," A.I.Ch.E. Journal, 1 (March, 1955), p. 28.

54. Fatt, I. "Pore Structure of Sintered Glass From Diffusion and Resistance Measurements," Journal of Phys. Chem., 63 (1959), p. 751.

55. Francl, J. and Kingery, W. D. "Thermal Conductivity: IX Experimental Investigation of Effect of Porosity on Thermal Conductivity," Journal of the American Ceramic Society, 37 (February, 1954), p. 99.

56. Frankel, S. P. "Mixing of Fluid Flowing in a Porous Medium," Conference on Theory of Fluid Flow in Porous Media, University of Oklahoma, (March 23-24, 1959).

57. Friedlander, S. K. "Mass and Heat Transfer to Single Spheres and Cylinders at Low Reynolds Numbers," A.I.Ch.E. Journal, 3 (1957), p. 43.

58. Furnas, C. C. "Heat Transfer From a Gas Stream to a Bed of Broken Solids," U.S. Bureau of Mines Bulletin, 361 (1932).

59. Gaffney, B. J. and Drew, T. B. "Mass Transfer From Packing to Organic Solvents in Single Phase Flow Through a Column," Ind. and Eng. Chem., 42 (1950), p. 1120.

60. Gamson, B. W. "Heat and Mass Transfer-Fluid Solid Systems," Chem. Eng. Prog., 47 (1951), p. 19.

61. Gamson, B. W., Thodos, G. and Hougen, O. A. "Heat, Mass and Momentum Transfer in the Flow of Gases Through Granular Solids," Transactions A.I.Ch.E., 39 (1943), p. 1.

62. Gates, C. F. and Ramey, H. J. Jr. "Field Results of South Belridge Thermal Recovery Experiment," A.I.M.E. Petroleum Transactions, T. P. 8032, (1958).

63. Gilliland, E. R. and Baddour, R. F. "The Rate of Ion Exchange," Ind. and Eng. Chem., 45 (1953), p. 330.

64. Gilliland, E. R., Baddour, R. F. and Russel, J. L. "Rates of Flow Through Microporous Solids," A.I.Ch.E. Journal, 4, (1958), p. 90.

65. Glaser, H. "Static Measurement of Heat Transfer of Packed Beds of Raschig Rings," Chem. Tech., 27 (1955), p. 637.

66. Glaser, H. and Thodos, G. "Heat and Momentum Transfer in the Flow of Gases Through Packed Beds," A.I.Ch.E. Journal, 4 (1958), p. 63.

67. Glasstone, Samuel. Textbook of Physical Chemistry. New York: D. Van Nostrand and Co., Inc., 1946.

68. Glueckauf, E. Trans. of the Faraday Society, 15 (1949), p. 286.

69. Gopalarathnom, C. D., Hoelscher, H. E. and Laddha, G. S. "Effective Thermal Conductivity in Packed Beds," A.I.Ch.E. Journal, 7 (June, 1961), p. 249.

70. Gore, D. E. and Fluker, B. J. "Experimental Determination of Heat Transfer Coefficients of Porous Solid-Liquid Systems," Status Report to the A.P.I., (September, 1958).

71. Gottschlich, C. F. "Axial Dispersion in Packed Beds," Presented at Fifty-Fourth Annual Meeting A.I.Ch.E., New York, (December 2-7, 1961).

72. Granet, I. and Gould, R. M. "Shortcuts for Transient Heat Flow," Chem. Eng., 63 (February, 1956), p. 183.

73. Green, D. W. and Perry, R. H. "Heat Transfer With A Flowing Fluid Through Porous Media," Chem. Eng. Symp. Series, 57, (1960), p. 61.

74. Green, L. Jr., Edmonson, R. B. and Nall, K. L. "Heat Transfer in Flow Through Porous Graphite with Internal Power Generation," Aerojet-General Corporation-Contract Nr AF33(616)-3767, (1959).

75. Greenstein, R. I. and Preston, F. W. "Heat Gain by Unconsolidated Sands During Hot Water Injection," Producers' Monthly, 17 (February, 1953), p. 16.

76. Hadidi, T. A. R. "Heat Transfer Mechanisms in Porous Media Containing Oil and Water," Pennsylvania State University Dissertation (Ph.D.), 1955.

77. Hadidi, T. A. R., Nielson, R. F. and Calhoun, J. C. Jr. "Studies on Heat Transfer During Linear Fluid Displacement in Porous Media," Producers' Monthly, 20 (August, 1956), p. 38.

78. Hamilton, R. L. "Thermal Conductivity of Heterogeneous Mixtures," University of Oklahoma Dissertation (Ph.D.), 1960.

79. Handy, L. L. "An Evaluation of Diffusion Effects in Miscible Displacement," Journal of Pet. Tech., 11 (1959), p. 61.

80. Hausen, H. Z Math. Mech., 9 (1929), p. 173.

81. Hausen, W. C. and Livovich, A. F. "Thermal Conductivity of Refractory Insulating Concrete," Journal of the American Ceramic Society, 36 (November, 1953), p. 356.

82. Hellman, S. K., Habetler, George and Babrou, H. "Use of Numerical Analysis in the Transient Solution of Two-dimensional Heat Transfer Problems with Natural and Forced Convection," Trans. of A.S.M.E., 78 (1956), p. 1155.

83. Hiester, N. K. and Vermeulen, T. "Saturation Performance of Ion Exchange and Adsorption Columns," Chem. Eng. Prog., 48 (1952), p. 505.

84. Hobson, M. and Thodos, G. "Mass Transfer in the Flow of Liquids Through Granular Solids," Chem. Eng. Prog., 45 (1949), p. 517.

85. _____. "Mass Transfer - Laminar Flow of Gases Through Granular Beds," Chem. Eng. Prog., 47 (1951), p. 370.

86. Hougen, O. A. "Engineering Aspects of Solid Catalysts," Ind. and Eng. Chem., 53 (July, 1961), p. 509.

87. Hougen, O. A. and Wilkie, C. R. "Mass Transfer in the Flow of Gases Through Granular Solids Extended to Low Modified Reynolds Numbers," Trans. of A.I.Ch.E., 41 (1945), p. 445.

88. Jacob, A. and Osberg, G. L. "Effect of Gas Thermal Conductivity on Local Heat Transfer in a Fluidized Bed," Canadian Journal of Chemical Engineering, 35 (1957), p. 5.

89. Jakob, Max. Heat Transfer. Vol. I. New York: John Wiley and Sons, 1949.

90. _____. Heat Transfer. Vol. II. New York: John Wiley and Sons, 1957.

91. Jacques, G. L. and Vermeulen, T. "Longitudinal Dispersion in Solvent Extraction Columns, Peclet Numbers for Ordered and Random Packings," U.S. Atomic Energy Comm., U.C.R.L. 8029 (1957).

92. Jenkins, R. and Aronofsky, J. S. "Analysis of Heat Transfer Processes in Porous Media - New Concepts in Reservoir Heat Engineering," 18th Technical Conference on Petroleum Production at Penn. State University, (October 6-8, 1954).

93. Kasten, P. R. and Amundson, N. R. "Analytical Solution for Simple Systems in Moving Bed Adsorbers," Ind. and Eng. Chem., 44 (1952), p. 1704.

94. Kasten, P. R., Lapidus, L. and Amundson, N. R. "Mathematics of Adsorption in Beds: V. Effect of Intraparticle Diffusion in Flow Systems in Fixed Beds," Journal of Phys. Chem., 56 (June, 1952), pp. 683-688.

95. Keulemans, A. I. M. Gas Chromatography. New York: Reinhold Publishing Corp., 1959.

96. Kimura, M. "Effective Thermal Conductivities of Packed Beds," Kagaku Kikai, 21 (1957), p. 472.

97. Klinkenberg, A. "Heat Transfer in Cross-Flow Heat Exchangers and Packed Beds - Evaluation of Equations for Penetration of Heat or Solutes," Ind. and Eng. Chem., 46 (1954), p. 2285.

98. _____. "Numerical Evaluations of Equations Describing Transient Heat and Mass Transfer in Packed Solids," Ind. and Eng. Chem., 40 (1948), p. 1992.

99. Klinkenberg, A. and Harmens, A. "Unsteady State Heat Transfer in Stationary Packed Beds," Chem. Eng. Sci., 11 (1960), p. 260.

100. Klinkenberg, A. and Sjenitzer, F. "Holding-time Distributions of the Gaussian Type," Chem. Eng. Sci., 5 (1956), p. 258.

101. Knudsen, J. G. and Katz, D. L. Fluid Dynamics and Heat Transfer. New York: McGraw-Hill Book Co., 1958.

102. Koch, R. L. "In-situ Combustion - Newest Method of Increasing Oil Recovery," Oil and Gas Journal, (August 10, 1953, p. 92.

103. Koch, R. L., Gleason, J. R. Jr. and Boston, W. G. "In-Situ Combustion Oil Recovery Process - Installation for Field Experiment in Jefferson County, Oklahoma," Pet. Mech. Eng. Conf., Los Angeles, California, (September 26-29, 1954).

104. Kramers, H. and Alberda, G. "Frequency Response Analysis of Continuous Flow Systems," Chem. Eng. Sci., 2 (1953).

105. Kunii, D. and Smith, J. M. "Heat Transfer Characteristics of Porous Rocks: I. Effective Thermal Conductivities of Porous Media Containing Stationary Fluid," Paper presented at San Francisco, California Meeting of the A.I.Ch.E., (December 6-9, 1959).

106. _____. "Heat Transfer Characteristics of Porous Rocks: II. Thermal Conductivities of Unconsolidated Particles with Flowing Fluids," A.I.Ch.E. Journal, 7 (March, 1961), p. 21.

107. Kwong, S. S. and Smith, J. M. "Radial Heat Transfer in Packed Beds," Ind. and Eng. Chem., 49 (1957), p. 894.

108. Lacey, J. W., Draper, A. L. and Binder, G. G. "Miscible Fluid Displacement in Porous Media," Journal Pet. Tech., 10 (1958), p. 76.

109. Lange, N. A. (ed.) Handbook of Chemistry. Sandusky, Ohio: Handbook Publishers Inc., (1952).

110. Lapidus, L. and Amundson, N. R. "Mathematics of Adsorption in Beds VI. The Effect of Longitudinal Diffusion in Ion Exchange and Chromatographic Columns," Journal Phys. Chem., 56 (1952), p. 984.

111. Lauwerier, H. A. "The Transport of Heat in an Oil Layer Caused by the Injection of Hot Fluid," Applied Scientific Research, Vol. V (1956).

112. Leppert, G. "The Numerical Solution of Unsteady-state Heat Conduction Problems by the Method of Crank and Nicolson," Journal of the American Society of Naval Engineers, 64 (1952), p. 611.

113. Levenspiel, O. and Smith, W. K. "Notes on the Diffusion Type Model for the Longitudinal Mixing of Fluids in Flow," Chem. Eng. Sci., 6 (1957), p. 227.

114. Liles, A. W. and Geankoplis, C. J. "Axial Diffusion of Liquids in Packed Beds and End Effects," A.I.Ch.E. Journal, 6 (1960), p. 591.

115. Loeb, A. L. "Thermal Conductivity VIII, A Theory of Thermal Conductivity of Porous Materials," Journal of the American Ceramic Society, 37 (February, 1954), p. 96.

116. Lof, G. G. and Hawley, R. W. "Unsteady-state Heat Transfer Between Air and Loose Solids," Ind. and Eng. Chem., 40 (June, 1948), p. 1061.

117. Martin, W. L., Alexander, J. D. and Dew, J. N. "Process Variables in In-situ Combustion," Journal of Pet Tech., 10 (February, 1958), p. 28.

118. McCune, L. K. and Wilhelm, R. H. "Mass and Momentum Transfer in Solid-Liquid System," Ind. and Eng. Chem., 41 (1949), p. 1124.

119. McHenry, K. W. Jr. "Axial Mixing of Binary Gas Mixtures Flowing in a Random Bed of Spheres," Princeton University Dissertation (Ph.D.), 1958.

120. McHenry, K. W. Jr. and Wilhelm, R. H. "Axial Mixing of Binary Gas Mixtures Flowing in a Random Bed of Spheres," A.I.Ch.E. Journal, 3 (1957), p. 83.

121. McNeil, J. S. Jr., Nelson, T. W. and Moss, J. "Oil Recovery by Thermal Methods," Producers Monthly, 23 (1959), p. 14.

122. McNeil, J. S. and Moss, J. T. "In-situ Combustion," Oil and Gas Journal, (September 15, 1958).

123. McQuarrie, M. "Thermal Conductivity VII: Analysis of Variation of Conductivity with Temperature for Al_2O_3, BeO, and MgO," Journal of the American Ceramic Society, 37 (1954), p. 91.

124. Mickley, H. S. and Fairbanks, D. F. "Mechanism of Heat Transfer to Fluidized Beds," A.I.Ch.E. Journal, 1 (1955), p. 374.

125. Mickley, H. S., Sherwood, T. K. and Reed, C. E. Applied Mathematics in Chemical Engineering. McGraw-Hill Book Co., 1957.

126. Miner, C. S. and Dalton, N. N. Glycerol. New York: Reinhold Publishing Co., 1953.

127. Molino, D. F. and Hougen, J. O. "Thermal Conductivity of Granular Solids Through Which Gases Are Flowing," Chem. Eng. Prog., 48 (1952), p. 147.

128. Morales, M., Spinn, C. W. and Smith, J. M. "Velocities and Effective Thermal Conductivities in Packed Beds," Ind. and Eng. Chem., 43 (1951), p. 225.

129. Morey, G. W. Properties of Glass. New York: Reinhold Publishing Co., 1938.

130. Moss, J. T., White, P. D. and McNeil, J. S. "In-situ Combustion Process - Results of a Five Well Experiment in Southern Oklahoma," Journal of Pet. Tech., 11 (April, 1959), p. 55.

131. Nelson, T. W. and McNeil, J. S. "Oil Recovery by Thermal Methods," Petroleum Engineer, 31 Parts I and II, (February and March, 1959), p. B-27 and B-75.

132. Nusselt, W. Z. Ver. deut. Ing. 71 (1927), p. 85.

133. Perry, J. H. (ed.) Chemical Engineers' Handbook. New York: McGraw-Hill Book Co., 1950.

134. Personal Communication. Pittsburgh Plate Glass Co., Pittsburg 22, Pa., (August 23, 1961).

135. Peskin, Richard, L. "Some Effects of Particle - Particle and Particle- Fluid Interaction in Two Phase Flow Systems," Proceedings of 1960 Heat Transfer and Fluid Mechanics Institute, 192 (1960).

136. Plautz, D. A. and Johnstone, H. F. "Heat and Mass Transfer in Packed Beds," A.I.Ch.E. Journal, 1 (1955), p. 193.

137. Prausnitz, J. M. "Longitudinal Dispersion in a Packed Bed," A.I.Ch.E. Journal, 4 (March, 1958), p. 14M.

138. Preston, F. W. "Mechanism of Heat Transfer in Unconsolidated Porous Media at Low Flow Rates," Penn. State Univ. Dissertation (Ph.D.), 1957.

139. Preston, F. W. and Hazen, R. D. "Further Studies on Heat Transfer in Unconsolidated Sands During Water Injection," Producers' Monthly, 18 (February, 1954), p. 24.

140. Raimondi, P., Gardner, G. H. F. and Petrick, C. B. "Effect of Pore Structure and Molecular Diffusion on the Mixing of Miscible Liquids Flowing in Porous Media," Paper presented at San Francisco, California Meeting of A.I.Ch.E., (December 6-9, 1959).

141. Ramey, H. J. Jr. "Transient Heat Conduction During Radial Movement of a Cylindrical Heat Source - Applications to the Thermal Recovery Process," Paper # 1133 G presented at the Dallas, Texas Meeting of the A.I.M.E., (1958).

142. Ranz, W. E. "Friction and Transfer Coefficients for Single Particles and Packed Beds," Chem. Eng. Prog., 48 (1952), p. 247.

143. Ranz, W. E. and Marshall, W. R. "Evaporation from Drops," Chem. Eng. Prog., 48 (1952), pp. 141, 173.

144. Reilly, P. M. "Unsteady-state Heat Transfer in Stationary Packed Beds," A.I.Ch.E. Journal, 3 (1957), p. 513.

145. Richtmyer, R. D. Difference Methods for Initial-value Problems. New York: Interscience Publishers Inc., 1957.

146. Roeser, W. R. and Lonberger, S. T. "Methods of Testing Thermocouples and Thermocouple Materials," Nat'l Bureau of Standards (U.S.), Gr # 590 (1958), p. 21.

147. Rosen, J. B. "General Numerical Solution for Solid Diffusion in Fixed Beds," Ind. and Eng. Chem., 46 (August, 1954), p. 1590.

148. _____. "Kinetics of a Fixed Bed System for Solid Diffusion into Spherical Particles," Journal of Chemical Physics, 20 (March, 1952), p. 387.

149. Rosen, J. B. and Winsche, W. E. "The Admittance Concept in the Kinetics of Chromatography," Journal of Chemical Physics, 18 (1950), p. 1587.

150. Saffman, P. G. and Taylor, Geoffrey. "The Penetration of a Fluid in a Porous Medium or Hele-Shaw Cell Containing a More Viscous Fluid," Proceedings Royal Society (London), A 245 (1958), p. 312.

151. Satterfield, C. N. and Resnick, H. "Simultaneous Heat and Mass Transfer in a Diffusion Controlled Chemical Reaction," Chem. Eng. Prog., 50 (October, 1954), p. 504.

152. Saunders, O. A. and Ford, H. "Heat Transfer in the Flow of Gas Through a Bed of Solid Particles," Iron and Steel Institute, (London), 141 (1940), p. 291.

153. Scheidegger, A. E. "An Evaluation of the Accuracy of the Diffusivity Equation for Describing Miscible Displacement in Porous Media," Conference on Theory of Fluid Flow in Porous Media, University of Oklahoma, (1959).

154. Scheidegger, A. E. The Physics of Flow Through Porous Media. New York: The MacMillan Co., 1957.

155. Schild, A. "A Theory for the Effect of Heating Oil Producing Wells," A.I.M.E. Transactions, 210 (1957), p. 1.

156. Schilson, R. E. "Study of Intraparticle Diffusion Effects in a Gas Phase Catalytic Reaction," University of Minnesota Dissertation (Ph.D.), 1957.

157. Schneider, P. J. "Numerical Method for Porous Heat Sources," Journal of Applied Physics, 24 (1953), p. 271.

158. Schuler, R. W., Stallings, V. P. and Smith, J. M. Chem. Eng. Prog. Symposium, Series No. 4, 48 (1952), p. 19.

159. Schumann, T. E. W. "Heat Transfer: A Liquid Flowing Through A Porous Prism," Jour. Franklin Inst., 208 (1929), p. 405.

160. Schumann, T. E. W. and Voss, V. "Heat Flow Through Granulated Material," Fuel, 13 (1934), p. 249.

161. Schwartz, C. E. and Smith, J. M. "Flow Distribution in Packed Beds," Ind. and Eng. Chem., 45 (1953), p. 1209.

162. Shand, E. B. Glass Engineering Handbook. New York: McGraw-Hill Book Co., 1958.

163. Singer, E. and Wilhelm, R. H. "Heat Transfer in Packed Beds," Chem. Eng. Prog., 46 (1950), p. 343.

164. Smith, J. M. Chemical Engineering Kinetics. New York: McGraw-Hill Book Co., 1956.

165. Smith, N. L. and Amundson, N. R. "Intraparticle Diffusion in Catalytic Heterogeneous Systems," Ind. and Eng. Chem., 43 (1951), p. 2156.

166. Somerton, W. H. "Some Characteristics of Porous Rocks," Journal of Petroleum Technology, 10 (May, 1958), p. 61.

167. Stewart, W. E. Personal Communication, (May 21, 1962).

168. Strang, D. A. and Geankoplis, C. J. "Longitudinal Diffusivity of Liquids in Packed Beds," Ind. and Eng. Chem., 50 (1958), p. 1305.

169. Strickler, H. S. "Thermal Conductivity of Granulated Beds," Ind. and Eng. Chem., 46 (1954), p. 828.

170. Sugiyama, S. and Nagasaka, K. "Unsteady-state Heat Transfer Between Fixed Beds and Flowing Fluid," Kagaku Kogaku, 22 (1958), p. 547.

171. Taylor, Sir Geoffrey. "Dispersion of Soluble Matter in a Solvent Flowing Slowly Through a Tube," Proceedings of the Royal Society of London, 219 (1953), pp. 186-202.

172. Topper, L. "Analysis of Porous Thermal Insulating Materials," Ind. and Eng. Chem., 47 (1955), p. 1377.

173. Tsu-ning Tsao, George. "Thermal Conductivity of Two Phase Materials," Ind. and Eng. Chem., 53 (1961), p. 395.

174. Van Deemter, J. J. "Heat and Mass Transport in a Fixed Catalyst Bed During Regeneration," Ind. and Eng. Chem., 45 (1953), p. 1227; 46 (1954), p. 2300.

175. Van Deemter, J. J., Zuiderweg, F. J. and Klinkenberg, A. "Longitudinal Diffusion and Resistance to Mass Transfer as Causes of Nonideality in Chromatography," Chem. Eng. Sci., 5 (1956), p. 271.

176. Vogel, L. C. and Krueger, R. F. "An Analog Computer for Studying Heat Transfer During a Thermal Recovery Process," A.I.M.E. Trans., 204 (1955), p. 205.

177. Von Rosenberg, D. V. "Mechanics of Steady State Single Phase Fluid Displacement from Porous Media," A.I.Ch.E. Journal, 2 (1956), p. 55.

178. Wagstaff, J. B. "Air Flow in Beds of Granular Solids," Ind. and Eng. Chem., 47 (1955), p. 1129.

179. Walter, H. "Application of Heat for Recovery of Oil: Field Test Results and Possibility of Profitable Operation," Journal of Pet. Tech., 9 (February, 1957).

180. Walter, J. E. "Rate Dependent Chromatographic Adsorption," Journal of Chem. Phys., 13 (1945), p. 332.

181. Weisman, J. "Effect of Void Volume and Prandtl Modulus on Heat Transfer in Tube Banks and Packed Beds," A.I.Ch.E. Journal, 1 (1955), p. 342.

182. Wilhelm, R. H., Johnson, W. C., Wynkoop, R. and Collier, D. W. "Reaction Rate, Heat Transfer and Temperature Distribution in Fixed Bed Catalytic Converters," Chem. Eng. Prog., 44 (1948), p. 105.

183. Wilks, S. S. Elementary Statistical Analysis. Princeton University Press, 1948.

184. Wilson, L. A., Wygal, R. J., Reed, D. W., Gergins, R. L. and Henderson, J. H. "Fluid Dynamics During an Underground Combustion Process," Paper # 9130 presented at the Dallas, Texas Meeting of the Soc. of Pet. Eng., A.I.M.E., (October, 1957).

185. Winterkamp, F. N. Ohio State University Thesis (M.Sc.), (1950).

186. Woodside, W. "Calculation of the Thermal Conductivity of Porous Media," Canadian Journal of Physics, 36 (1958), p. 815.

187. Yagi, S. and Kunii, D. "Studies of Effective Thermal Conductivities in Packed Beds," A.I.Ch.E. Journal, 3 (September, 1957), p. 373.

188. Yagi, S., Kunii, D. and Shimomura, Y. "Heat Transfer in a Packed Bed with Fluid Flow," Kagaku Kikai, 21 (1957), p. 342.

189. Yagi, S., Kunii, D. and Wakao, N. "Studies on Axial Effective Thermal Conductivities in Packed Beds," A.I.Ch.E. Journal, 6 (1960), p. 543.

190. Yoshida, F., Ramaswami, D. and Hougen, O. A. "Temperatures and Partial Pressures at the Surfaces of Catalyst Particles," A.I.Ch.E. Journal, 8 (1962), p. 5.

191. Zierfuss, H. and Van der Vliet, G. "Laboratory Measurement of Heat Conductivity of Sedimentary Rocks," Bulletin of the American Soc. of Pet. Geologists, 40 (October, 1956), p. 2475.

APPENDIX A

NOMENCLATURE

NOMENCLATURE

a = particle area per unit bed volume, ft^2/ft^3

b = constant

B = coefficient defined in Equation (K-2)

C = heat capacity, Btu/#°F

C = concentration, moles/ft^3

C_1 = $\rho_w C_w \phi$, Btu/ft^3 °F

C_2 = $\rho_s C_s (1-\phi)$, Btu/ft^3 °F

D = molecular diffusivity; $k_{wc}/\rho_w C_w$ for fluid-phase heat transfer, ft^2/hr

d_p = particle diameter, in. or ft.

d_t = inside diameter of tube, ft

E = eddy-dispersion diffusivity, $k_{wm}\phi/\rho_w C_w \phi$ for heat transfer, ft^2/hr

erf ~ denotes error function, Equation (II-15)

erfc ~ denotes co-error function, 1 - erf

F = $x/\sqrt{\theta} - V_F\sqrt{\theta}$

G = mass velocity, based on open tube area, #/hr-ft^2

Gr = Grashof number, Equation (IV-1)

g_c = 32.2 (# mass/# force)(ft/sec^2)

H = mass-transfer coefficient, # moles/hr-atm-ft^2

h = heat-transfer coefficient , Btu/hr-ft^2 °F

ha = heat-transfer coefficient, based on unit volume of porous media, Btu/hr-ft^3 °F

I ~ denotes Bessel function

j ~ empirical "j" factor, Equation (II-19)

K = effective thermal diffusivity of porous media, $k_e/[\rho_w C_w \phi + \rho_s C_s (1-\phi)]$, ft^2/hr

K^o = effective static thermal diffusivity of porous media,

$$k_e{}^o / \left[\rho_w C_w \phi + \rho_s C_s (1-\phi) \right], \ ft^2/hr$$

k_e = effective thermal conductivity of porous media, Btu/hr-ft^{2o}F/ft

$k_e{}^o$ = static thermal conductivity of porous media, i.e., thermal conductivity of porous media with fluid in-place but not moving, Btu/hr-ft^{2o}F/ft

$k_{e(v)}$ = velocity dependent component of the effective thermal conductivity, Btu/hr-ft^{2o}F/ft

$k_{e(num)}$ = effective thermal conductivity of porous media; calculated from numerical solution to Equations (III-1) and (III-2), Btu/hr-ft^{2o}F/ft

k_{ha} = effective dispersion coefficient characterizing a finite heat-transfer rate between the fluid and solid phases of porous media; heat-transfer rate controlled by fluid "film" around particle, Equation (III-30), Btu/hr-ft^{2o}F/ft

k_s = pseudo thermal conductivity of the solid phase of porous media, Btu/hr-ft^{2o}F/ft

$k_s{}'$ = $k_s(1-\phi)$

k_{sc} = molecular thermal conductivity of solid, Btu/hr-ft^{2o}F/ft

$k_{s(ha)}$ = effective dispersion coefficient characterizing a finite heat-transfer rate between the fluid and solid phases of porous media; heat-transfer rate controlled by solid intra-particle resistance, Equation (V-10), Btu/hr-ft^{2o}F/ft

k_{sv} = Schumann and Voss static thermal conductivity, Equations (II-28), (II-29) and (II-30), Btu/hr-ft^{2o}F/ft

k_w = pseudo thermal conductivity of the fluid phase, Equation (III-3), Btu/hr-ft^{2o}F/ft

$k_w{}'$ = $k_w\phi$

k_{wm} = eddy dispersion coefficient, Btu/hr-ft^{2o}F/ft

k_{wc} = molecular thermal conductivity of fluid, Btu/hr-ft^2°F/ft

k_1 = constant, Equation (II-36)

k_2 = constant, Equation (II-36)

L = length, ft

M = molecular weight

m = empirical constant

n = amount of adsorbate on adsorbent, Equation (II-35)

P = pressure-film factor (analogous to the mean partial pressure of the inert gas in a single diffusing component in a stagnant gas), atm.

p = constant in Equation (II-28) and (II-30)

Pe = Peclet number, $\frac{vd_p}{E+D}$

Pr = Prandtl number, $\frac{C_w\mu}{k_{wc}}$ for heat transfer

R = second term of solution to equation of thermal conduction, Equation (III-9)

Re = Reynolds number, $\frac{d_p\, v\, \rho_w}{\mu}$

Re_s = modified Reynolds number, $\frac{d_p\, G}{\mu}$

R_p = particle radius, ft or in

T = temperature, °F

t = accomplished temperature fraction, $\frac{T - T_o}{T_i - T_o}$

u ~ dummy variable, Equations (II-10) and (II-11)

v = fluid interstitial velocity, ft/hr

v_F = square heat-front velocity, Equation (II-5), ft/hr

x = distance, ft

y ~ denotes y direction

y = dimensionless distance, $\left(\frac{ha}{k_w\phi}\right)^{\frac{1}{2}} x$

Y = $\frac{ha\ x}{\rho_w C_w \phi v}$, dimensionless

z ~dummy variable, Equation (III-39)

z ~denotes z direction

Z = $\frac{ha}{\rho_s C_s (1-\phi)}$ $(\theta - x/v)$, dimensionless

Greek Letters

α_s = thermal diffusivity of solid phase, $k_s/\rho_s C_s$ where k_s is a pseudo solid-phase thermal conductivity, ft^2/hr

α_w = thermal diffusivity of fluid phase including both molecular conduction and eddy dispersion, $k_w/\rho_w C_w$, ft^2/hr

β = coefficient of thermal cubical expansion, Equation (IV-1)

β = $\rho_w C_w \phi / \left[\rho_w C_w \phi + \rho_s C_s (1-\phi) \right]$

γ = constant characterizing distance between successive mixing layers in porous media, Equation (II-33)

ϵ = phase shift

η = empirical constant, Equation (II-32)

θ = time, hr or min

θ_o = small increment of time, hr or min

λ = dimensionless constant, $\left(\frac{ha}{k_w \phi}\right)^{\frac{1}{2}} \frac{\alpha_w}{v}$

μ = viscosity, #/ft-hr

ρ = density, $\#/ft^3$

σ = standard deviation; σ^2 = variance; particular variances denoted by subscripts are defined in text

σ^* = standard deviation = $\sqrt{2K}$

τ = dimensionless time, $\left(\frac{ha}{k_w \phi}\right)^{\frac{1}{2}} v\ \theta$

ϕ = porosity, i.e., packed-bed void fraction, dimensionless

ω = frequency, cycles/sec

Subscripts

avg ~ denotes an average

h ~ denotes a heat-transfer coefficient or constant

i ~ denotes inlet fluid conditions, at x=0

m ~ denotes a mass-transfer coefficient or constant

max ~ denotes maximum value

o ~ denotes initial conditions; at θ=0

s ~ denotes solid phase

sc ~ denotes molecular conductivity of solid

w ~ denotes fluid phase

wc ~ denotes molecular conductivity of fluid

wm ~ denotes eddy dispersion

APPENDIX B

NUMERICAL SOLUTION DIFFERENCE EQUATIONS

NUMERICAL SOLUTION DIFFERENCE EQUATIONS

The differential equations to be solved numerically are,

$$\frac{\partial t_w}{\partial \tau} = - \frac{\partial t_w}{\partial y} + \lambda \frac{\partial^2 t_w}{\partial y^2} - \lambda (t_w - t_s) \qquad \text{(III-5)}$$

$$\frac{\partial t_s}{\partial \tau} = \frac{\alpha_s}{\alpha_w} \frac{\partial^2 t_s}{\partial y^2} + \lambda \frac{\alpha_s}{\alpha_w} \frac{k_w \phi}{k_s (1-\phi)} (t_w - t_s) \qquad \text{(III-6)}$$

with boundary conditions,

$$t_w = t_s = 0, \qquad \tau = 0, \qquad y > 0 \qquad \text{(B-1)}$$

$$t_w = 1, \qquad \tau > 0, \qquad y = 0 \qquad \text{(B-2)}$$

$$t_s = 1, \qquad \tau > 0, \qquad y = 0 \qquad \text{(B-3)}$$

$$t_w = t_s = 0, \qquad \text{all } \theta, \qquad y = \infty \qquad \text{(B-4)}$$

Finite-difference equations of the forward difference type are now formulated. Let "i" denote an increment in τ and "j" an increment in y. The following substitutions are made for the partial derivitives:

$$\left(\frac{\partial t}{\partial \tau}\right)_{j,i+1} = \frac{t_{j,i+1} - t_{j,i}}{\Delta \tau} \qquad \text{(B-5)}$$

$$\left(\frac{\partial t}{\partial y}\right)_{j,i} = \frac{t_{j,i} - t_{j-1,i}}{\Delta y} \qquad \text{(B-6)}$$

$$\left(\frac{\partial^2 t}{\partial y^2}\right)_{j,i} = \frac{t_{j+1,i} - 2t_{j,i} + t_{j-1,i}}{\Delta y^2} \qquad \text{(B-7)}$$

Making these substitutions in Equations (III-5) and (III-6), letting $t = t_w$ and $T = t_s$, and rearranging,

$$t_{j,i+1} = \left(\lambda \frac{\Delta \tau}{\Delta y^2}\right) t_{j+1,i} + \left(1 - \frac{\Delta \tau}{\Delta y} - 2\lambda \frac{\Delta \tau}{\Delta y^2} - \lambda \Delta \tau\right) t_{j,i}$$

$$+ \left(\frac{\Delta \tau}{\Delta y} + \lambda \frac{\Delta \tau}{\Delta y^2}\right) t_{j-1,i} + \lambda \Delta \tau T_{j,i} \qquad \text{(B-8)}$$

$$T_{j,i+1} = \left(\lambda \frac{a_s}{a_w} \frac{\Delta\tau}{\Delta y^2}\right) T_{j+1,i} + \left(1-2\lambda \frac{a_s}{a_w} \frac{\Delta\tau}{\Delta y^2} - \lambda \frac{a_s}{a_w} \frac{k_w \phi}{k_s(1-\phi)} \Delta\tau\right) T_{j,i}$$

$$+ \left(\lambda \frac{a_s}{a_w} \frac{\Delta\tau}{\Delta y^2}\right) T_{j-1,i} + \left(\lambda \frac{a_s}{a_w} \frac{k_w \phi}{k_s(1-\phi)} \Delta\tau\right) t_{j,i} \qquad \text{(B-9)}$$

Starting with conditions (B-1) - (B-4), t_w and t_s are calculated at all "j" points at time (i+1). The time increment is increased to (i+2) and the calculations repeated.

Dusinberre (45) suggests as convergence criteria that the coefficients of all terms in Equations (B-8) and (B-9) be positive. This condition leads to,

$$\Delta\tau \leqq \frac{1}{\frac{1}{\Delta y} + \frac{2\lambda}{\Delta y^2} + \lambda} \qquad \text{(B-10)}$$

$$\Delta\tau \leqq \frac{1}{2\lambda \frac{a_s}{a_w} \frac{1}{\Delta y^2} + \lambda \frac{a_s}{a_w} \frac{k_w \phi}{k_s(1-\phi)}} \qquad \text{(B-11)}$$

APPENDIX C

SIMPLIFICATION OF THE ANALYTICAL SOLUTION FOR A FINITE HEAT-TRANSFER COEFFICIENT

SIMPLIFICATION OF THE ANALYTICAL SOLUTION FOR A FINITE HEAT-TRANSFER COEFFICIENT

The solution to Equations (III-17) and (III-18), for the boundary condition of a pulse input, is here simplified to an expression which is Gaussian in the holding-time variable, θ. Starting with the general solution for a step-function temperature input, previously given in Chapter II,

$$t_w = \int_0^Z \exp\left|-Y-Z\right| \; I_o\left(2\sqrt{YZ}\right) dZ$$

$$+ \exp\left|-Y-Z\right| \; I_o\left(2\sqrt{YZ}\right) \qquad \text{(II-10)}$$

Substituting for Y and Z and letting $C_1 = \rho_w C_w \phi$ and $C_2 = \rho_s C_s (1-\phi)$,

$$t_w = \int_{\frac{x}{v}}^{\theta} \frac{ha}{C_2} \exp\left[\frac{-hax}{C_1 v} - \frac{ha}{C_2}(\theta - x/v)\right] I_o\left[2\sqrt{\frac{(ha)^2 x(\theta-x/v)}{C_1 C_2 v}}\right] d\theta$$

$$+ \exp\left[\frac{-hax}{C_1 v} - \frac{ha}{C_2}(\theta - x/v)\right] I_o\left[2\sqrt{\frac{(ha)^2 x(\theta-x/v)}{C_1 C_2 v}}\right] \qquad \text{(III-19)}$$

For a pulse input

$$\frac{t_w}{\theta_o} = \frac{ha\,x}{\sqrt{C_1 C_2 v x\,(\theta - x/v)}} \exp\left[\frac{-hax}{C_1 v} - \frac{ha}{C_2}(\theta - x/v)\right]$$

$$I_1\left[2\sqrt{\frac{(ha)^2 x(\theta-x/v)}{C_1 C_2 v}}\right] \qquad \text{(C-1)}$$

Using the asymptotic expansion for the Bessel function,

$$\frac{t_w}{\theta_o} = \frac{\exp\left[\frac{-hax}{C_1 v} - \frac{ha}{C_2}(\theta - x/v)\right] \exp\left[2ha\sqrt{\frac{x(\theta-x/v)}{C_1 C_2 v}}\right] hax}{\left[C_2^2 4\pi\, ha \sqrt{\frac{x(\theta-x/v)}{C_1 C_2 v}}\right]^{\frac{1}{2}} \left[\frac{x(\theta-x/v)\, C_1 v}{C_2}\right]^{\frac{1}{2}}} \qquad \text{(III-20)}$$

Combining exponents and rearranging,

$$\frac{t_w}{\theta_o} = \left[\frac{ha}{4\pi C_2^2 \sqrt{\frac{x(\theta-x/v)}{C_1 C_2 v}}}\right]^{\frac{1}{2}} \left[\frac{C_2 x}{(\theta - x/v) C_1 v}\right]^{\frac{1}{2}}$$

$$\exp\left\{\frac{\left[-\frac{hax}{C_1 v} - \frac{ha(v\theta - x)}{C_2 v}\right]^2}{\left[\left|\frac{hax}{C_1 v}\right|^{\frac{1}{2}} + \left|\frac{ha(\theta - x/v)}{C_2}\right|^{\frac{1}{2}}\right]^2}\right\} \qquad \text{(C-2)}$$

Now, expand and rearrange the numerator of the exponential argument.

$$\frac{t_w}{\theta_o} = \left[\frac{ha}{4\pi C_2^2 \sqrt{\frac{x(\theta-x/v)}{C_1 C_2 v}}}\right]^{\frac{1}{2}} \left[\frac{C_2 x}{(\theta - x/v) C_1 v}\right]^{\frac{1}{2}}$$

$$\exp\left\{\frac{-\left|\frac{ha}{C_2}\right|^2 (x/V_F - \theta)^2}{\left[\left|\frac{hax}{C_1 v}\right|^{\frac{1}{2}} + \left|\frac{ha(\theta - x/v)}{C_2}\right|^{\frac{1}{2}}\right]^2}\right\} \qquad \text{(C-3)}$$

Let all holding times be near the mean holding time, x/V_F. With this assumption, x/V_F may be substituted for θ in all terms <u>except</u> the numerator of the exponent. The result is

$$\frac{t_w}{\theta_o} = \left[\frac{ha\, v\, C_1}{4\pi C_2^2 x}\right]^{\frac{1}{2}} \exp\left[\frac{-ha\, C_1 v}{4 C_2^2 x}(x/V_F - \theta)^2\right] \qquad \text{(C-4)}$$

Let

$$\sigma_2^2 = \frac{2\,C_2^2 x}{C_1 v\, ha} \qquad \text{(III-23)}$$

giving as the simplified expression,

$$\frac{t_w}{\theta_o} = \frac{1}{\sqrt{2\,\Pi\,\sigma_2^2}} \exp\left[\frac{-(x/V_F - \theta)^2}{2\,\sigma_2^2}\right] \qquad \text{(III-22)}$$

The necessary assumptions were

$$2\left[\frac{(ha)^2\, x\, (\theta - x/v)}{C_1\, C_2\, v}\right]^{\frac{1}{2}} \ll 1 \qquad \text{(C-5)}$$

and

$$\frac{2C_2^2\, x}{ha\, C_1\, v} \ll \left(\frac{x}{V_F}\right)^2 \qquad \text{(C-6)}$$

APPENDIX D

ADDITION OF VARIANCES; VAN DEEMTER DERIVATION

ADDITION OF VARIANCES; VAN DEEMTER DERIVATION

The derivation of Van Deemter et al. (175), simplifying the solution of Equations (III-37) and (III-38) to a form which is Gaussian and in which the variances of the individual dispersion mechanisms are additive, follows. The differential equations for heat transfer are,

$$\rho_w C_w \phi \frac{\partial T_w}{\partial \theta} = - v \rho_w C_w \phi \frac{\partial T_w}{\partial x} + k_w \phi \frac{\partial^2 T_w}{\partial x^2} - ha\ (T_w - T_s) \qquad \text{(III-37)}$$

$$\rho_s C_s (1-\phi) \frac{\partial T_s}{\partial \theta} = ha\ (T_w - T_s) \qquad \text{(III-38)}$$

Now, let $C_1 = \rho_w C_w \phi$ and $C_2 = \rho_s C_s (1-\phi)$.

The solution according to Lapidus and Amundson (110) for a step-function temperature input is

$$t_w = e^{vx/2\alpha_w} \left[F(\theta) + \frac{ha}{C_2} \int_0^\theta F(\theta)\, d\theta \right] \qquad \text{(D-1)}$$

where

$$F(\theta) = e^{-ha\,\theta/C_2} \int_0^\theta \frac{x}{2\sqrt{\pi\ \alpha_w\ z^3}}\ I_o \left[2\sqrt{\frac{(ha)^2 z(\theta - z)}{C_1\ C_2}} \right] \exp\left[\frac{-x^2}{4\alpha_w z} - zf \right] dz \qquad \text{(D-2)}$$

with $f = \frac{v^2}{4\alpha_w} + \frac{ha}{C_1} - \frac{ha}{C_2}$.

The corresponding solution for a pulse input over a small increment of time, θ_o, is derived from Equation (D-1) by differentiation,

$$\frac{t_w}{\theta_o} = e^{vx/2k_w}\left[F'(\theta) + \frac{ha}{C_2}F(\theta)\right] \qquad (D\text{-}3)$$

where

$$F'(\theta) = e^{-ha\,\theta/C_2}\frac{d}{d\theta}\int_o^\theta \frac{x}{2\sqrt{\Pi\ a_w z^3}} I_o\left[2\sqrt{\frac{(ha)^2 z(\theta-x)}{C_1\ C_2}}\right]$$

$$\exp\left[\frac{-x^2}{4\,a_w z} - z\,f\right] d\,z \;-\; \frac{ha}{C_2}F(\theta) \qquad (D\text{-}4)$$

Application of Leibnitz's rule yields

$$\frac{t_w}{\theta_o} = \frac{x}{2\theta\sqrt{\Pi\ a_w\theta}}\exp\left[\frac{-(x-v\theta)^2}{4\,a_w\theta} - \frac{ha\theta}{C_1}\right]$$

$$+\int_o^\theta \frac{x}{2z\sqrt{\Pi\,a_w z}}\exp\left[\frac{-(x-vz)^2}{4\,a_w z}\right]F_2(z)\,dz \qquad (III\text{-}39)$$

where

$$F_2(z) = \left[\frac{(ha)^2 z}{C_1C_2(\theta-z)}\right]^{\frac{1}{2}}\exp\left[\frac{-ha\,(\theta-z)}{C_2} - \frac{ha\,z}{C_1}\right]$$

$$I_1\left[2\sqrt{\frac{(ha)^2\,z\,(\theta-z)}{C_1\ C_2}}\right] \qquad (III\text{-}40)$$

Assume the Bessel function argument is sufficiently large so that the asymptotic expansion may be used. Then

$$F_2(z) = \frac{1}{2\sqrt{\Pi}}\left[\frac{(ha)^2\,z}{C_1\ C_2\ (\theta-z)^3}\right]^{\frac{1}{4}}$$

$$\exp\left\{\frac{-\,ha}{C_1(1-\phi)}\left[\left|\frac{C_1(\theta-z)}{\rho_s C_s}\right|^{\frac{1}{2}} - \left|z(1-\phi)\right|^{\frac{1}{2}}\right]^2\right\} \qquad (D\text{-}5)$$

Rearranging and multiplying the numerator and denominator of the exponent by

$$\left[\frac{C_1(\theta-z)}{\rho_s C_s}\right]^{\frac{1}{2}} + \left[z(1-\phi)\right]^{\frac{1}{2}} ,$$

there follows

$$F_2(z) = \frac{1}{2\sqrt{\pi}} \left[\frac{(ha)^2 z}{C_1 C_2 (\theta-z)^3}\right]^{\frac{1}{4}} \exp\left\{\frac{-haC_1}{C_2}\left[\frac{\theta - z/\beta}{\left(C_1(\theta-z)\right)^{\frac{1}{2}}+(C_2 z)^{\frac{1}{2}}}\right]^2\right\} \qquad \text{(D-6)}$$

with $\beta = \dfrac{C_1}{C_1 + C_2}$.

The following simplifications are due mainly to van der Waerden, B.L. [referenced by Van Deemter et al. (175)]. In the integral of (III-39), the maximum values of the exponentials are at $z = x/v$ and $z = \beta\,\theta$ respectively. If the effects of longitudinal diffusion are small and the solid-fluid temperatures are nearly equal, all retention times in the bed will be close to the mean $\bar{\theta} = x/\beta\, v$. Therefore, the two maxima in the integrals are close together. The main contributions of the integrals will be in a small region near the maxima where $z \approx \beta\,\theta \approx x/v$. Then, z may be replaced by x/v or by $\beta\,\theta$ <u>except</u> in the numerators of the exponentials. $F_2(z)$ now simplifies to,

$$F_2(z) = \frac{\beta}{\sqrt{2\,\pi}} \left[\frac{ha\, C_1\, v}{2\,\beta^2\, C_2^2 x}\right]^{\frac{1}{2}} \exp\left[\frac{-haC_1 v}{4C_2^2\, x}\,(\theta - z/\beta\,)^2\right] \qquad \text{(D-7)}$$

Define

$$\sigma_5^2 = \frac{2\, k_w \phi\, x}{C_1\, v^3} \qquad \text{(D-8)}$$

$$\sigma_6^2 = \frac{2\, \beta^2\, C_2^2\, x}{ha\, C_1\, v} \qquad \text{(D-9)}$$

As long as x is markedly different from $v\theta$, the first term of Equation (III-39) will be negligible. Therefore, Equation (III-39) reduces, upon combining Equations (III-39), (D-7), (D-8) and (D-9) and substituting $z = x/v$ in all terms except the numerator of the exponentials, to

$$\frac{t_w}{\theta_o} = \beta \int_o^{\theta} \frac{1}{\sigma_5\sqrt{2\pi}} \exp\left[\frac{-(x/v - z)^2}{2\,\sigma_5^2}\right] \frac{1}{\sigma_6\sqrt{2\pi}} \exp\left[\frac{-(\beta\,\theta - z)^2}{2\,\sigma_6^2}\right] dz \qquad \text{(D-10)}$$

The integral may be approximated. The exponential arguments are expanded, combined and factored for z. The result gives, letting $\eta = z - \left[\dfrac{\sigma_5^2 \frac{x}{v} + \sigma_6^2 \beta\,\theta}{\sigma_5^2 + \sigma_6^2}\right]$,

$$\frac{t_w}{\theta_o} = \int_{a_1}^{b_1} \frac{\beta}{2\pi\,\sigma_5\,\sigma_6} \exp - \left[\frac{(\sigma_5^2 + \sigma_6^2)}{2\,\sigma_5^2\,\sigma_6^2}\,\eta^2 + \frac{(x/v - \beta\,\theta)^2}{2(\sigma_5^2 + \sigma_6^2)}\right] d\eta \qquad \text{(D-11)}$$

where $a_1 = \dfrac{-(\sigma_5^2 \frac{x}{v} + \sigma_6^2 \beta\,\theta)}{\sigma_5^2 + \sigma_6^2}$ and $b_1 = \theta + a_1$.

Let

$$\xi = \frac{(\sigma_5^2 + \sigma_6^2)^{\frac{1}{2}}}{\sqrt{2}\,\sigma_5\,\sigma_6}\,\eta \qquad \text{(D-12)}$$

Then

$$\frac{t_w}{\theta_o} = \int_{a_2}^{b_2} \frac{\beta}{\pi\sqrt{2(\sigma_5^2 + \sigma_6^2)}} \exp - \left[\xi^2 + \frac{(x/v - \beta\theta)^2}{2(\sigma_5^2 + \sigma_6^2)}\right] d\xi \qquad \text{(D-13)}$$

where $a_2 = \frac{(\sigma_5^2 + \sigma_6^2)^{\frac{1}{2}}}{\sqrt{2}\,\sigma_5\,\sigma_6}\, a_1$ and $b_2 = \frac{(\sigma_5^2 + \sigma_6^2)^{\frac{1}{2}}}{\sqrt{2}\,\sigma_5\,\sigma_6}\, b_1$.

$$\frac{t_w}{\theta_o} = \frac{\beta}{\pi\sqrt{2(\sigma_5^2 + \sigma_6^2)}} \exp\left[\frac{-(x/v - \beta\theta)^2}{2(\sigma_5^2 + \sigma_6^2)}\right] \int_{a_2}^{b_2} \exp(-\xi^2)\, d\xi \qquad \text{(D-14)}$$

Examination of the integral in Equation (D-14) shows that it may be adequately approximated by

$$\int_{a_2}^{b_2} \exp(-\xi^2)\, d\xi = \int_{-\infty}^{\infty} \exp(-\xi^2)\, d\xi = \sqrt{\pi} \qquad \text{(D-15)}$$

The simplified expression is then

$$\frac{t_w}{\theta_o} = \frac{\beta}{\sqrt{2\pi(\sigma_5^2 + \sigma_6^2)}} \exp\left[\frac{-(x/v - \beta\theta)^2}{2(\sigma_5^2 + \sigma_6^2)}\right] \qquad \text{(D-16)}$$

or

$$\frac{t_w}{\theta_o} = \frac{1}{\sqrt{2\pi(\sigma_1^2 + \sigma_2^2)}} \exp\left[\frac{-(x/V_F - \theta)^2}{2(\sigma_1^2 + \sigma_2^2)}\right] \qquad \text{(III-42)}$$

where σ_1^2 and σ_2^2 are defined as

$$\sigma_1^2 = \frac{2\,k_w \phi\, x}{C_1\, v\, V_F^2} \qquad \text{(D-17)}$$

$$\sigma_2^2 = \frac{2\,C_2^2 x}{ha\,C_1 v} = \frac{2k_{ha}\,x}{C_1\, v\, V_F^2} \qquad \text{(D-18)}$$

The basic assumptions in this simplification are now summarized,

$$2\left[\frac{(ha)^2\ z\ (\theta-z)}{C_1\ C_2}\right]^{\frac{1}{2}} \approx \frac{2x\ ha}{v\ C_1} \gg 1 \qquad \text{(D-19)}$$

$$\sigma_1^2 \ll \left|\frac{x}{V_F}\right|^2 \qquad \text{(D-20)}$$

$$\sigma_2^2 \ll \left|\frac{x}{V_F}\right|^2 \qquad \text{(D-21)}$$

Equations (D-20) and (D-21) specify that the dispersion in holding time due to either of the heat-transfer mechanisms considered is small compared to the total time of travel in the bed.

APPENDIX E

SOME PROPERTIES OF THE JENKINS - ARONOFSKY SOLUTION TO THE THERMAL CONDUCTION EQUATION

SOME PROPERTIES OF THE JENKINS - ARONOFSKY SOLUTION TO THE THERMAL CONDUCTION EQUATION

The Jenkins and Aronofsky (92) solution to the thermal-conduction equation, (III-7), is

$$t = \frac{1}{2}\left[1 - \operatorname{erf}\frac{1}{2\sqrt{K}}\left(\frac{x}{\sqrt{\theta}} - V_F\sqrt{\theta}\right)\right] + \frac{1}{2}\,e^{\rho_w C_w \phi v x/k_e}\left[1 - \operatorname{erf}\frac{1}{2\sqrt{K}}\left(\frac{x}{\sqrt{\theta}} + V_F\sqrt{\theta}\right)\right] \quad \text{(III-9)}$$

Simplification of Second Term

The second term has been designated R. Preston (138) simplified R as follows. The co-error function is expanded in series,

$$\operatorname{erfc}(s) = \frac{e^{-s^2}}{s\sqrt{\pi}}\left(1 - \frac{1}{2s^2} + \frac{1\cdot 3}{(2s^2)^2} - \frac{1\cdot 3\cdot 5}{(2s^2)^3} + \ldots\ldots\right) \quad \text{(E-1)}$$

For s = 3, all terms beyond the first may be neglected,

$$\operatorname{erfc}(s) \quad \frac{e^{-s^2}}{s\sqrt{\pi}} \quad \text{(E-2)}$$

Therefore R reduces to

$$R = \frac{e^{(z-w^2)}}{2\,w\sqrt{\pi}} \quad \text{(III-44)}$$

where $z = \dfrac{x\ v\ \rho_w C_w\ \phi}{k_e}$ and $w = \dfrac{1}{2\sqrt{K}}\left(\dfrac{x}{\sqrt{\theta}} + V_F\sqrt{\theta}\right)$.

The error in using this approximation is about 5% of R at s = 3.

Maximum Value of R

The maximum R was determined by differentiation of R with respect to θ and setting the derivitive equal to zero. The simplified R expression, Equation (III-44), was used. The results obtained by Preston (138) were as follows.

(1) R_{max} occurs at $\frac{x}{V_F} = \theta$ i.e., the arrival time of the "square" front.

(2) $$R_{max} = \frac{1}{2\sqrt{\Pi}} \sqrt{\frac{k_e}{\rho_w C_w \phi\, vx}}$$

Calculation of k_e, Importance of R

Values of R_{max} encountered in the experimental data were generally .03 or less. The significance of R values of this magnitude in the determination of k_e is now examined through sample calculation. Equation (III-9) reads

$$t_w = \frac{1}{2}\left[1 - \text{erf}\,\frac{F}{2\sqrt{K}}\right] + R \qquad \text{(E-3)}$$

or

$$t_w - R = \frac{1}{2}\left[1 - \text{erf}\,\frac{F}{2\sqrt{K}}\right] \qquad \text{(E-4)}$$

The method of k_e calculation was discussed Chapters III and V. It consists essentially of taking the difference in F values at two temperature points, such as $t_w = .1$ and $t_w = .9$. For an R_{max} value of .03, calculations show R at $t_w = .1$ and $t_w = .9$ to be on the order of .005. This value will be assumed here. At $t_w = .1$

$$2\,(.1 - .005) - 1 = -\,\text{erf}\,\frac{F}{2\sqrt{K}} \qquad \text{(E-5)}$$

$$-.81 = - \operatorname{erf} \frac{F}{2\sqrt{K}} \tag{E-6}$$

From error-function tables

$$\frac{F_{t_w=.1}}{2\sqrt{K}} = .9267 \tag{E-7}$$

At $t_w = .9$

$$2\,(.9 - .005) - 1 = - \operatorname{erf} \frac{F}{2\sqrt{K}} \tag{E-8}$$

$$.79 = - \operatorname{erf} \frac{F}{2\sqrt{K}} \tag{E-9}$$

and from error-function tables

$$\frac{F_{t_w=.9}}{2\sqrt{K}} - .8865 \tag{E-10}$$

Subtracting Equation (E-10) from Equation (E-7),

$$(F_{t_w=.1} - F_{t_w=.9}) = 1.8132 \left| 2\sqrt{K} \right| \tag{E-11}$$

Neglecting R, an F difference factor of 1.8124 rather than 1.8132 is obtained. On this basis, R_{max} values up to about .07 may be assumed negligible in the experimental k_e calculations.

Data for a typical experimental run are shown on a probability-paper plot in Figure 38. The experimental points are plotted as t_w vs. F. The solution, Equation (III-9), is also shown both including and neglecting R. On the probability plot, at relatively low R values, the linear curve is merely "shifted" with negligible change in slope.

Determination of k_e by Slope Method. Preston (138) has shown that his derived expression for the slope of the

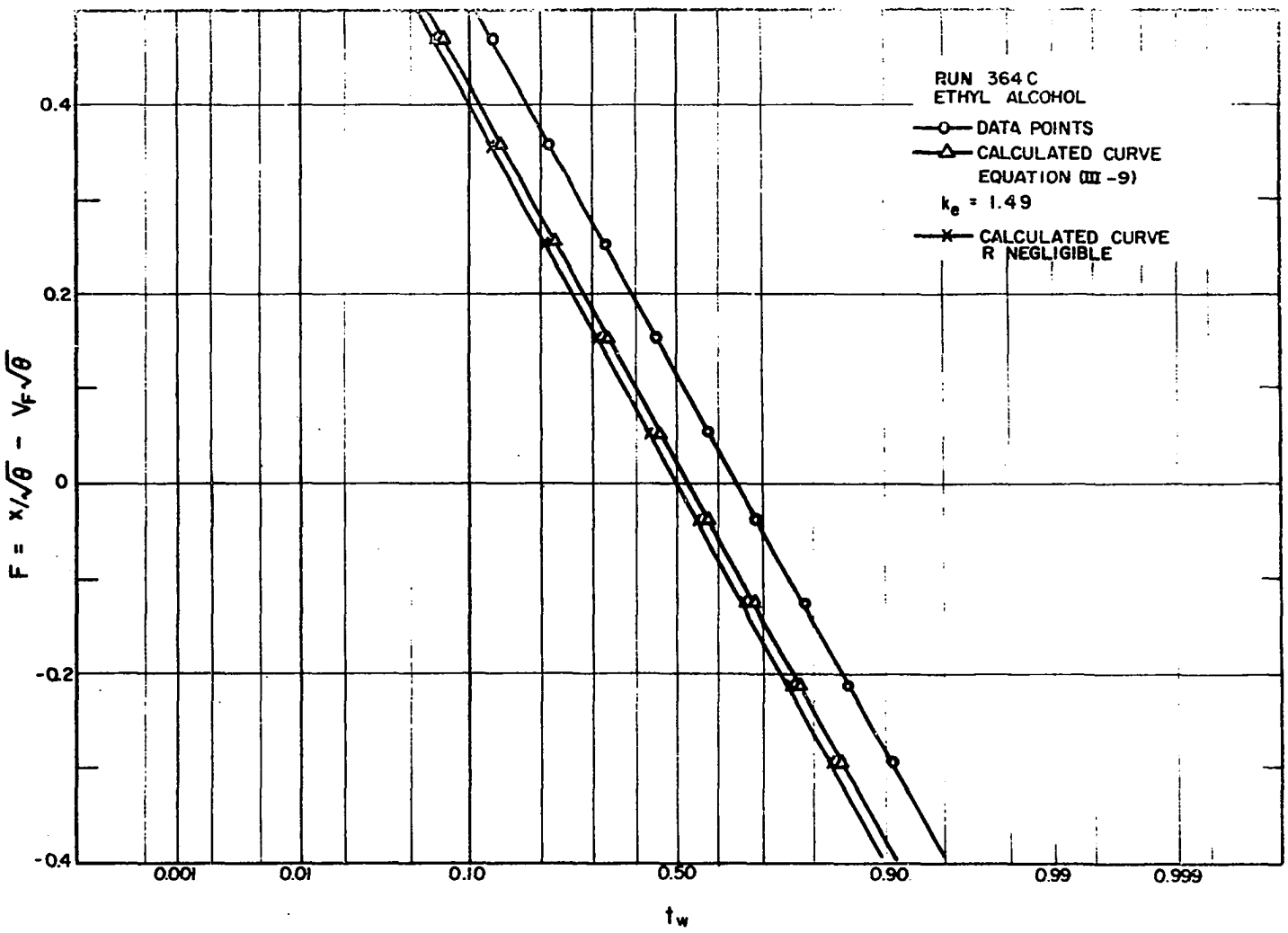

Figure 38- Importance of R in Jenkins - Aronofsky Solution to the Thermal-Conduction Equation; Run 364C

t_w vs. θ curve, evaluated at $x/V_F = \theta$,

$$\frac{dt_w}{d\theta} = \frac{x}{2\theta\sqrt{\pi\ K\ \theta}} \qquad (V\text{-}4)$$

is the same whether or not R is included.

APPENDIX F

SAMPLE CALCULATIONS

SAMPLE CALCULATIONS

A. Sample Calculation of $k_{e(num)}$ from the Numerical Solution*

Numerical Run P-5

$\lambda = .114$, $\alpha_w / \alpha_s = .316$, $k_w\phi / k_s(1-\phi) = .337$

Specific Conditions

$\alpha_w = .006$, $\alpha_s = .019$, $k_w\phi = .132$, $k_s(1-\phi) = .392$,

$\phi = .355$, $x = .35$ ft $v = 5.263$ ft/hr, $V_F = 2.717$ ft/hr

Numerical Calculation Results:

t_w	θ (min)	F
.982	15.76	-.7096
.968	14.37	-.6147
.890	11.32	-.3691
.804	9.816	-.2337
.743	9.066	-.1557
.573	7.524	.0263
.467	6.774	.1288
.350	6.018	.2446
.230	5.268	.3762
.119	4.512	.5314

$(F_{t=.16} - F_{t=.84}) = .750$ ‡

From Equation (III-55)

$$K = \frac{(.750)^2}{7.897} = .07122 \text{ ft}^2/\text{hr}$$

$k_{e(num)} = .07122\ (42.63)$

$= 3.036$ Btu/hr-ft^2°F/ft

Addition of Conductivities:

$k_w\phi = .132$

$k_s(1-\phi) = .392$

$$k_{ha} = \frac{V_F^2 \left[\rho_s C_s (1-\phi)\right]^2}{ha} = \frac{(2.676)^2\ (20.63)^2}{1319.9}$$

Equation (III-30)

$k_{ha} = 2.380$

$k_e = .132 + .392 + 2.380 = 2.904$

*Refer to Chapter III, Theoretical Investigation

‡See Figure 39

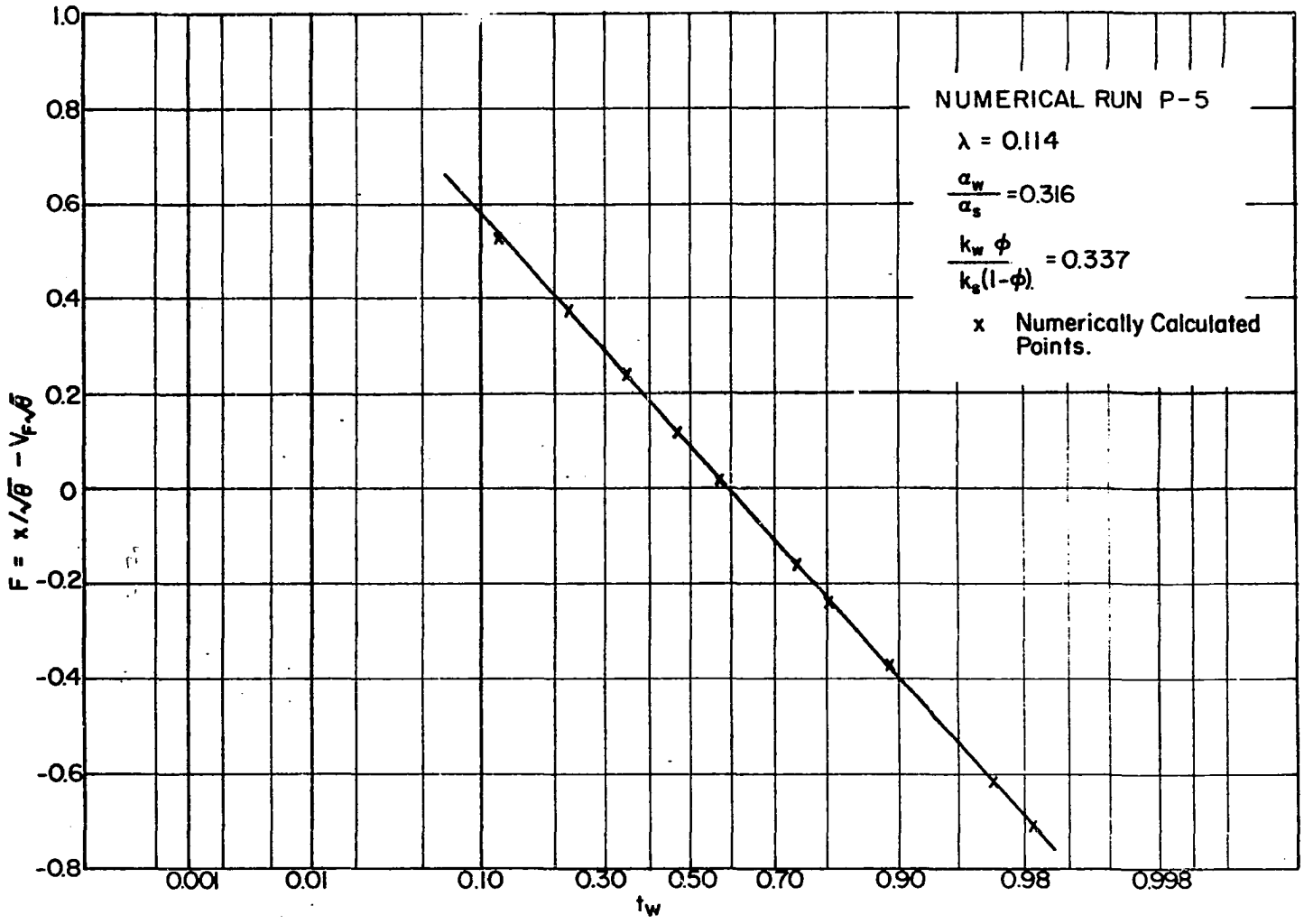

Figure 39- Calculation of $k_{e(num)}$; Probability Paper

B. Sample Calculation of Experimental k_e, Run 359C, 30% Glycerol‡

$v = 19.82$ ft/hr

$vd_p = .195$ ft^2/hr $T_{avg} = 104.85$ T.C. Position No. 1 & 8

$x = .921$ ft

$T_{(initial)} = 123.8^oF$ $T_{(inlet)} = 85.9^oF$ $T_{(initial)} - T_{(inlet)} = 37.9^oF$

T	θ' Time (min)	t_w	$x/\sqrt{\theta}$	$V_F\sqrt{\theta}$	F
122.2	4.40	.042	3.400	2.714	.686
120.5	4.60	.087	3.326	2.775	.551
117.7	4.80	.161	3.256	2.834	.422
113.7	5.01	.266	3.188	2.895	.293
108.8	5.21	.396	3.125	2.953	.172
103.3	5.41	.541	3.067	3.009	.058
98.4	5.61	.670	3.011	3.065	-.054
94.2	5.82	.781	2.958	3.120	-.162
91.0	6.02	.865	2.907	3.175	-.268
87.3	6.42	.963	2.815	3.279	-.464

$$V_F = \frac{\rho_w C_w \phi\, v}{\rho_w C_w \phi + \rho_s C_s (1-\phi)} = .5056\, v = 10.02 \text{ ft/hr}$$

$F_{t=.1} - F_{t=.9} = .840$*

From Equation (V-2)

$$K = \frac{(.840)^2}{13.139} = .0537 \text{ ft}^2/\text{hr}$$

$$k_e = (.0537)\left[\rho_w C_w \phi + \rho_s C_s (1-\phi)\right] = .0537\ (40.8)$$

$$= 2.19 \text{ Btu/hr - ft}^{2o}\text{F/ft}$$

‡Refer to Chapter V, Data Reduction Section

*See Figure 40, for plot of F vs. t_w on probability graph paper.

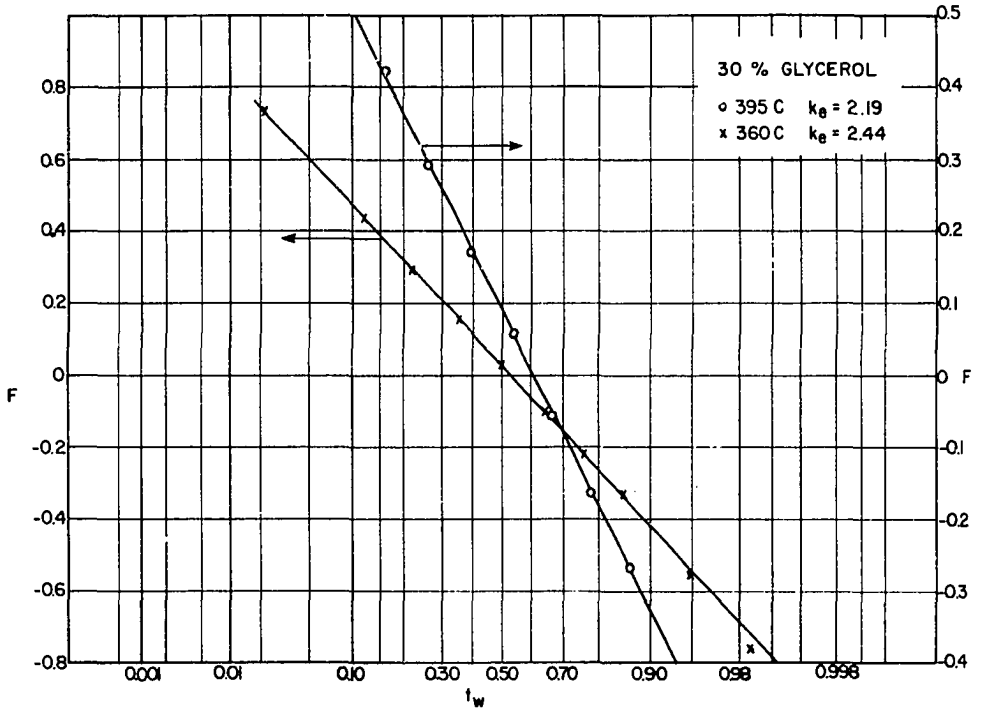

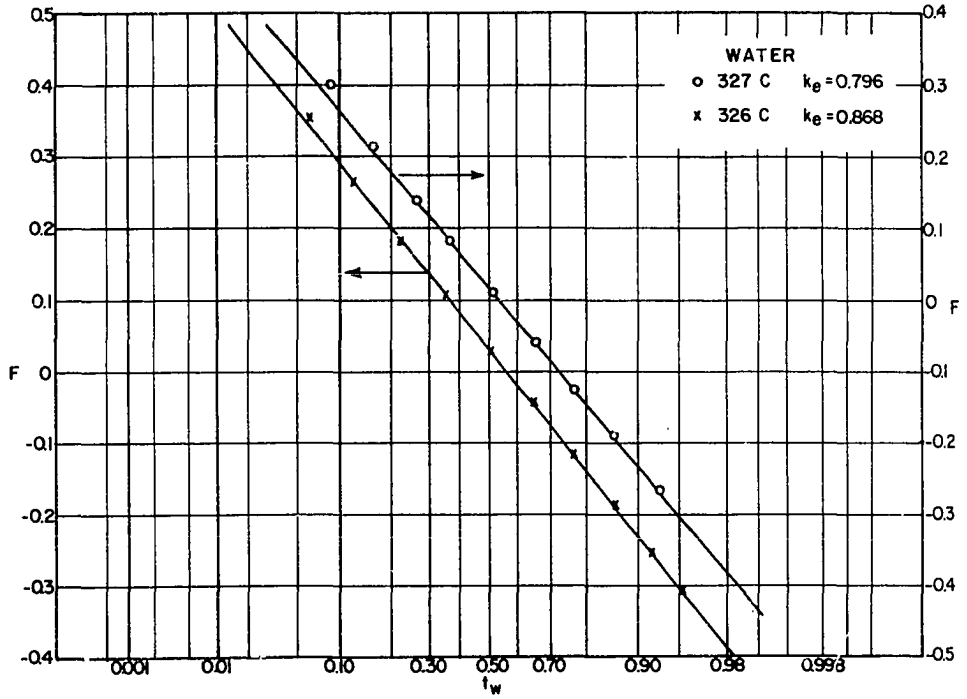

Figure 40- Experimental Data, Probability-Paper Plots; Runs 359C, 360C, 326C, 327C

C. Calculation of Temperature Profile, Equation (III-34).

Run 359C, 30% Glycerol

θ (min)	$F/2\sqrt{K}$	t_w (calculated)*
4.40	1.483	.0180
4.60	1.190	.0462
4.80	.912	.0986
5.01	.633	.1854
5.21	.372	.2994
5.41	.125	.4299
5.61	-.117	.5657
5.82	-.350	.6897
6.02	-.579	.7936
6.42	-1.001	.9216

k_e(From Data) = 2.19 Btu/hr-ft^2°F/ft

$K = .0537$ ft^2/hr

$2\sqrt{K} = .4630$

Plot of t_w vs. θ ~ Figure 41

* Equation (III-34)

D. k_{ha} and $k_{wm}\phi$ Calculation, Run 359C, 30% Glycerol*

$k_e = 2.19$ Btu/hr-ft^2°F/ft (From data)

$k_e^o = .50$ (Table 5)

$k_e(v) = 2.19 - .50 = 1.69$ Btu/hr-ft^2°F/ft Equation (V-5)

$T_{avg} = 104.9$°F

$d_p = .118$ inch

$vd_p = .195$ ft^2/hr, $v = 19.8$ ft/hr

$$Re = \frac{.195 \times 66.39}{3.51} = 3.69$$

$$k_{ha} = \frac{V_F^2 \left[\rho_s C_s (1-\phi)\right]^2}{ha}$$ Equation (III-30)

$$j_h\phi = \frac{h\phi}{C_w G}\left(\frac{C_w \mu}{k_{wc}}\right)^{2/3}$$

From Figure 50 at Re = 3.69 Dryden et al. correlation

$j_h\phi = .785$

$$ha = (j_h\phi)\ \rho_w C_w v \left(\frac{C_w \mu}{k_{wc}}\right)^{-2/3} \frac{6(1-\phi)}{d_p} \text{ Btu/hr-ft}^3\text{°F}$$

$$ha = .785 \times 58.29 \times 19.8 \left(\frac{.878 \times 3.51}{.290}\right)^{-2/3} \frac{6 \times .647}{.00983}$$

$ha = 74{,}200$ Btu/hr-ft^3°F

*Refer to Chapter V, Data Correlation Section

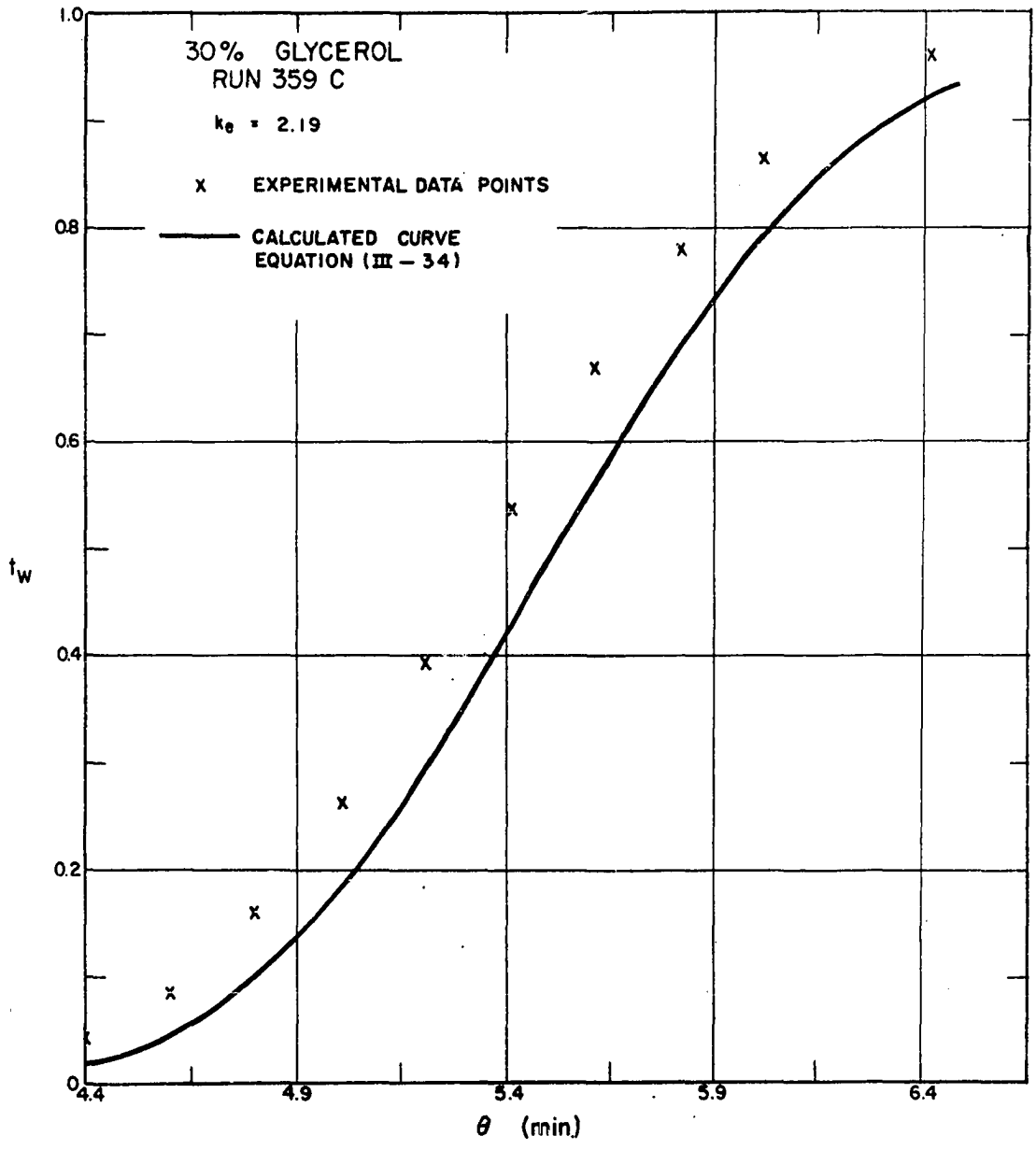

Figure 41- Experimental and Calculated Temperature Profiles; Run 359C; 30 Per Cent Glycerol System

$$V_F = \frac{\rho_w C_w \phi\ v}{\rho_w C_w \phi + \rho_s C_s (1-\phi)} = \frac{58.29 \times .353 \times 19.8}{(58.29 \times .353) + (2.47 \times 62.4 \times .202 \times .647)}$$

$V_F = 10.0$ ft/hr

$$k_{ha} = \frac{(10.0)^2 \times (20.14)^2}{74,200} = .545 \text{ Btu/hr-ft}^2{}^\circ\text{F/ft}$$

Calculation of $k_{wm}\phi$:

$k_{wm}\phi = k_e(v) - k_{ha}$ Equation (V-11)

$k_{wm}\phi = 1.69 - .545 = 1.145$

Peclet Number:

$$Pe = \frac{vd_p}{E_h + D_h}$$ Equation (V-12)

$$D_h = \frac{k_{wc}}{\rho_w C_w} = \frac{.290}{58.29} = .00498 \text{ ft}^2/\text{hr}$$

$$E_h = \frac{k_{wm}\phi}{\rho_w C_w \phi} = \frac{1.145}{58.29 \times .353} = .0557 \text{ ft}^2/\text{hr}$$

$$Pe = \frac{.195}{.0607} = 3.21$$

Eddy-Dispersion Correlation:

$$\frac{E_h}{D_h} = 11.18$$

$$\frac{vd_p}{D_h} = 39.16$$

E. Eddy-Dispersion Correlation, Liquid-Phase, Mass-Transfer Literature Data*

Example Calculations:

1. Carberry and Bretton (29)

d_p = 3 mm, Re = 100, Pe = .435, vd_p = 3.87 ft^2/hr, E_m = 8.91 ft^2/hr

$D_m = 1.935 \times 10^{-5}$ ft^2/hr

$\frac{E_m}{D_m} = 4.61 \times 10^5$

$\frac{vd_p}{D_m} = 1.995 \times 10^5$

2. Cairns (22, 25)

d_p = 3.196 mm, Re = 147, Pe = .678, vd_p = 6.20 ft^2/hr, E_m = 9.14 ft^2/hr

$D_m = 5.23 \times 10^{-5}$ ft^2/hr

$\frac{E_m}{D_m} = 1.746 \times 10^5$

$\frac{vd_p}{D_m} = 1.185 \times 10^5$

3. Liles and Geankoplis (114)

d_p = .47 mm, Re = 6.54, Pe = .370 E_m = .636 ft^2/hr

vd_p = .235 ft^2/hr, $D_m = 3.47 \times 10^{-5}$ ft^2/hr ~ Ref (118)

$\frac{E_m}{D_m} = .1835 \times 10^5$

$\frac{vd_p}{D_m} = .0678 \times 10^5$

*Refer to Chapter V, Data Correlation Section

F. Eddy Dispersion Correlation, Gas-Phase, Mass-Transfer Literature Data*

1. McHenry and Wilhelm (120)

H_2 - N_2 Equi-molar

d_p = .127 in, Re = 26.8, Pe = 2.26 ± .07

T_{avg} ≈ room temp

D_m = 3.79 ft^2/hr Gilliland Equation, Ref (19)

E_m = 8.89 ± .39 ft^2/hr

vd_p = 28.6 ft^2/hr

μ_{avg} = .041 #/ft-hr Calculated From Correlation in McHenry (119)

ρ_{avg} = .0384 $\#/ft^3$

$\frac{E_m}{D_m}$ = 2.35 ± .10

$\frac{vd_p}{D_m}$ = 7.55

2. Deisler (39, 40)

H_2 - N_2 Equi-molar, Room Temp.

Re range 3.8 - 48.4

Pe = 4.33 (Avg. value over Re range)

D_m = 3.79 ft^2/hr Gilliland Equation Ref (19)

E_m = 2.57 ± 1.47 ft^2/hr

$\frac{E_m}{D_m}$ = .679 ± .388

$\frac{vd_p}{D_m}$ = 7.35

*Refer to Chapter V, Data Correlation Section

APPENDIX G

IMPROVED APPROXIMATE SOLUTION TO THE GENERAL DIFFERENTIAL EQUATIONS

IMPROVED APPROXIMATE SOLUTION TO THE GENERAL DIFFERENTIAL EQUATIONS

A proposed approximate solution to Equations (III-1) and (III-2) with boundary condition (III-4) is given by the following:

$$t_w = \frac{1}{2}\left\{1 - \operatorname{erf}\left[\frac{1}{2\sqrt{K}}\left(\frac{x}{\sqrt{\theta}} - V_F\sqrt{\theta}\right) - \frac{1}{8\sqrt{Z}} - \frac{1}{8\sqrt{Y}}\right]\right\} + R \quad \text{(G-1)}$$

$$t_s = \frac{1}{2}\left\{1 - \operatorname{erf}\left[\frac{1}{2\sqrt{K}}\left(\frac{x}{\sqrt{\theta}} - V_F\sqrt{\theta}\right) + \frac{1}{8\sqrt{Z}} + \frac{1}{8\sqrt{Y}}\right]\right\} + R \quad \text{(G-2)}$$

where

$$R = \exp\left[\frac{x\,\rho_w C_w \phi\, v}{k_w\phi + k_s(1-\phi)}\right] \operatorname{erfc}\left[\frac{1}{2\sqrt{K^o}}\left(\frac{x}{\sqrt{\theta}} + V_F\sqrt{\theta}\right)\right] \quad \text{(G-3)}$$

$$K = \frac{k_w\phi + k_s(1-\phi) + k_{ha}}{\rho_w C_w \phi + \rho_s C_s(1-\phi)} \quad \text{(G-4)}$$

$$K^o = \frac{k_w\phi + k_s(1-\phi)}{\rho_w C_w \phi + \rho_s C_s(1-\phi)} \quad \text{(G-5)}$$

$$Y = \frac{ha\,x}{\rho_w C_w\, \phi\, v} \quad \text{(G-6)}$$

$$Z = \frac{ha}{\rho_s C_s(1-\phi)}\left(\theta - \frac{x}{v}\right) \quad \text{(G-7)}$$

This approximation resulted from a combination of the Jenkins and Aronofsky solution to the thermal-conduction equation, Equation (III-9), and the Klinkenberg approximation to the solution for a finite heat-transfer coefficient, Equations (II-16) and (II-17).

The approximation was checked by a comparison with

the numerical solutions as shown in Figures 42 and 43. Tabulated calculations are given in Table 8. The fluid-phase temperature agreement between the numerical solution and Equation (G-1) is good, but the solid-phase temperature agreement is only fair. The approximation appears to be applicable to systems and conditions of the type considered in this research. However, the generality of Equations (G-1) and (G-2) has not been shown. It should not be used for Z less than 1 or Y less than 2.

TABLE 8

CALCULATED TEMPERATURE PROFILES; NUMERICAL SOLUTION AND ANALYTICAL APPROXIMATION

I. P - 6 (Computer Run)

λ = .342, α_w = .006, α_s = .019, $k_w\phi$ = .132, $k_s(1-\phi)$ = .392

ϕ = .355, k_{ha} = .264, v = 6 ft/hr, Θ = .163 hr

	Numerical Solution	Approximation
x (ft)	t_w	t_w
.307	.994	.995
.395	.924	.933
.439	.815	.827
.461	.736	.746
.483	.642	.647
.504	.539	.537
.526	.434	.424
.548	.332	.315
.570	.242	.221
.592	.166	.145
.614	.108	.080
.636	.066	.051
.658	.038	.027
.702	.010	.006

TABLE 8 - Continued

II. P - 5 (Computer Run)

$\lambda = .114$, $a_w = .006$, $a_s = .019$, $k_w\phi = .132$, $k_s(1-\phi) = .392$,

$\theta = .355$, $k_{ha} = 2.46$, $v = r.26$ ft/hr, $x = .35$ ft

θ (hr)	Numerical Solution t_w	Numerical Solution t_s	Approximation t_w	Approximation t_s
.263	.982	.969	.975	.963
.240	.968	.947	.965	.936
.189	.890	.830	.877	.803
.164	.804	.714	.796	.692
.151	.743	.638	.739	.619
.125	.573	.441	.572	.430
.113	.467	.332	.458	.316
.100	.350	.223	.334	.201
.0878	.230	.125	.220	.106
.0752	.119	.050	.133	.039

III. P - 25 (Computer Run)

$\lambda = .167$, $a_w = .00945$, $a_s = .077$, $k_w\phi = .239$,

$k_s(1-\phi) = 1.428$, $k_{ha} = 1.53$, $v = 5.0$ ft/hr, $\theta = .1053$ hr

x (ft)	Numerical Solution t_w	Numerical Solution t_s	Approximation t_w	Approximation t_s
.1132	.973	.949	.968	.918
.1698	.924	.877	.921	.841
.2263	.831	.759	.833	.722
.2829	.689	.597	.690	.560
.3395	.508	.413	.503	.374
.3961	.321	.242	.317	.206
.4527	.166	.116	$Y < 2.0$	
.5093	.067	.043		

TABLE 8 - Continued

IV. P - 23 (Computer Run)

$\lambda = .342$, $\alpha_w = .006$, $\alpha_s = .077$, $k_w\phi = .152$,

$k_s(1-\phi) = 1.428$, $k_{ha} = .232$, $v = .461$ ft

Numerical Solution		Approximation	
θ (hr)	t_w	θ (hr)	t_w
.210	.073	.250	.184
.237	.132	.280	.263
.252	.174	.330	.416
.295	.302	.380	.554
.311	.352	.385	.574
.342	.448	.398	.607
.359	.495	.420	.658
.369	.524	.480	.773
.401	.605	.680	.949
.443	.696		
.459	.725		
.475	.758		

Computer Run Terminated

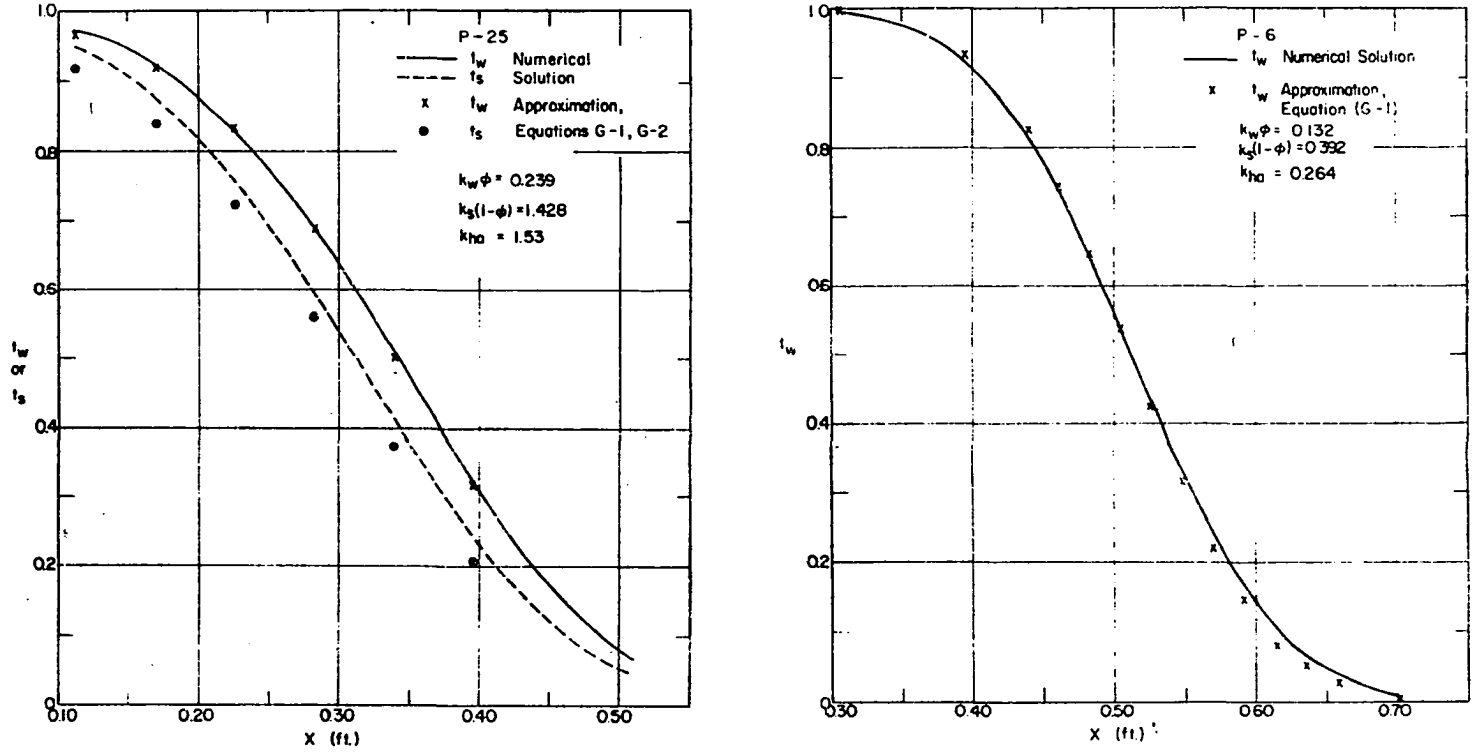

Figure 42- Comparison of the Improved Analytical Approximation with the Numerical Solution to the General Differential Equations; t vs. x

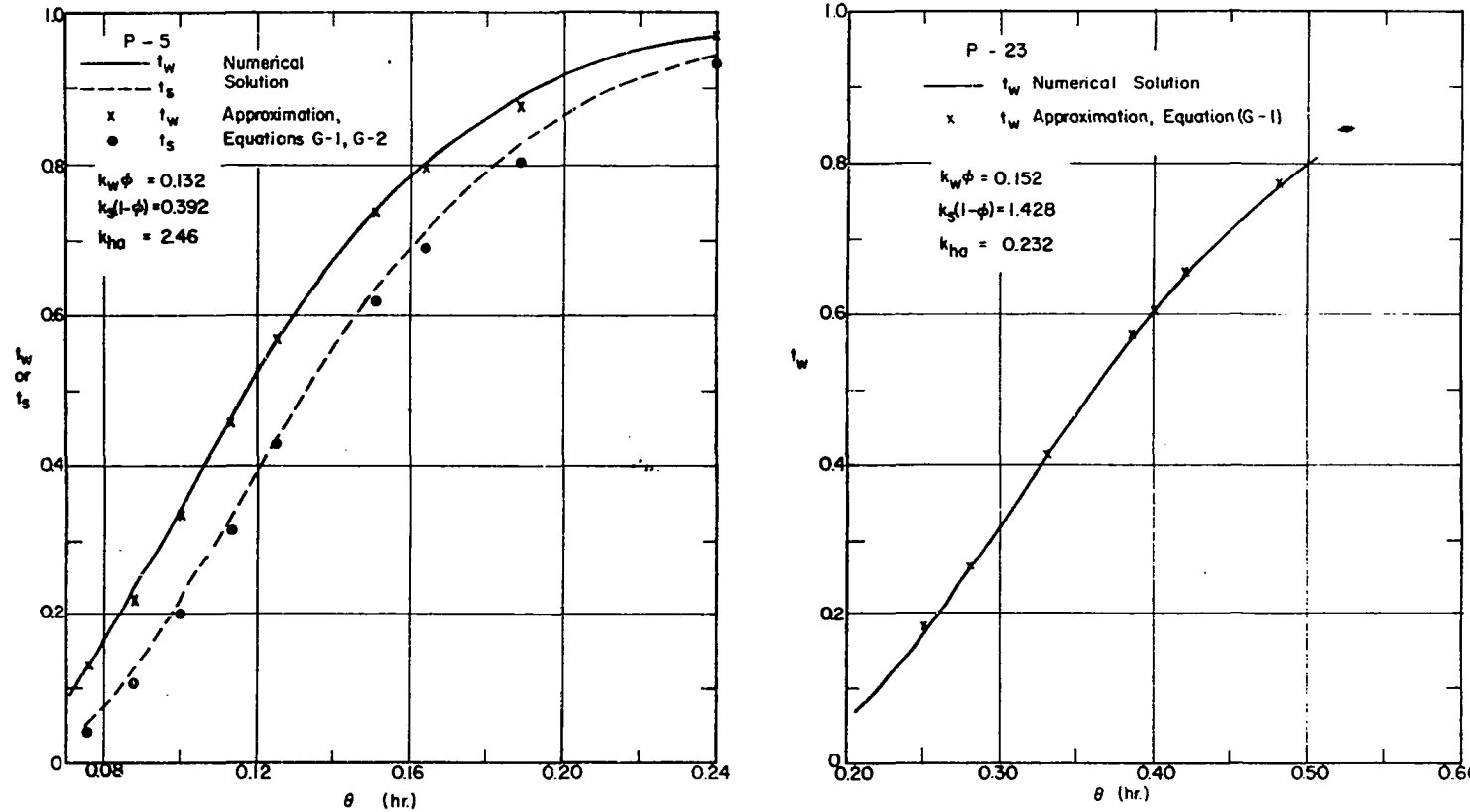

Figure 43- Comparison of the Improved Analytical Approximation with the Numerical Solution to the General Differential Equations; t vs. θ

APPENDIX H

EXPERIMENTAL MATERIALS

TABLE 9

SOURCE AND SPECIFICATIONS OF LIQUIDS

1. Distilled Water
   Source: University of Oklahoma, Power Plant

2. Ethyl Alcohol
   Source: Anderson Laboratories, Fort Worth, Texas
   Catalog Number 385
   Specifications:
   Ethyl Alcohol - Not less than 90%
   Methyl Alcohol - Not more than 5%
   Isopropyl Alcohol - Not more than 5%
   Total Alcohols - Not less than 99.9%

   Refractive Index 1.35935 @ 25° C

3. Glycerol
   Source: J. T. Baker Co., Phillipsburg, N. J.
   Specifications:

Assay ($C_8H_5(OH)_3$)	96.0%
Color	Pass ACS test
Density @ 25°C	1.251
Residue after ignition	.001%
Neutrality	Pass ACS test

TABLE 10

SOURCE AND DESCRIPTION OF GLASS SPHERES

1. 140-170 US Sieve (0.0038")
   Source: Minnesota Mining and Manufacturing Co., 900 Bush Avenue, Saint Paul 6, Minnesota

   Description:
   Catalog Number 130
   3 M "Superbrite" Glass Beads
   Soda-lime-silica glass

2. 35-40 US Sieve (0.0181")
   Source: Minnesota Mining and Manufacturing Co., 900 Bush Avenue, Saint Paul 6, Minnesota

   Description:
   Catalog Number 070
   3 M "Superbrite" Glass Beads
   Soda-lime-silica

3. 16-18 US Sieve (0.0425")
   Source: W. H. Curtin and Co., Houston, Texas
   Special Order - Melvin Ader (Subcontractor)

   Description:
   Lead-silica glass

4. 6-7 US Sieve (0.118")
   Source: W. H. Curtin and Co., Houston, Texas
   Catalog Number 9371

   Description:
   Soda-lime-silica glass

TABLE 11

CHEMICAL COMPOSITION OF GLASS SPHERES

Approximate Percentages of Major Constituents

1. 0.0038" and 0.0181" spheres
   Designated by manufacturer to resemble plate and window glass in composition. Composition data from Ref (134).

Compound	Approximate %
SiO_2	72
Na_2O	13
CaO	12
MgO	2
(Misc)	1

2. 0.0425" spheres
   Calculated from semi-quantitative spectrographic analysis; Shilstone Testing Laboratory, 1714 West Capital, Houston, Texas

Compound	Approximate %
SiO_2	60
PbO	30
K_2O	3
Na_2O	3
(Misc)	4

3. 0.118" spheres
   Calculated from semi-quantitative spectrographic analysis; Shilstone Testing Laboratory, 1714 West Capitol, Houston, Texas

Compound	Approximate %
SiO_2	69
CaO	8
Na_2O	16
K_2O	1
PbO	3
(Misc)	3

TABLE 12

THERMAL CONDUCTIVITY OF LIQUIDS AND SOLIDS

Units, Btu/hr - ft^2 $^oF/ft$

Temperature, ^oF

Material	Ref	80°	100°	120°	140°	160°	180°
Glass Beads 0.0038"	134	.54	.55	.56	.57	.58	.59
0.0181"	134	.54	.55	.56	.57	.58	.59
0.0425"	‡	.55		.56			
0.118"	134	.54	.55	.56	.57	.58	.59
Water	133	.357	.363	.369	.375	.381	.387
30% Glycerol (Aqueous)	126	.280	.288	.294	.300	.306	
60% Glycerol (Aqueous)	126	.220	.222	.224	.227	.230	
Ethyl Alcohol	* 133	.102	.095	.089	.082		

*Measured at 75° F by Prabhudesai, University of Oklahoma, Sept., 1961, k_{wc} = .104; Data extrapolated using this value and literature reference

‡Estimated from data, Ref (129) p. 221.

TABLE 13

SPECIFIC HEAT OF LIQUIDS AND SOLIDS

Units, Btu/#° F

Temperature, ° F

Material	Ref						
Glass 0.0038"	134	.202					
Beads 0.0181"	134	.202	(Mean values between T_i = 80°F, T_o = 150°F. These values were used in all calculations)				
0.0425"	‡	.16					
0.118"	134	.202					
		80°	100°	120°	140°	160°	180°
Water	133	.999	.999	.999	1.000	1.002	1.003
30% Glycerol (Aqueous)	133	.886	.880	.874	.868	.862	
60% Glycerol (Aqueous)	133	.759	.754	.749	.744	.739	
Ethyl Alcohol	*	.586	.613	.648	.687	.725	.765

*Linear interpolation between Ref (109) and Ref (123)

‡Estimated from data, Ref (129) p. 212, Ref (162) p. 25

TABLE 14

DENSITY OF LIQUIDS AND SOLIDS

Material	Density #/ft^3
Glass 0.0038"	155
0.0181"	156
0.0425	187
0.118"	154

Densities were experimentally determined

Material	Ref	Density #/ft^3 80°F	100°F	120°F	140°F	160°F	180°F
Water	133	62.2	62.0	61.6	61.3	61.0	60.5
30% Glycerol (Aqueous)	126	66.8	66.5	66.2	65.9	65.6	
60% Glycerol (Aqueous)	126	71.7	71.4	7.10	70.6	70.2	
Ethyl Alcohol	109 133	48.9	48.3	47.6	47.0		

TABLE 15

VISCOSITY OF LIQUIDS

Units, centipoise

Material	Ref	80°F	100°F	120°F	140°F	160°F	180°F
Water	133	.857	.686	.560	.470	.404	.350
30% Glycerol (Aqueous)	126	2.10	1.55	1.20	.98	.85	
60% Glycerol (Aqueous)	126	8.14	5.47	3.88	2.86	2.22	
Ethyl Alcohol	133	1.08	.38	.735	.610		

TABLE 16

PHYSICAL PROPERTIES; SOLTROL "130"*

ρ_w = 40.8 #/ft^3 @ 60°F

C_w = .50 Btu/#°F @ 75°F

k_{wc} = .0812 Btu/hr-ft^2°F/ft @ 75°F

Physical Property Values Used in Calculations:

T = 110°F

ρ_w = 45.2 #/ft^3

C_w = .52 Btu/#°F

k_{wc} = .080 Btu/hr-ft^2°F/ft

μ = .92 cp.

*Phillips Petroleum Company Trade Name, Bartlesville, Oklahoma

APPENDIX I

EXPERIMENTAL DATA

EXPERIMENTAL DATA

Index to Data

Tables 17 to 20*

US Sieve	ϕ	Liquid	Run Numbers (Incl)
140 - 170	.355	Water	33C - 101C
		30% Glycerol	106C - 118C
		60% Glycerol	119C - 122C
35 - 40	.356	Water	123C - 163C
		30% Glycerol	165C - 179C
		60% Glycerol	185C - 190C
		Ethyl Alcohol	191C - 208C
			375C - 379C
16 - 18	.360	Water	393C - 400C
			431C - 439C
		30% Glycerol	412C - 420C
		60% Glycerol	401C - 411C
		Ethyl Alcohol	422C - 430C
6 - 7	.353	Water	318C - 340C
		30% Glycerol	347C - 361C
		60% Glycerol	273C - 293C
			341C - 346C
		Ethyl Alcohol	362C - 373C

*Where run numbers are omitted in the tables, the reason is one of the following: 1) Run was a heating run, 2) Channeling occurred, 3) Experimental error such as long preheat, poor inlet temperature control, etc.

TABLE 17

EXPERIMENTAL DATA; WATER SYSTEM

Run #	vd_p	k_e	$k_e(v)$	k_e^o	T_{avg}	Re
33C	.00203	.534	.024	.51	118.5	.090
34C	.00168	.577	.067	.51	119.4	.075
35C	.00140	.577	.067	.51	120.9	.064
36C	.00091	.561	.051	.51	122.7	.043
38C	.00300	.560	.050	.51	117.9	.134
39C	.00395	.534	.024	.51	116.1	.174
40C	.00498	.540	.030	.51	117.8	.222
41C	.00606	.509	-.001	.51	114.8	.261
42C	.00647	.509	-.001	.51	118.5	.289
43C	.00715	.519	.009	.51	118.2	.319
44C	.00843	.498	-.012	.51	117.6	.376
45C	.00917	.519	.009	.51	119.4	.409
46C	.00295	.519	.009	.51	116.9	.130
47C	.00262	.529	.019	.51	116.5	.115
48C	.00350	.545	.035	.51	116.5	.154
49C	.00233	.545	.035	.51	119.5	.106
51C	.00172	.550	.040	.51	120.1	.078
52C	.00418	.514	.004	.51	119.4	.187
53C	.00475	.509	-.001	.51	122.1	.219
56C	.00164	.545	.035	.51	117.2	.072
57C	.00138	.550	.040	.51	116.7	.061
58C	.00219	.503	-.007	.51	116.2	.096
59C	.00320	.524	.014	.51	113.3	.135
60C	.00387	.506	-.004	.51	115.7	.170
61C	.00458	.514	.004	.51	113.9	.196
62C	.00505	.493	-.017	.51	115.7	.222
63C	.00562	.499	-.011	.51	117.8	.251
64C	.00618	.510	0	.51	117.2	.272
65C	.00665	.514	.004	.51	118.2	.297
66C	.00728	.498	-.012	.51	117.2	.320
67C	.00745	.514	.004	.51	117.0	.328
68C	.00788	.514	.004	.51	116.9	.347
69C	.00812	.524	.014	.51	119.8	.370
70C	.00370	.530	.020	.51	115.8	.159
71C	.00444	.488	-.022	.51	115.0	.191
72C	.00528	.503	-.007	.51	118.5	.236
73C	.00614	.534	.024	.51	118.8	.274
74C	.00655	.540	.030	.51	118.5	.292
76C	.00763	.539	.029	.51	118.9	.341
86C	.00149	.540	.030	.51	98.5	.055
87C	.00215	.529	.019	.51	98.5	.080

TABLE 17 - Continued

Run #	vd_p	k_e	$k_e(v)$	k_e^0	T_{avg}	Re
88C	.00299	.535	.025	.51	99.4	.111
89C	.00370	.539	.029	.51	101.0	.139
90C	.00435	.514	.004	.51	98.5	.161
91C	.00511	.523	.013	.51	98.7	.189
92C	.00591	.551	.041	.51	100.8	.222
93C	.00638	.525	.015	.51	100.7	.240
94C	Poor fit to erf curve					
95C	.00277	.549	.039	.51	131.6	.138
96C	.00396	.498	-.012	.51	132.6	.202
97C	.00524	.550	.040	.51	134.3	.268
98C	.00552	.524	.014	.51	136.0	.287
99C	.00674	.513	.003	.51	135.8	.350
100C	.00787	.507	-.003	.51	135.1	.408
101C	.00236	.554	.044	.51	133.9	.121
123C	.0289	.594	.084	.51	111.0	1.210
124C	.0254	.594	.084	.51	111.0	1.070
125C	.0120	.567	.057	.51	114.6	.523
126C	.0220	.583	.073	.51	114.1	.946
127C	.0191	.577	.067	.51	114.2	.820
128C	.0337	.645	.135	.51	115.1	1.461
129C	.0371	.622	.111	.51	115.6	1.635
130C	.0078	.588	.078	.51	115.1	.340
131C	.0093	.584	.074	.51	117.2	.412
132C	.0161	.546	.036	.51	116.3	.708
133C	.0178	.557	.047	.51	113.1	.761
134C	.0207	.568	.058	.51	113.6	.889
135C	.0234	.600	.090	.51	113.0	1.000
137C	.0278	.595	.085	.51	112.2	1.177
138C	.0312	.617	.107	.51	113.6	1.340
139C	.0317	.646	.136	.51	115.3	1.374
140C	.0359	.584	.074	.51	116.4	1.585
141C	.0120	.551	.041	.51	118.9	.539
142C	.0152	.529	.019	.51	119.6	.694
143C	.0307	.633	.123	.51	120.5	1.408
144C	.0352	.638	.128	.51	121.3	1.613
145C	.0305	.615	.105	.51	113.7	1.313
152C	.0111	.550	.040	.51	112.1	.472
153C	.0138	.558	.048	.51	114.0	.593
154C	.0134	.566	.056	.51	114.8	.581
155C	.0324	.594	.084	.51	114.2	1.394
156C	.0301	.540	.030	.51	114.5	1.308
157C	.0294	.566	.056	.51	116.2	1.300
158C	.0312	.571	.061	.51	117.5	1.388

TABLE 17 - Continued

Run #	vd_p	k_e	$k_e(v)$	k_e^o	T_{avg}	Re
159C	.0145	.544	.034	.51	129.2	.706
160C	.0217	.615	.105	.51	132.7	1.103
161C	.0293	.620	.110	.51	132.5	1.489
163C	.0340	.632	.122	.51	129.7	1.697
318C	.181	1.99	1.48	.51	122.9	8.58
319C	.146	1.56	1.05	.51	120.0	6.62
320C	.123	1.32	.81	.51	121.2	5.58
321C	.202	2.11	1.60	.51	119.4	9.16
322C	.246	2.76	2.25	.51	118.6	11.16
324C	.184	1.92	1.41	.51	124.4	8.72
325C	.165	1.65	1.14	.51	115.1	7.18
326C	.0695	.868	.358	.51	116.9	3.02
327C	.0558	.796	.286	.51	117.8	2.53
328C	.114	1.18	.67	.51	117.5	5.06
329C	.0580	.855	.345	.51	120.8	2.63
330C	.0944	1.11	.60	.51	121.2	4.28
331C	.232	2.43	1.92	.51	120.3	10.52
332C	.223	2.32	1.81	.51	120.6	10.11
333C	.255	2.65	2.14	.51	120.5	11.56
334C	.230	2.70	2.19	.51	120.4	10.43
335C	.0921	1.00	.49	.51	101.7	3.26
336C	.148	1.57	1.06	.51	101.9	5.24
337C	.189	1.94	1.43	.51	102.3	6.69
338C	.232	2.70	2.19	.51	105.2	9.15
339C	.121	1.31	.80	.51	100.0	4.28
340C	.181	1.92	1.41	.51	100.0	6.41
393C	.0433	.692	.182	.51	102.2	1.53
394C	.0270	.636	.126	.51	102.4	.845
395C	.069	.862	.352	.51	101.6	2.46
398C	.0216	.592	.082	.51	102.2	.765
399C	.0378	.665	.155	.51	101.3	1.34
400C	.0656	.805	.295	.51	100.8	2.32
431C	.0761	.910	.400	.51	106.6	3.00
432C	.0461	.712	.202	.51	107.8	1.82
433C	.0219	.625	.115	.51	109.2	.903
434C	.0646	.838	.328	.51	106.9	2.55
435C	.0328	.660	.150	.51	109.1	1.35
436C	.0818	.964	.454	.51	106.5	3.23
437C	.0471	.700	.190	.51	108.4	1.94

TABLE 18

EXPERIMENTAL DATA; ETHYL ALCOHOL SYSTEM

Run #	vd_p	k_e	$k_e(v)$	k_e^o	Tavg	Re
191C	.0136	.482	.082	.40	111.4	.340
192C	.0194	.521	.121	.40	112.1	.489
193C	.0269	.521	.121	.40	115.9	.700
194C	.0364	.544	.144	.40	116.2	.948
195C	.0159	.449	.049	.40	112.0	.400
196C	.0193	.495	.095	.40	112.9	.490
197C	.0236	.517	.117	.40	112.1	.595
198C	.0253	.557	.057	.40	113.9	.646
200C	.0291	.523	.123	.40	115.9	.758
201C	.0101	.442	.042	.40	113.0	.255
202C	.0107	.414	.014	.40	110.8	.267
203C	.0353	.628	.228	.40	111.3	.882
205C	.0410	.597	.197	.40	113.2	1.041
206C	.0130	.463	.063	.40	112.7	.329
207C	.0430	.560	.160	.40	114.8	1.107
208C	.0165	.476	.076	.40	114.4	.422
362C	.120	1.17	.77	.40	101.7	2.73
363C	.121	1.16	.76	.40	93.0	2.61
364C	.162	1.49	1.09	.40	93.3	3.49
365C	.209	1.91	1.51	.40	94.4	4.50
366C	.093	.940	.540	.40	96.3	2.00
367C	.076	.765	.365	.40	95.8	1.64
368C	Poor fit to erf curve					
369C	.137	1.22	.82	.40	95.0	2.95
370C	.068	.776	.376	.40	95.9	1.47
371C	.248	2.36	1.96	.40	91.9	5.02
372C	.128	1.14	.74	.40	94.4	2.76
373C	.158	1.44	1.04	.40	95.8	3.40
375C	.0236	.489	.090	.40	96.5	.508
376C	.0339	.510	.110	.40	96.3	.730
377C	.0113	.465	.065	.40	99.3	.400
378C	.0194	.457	.057	.40	98.8	.687
379C	.0354	.514	.114	.40	99.4	1.25
422C	.0676	.685	.285	.40	101.7	1.54
423C	.0855	.872	.472	.40	100.6	1.95
424C	.0915	.803	.403	.40	103.3	2.18
425C	.0995	.875	.475	.40	103.1	2.37
426C	.0516	.649	.249	.40	103.5	1.23
427C	.0415	.569	.169	.40	103.0	.989

TABLE 18 - Continued

Run #	vd_p	k_e	$k_e(v)$	k_e^o	T_{avg}	Re
428C	.0350	.569	.169	.40	105.0	.834
429C	.0729	.693	.293	.40	105.0	1.74
430-A C	.0334	.571	.171	.40	112.2	.826
430-B C	.106	1.05	.65	.40	112.0	2.62
430-C C	.0989	1.04	.64	.40	107.5	2.39
430-D C	.0337	.571	.171	.40	109.2	.834

TABLE 19

EXPERIMENTAL DATA; 30 PER CENT GLYCEROL SYSTEM

Run #	vd_p	k_e	$k_e(v)$	k_e^o	T_{avg}	Re
106C	.00371	.537	.037	.50	121.5	.0876
107C	.00342	.527	.027	.50	121.5	.0809
108C	.00276	.521	.021	.50	121.3	.064
109C	.00560	.527	.027	.50	117.0	.123
110C	.00548	.531	.031	.50	117.6	.123
111C	.00427	.511	.011	.50	120.9	.099
112C	.00210	.486	-.014	.50	119.7	.048
113C	.00139	.558	.058	.50	119.8	.032
114C	Poor fit to erf curve					
115C	.00655	.537	.037	.50	120.1	.151
116C	.00214	.506	.006	.50	118.4	.048
117C	.00389	.511	.011	.50	118.2	.087
118C	.00565	.506	.006	.50	119.2	.129
156C	.0138	.554	.054	.50	116.3	.296
166C	.0182	.570	.070	.50	118.2	.408
167C	.0216	.591	.091	.50	121.1	.501
168C	.0262	.586	.086	.50	120.0	.602
169C	.0267	.559	.059	.50	121.1	.619
170C	.0314	.575	.075	.50	120.8	.728
171C	.0287	.597	.097	.50	123.1	.682
172C	.0107	.580	.080	.50	119.7	.247
173C	.0148	.533	.033	.50	118.0	.333
174C	.0272	.554	.054	.50	121.5	.630
175C	.0120	.564	.064	.50	123.3	.285
176-I C	.0206	.586	.086	.50	122.9	.489
176-II C	.0186	.559	.059	.50	122.9	.443
177C	.0209	.586	.086	.50	116.8	.456
178C	.0186	.580	.080	.50	118.2	.419
179C	.0275	.591	.091	.50	122.2	.649
347C	.147	1.61	1.11	.50	107.6	2.98
348C	.169	1.88	1.38	.50	111.5	3.43
349C	.200	2.19	1.69	.50	114.6	4.32
350C	.134	1.37	.87	.50	113.6	2.89
351C	.119	1.30	.80	.50	116.0	2.57
352C	.096	1.13	.63	.50	117.1	2.07
353C	.0675	.812	.31	.50	115.5	1.46
354C	.200	2.32	1.82	.50	110.8	4.06
355C	.053	.790	.290	.50	120.1	1.21
356C	.071	.916	.416	.50	109.4	1.44

TABLE 19 - Continued

Run #	vd_p	k_e	$k_e(v)$	k_e°	T_{avg}	Re
357C	.064	.870	.370	.50	107.2	1.30
358C	.089	1.03	.53	.50	106.3	1.68
359C	.195	2.19	1.69	.50	104.9	3.69
360C	.212	2.44	1.94	.50	116.8	4.58
361C	.220	2.64	2.14	.50	114.3	4.75
412C	.0753	.837	.337	.50	112.3	1.53
413C	.0583	.756	.256	.50	113.5	1.26
414C	.0445	.742	.242	.50	117.0	.961
415C	.0308	.638	.138	.50	118.8	.703
416C	.0804	.907	.407	.50	117.2	1.74
417C	.0589	.881	.381	.50	121.4	1.34
418C	.0279	.607	.107	.50	111.3	.566
419C	.0562	.775	.275	.50	107.2	1.06
420C	.0585	.795	.295	.50	113.8	1.26

TABLE 20

EXPERIMENTAL DATA; 60 PER CENT GLYCEROL SYSTEM

Run #	vd_p	k_e	$k_e(v)$	k_e^o	T_{avg}	Re
119C	.00220	.491	.041	.45	117.3	.0148
120C	.00244	.491	.041	.45	118.0	.0169
121C	.00252	.462	.012	.45	120.2	.0179
122C	.00242	.444	-.006	.45	116.4	.0161
185C	.0127	.568	.118	.45	116.5	.0861
186C	.0185	.573	.123	.45	123.7	.139
187C	.0194	.552	.102	.45	123.5	.145
188C	.0133	.568	.118	.45	121.0	.095
189C	.0177	.563	.113	.45	123.5	.132
190C	.0192	.512	.062	.45	125.5	.146
273C	.121	1.23	.78	.45	126.3	.987
275C	.118	1.22	.77	.45	104.5	.687
277C	.109	1.12	.67	.45	104.5	.635
278C	.109	1.09	.64	.45	104.3	.635
279C	.109	1.12	.67	.45	104.4	.635
280C	.135	1.43	.98	.45	98.8	.728
281C	.141	1.58	1.13	.45	99.5	.760
282C	.155	1.77	1.32	.45	102.6	.904
283C	.173	2.00	1.55	.45	104.4	1.01
284C	.175	1.89	1.44	.45	102.8	1.02
285C	.173	1.90	1.45	.45	103.6	1.01
286C	.189	2.05	1.60	.45	103.6	1.10
287C	.191	2.05	1.60	.45	103.1	1.11
288C	.193	2.19	1.74	.45	105.2	1.12
289C	.192	1.97	1.52	.45	104.9	1.12
290C	.0855	.980	.530	.45	102.7	.498
291C	.0745	.850	.400	.45	103.1	.434
292C	.0732	.844	.394	.45	103.9	.427
293C	.0717	.850	.400	.45	106.3	.418
341C	.070	.893	.443	.45	111.4	.448
342C	.163	1.76	1.31	.45	109.7	1.04
343C	.146	1.47	1.02	.45	112.3	.934
344C	.122	1.35	.90	.45	112.7	.781
345C	.195	2.25	1.80	.45	113.9	1.37
346C	.172	1.77	1.32	.45	114.7	1.20
401C	.0529	.761	.311	.45	102.2	.285
402C	.0532	.658	.208	.45	101.9	.287
403C	.0423	.738	.288	.45	104.0	.247

TABLE 20 - Continued

Run #	vd_p	k_e	$k_e(v)$	k_e^o	T_{avg}	Re
404C	.0278	.635	.185	.45	105.2	.162
405C	.0237	.636	.186	.45	106.0	.138
406C	.036	.599	.149	.45	106.6	.210
407C	.0526	.670	.220	.45	106.3	.307
408C	.0392	.691	.241	.45	101.9	.211
409C	.0422	.691	.241	.45	103.8	.246
410C	.0246	.710	.260	.45	104.5	.143
411C	.0618	.780	.330	.45	103.5	.360

APPENDIX J

TABULATED CORRELATION CALCULATIONS

TABLE 21

CORRELATION CALCULATIONS; WATER SYSTEM, HEAT-TRANSFER COEFFICIENT FROM DRYDEN, STRANG, WITHROW

Run #	vd_p	k_{ha}	$k_{wm}\phi$	$\frac{k_{wm}\phi}{k_{wc}\phi}$	Pe	$\frac{vd_p}{D_h}$
318C	.181	.439	1.04	7.94	3.37	30.02
319C	.146	.303	.747	5.75	3.61	24.37
320C	.123	.226	.584	4.49	3.74	20.53
321C	.202	.485	1.12	8.62	3.52	33.72
322C	.246	.733	1.52	11.69	3.24	41.07
324C	.184	.451	.959	7.32	3.67	30.92
325C	.165	.375	.765	5.88	4.01	27.73
326C	.0695	.085	.273	2.10	3.75	11.68
327C	.0558	.059	.227	1.75	3.39	9.32
328C	.114	.200	.470	3.62	4.13	19.03
329C	.0580	.063	.282	2.17	3.07	9.68
330C	.0944	.145	.455	3.50	3.86	15.76
331C	.232	.668	1.25	9.62	3.65	38.73
332C	.223	.625	1.19	9.15	3.68	37.23
333C	.255	.770	1.37	10.54	3.70	42.57
334C	.230	.658	1.53	11.77	3.02	38.40
335C	.0921	.138	.352	2.75	4.19	15.72
336C	.148	.315	.745	5.82	3.71	25.26
337C	.189	.476	.954	7.45	3.82	32.35
338C	.232	.673	1.52	11.78	3.08	39.32
339C	.121	.224	.576	4.50	3.76	20.65
340C	.181	.445	.965	7.54	3.63	30.89
393C	.0433	.043	.139	1.061	3.57	7.39
394C	.0270	.016	.110	.84	2.50	4.61
395C	.069	.084	.268	2.05	3.86	11.77
398C	.0216	.011	.071	.542	2.38	3.69
399C	.0378	.029	.126	.962	2.28	6.45
400C	.0656	.077	.218	1.66	4.19	11.19
431C	.0761	.077	.323	2.47	3.74	12.90
432C	.0461	.042	.160	1.21	3.51	7.81
433C	.0219	.012	.103	.780	2.07	3.70
434C	.0646	.075	.253	1.93	3.74	10.95
435C	.0328	.023	.127	.962	2.82	5.54
436C	.0818	.112	.342	2.61	3.85	13.86
437C	.0471	.044	.146	1.11	3.76	7.96

TABLE 22

CORRELATION CALCULATIONS; ETHYL ALCOHOL SYSTEM; HEAT-TRANSFER COEFFICIENT FROM DRYDEN, STRANG, WITHROW

Run #	vd_p	k_{ha}	$k_{wm}\phi$	$\frac{k_{wm}\phi}{k_{wc}\phi}$	Pe	$\frac{vd_p}{D_h}$
362C	.120	.286	.484	14.28	2.42	37.04
363C	.121	.290	.470	13.74	2.48	36.56
364C	.162	.481	.609	17.81	2.61	48.94
365C	.209	.750	.760	22.22	2.72	63.14
366C	.093	.187	.353	10.32	2.48	28.10
367C	.076	.134	.231	6.75	2.97	22.96
369C	.137	.359	.461	13.47	2.87	41.39
370C	.068	.110	.266	7.78	2.35	20.54
371C	.248	.978	.982	28.14	2.38	74.92
372C	.128	.320	.420	12.28	2.92	38.67
373C	.158	.461	.579	16.93	2.67	47.73
422C	.0676	.111	.174	5.03	3.44	20.86
423C	.0855	.168	.304	8.79	2.69	26.39
424C	.0915	.189	.214	6.31	3.97	29.14
425C	.0995	.218	.257	7.58	3.68	31.69
426C	.0516	.070	.179	5.28	2.60	16.43
427C	.0415	.046	.123	3.63	2.84	13.22
428C	.0350	.034	.135	3.98	2.23	11.15
429C	.0729	.126	.167	4.93	3.91	23.22
430-A C	.0334	.031	.140	4.23	2.10	10.95
430-B C	.106	.245	.405	12.24	2.63	34.75
430-C C	.0989	.217	.423	12.78	2.34	32.43
430-D C	.0337	.032	.139	4.20	2.13	11.05

TABLE 23

CORRELATION CALCULATIONS; 30 PER CENT GLYCEROL SYSTEM; HEAT-TRANSFER COEFFICIENT FROM DRYDEN, STRANG, WITHROW

Run #	vd_p	k_{ha}	$k_{wm}\phi$	$\frac{k_{wm}\phi}{k_{wc}\phi}$	Pe	$\frac{vd_p}{Dh}$
347C	.147	.339	.771	7.49	3.45	29.34
348C	.169	.426	.954	9.26	3.26	33.73
349C	.200	.568	1.12	10.87	3.45	39.92
350C	.134	.289	.581	5.64	4.01	26.53
351C	.119	.235	.565	5.49	3.64	23.56
352C	.096	.162	.468	4.54	3.44	10.01
353C	.0675	.090	.220	2.14	4.28	13.37
354C	.200	.568	1.25	12.14	3.04	39.92
355C	.053	.059	.231	2.22	3.22	10.41
356C	.071	.099	.317	3.08	3.47	14.17
357C	.064	.082	.288	2.82	3.37	12.77
358C	.089	.094	.436	4.27	3.39	17.87
359C	.195	.545	1.15	11.18	3.21	39.16
360C	.212	.625	1.32	12.82	3.05	41.98
361C	.220	.666	1.47	14.27	2.87	43.56
412C	.0753	.103	.234	2.23	4.65	15.03
413C	.0583	.065	.191	1.82	4.11	11.54
414C	.0445	.039	.203	1.93	3.01	8.81
415C	.0308	.021	.117	1.10	2.87	6.05
416C	.0804	.117	.290	2.76	4.26	15.92
417C	.0589	.067	.314	2.96	2.91	11.57
418C	.0279	.017	.090	.857	2.99	5.57
419C	.0562	.062	.213	2.05	3.71	11.29
420C	.0585	.065	.230	2.19	3.65	11.58

TABLE 24

CORRELATION CALCULATIONS; 60 PER CENT GLYCEROL SYSTEM; HEAT-TRANSFER COEFFICIENT FROM DRYDEN, STRANG, WITHROW

Run #	vd_p	k_{ha}	$k_{wm}\phi$	$\frac{k_{wm}\phi}{k_{wc}\phi}$	Pe	$\frac{vd_p}{D_h}$
275C	.118	.237	.533	6.80	3.66	28.50
277C	.109	.205	.465	5.93	3.81	26.33
278C	.109	.205	.435	5.55	4.02	26.33
279C	.109	.205	.533	6.80	3.37	26.33
280C	.135	.302	.678	8.65	3.41	32.77
281C	.141	.326	.804	10.26	3.04	34.22
282C	.155	.387	.933	11.90	2.90	37.44
283C	.173	.424	1.13	14.41	2.71	41.79
284C	.175	.435	1.01	12.88	3.05	42.27
285C	.173	.424	1.03	13.14	2.95	41.79
286C	.189	.557	1.04	13.27	3.20	45.65
287C	.191	.567	1.03	13.14	3.26	46.14
288C	.193	.578	1.16	14.80	2.95	46.62
289C	.192	.572	.948	12.09	3.54	46.38
290C	.0855	.133	.397	4.54	3.41	20.65
291C	.0745	.105	.295	3.76	3.79	18.00
292C	.0732	.100	.294	3.75	3.73	17.68
293C	.0717	.097	.303	3.86	3.56	17.32
341C	.070	.093	.350	4.45	3.08	16.79
342C	.163	.377	.933	11.86	3.04	39.09
343C	.146	.346	.674	8.56	3.67	35.01
344C	.122	.252	.648	8.23	3.16	29.05
345C	.195	.588	1.21	15.30	2.84	46.43
346C	.172	.469	.851	10.76	3.48	40.95
401C	.0529	.053	.258	3.23	3.05	12.84
402C	.0532	.054	.154	1.93	4.40	12.91
403C	.0423	.037	.251	3.14	3.14	10.22
404C	.0278	.017	.168	2.10	2.16	6.71
405C	.0237	.013	.173	2.16	1.82	5.72
406C	.036	.027	.122	1.53	3.44	8.70
407C	.0526	.052	.168	2.10	4.10	12.71
408C	.0392	.032	.209	2.61	2.64	9.51
409C	.0422	.037	.204	2.55	2.88	10.19
410C	.0246	.014	.246	3.08	1.45	5.94
411C	.0618	.045	.285	3.56	3.26	14.93

APPENDIX K

SOLID-PHASE INTRA-PARTICLE RESISTANCE

SOLID-PHASE INTRA-PARTICLE RESISTANCE

Deisler (39) conducted a frequency-response analysis of longitudinal mass transfer in a gas-porous solid, packed-bed system. For an input into the bed of the form,

$$X(0) = X_m + A(0) \cos(\omega \theta) \qquad \text{(K-1)}$$

where X is mole fraction of a selected gas and X_m is the mean X value, the output may be written as

$$X(L) = X_m + A(0)\, e^{-B} \cos(\omega - \epsilon\theta) \qquad \text{(K-2)}$$

A(0) is the amplitude of the input sine concentration wave. The term e^{-B} is an amplitude attenuation factor and ϵ is the phase shift. Deisler derived an expression for B which holds under certain conditions concerning system parameters. The mass-transfer mechanisms considered significant in the development were longitudinal diffusion and eddy dispersion in the gas phase, and intra-particle diffusion in each porous solid particle. In this model then, a finite rate of fluid-solid mass transfer was treated, but the resistance for this transfer was assumed to be in the solid particle and not in a fluid "film" surrounding the particle. Deisler's expression for B is, for the analogous case of heat transfer,

$$\frac{B}{\omega^2} = \frac{\left[\rho_s C_s (1-\phi)\right]^2}{15\, \rho_w C_w \phi\, v\, k_{sc}(1-\phi)} R_p^2 L + \frac{k_w \phi L}{\rho_w C_w \phi\, v^3} \left[\left[\frac{\rho_s C_s (1-\phi)}{\rho_w C_w \phi} \right]^2 + 1 \right] \qquad \text{(K-3)}$$

Equation (K-3) may be rearranged to give

$$\frac{B}{\omega^2} = \frac{\left[\rho_s C_s (1-\phi)\right]^2}{\rho_w C_w \phi\, v\, k_{sc}(1-\phi)} \frac{R_p^2 L}{15} + \frac{k_w \phi L}{\rho_w C_w \phi\, v\, V_F^2} \qquad \text{(K-4)}$$

The second term on the right is equal to one-half the fluid-phase variance for the mechanisms of conduction and eddy dispersion [See Equation (III-12)]. The first term may analogously be taken as the variance for the solid-phase intraparticle resistance.

$$\sigma_4^2 = \frac{2\left[\rho_s C_s(1-\phi)\right]^2 R_p^2 L}{15\ \rho_w C_w \phi\ v\ k_{sc}(1-\phi)} \qquad \text{(K-5)}$$

An effective longitudinal conductivity for the solid-phase resistance is then written as

$$k_{s(ha)} = \frac{V_F^2\left[\rho_s C_s(1-\phi)\right]^2}{60\ k_{sc}(1-\phi)}\ d_p^2 \qquad \text{(V-10)}$$

The condition for application of this expression follows from Equation (III-14),

$$\frac{2\ k_{s(ha)}}{\rho_w C_w \phi\ v\ x} \ll 1 \qquad \text{(K-6)}$$

It may be assumed as a first approximation that $k_{s(ha)}$ is additive with the other conductivities previously discussed. However it is difficult to reconcile the addition of $k_{s(ha)}$ and $k_s(1-\phi)$, since the assumptions used in the two models are conflicting. That is, in deriving the $k_{s(ha)}$ expression, each spherical particle is assumed to be surrounded by fluid at one temperature, i.e., the temperature gradients within a particle are symmetrical. The term $k_s(1-\phi)$ accounts for conduction in a longitudinal direction because of longitudinal temperature gradients within the particles.

APPENDIX L

ADDITIONAL WORK

ADDITIONAL WORK

The additional work presented in this appendix consists of data in which flow channeling occurred in the porous media, and the limited amount of heating-run data in which no measurable channeling was present. These data were discussed in Chapter IV.

Heating-Run Data, No Channeling

In the .118 inch bead packed bed, no measurable channeling was observed in heating runs with water or ethyl alcohol where the flow direction was downward. This was in contrast to runs with smaller size beads and runs with liquids of higher viscosity, (See Table 2). The channeling which did occur in heating runs was discussed in Chapter IV, and was proposed to be the result of an unfavorable viscosity ratio between the displacing and displaced liquids. The absence of fingering in the water and ethyl alcohol - .118 inch bead systems indicates that the viscous resistance of the bed at these conditions was reduced to a point such that measurable flow fingers were not formed. However, a more sensitive measuring system than used here would quite likely indicate the presence of small flow fingers.

Effective thermal conductivities were calculated for systems where there was a negligible amount of channeling. These data are shown in Figure 44 and are tabulated in Tables 25 and 26. The k_e values for ethyl alcohol are in

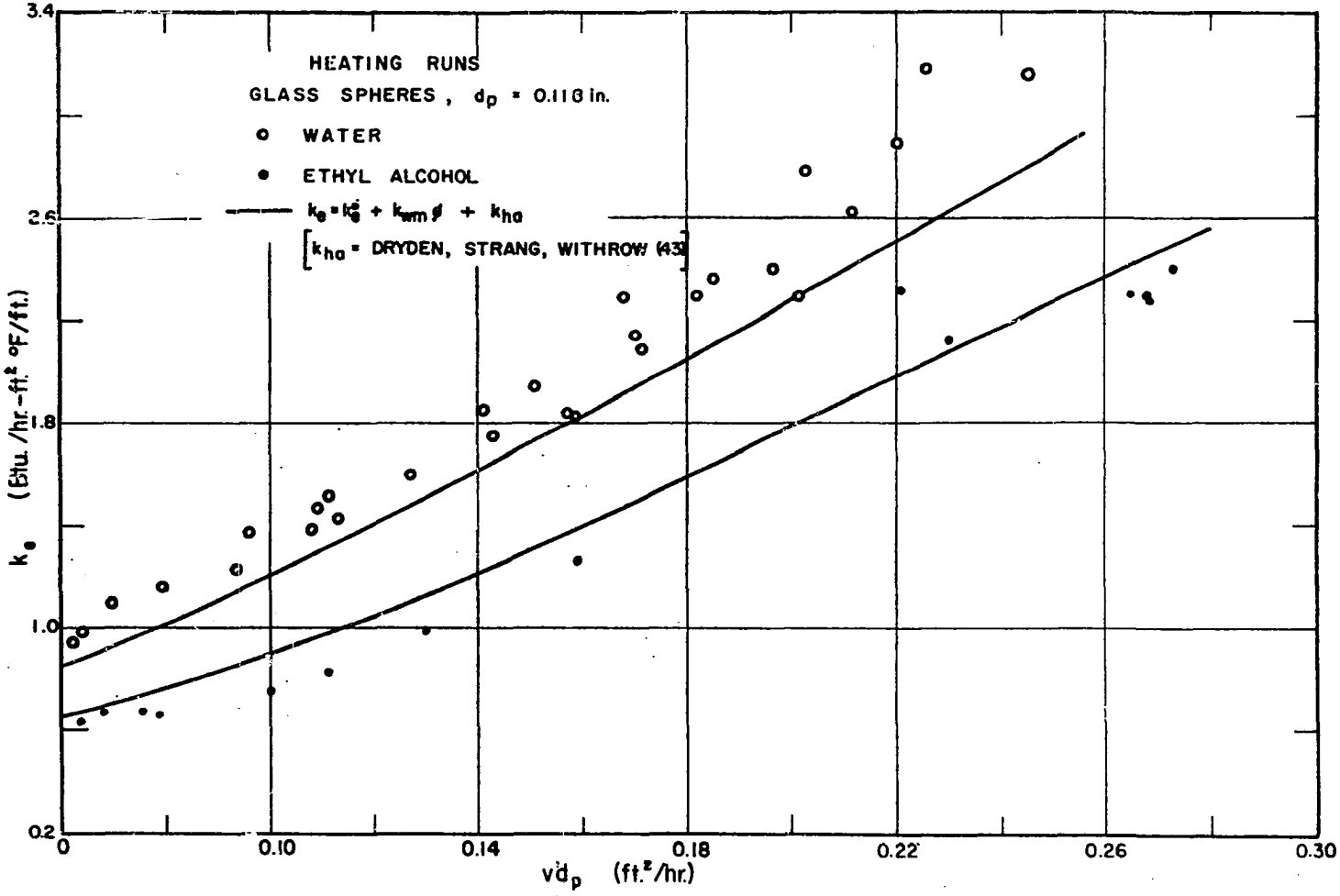

Figure 44- Heating-Run Data; Effective Thermal Conductivity vs. vd_p; Water and Ethyl Alcohol Systems

TABLE 25

EXPERIMENTAL HEATING-RUN DATA; WATER SYSTEM

Run #	vd_p	k_e	$k_e(v)$	k_e^o	T_{avg}	Re
209H	.168	2.28	1.77	.51	101.4	6.33
211H	.0961	1.37	.86	.51	105.1	3.78
214H	.113	1.42	.91	.51	105.1	4.42
215H	.127	1.59	1.08	.51	105.4	4.99
216H	.143	1.74	1.23	.51	110.2	5.93
217H	.159	1.82	1.31	.51	110.1	6.56
218H	.171	2.09	1.58	.51	110.5	7.05
219H	.182	2.29	1.78	.51	110.6	7.50
220H	.196	2.40	1.89	.51	110.9	8.20
221H	.211	2.62	2.11	.51	111.2	8.80
222H	.220	2.88	2.37	.51	111.0	9.07
223H	.245	3.16	2.65	.51	111.1	10.23
224H	.0614	.95	.44	.51	106.7	2.46
225H	.0789	1.16	.65	.51	107.7	3.25
226H	.0696	1.10	.59	.51	107.8	2.87
230H	.108	1.38	.87	.51	94.9	3.80
231H	.157	1.84	1.33	.51	95.6	5.58
232H	.201	2.29	1.78	.51	95.3	7.09
237H	.0934	1.23	.72	.51	124.7	4.46
239H	.185	2.36	1.85	.51	128.6	9.08
240H	.109	1.47	.96	.51	122.1	5.06
241H	.141	1.85	1.34	.51	122.3	6.54
242H	.203	2.78	2.27	.51	124.5	9.57
243H	.226	3.18	2.67	.51	124.1	10.69
246H	.111	1.51	1.00	.51	123.8	5.26
247H	.151	1.94	1.43	.51	130.9	7.15
248H	.170	2.14	1.63	.51	131.2	8.05

TABLE 26

EXPERIMENTAL HEATING-RUN DATA; ETHYL ALCOHOL SYSTEM

Run #	vd_p	k_e	$k_e(v)$	k_e^o	Tavg	Re
296H	.159	1.26	.86	.40	96.3	3.42
298H	.130	.99	.59	.40	92.1	2.63
299H	.100	.75	.35	.40	92.1	2.03
300H	.0791	.66	.26	.40	92.5	1.60
301H	.0638	.64	.24	.40	92.9	1.37
308H	.0755	.67	.27	.40	98.3	1.72
309H	.111	.83	.43	.40	98.1	2.53
310H	.0683	.67	.27	.40	96.5	1.47
311H	.273	2.40	2.00	.40	100.1	6.22
312H	.265	2.30	1.90	.40	101.1	6.04
314H	.268	2.29	1.89	.40	96.9	5.77
315H	.268	2.29	1.89	.40	97.7	6.11
316H	.230	2.12	1.72	.40	94.7	4.95
317H	.221	2.31	1.91	.40	94.2	4.76

agreement with the corresponding cooling-run data, Figure 25, but the water k_e values are higher than the cooling-run results, Figure 23. The fit of the experimental temperature profiles to the conduction-equation solution, Equation (III-34), was good for the water data but only fair for ethyl alcohol. This is illustrated in Figure 45.

The difference in measured effective thermal conductivities between the water heating and cooling runs has not been explained. An initial postulate would be that the unfavorable viscosity ratio, while not causing measurable channeling, does result in an increased eddy dispersion. This result has been noted in a mass-transfer investigation of longitudinal dispersion (17). However, this is not supported by the ethyl alcohol data where the heating and cooling results are in agreement. Additional work on the effect of an unfavorable viscosity ratio is needed.

Heating-Run Data with Channeling

In most of the heating run experiments, flow channeling was indicated. An attempt to calculate values of k_e from such data yielded poor fits to Equation (III-34). Tabulated effective thermal conductivities are therefore not presented.

Preston (138) carried out heating-run experiments in his investigation and values of k_e determined are considerably higher than the results of this work. This is

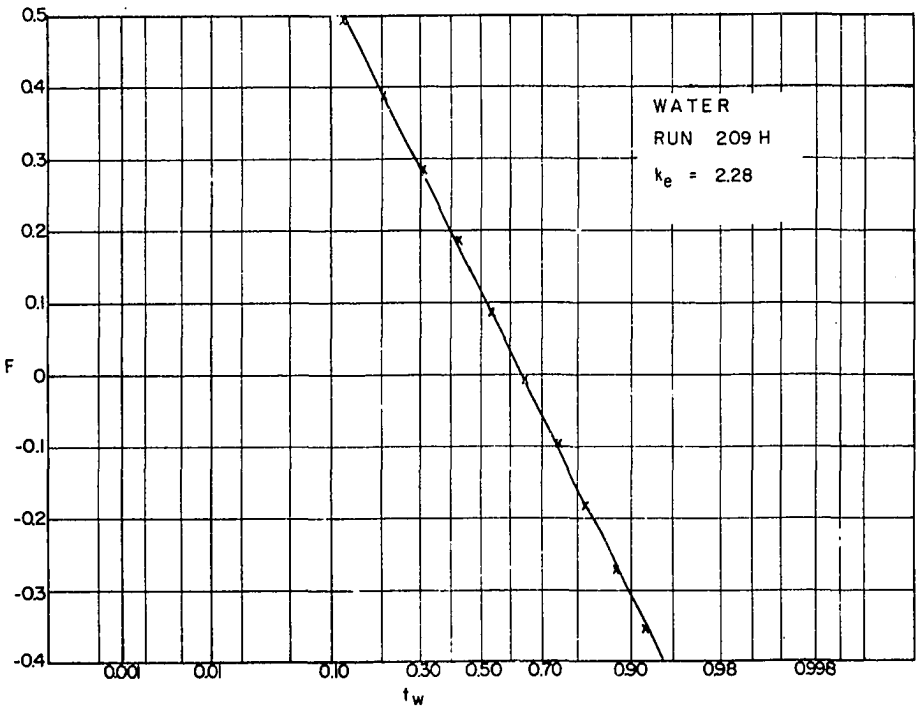

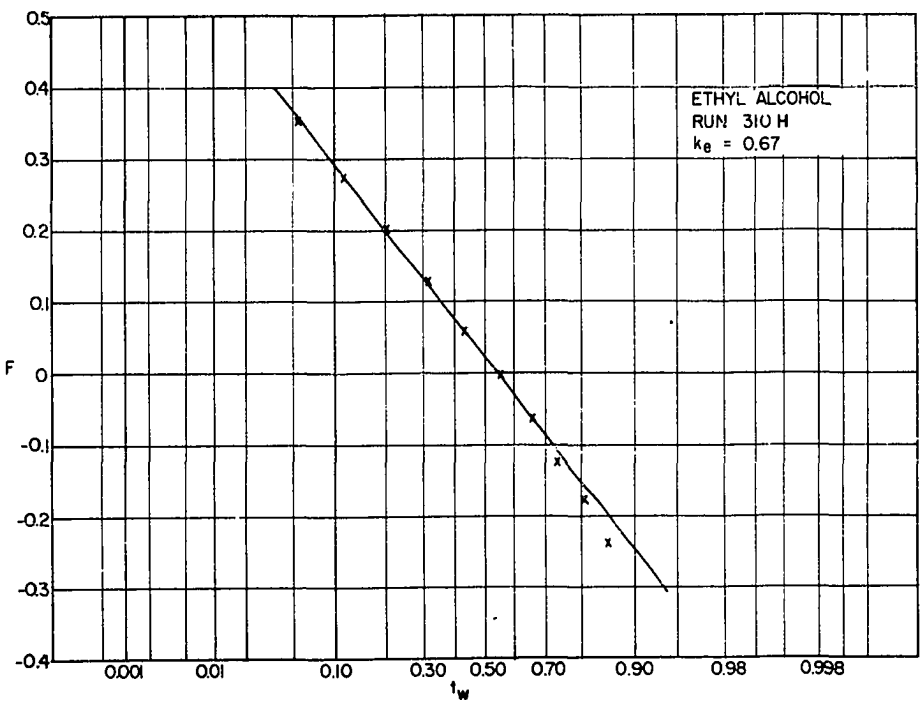

Figure 45- Heating-Run Data; Probability-Paper Plots; Water and Ethyl Alcohol Systems

illustrated in Figure 46. The difference is believed to be the result of flow channeling which most probably occurred in Preston's system. Further, in his experimental apparatus, Preston measured the packed-bed effluent temperature at the opening of the exit tubing. A "mixing-cup" temperature was thus obtained. Since an average effluent temperature was measured, flow channeling would cause a spread of the temperature profile resulting in a larger apparent k_e. The effect of channeling on measured dispersion coefficients has been discussed by Cairns and Prausnitz (25).

As a check on this hypothesis, several heating runs were made in the water - .0181 inch bead system in which an average packed-bed effluent temperature was measured. This was done in a manner similar to that of Preston, by inserting a thermocouple in the mouth of the packed-bed exit tubing. The scatter in the resulting calculated effective thermal conductivities was large due to a poor fit of the data to Equation (III-34), however, the calculated k_e values were in good agreement with the results of Preston. Experimental conductivities are shown in Table 27.

Natural Convection Channeling

Channeling caused by natural-convection effects was discussed in Chapter IV. Effective thermal conductivities were not calculated for these runs as the data fit to Equation (III-34) was very poor.

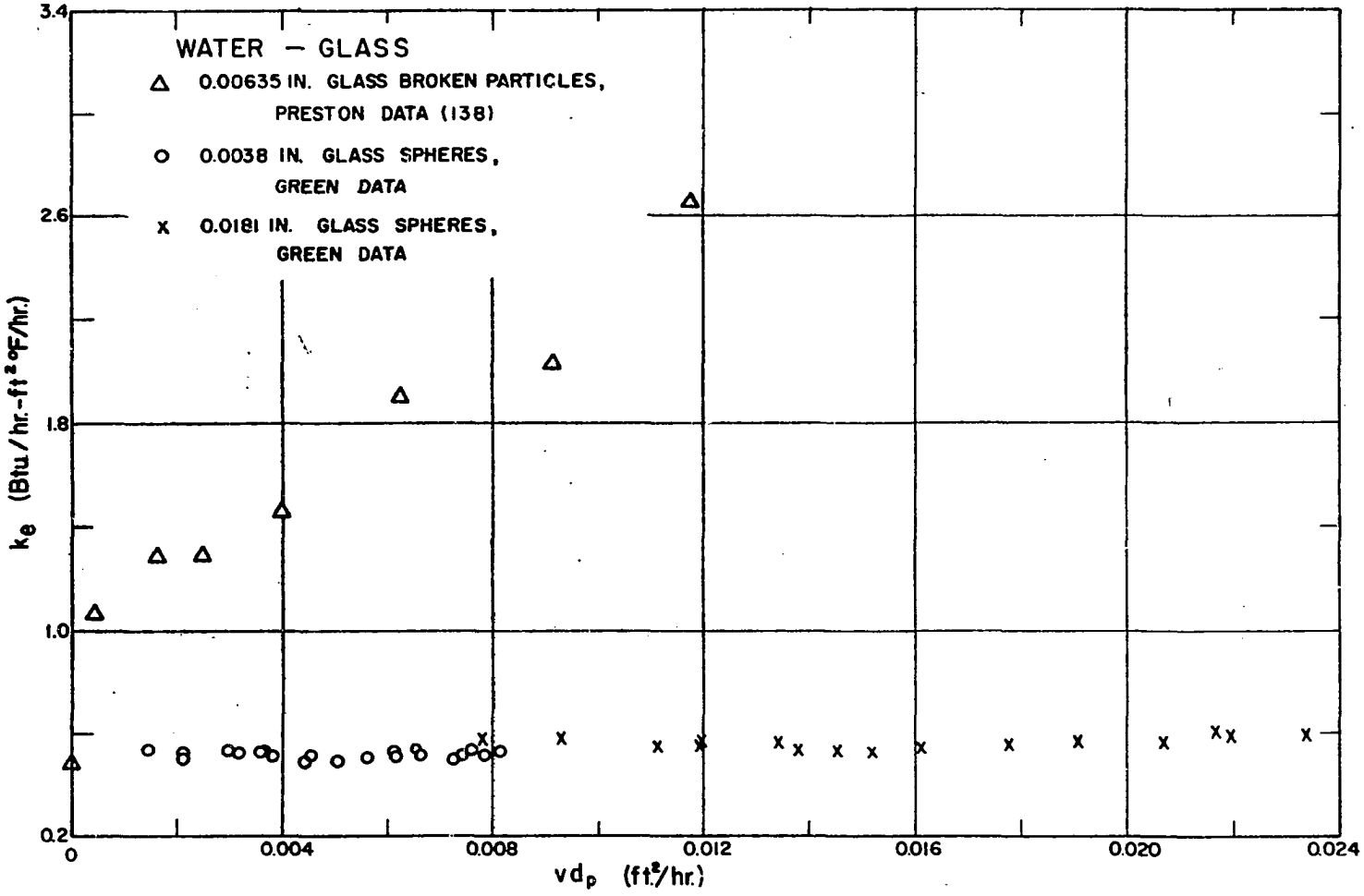

Figure 46- Comparison of the Experimental Data of Preston and Green

TABLE 27

HEATING-RUN DATA; EFFECTIVE THERMAL CONDUCTIVITY DETERMINED FROM THE AVERAGE PACKED-BED EFFLUENT TEMPERATURE

A. Green Data Glass Beads - Water d_p = .0181 inch				B. Preston Data Glass Particles - Water 80 - 100 mesh d_p = .0063 inch (Avg. of screen opening		
Run #	vd_p	k_e	$k_e(v)$	vd_p	k_e	$k_e(v)$
146H	.0176	2.27	1.76	.000469	1.07	.58
147H	.0236	2.17	1.66	.00163	1.29	.80
148H	.0274	2.49	1.98	.00250	1.29	.80
149H	.0328	2.66	2.15	.0040	1.46	.97
162H	.0296	2.80	2.29	.00625	1.91	1.42
164H	.0327	2.0-3.0	1.49-1.59	.00919	2.04	1.55
				.0117	2.66	2.17

APPENDIX M

ADDENDUM TO CHAPTER V

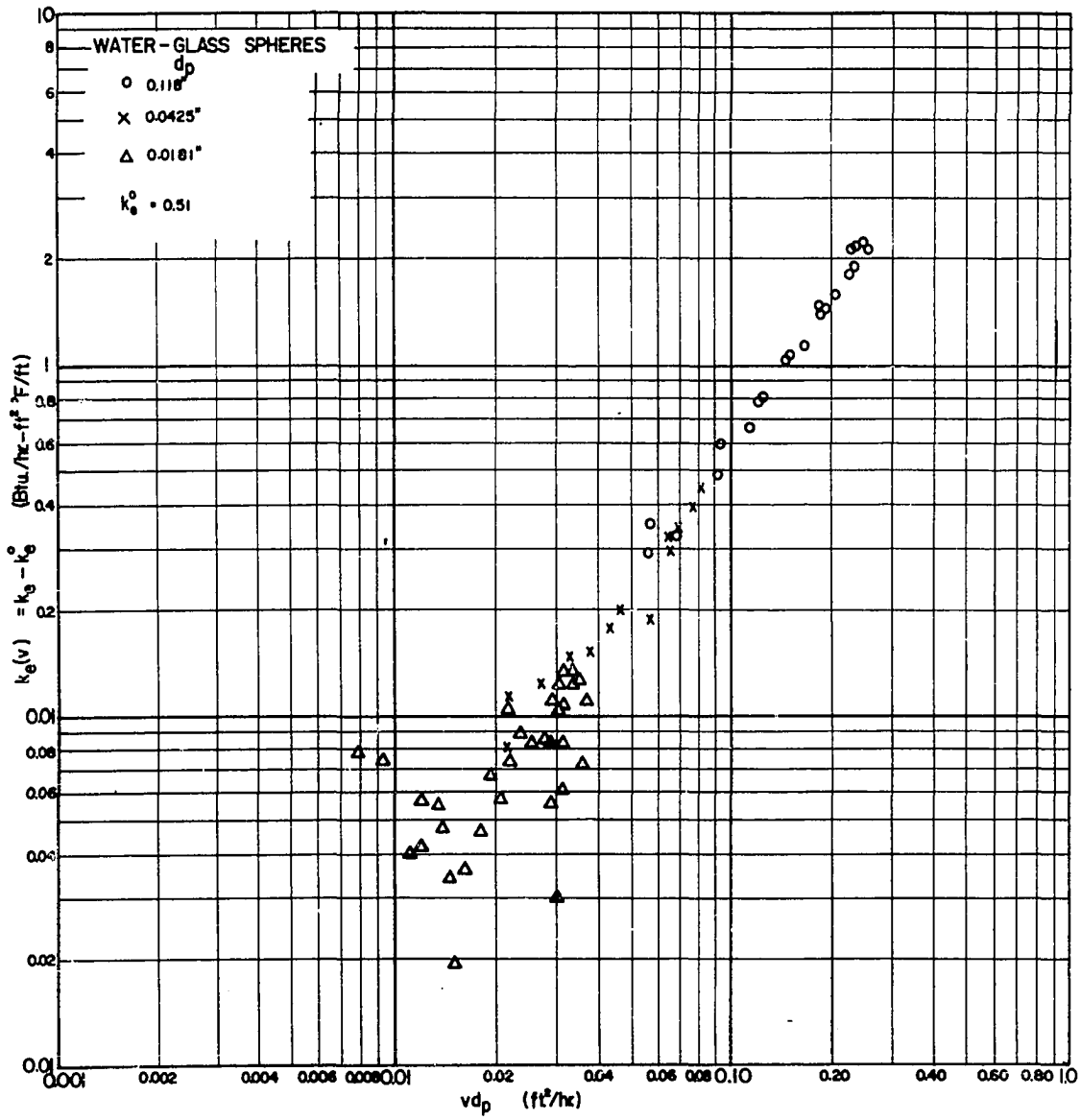

Figure 47- Velocity Component of the Effective Thermal Conductivity; Water System

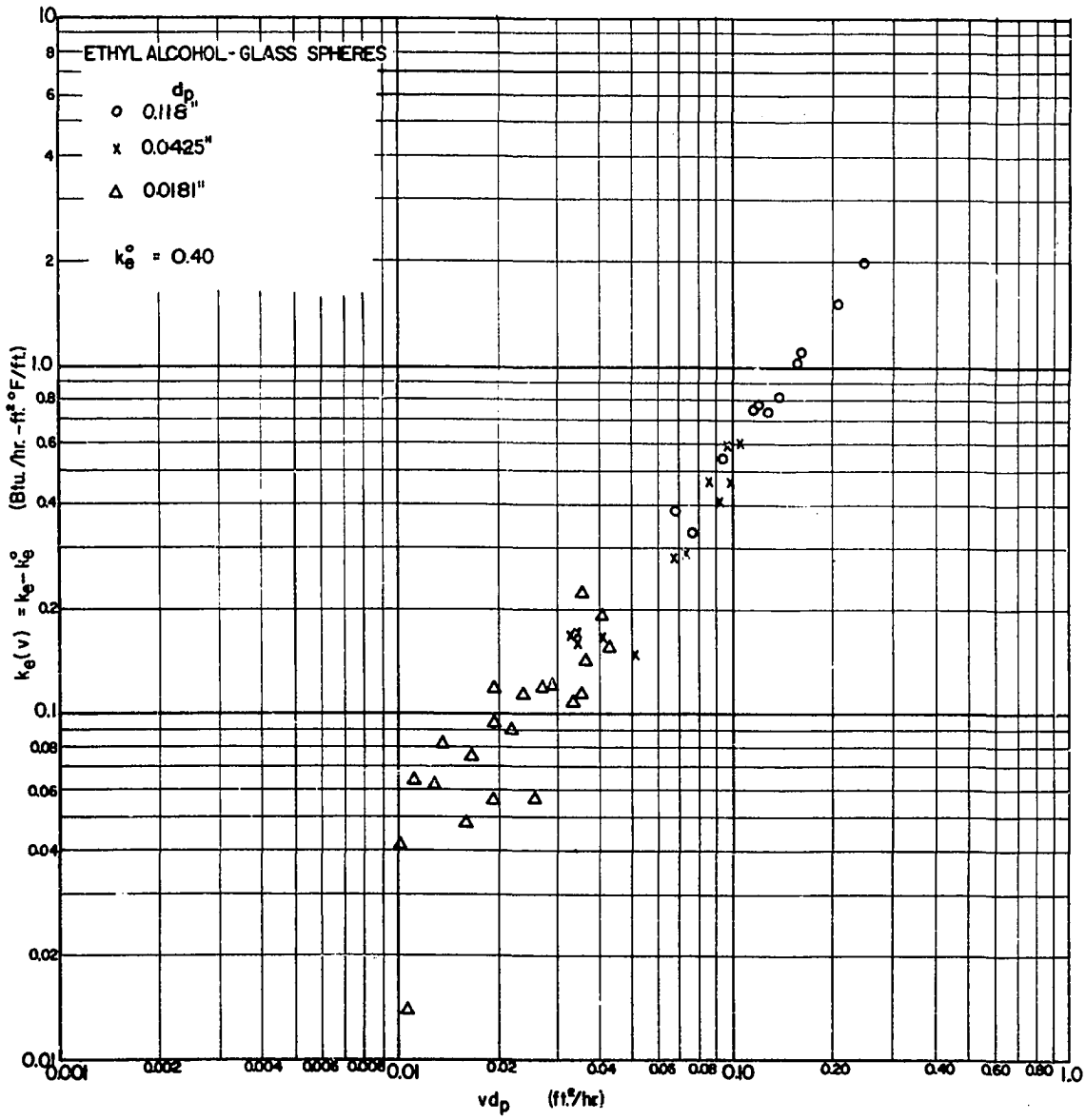

Figure 48- Velocity Component of the Effective Thermal Conductivity; Ethyl Alcohol System

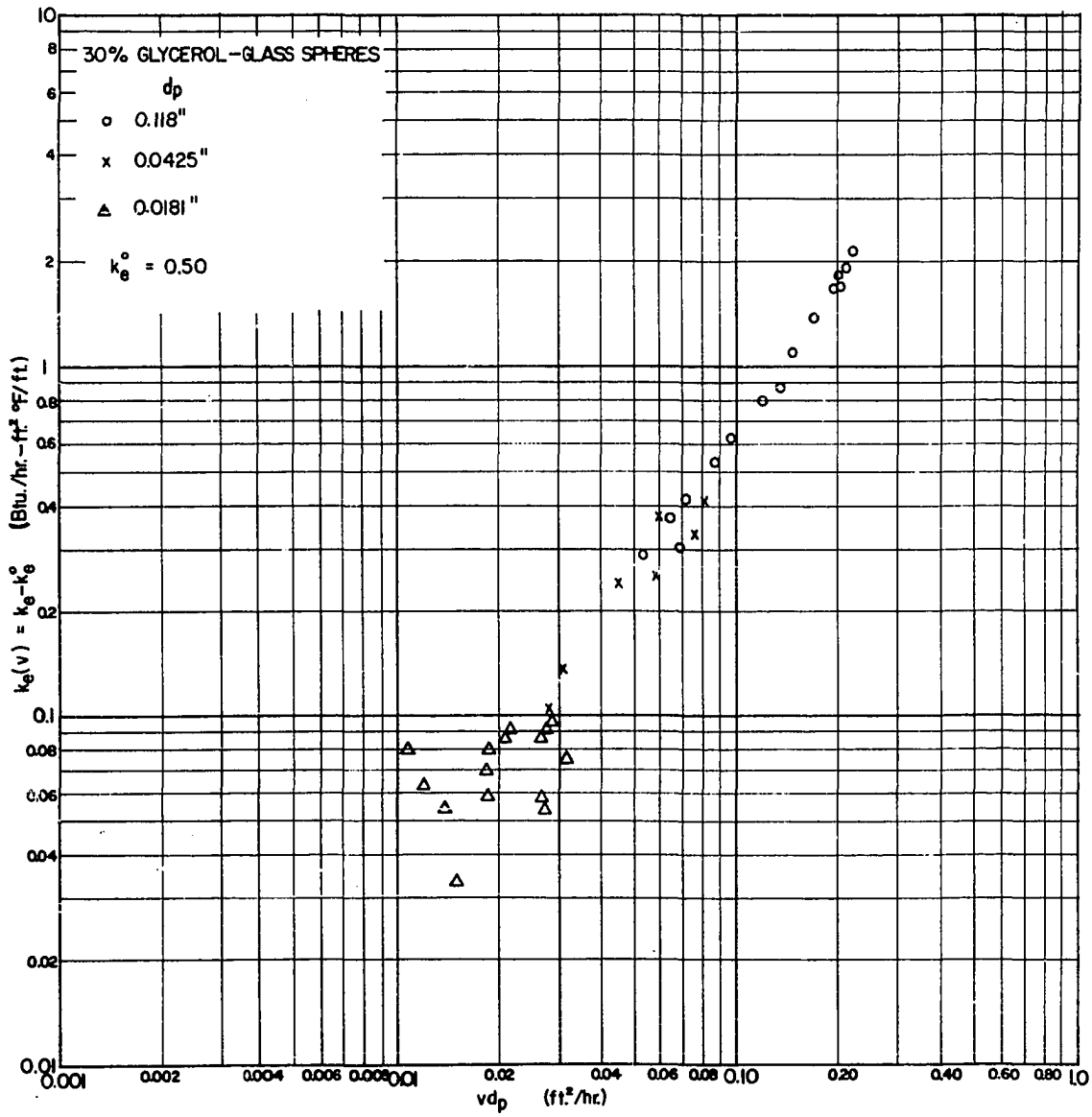

Figure 49- Velocity Component of the Effective Thermal Conductivity; 30 Per Cent Glycerol System

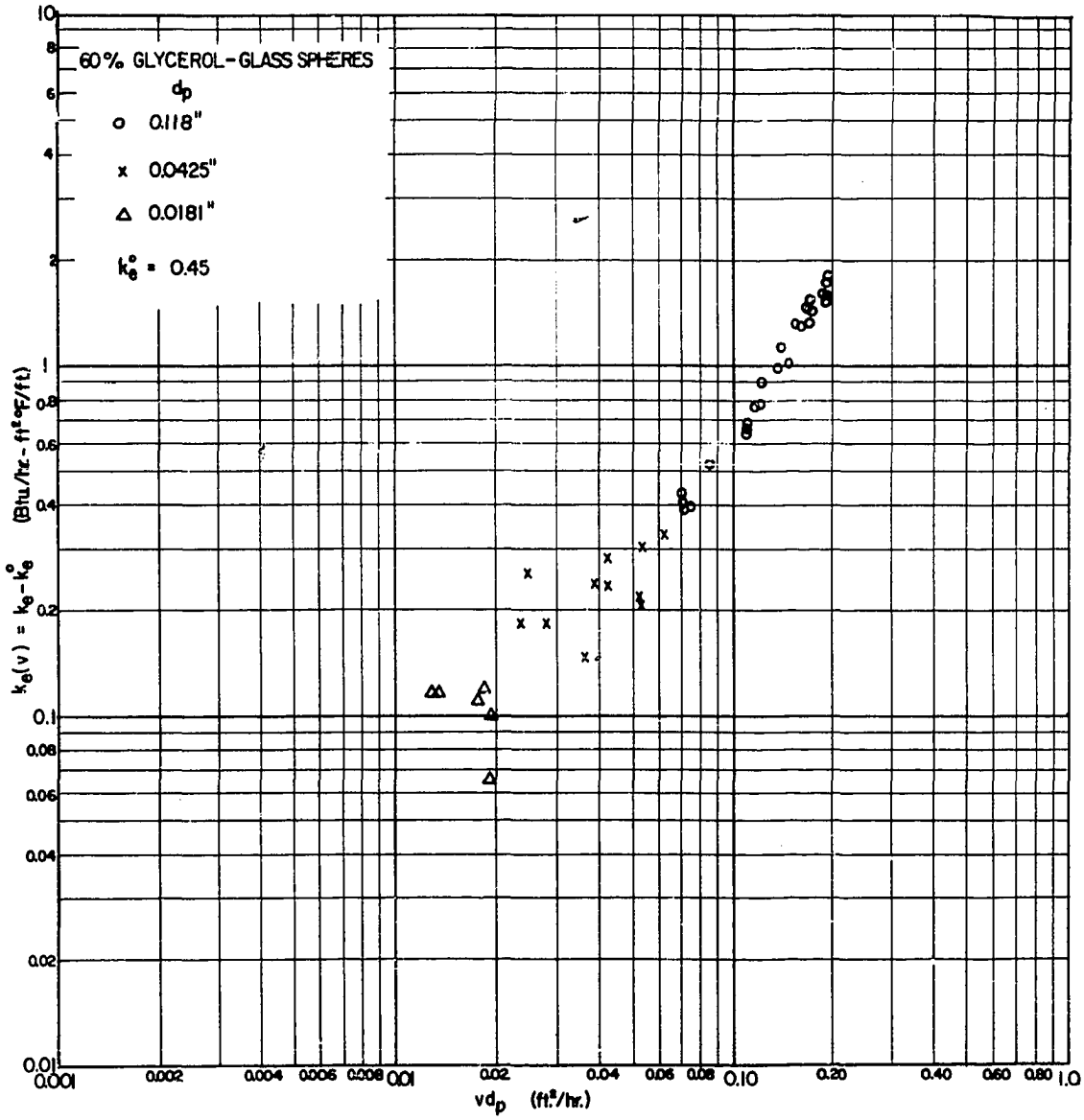

Figure 50- Velocity Component of the Effective Thermal Conductivity; 60 Per Cent Glycerol System

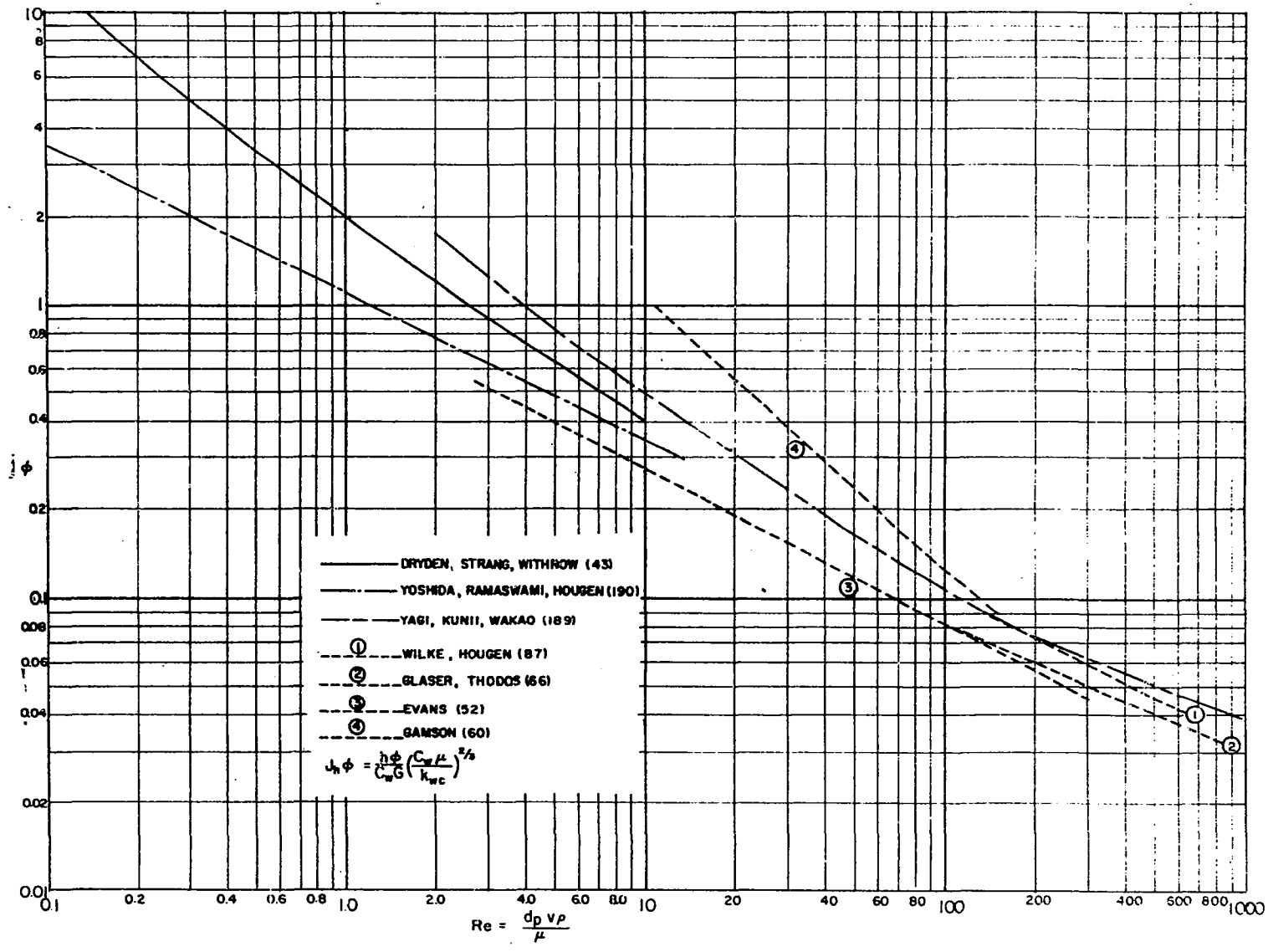

Figure 51- Heat-Transfer Coefficients; $j_h\phi$ vs. Re

Eddy-Dispersion Correlation; k_{ha} from Yoshida, Ramasuami, Hougen "j" Factor Correlation

The "j" factor correlation of Yoshida, Ramasuami, and Hougen (190) is

$$j_h = .91 \quad Re_B^{-.51} \tag{L-1}$$

where

$$Re_B = \frac{\rho_w v \phi}{\mu a \psi} = \frac{v \rho_w \phi d_p}{6 \mu (1-\phi)} \tag{L-2}$$

and where ψ is the sphericity (1.0 for spheres) and j_h was defined in Equation (II-19). Equations (L-1), (L-2) and (V-9) were used to determine ha and correspondingly k_{ha} for the liquid systems studied. Plots of k_{ha} versus vd_p for these liquid systems are shown in Figure 52.

Calculations of the eddy-dispersion coefficient, $k_{wm}\phi$, were then made for the experimental cooling-run data just as discussed in Chapter V [See Equation (V-11)]. A plot of $k_{wm}\phi/k_{wc}\phi$ versus $\frac{vd_p}{D_h}$ is shown in Figure 53, and a straight line fit to the data yielded

$$\frac{k_{wm}\phi}{k_{wc}\phi} = .084 \quad \left(\frac{vd_p}{D_h}\right)^{1.25} \tag{L-3}$$

Values of $k_{wm}\phi$ are approximately 30% below corresponding values using the Dryden et al. (43) "j" factor.

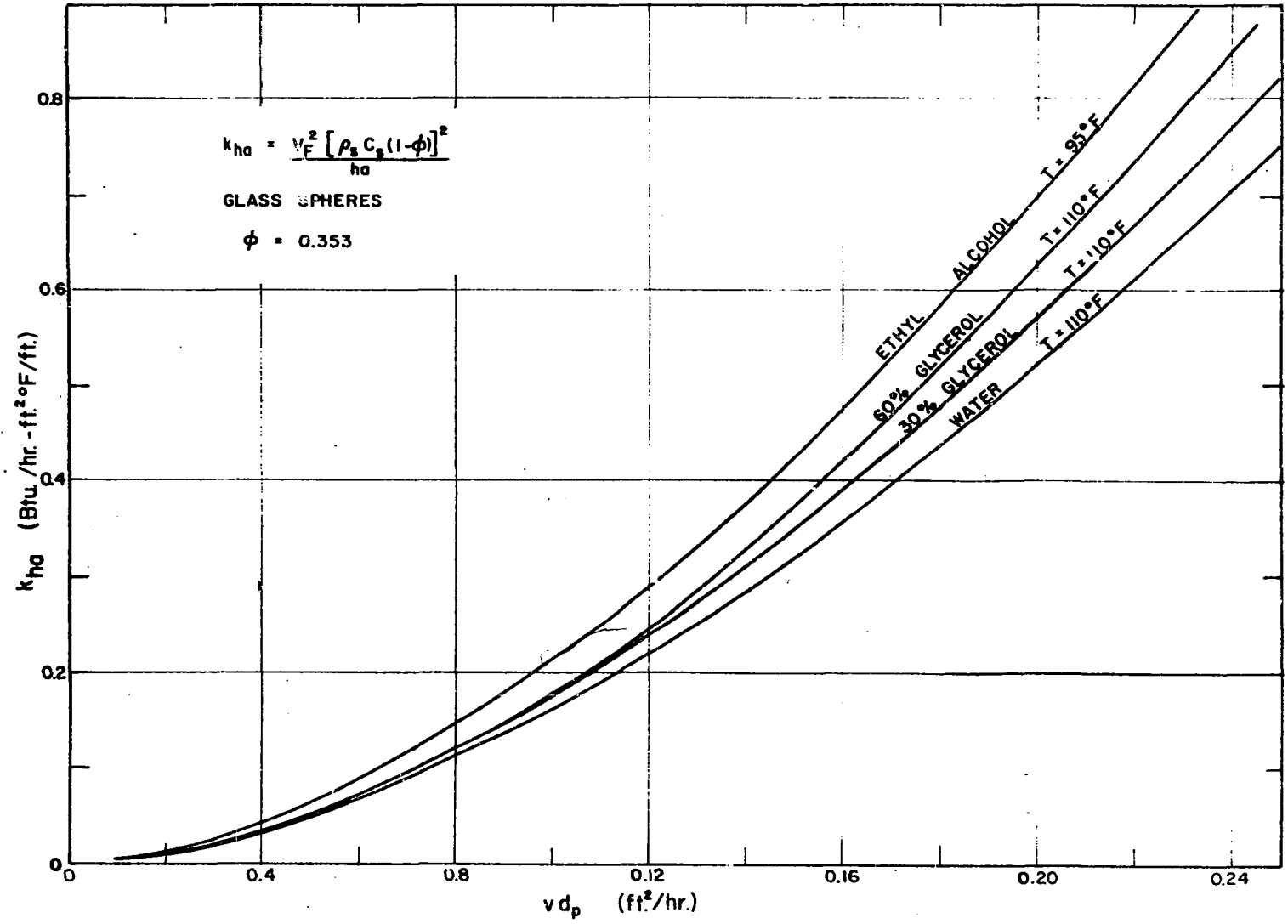

Figure 52- k_{ha} vs. vd_p; Heat-Transfer Coefficient
Data from Yoshida, Ramasuami, Hougen

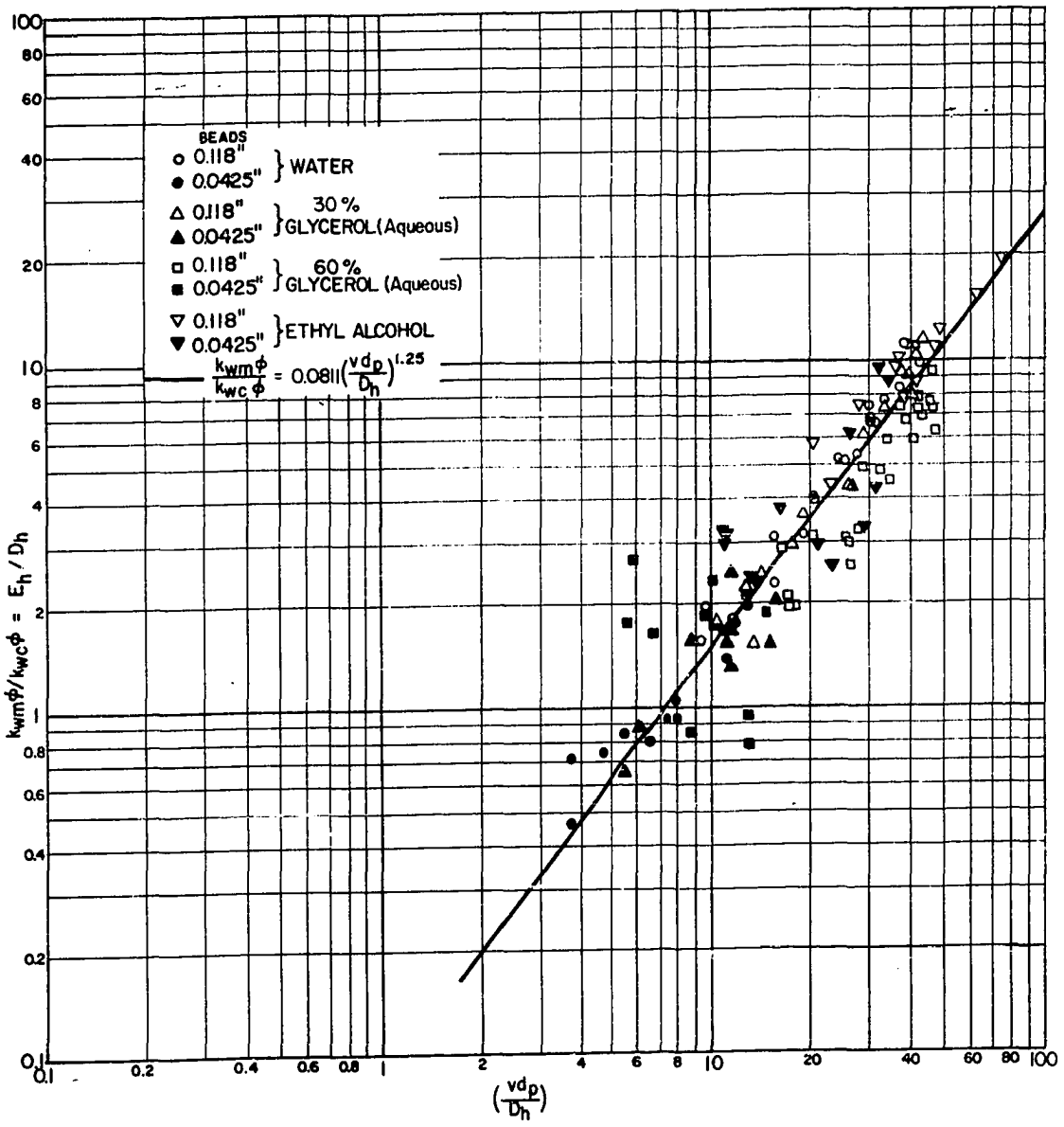

Figure 53- Correlation of Eddy-Dispersion Data; E/D vs. (vd_p/D); k_{ha} from Yoshida, Ramasuami, Hougen Correlation

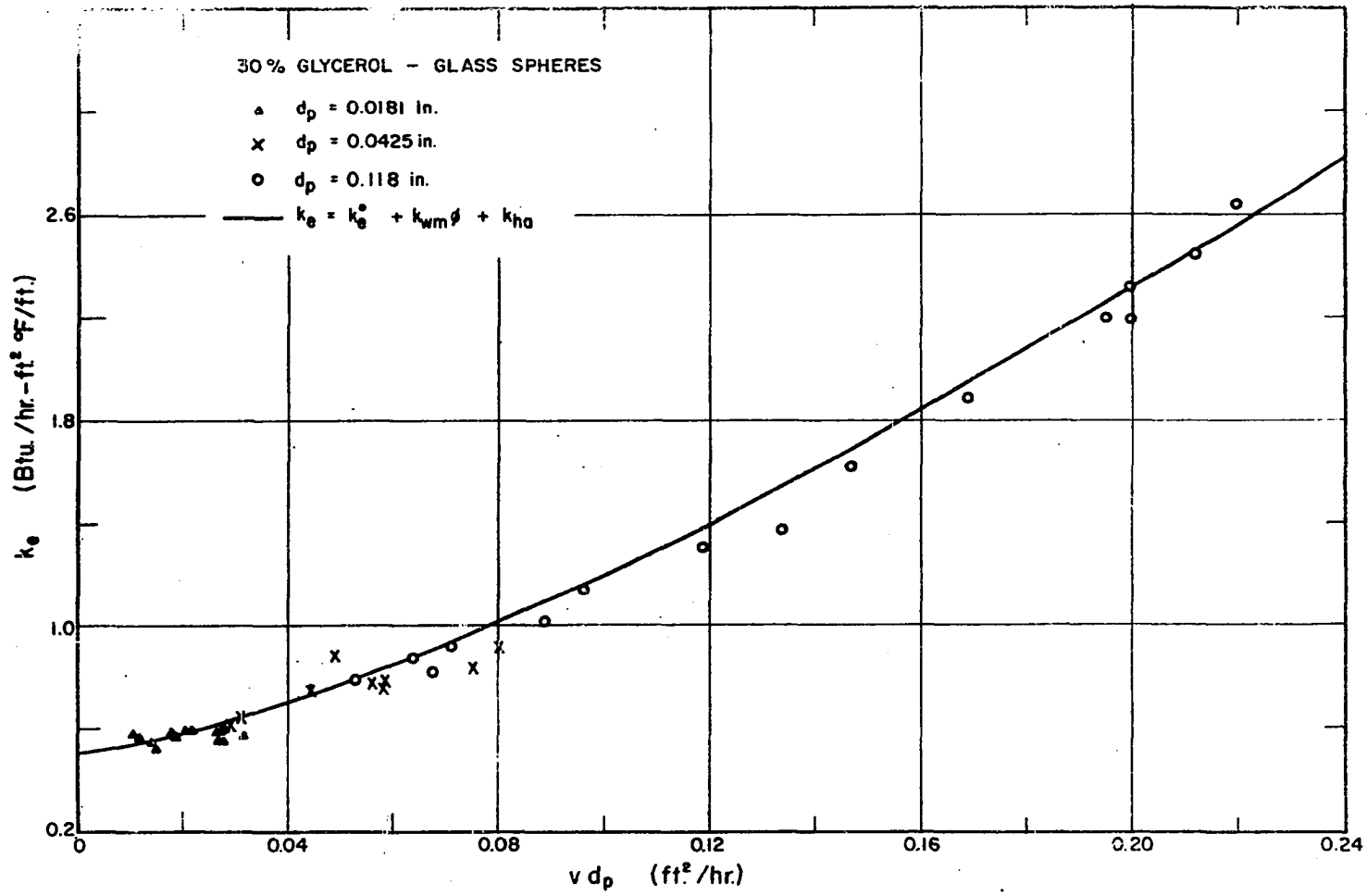

Figure 54- Summation of Conductivities; k_{ha} from Dryden, Strang, Withrow Data; 30 Per Cent Glycerol System

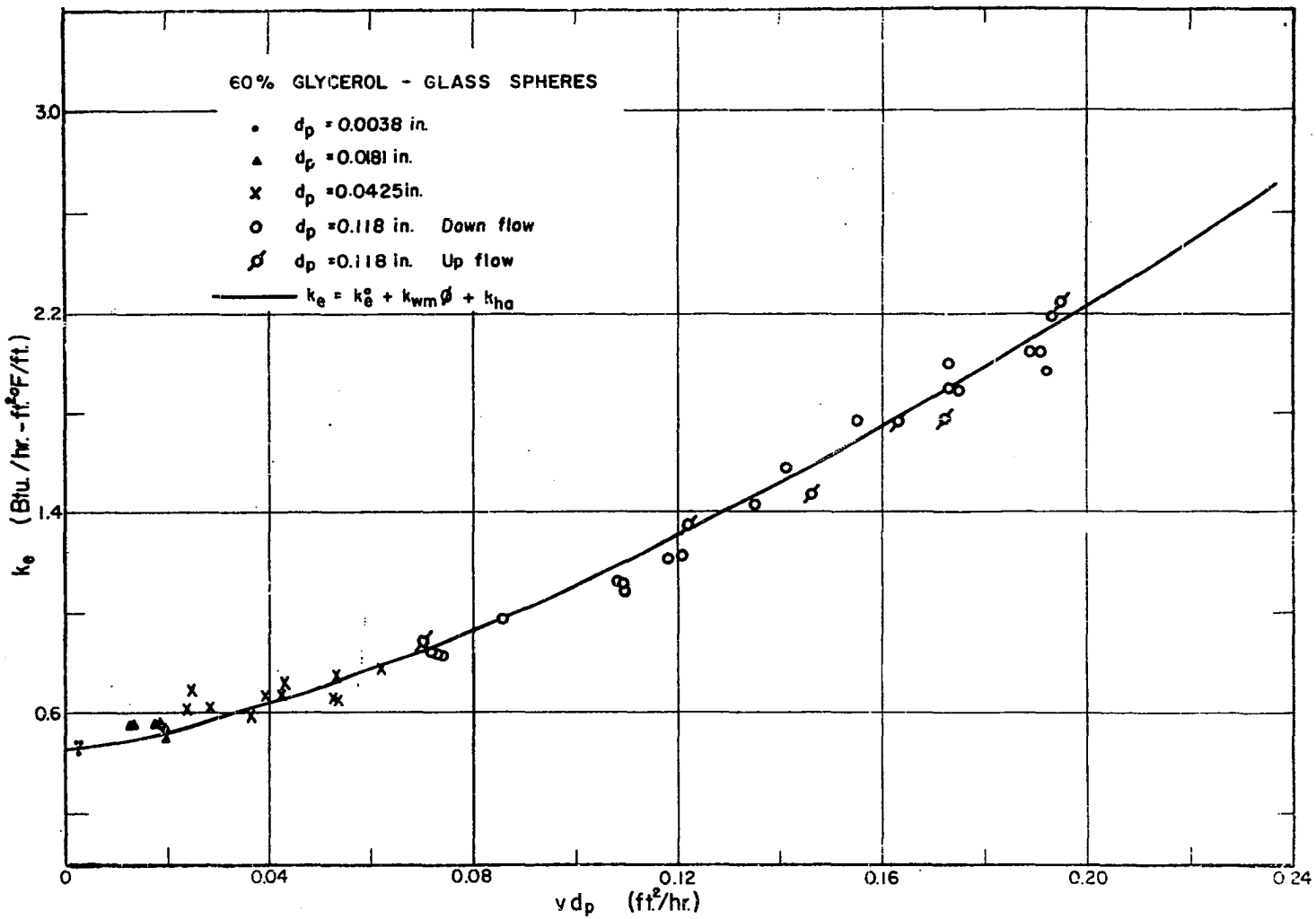

Figure 55- Summation of Conductivities; k_{ha} from Dryden, Strang, Withrow Data; 60 Per Cent Glycerol System

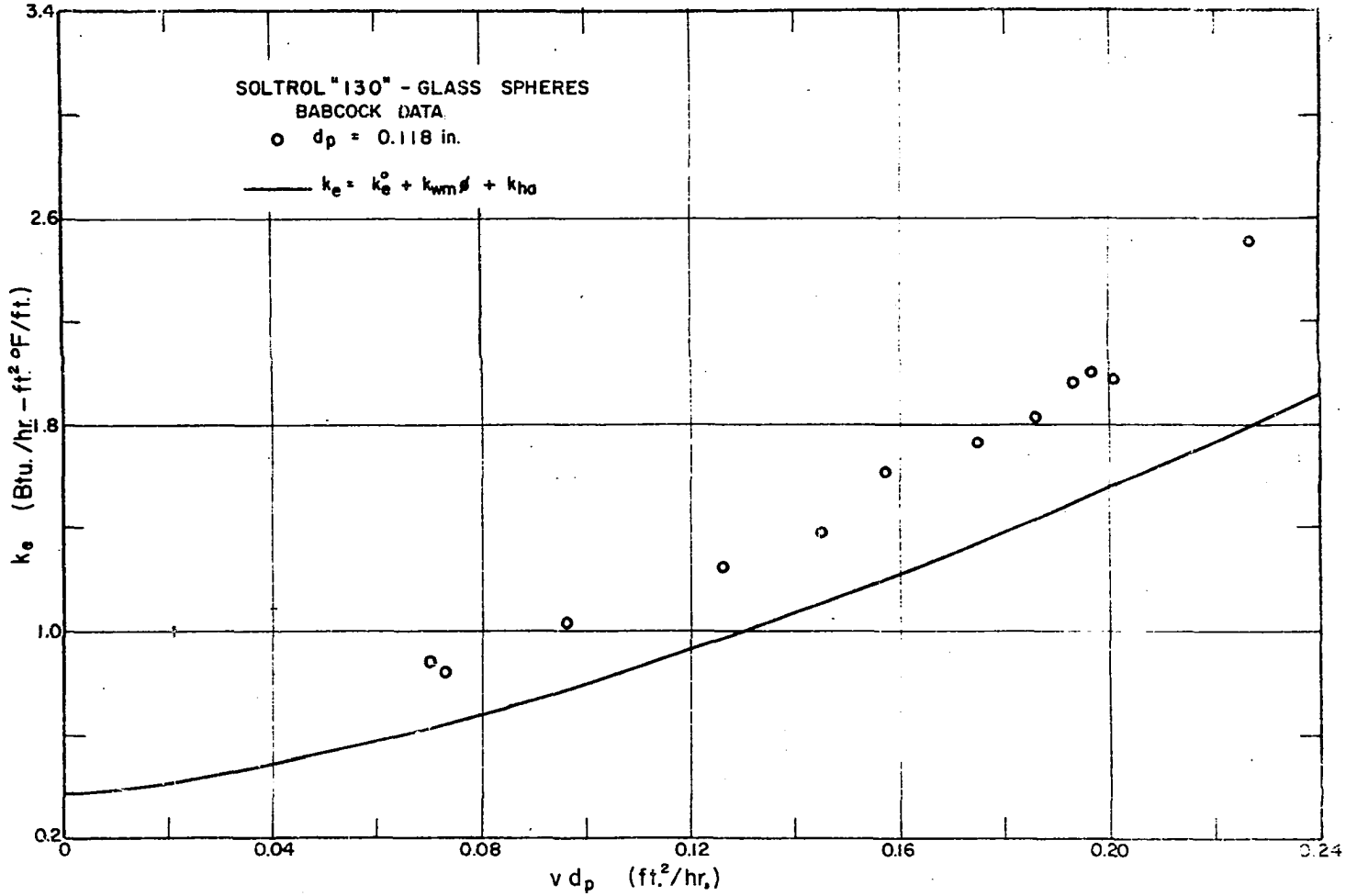

Figure 56- Summation of Conductivities; k_{ha} from Dryden, Strang, Withrow Data; Soltrol "130", Babcock Data

TABLE 28

SUMMATION OF CONDUCTIVITIES; k_{ha} FROM DRYDEN, STRANG, WITHROW DATA; 30% GLYCEROL, 60% GLYCEROL, AND SOLTROL "130" SYSTEMS

30% Glycerol: T = 110°F ϕ = .356

vd_p	k_e^o	k_{ha}	$k_{wm}\phi$	k_e
.01	.50	.003	.029	.532
.02		.01	.069	.579
.05		.052	.218	.770
.10		.175	.520	1.195
.15		.349	.860	1.709
.20		.568	1.230	2.298
.24		.772	1.53	2.802

60% Glycerol: T = 105°F ϕ = .356

vd_p	k_e^o	k_{ha}	$k_{wm}\phi$	k_e
.01	.45	.003	.027	.480
.02		.01	.064	.524
.05		.053	.203	.706
.10		.178	.480	1.108
.15		.372	.805	1.627
.20		.625	1.150	2.225
.24		.850	1.450	2.75

Soltrol "130" Babcock Data T = 110°F ϕ = .359

vd_p	k_e^o	k_{ha}	$k_{wm}\phi$	k_e
.01	.37	.004	.013	.387
.02		.012	.031	.413
.05		.058	.097	.525
.10		.193	.230	.793
.15		.386	.382	1.138
.20		.633	.545	1.548
.24		.860	.680	1.910
.307		1.307	.930	2.607
.345		1.585	1.070	3.025

ERRATA

HEAT TRANSFER WITH A FLOWING FLUID THROUGH POROUS MEDIA

Ph. D. Thesis, Don W. Green, Univ. of Oklahoma, 1962

1. Figures 28 and 52 should be interchanged, that is, the graph on page 246 should go with the title and figure number on page 119, and the graph on page 119 should go with the title and figure number on page 246.

2. On page 137 in the heading row on the bottom-half of the table $k_e(ha)$ should read k_{ha}.

3. On page 227, the next to last sentence should read, "Deisler's expression for B, for the analogous case of heat transfer, may be correctly shown to be,

$$\frac{B}{w^2} = \frac{\left[\rho_s C_s (1-\phi)\right]^2 R_p^2 L}{15\, \rho_w C_w \phi v\, k_{sc}\, (1-\phi)} + \frac{k_w \phi L}{\rho_w C_w \phi v^3} \left[\left[\frac{\rho_s C_s (1-\phi)}{\rho_w C_w \phi} \right]^2 + \frac{2\rho_s C_s (1-\phi)}{\rho_w C_w \phi} + 1 \right] \qquad (K-3)$$

(Equation 49, page 147 of Reference 39 appears to be in error.)

4. In Figure 52, page 246, the second and third units of the abscissa should read 0.04 and 0.08 respectively.